Title
Nitroacetylenes Harnessed by Cobalt

Author
Windler, Gary Kenneth

Publication Date
2011

Peer reviewed|Thesis/dissertation

Nitroacetylenes Harnessed by Cobalt

By

Gary Kenneth Windler, Jr.

A dissertation submitted in partial satisfaction of the

requirements for the degree of

Doctor of Philosophy

in

Chemistry

in the

Graduate Division

of the

University of California, Berkeley

Committee in charge:

Professor K. Peter C. Vollhardt, chair
Dr. Philip F. Pagoria (LLNL)
Professor Robert G. Bergman
Professor Clayton J. Radke

Fall 2011

Nitroacetylenes Harnessed by Cobalt

by Gary Kenneth Windler, Jr.

Abstract

Nitroacetylenes Harnessed by Cobalt

by

Gary Kenneth Windler, Jr.

Doctor of Philosophy in Chemistry

University of California, Berkeley

Professor K. Peter C. Vollhardt, Chair

The syntheses and characterization of nitroacetylenes have been studied with respect to their large-scale production, purification, and NMR spectra, respectively. The ^{13}C NMR spectrum of 1-nitro-2-(trimethylsilyl)ethyne (**18**) evidenced $^{13}C–^{14}N$ coupling between the alkynyl carbon and the attached nitrogen, in agreement with the previously reported spectrum of 1-nitroethyne (**16**). The multi-gram preparation of high purity **18** is described. A history of previous work with nitroacetylenes is reviewed.

The stabilization of nitroacetylenes as hexacarbonyl dicobalt alkyne complexes was investigated. In conjunction with appropriate oxidizers, such complexes were shown to be long-term storage media for free nitroalkynes. The syntheses and complete characterization of the first two nitroalkyne transition metal complexes, [μ-1-nitro-2-(trimethylsilyl)ethyne-1,2-diyl]bis(tricarbonylcobalt)(*Co–Co*) (**25**) and [μ-1-nitroethyne-1,2-diyl]bis(tricarbonylcobalt)(*Co–Co*) (**26**), are described. Phosphine derivatives of **25** were prepared and studied. The synthesis of [μ-1,2-dinitroethyne-1,2-diyl]bis(tricarbonylcobalt)(*Co–Co*) (**24**) by direct ligation, transformation of functional groups on existing complexes, and nitration of such complexes was unsuccessful.

Complexes **25** and **26** were applied to the synthesis of organic molecules. While they did not yield cyclopentenones via the Pauson-Khand cyclization, they rendered benzene derivatives by the [2 + 2 + 2] cobalt-mediated cyclotrimerization. In addition to two nitroindanes and a nitrotetralin, several new trinitrobenzene isomers were made, all potential precursors to energetic materials. The X-ray crystal structure of one of these, 1,3,5-trinitro-2,4,6-tris(trimethylsilyl)benzene (**325**), showed a planar, but distorted aromatic ring.

For my mother,
Rev. Dr. Diane Earle Windler,
who taught me to never, never, never give up.

Table of Contents

Abbreviations and Acronyms

Ac - Acyl
BDE - Bond Dissociation Energy
Boc - *N*-*t*-Butoxycarbonyl
Bu - Butyl
***sec*-Bu** - *sec*-Butyl
***t*-Bu** - *tert*-Butyl
Bz - Benzoyl
CAN - Ceric Ammonium Nitrate
CL-20 - China Lake formulation 20, 2,4,6,8,10,12-hexanitro-2,4,6,8,10,12-hexaazaisowurtzitane
Cp - Cyclopentadiene
***m*-CPBA** - *meta*-Chloroperoxybenzoic acid
CV - Cyclic Voltammetry
DFT - Density Functional Theory
DH_{50} - Drop hammer Height, 50 % probability level
DMAD - Dimethyl Acetylene Dicarboxylate
DMDO - Dimethyldioxirane
DMF - Dimethylformamide
DMSO - Dimethylsulfoxide
DNA - Dinitroacetylene
DPPA - Diphenylphosphoryl Azide
DSC - Differential Scanning Calorimetry
EI-MS - Electron Impact Mass Spectrometry
Et - Ethyl
FID - Flame Ionization Detector
FOX-7 - Försvarets forskningsanstalt explosive 7, 1,1-diamino-2,2-dinitroethene
FT - Fourier Transform
GC-IR - Gas Chromatography Infrared Spectrometry
GC-MS - Gas Chromatography Mass Spectrometry
Hex - Hexyl
HF - Hartree Fock or hydrofluoric acid
HHTDD - 2,4,6,8,10,12-Hexanitro-2,4,6,8,10,12-hexaaza-tricyclo (7,3,0,$0^{3,7}$) dodecane-5,11-dione
HMDS - Hexamethyldisilizane
HMX - High Melting explosive, octahydro-1,3,5,7-tetranitro-1,3,5,7-tetrazocine
HNB - Hexanitrobenzene
IR - Infrared
LAH - Lithium Aluminum Hydride
LLNL - Lawrence Livermore National Laboratory
Me - Methyl
MINDO/3 - Modified Intermediate Neglect of Differential Overlap
MS - Mass Spectrometry or Mass Spectrum
NMO - *N*-methylmorphonline-*N*-oxide
NMP - *N*-methylpyrrolidinone
NMR - Nuclear Magnetic Resonance
Npht - phthalimido
OB - Oxygen Balance
ORTEP - Oak Ridge Thermal Elipsoid Plot (computer program)
POV-Ray - Point Of View Ray tracer (computer program)
Pent - Pentyl
***neo*-Pent** - *neo*-Pentyl
PETN - Pentaerythrite Tetranitrate
Ph - Phenyl
Pr - Propyl
***i*-Pr** - *iso*-Propyl
RDX - Research Department explosive, 1,3,5-Trinitroperhydro-1,3,5-triazine
rt, RT - Room Temperature
TATB - 1,3,5-Triamino-2,4,6-trinitrobenzene
TBAF - Tetrabutylammonium Fluoride
TFA - Trifluoroacetic Acid
TGA - Thermogravimetric Analysis
THF - Tetrahydrofuran
TIPS - Tri(*iso*-propyl)silyl
TLC - Thin Layer Chromatography
TMANO - Trimethylamine-*N*-oxide
TMEDA - Tetramethylethylenediamine
TMG - Tetramethylguanidine
TMP - Tetramethylpipiridine

TMS - Trimethylsilyl
TNB - 1,3,5-Trinitrobenzene
TNGU - Tetranitroglycouril
TNT - 2,4,6-Trinitrotoluene
UV-Vis - Ultraviolet Visible

Acknowledgements

Anyone who has attempted to produce a work of this magnitude knows of the difficulty and frustration not only of writing, but of the chemical syntheses and analyses involved as well. In the laboratory, I would like to thank Rudi Nunlist for his invaluable help obtaining NMR spectra and many amusing anecdotes, Dr. Fred Hollander for the crystal structures herein and our discussions of crystallography, the analytical staff at LLNL/HEAF for DSC, TGA, and drop hammer data, and Dr. Dean Goedde, my undergraduate mentor, who instilled in me my lab technique (and love for large quantities of mercury). I would especially like to thank Dr. Mao-Xi Zhang, one of the greatest living synthetic chemists, whose help with particularly dangerous and difficult syntheses was both invaluable and educational.

I would like to thank Lawrence Livermore National Laboratory for the SEGRF/LSP fellowship, funding, and the opportunity to work on site at HEAF.

I owe thanks to the organizations and people whose activities and friendships kept me sane through various stages of my graduate career: the Organomets and Circuit Riders softball teams, the Golden Gate Raptor Observatory, the Livermore Amador Symphony, Lisa Lauderbach, and Bronwyn Hagerty. I wish to also thank Lisa, Phil Pagoria, my parents, and Kara Reagan for their constant, unwavering support. Special thanks go to Dave Wise for many conversations that helped me keep perspective, and his encouragement when I was the most defeated. I owe Lynn Keithlin a debt of gratitude for helping me navigate the endless, senseless, and ever-changing red-tape of the University of California.

The greatest support I received from any of my peers was from Dr. Philip Leonard, and he is deserving of his own paragraph. His friendship, loyalty, chemistry lessons, and insanely cheerful (or maybe cheerfully insane?) attitude made an otherwise unbearable existence tolerable under the worst of circumstances. My thanks to you, Phil.

The two advisors who made this work possible, Philip Pagoria and Peter Vollhardt, also have my gratitude for dreaming up this project and setting the wheels in motion to bring it to fruition. I would like to thank Phil for his constant support and encouragement, without which this thesis may have never been finished, and Peter for never losing faith or giving up on me, both in research and completing this thesis.

Finally, I would like to thank my parents. Their care and support throughout my life have given me the foundation upon which all of my accolades and achievements have been based. I could not have been blessed with better parents. Although my mom did not live to see the completion of this thesis, it was her zest for life and perseverance through trials far more difficult than a PhD that have been and will continue to be an inspiration to me.

Chapter 1. Introduction: History of Explosives and Goals of this Thesis

1.1 Examples of Explosives

"When the flame of black powder toucheth the soul of man, it burneth exceeding deep."

Roger Bacon, *Opus Majus*, 1242.

Roger Bacon was correct when he mused on black powder's hold on humanity. Its appearance in China in 808 AD ignited a fascination with propellants and explosives that continues today.[1] Since antiquity, humans have harnessed fire: the combination of a fuel with oxygen, which emits a great deal of energy in the form of heat and light, usually over relatively long periods. This process is considerably shortened in the case of propellants such as black powder.

The discovery of black powder represented a great technological leap. It incorporated an oxidizing agent, namely potassium nitrate (saltpeter), thus circumventing the need for atmospheric oxygen. Because saltpeter was intimately mixed with the fuel (charcoal and sulfur), combustion could take place rapidly and occur in a confined space, in turn generating tremendous temperatures and pressures. This was sufficient to break rocks or cause other damage, and it became a mainstay in the civilian sector for mining, and in the military for the obvious application to warfare.[2]

The next major advance came in 1846, when Sobrero first prepared 1,3-dinitrooxypropan-2-yl nitrate (nitroglycerin) (**1**),[3] and Schönbein and Böttger simultaneously isolated nitrocellulose (**2**).[4] Within a year, **2** was in artillery powders, and by 1864 Alfred Nobel had patented the use of **1** for blasting.[5,6] The power of these new compounds, known as secondary high explosives,[*] eclipsed the old by orders of magnitude in both quantity and speed of release. The importance of this was recognized, and the field soon exploded with discoveries of new energetic materials.[7]

Black powder owed its advance in performance to an intimate mixing of oxidizing agent and fuel. Nitroglycerin and nitrocellulose had improved this combination to an atomic level. Electrophilic nitration, which had become popular in 1842,[8] made it possible to introduce the nitro group effectively. This group bore oxidized nitrogen that served as an oxidizing agent for the rest of the molecule,[9] thus enabling powerful explosions, called detonations,[*] by a fast internal redox process.

New detonable materials are still developed and most contain the nitro group.[10,11] They are organized by chemical functionality,[12] differing only at the atom to which the nitro group is attached. The following sections will provide a glimpse of their diversity.

1.1.1 Nitric Esters

Nitroglycerin and nitrocellulose both belong to the class known as nitric esters (or nitrates), in which the nitro group is connected through an oxygen atom to the remainder of the molecule. Nitric esters possess a weak O—NO_2 bond (~40 kcal/mol),[13] which heightens sensitivity to initiation and lowers thermal stability. Because of these

[*] See Appendix A, section A1.

drawbacks, few are commercially available. Exceptions are **1**, **2**, and [3-nitrooxy-2,2-bis(nitrooxymethyl)propyl] nitrate (PETN) (**3**).

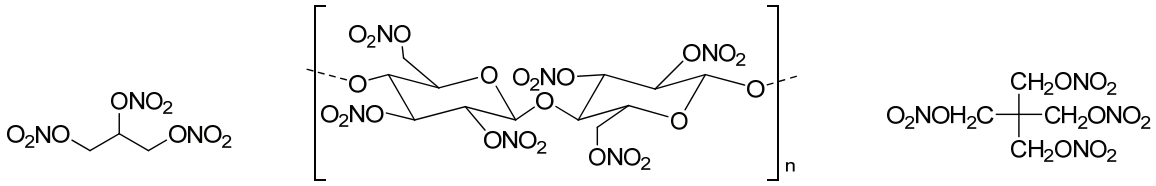

1 **2** **3**

Nitroglycerin is dangerous to handle, but can be stabilized by absorption on Kieselguhr (diatomaceous earth) to make dynamite.[14] Dissolved in cotton, **1** becomes blasting gelatin.[15] Nitrocellulose can be found today in lacquers and smokeless powder for small arms.[16] PETN is the most stable nitric ester and constitutes the bulk of detonation cord, some detonators, and the plastic explosive Semtex A, notorious for the bombing of PanAm Flight 103 in 1988.[17,18]

1.1.2 Nitroarenes

Nitroarenes are older than the nitric esters, but were applied later to warfare and mining.[19] The nitro groups in these compounds are bound to aromatic carbons. Nitroarenes have a wide range of powers and stabilities and constitute the bulk of modern arsenals.[20,21]

The oldest example is 2,4,6-trinitrophenol (picric acid) (**4**), which was first synthesized in 1771 as a yellow dye.[19] Its destructive utility was recognized in 1867, when it was adopted by the world's armies.[19] It had the drawback of corroding metal because of its acidity,[22] leading to the easy formation of picrate salts. Some of the salts are very sensitive, but others are stable enough for commerce. The ammonium salt of picric acid filled naval artillery shells from the turn of the century through World War II; 6.5 million pounds per month were consumed in 1944 alone.[23] In the civilian sector, the first whistling fireworks, which appeared around 1888, relied on potassium picrate to generate their sound.[24,25]

The most famous nitroarene, 2,4,6-trinitrotoluene (TNT) (**5**), was described initially in 1863 by Wilbrand,[26] but did not find much military application until 1901.[27] Its acidity and sensitivity were lower than those of picric acid, which made it compatible with a wider variety of substances, and in 1912 the United States replaced picric acid with TNT in all munitions.[21] To this day, TNT comprises the majority of the world's ordnance.

Anyone who has played with novelty black snake fireworks has likely come into contact with *N*-methyl-*N*,2,4,6-tetranitroaniline (tetryl) (**6**).[28] These snakes require a high energy fuel to sustain burning, and surplus tetryl from World War II Tetrytol munitions served this purpose for many years.[29] Originally isolated by Michler and Meyer in 1879,[30] tetryl is both a nitroarene and a nitramine (Section 1.1.4) and is more readily detonated than TNT.

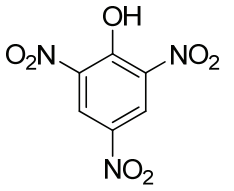

4

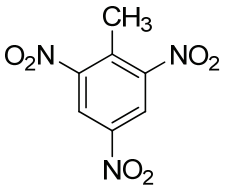

5

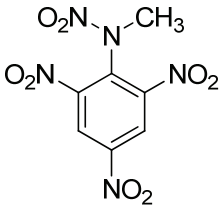

6

The most insensitive high explosive known is 1,3,5-triamino-2,4,6-trinitrobenzene (TATB) (**7**).[31] Even though it is less powerful than other nitroarenes, it is slowly replacing TNT in many devices, because only the most aggressive insult from friction, spark, or impact causes it to explode.

In 1966, the height of nitroarene performance was achieved in hexanitrobenzene (HNB) (**8**).[32,33] It exhibits the second greatest recorded detonation velocity,[†] at 9500 m/s, but has not become practical due to the dangerous precursors required for its preparation and its reactivity with moisture and light.[34]

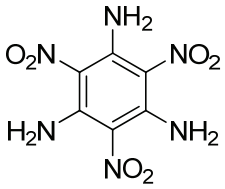

7

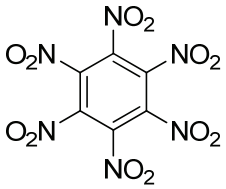

8

1.1.3 Nitroalkanes

The mid-nineteenth century saw the advent of nitroalkanes, which have a nitro group attached to an sp^3-hybridized carbon. They are more stable than nitric esters or nitramines, but are generally more toxic and difficult to create.[35,36,37,38]

Discovered in 1861, tetranitromethane (**9**) was recognized as both an energetic material and a virulent poison.[39] In the first World War, hundreds of workers died of 'TNT intoxication,' actually caused by the presence of **9** in trace quantity as a byproduct of the nitration of toluene.[40] Weapons designers shunned **9** because it was too difficult to handle, but synthetic chemists used it as a nitrating agent.[38] It is still sold as a reagent for this purpose today.

Octanitrocubane (**10**) is a modern nitroalkane which was sought for decades.[35] Although its detonation velocity did not set records as predicted, it still ranks highly.[35,41,42,43] Unfortunately, its long, difficult, low-yielding synthesis, illustratively reproduced in Scheme 1 on the next page, has precluded large-scale production.[35,44,45,43]

[†] See Appendix A, sections A1 and A2.

Scheme 1. The lengthy synthesis of **10**.

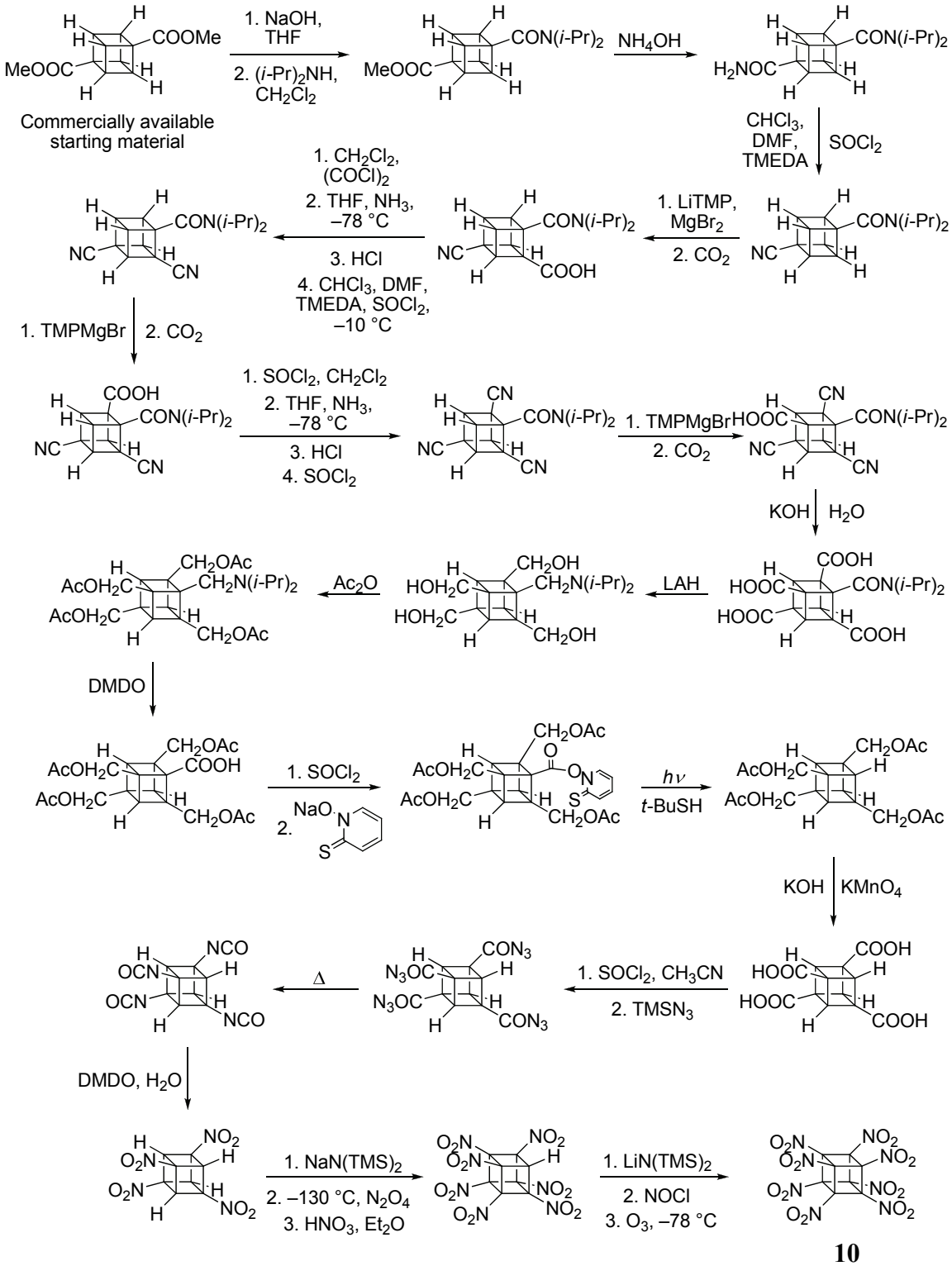

1.1.4 Nitramines

A nitro group connected to a nitrogen atom constitutes a nitramine. In general, nitramines fall between nitric esters and nitroarenes in sensitivity, and are less toxic than both.[46] Among them, 1,3,5-trinitro-1,3,5-triazinane (RDX) (**11**), 1,3,5,7-tetranitro-1,3,5,7-tetrazocane (HMX) (**12**), and 2,4,6,8,10,12-hexanitro-2,4,6,8,10,12-hexaazaisowurtzitane (CL-20) (**13**) are best known.

RDX, the main component of the famous plastic explosive C4, was patented as a medicine in 1899.[47,48] After World War I greater availability of feedstock chemicals enabled large scale manufacture, and subsequently its value in munitions was recognized.[49,50,51]

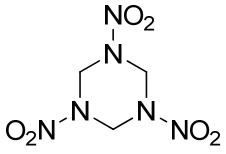

11

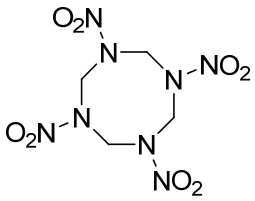

12

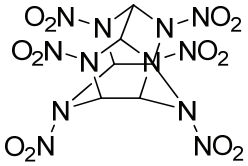

13

HMX and CL-20 are less common in formulations than RDX, but do find special application because of their excellent performance characteristics.[52,53]

1.1.5 Nitroalkenes

Nitro groups attached to alkenyl carbons give nitroalkenes, which have been the subject of recent investigations.[54,55,56,57,58,59,60] A few nitroalkenes, such as 1,1-diamino-2,2-dinitroethylene (FOX-7) (**14**),[61] have found commercial employ, but most are too reactive. As reagents, however, nitroalkenes can be good building blocks.[62] For instance, tetranitroethylene (**15**)[63,56,64] has the potential to cyclize or add to other substances. Because **15** is overoxidized,[‡] combination with an underoxidized[§] molecule can result in an energetic material.

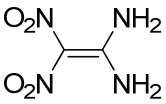

14

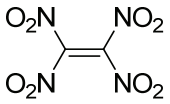

15

1.2 Nitroacetylenes

The first nitroacetylenes were not isolated until 1969,[65,66,67] making them one of the most recently discovered class of explosives. They are characterized by a nitro group attached to an *sp*-hybridized carbon. Because the nitro group is inductively withdrawing, when attached to an electron-poor acetylenic bond, it forms a reactive, powerful electron acceptor. One can take advantage of these characteristics by applying traditional

[‡] See Appendix A, section A3.

acetylene chemistry to nitroacetylenes.[68,69] For example, acetylenes can undergo oligomerization, or react with alkenes or azides to give cyclic products, including cyclopentenones,[70] benzenes,[71,72,73] cyclobutadienes,[74,75,76,77] and triazoles,[78,79,80,81] all of which could yield energetic materials when made with nitroacetylenes. Cyclic trimerization of 1-nitroethyne (nitroacetylene) (**16**) would generate 1,3,5-trinitrobenzene (TNB) (**17**) (Scheme 2), and the reaction of 1-nitro-2-(trimethylsilyl)ethyne (**18**) with (trimethylsilyl)azide has been shown to produce 4-nitro-5-(trimethylsilyl)-1,2,3-triazole (**19**) (Scheme 3).[81]

Scheme 2. Potential cyclotrimerization of **16** to **17**.

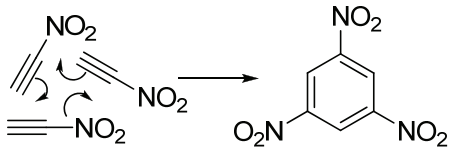

16 **17**

Scheme 3. Conversion of **18** to **19**.[81]

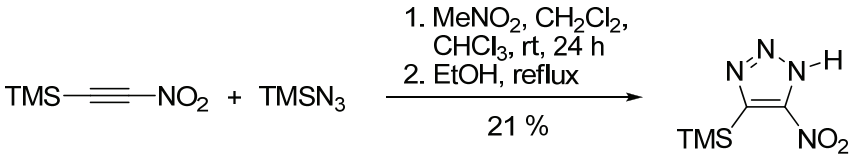

18 **19**

One could even envisage forming a polynitrocubane from the appropriate nitroacetylene, similar to the known conversion of bis(trifluoromethyl)acetylene (**20**) to octakis(trifluoromethyl)cubane (**21**) (Scheme 4, next page).[82]

The unknown dinitroacetylene (DNA) (**22**) is considered the holy grail of all nitroacetylenes due to its perfect oxygen balance.[§,85,86,87,88,89,90,84]

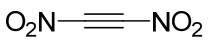

22

The reactivity of two nitro groups attached to a triple bond will likely make pure DNA impractical as an explosive, but it has potential as a versatile monomer for oligomerization.[85,91,92,93] Any oligomers of DNA, such as **8** and **10**, will also have perfect oxygen balance.[91] Such compounds represent the pinnacle of explosive power and are the culmination of the journey began by Sobrero, Schönbein, and Böttger in 1846.

[§] See Appendix A, section A2.

Scheme 4. Preparation of **21** from **20**.[83,82]

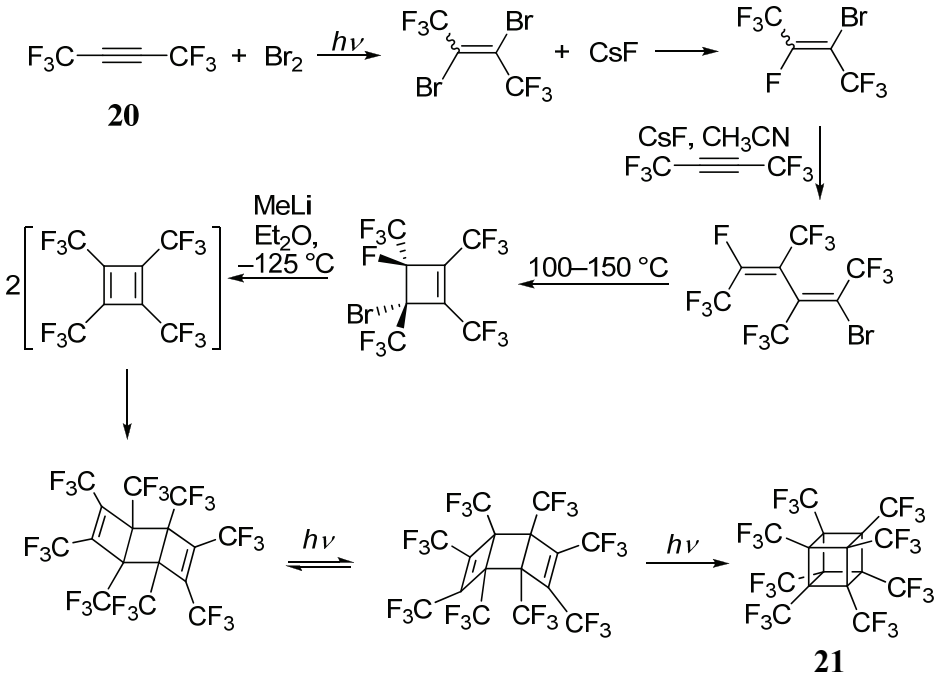

1.3 Goals

The goals of this work were fourfold: 1. the production of free nitroacetylenes and their complete characterization; 2. the stabilization of these alkynes as transition metal complexes; 3. the synthesis of a complex of DNA; and 4. the exploration of the chemistry of these compounds. The following sections elaborate on these aims.

1.3.1 Production of Nitroacetylenes

Few nitroacetylenes of synthetic value are known and most have not been adequately characterized. Conflicting procedures and little data were reported for **18**, and **16** was difficult to prepare, but these acetylenes held the most promise for further transformations. The first objective of this work was therefore to create **16** and **18** by literature methods, to maximize yields, and to better characterize **18**.

1.3.2 Stabilization of Nitroacetylenes as Metal Complexes

Working with nitroacetylenes is difficult because of their reactivity and thermal instability. One of the main foci of this study was to obtain nitroacetylenes in a stable form that could either store or directly replace the free acetylene in synthetic transformations. Transition metals are known to stabilize reactive alkynes through a combination of back donation of electrons from filled d_π orbitals on the metal to empty π^* orbitals of the acetylene and forward donation from the π bonds of the acetylene into the empty d_σ orbital on the metal (Figure 1).[94]

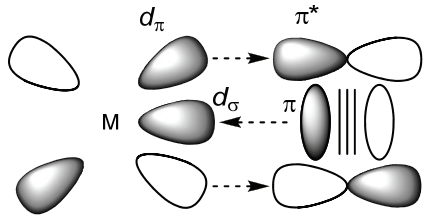

Figure 1. Bonding between a transition metal fragment and acetylene.

The selection of the metal was based on three criteria: compatibility with the nitro group, mild conditions for removal, and ready availability at reasonable cost. On this basis, cobalt was chosen as the stabilizing auxiliary. Specifically, octacarbonyldicobalt (**23**) has been shown to decarbonylate and ligate reactive alkynes bearing electron withdrawing groups;[95,96] the metal in such complexes can be removed with mild oxidizing agents such as iron(III);[97] and the starting cobalt carbonyl is available commercially. These complexes enjoy the additional benefits of being air-tolerant and functioning as synthons for further reactions.[95] Consequently, methods were developed to synthesize hexacarbonyldicobalt stabilized **16** and **18**.

1.3.3 Preparation of Hexacarbonyldicobalt Dinitroacetylene

Despite numerous attempts since at least 1901,[88] DNA remains unknown. Instead of arriving at DNA through traditional methods, an objective of this work was to obtain it from a hexacarbonyldicobalt complex. Two approaches to [μ-1,2-dinitroethyne-1,2-diyl]bis(tricarbonylcobalt)(*Co–Co*) (**24**) were envisaged. The first involved the direct trapping of DNA, if it could be generated *in situ*. The second entailed functional group manipulation of an appropriately substituted alkyne complex to introduce one or both nitro substituents.

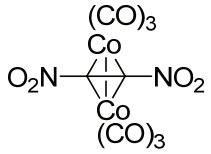

24

Both methods were investigated, with emphasis on the latter, an area that was largely unexplored.[98,99,100]

1.3.4 Nitroacetylene Complexes as Synthons

In addition to constituting novel molecules, the physical and structural properties of which were of intrinsic interest, it was hoped that hexacarbonyldicobalt(nitroalkyne) complexes would provide air and thermally stable synthons for a variety of potential transformations.[97] One such avenue was the Pauson-Khand reaction, which transforms hexacarbonyldicobalt alkyne complexes in the presence of alkenes into cyclopentenones (Scheme 5).[101]

Scheme 5. Pauson-Khand reaction.

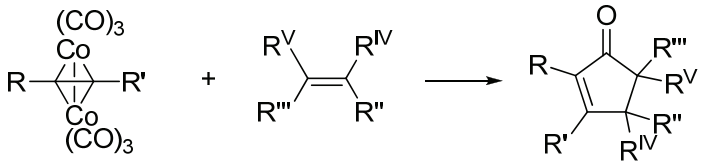

Such reactivity was unexplored for nitroalkynes.

A second possibility was the cobalt-mediated [2 + 2 + 2] co-cyclization of the ligand with other alkynes to furnish nitroarenes,[67] the regioselectivity of which was of additional interest (Scheme 6).[102,103]

Scheme 6. Cobalt-mediated [2 + 2 + 2] cycloaddition.

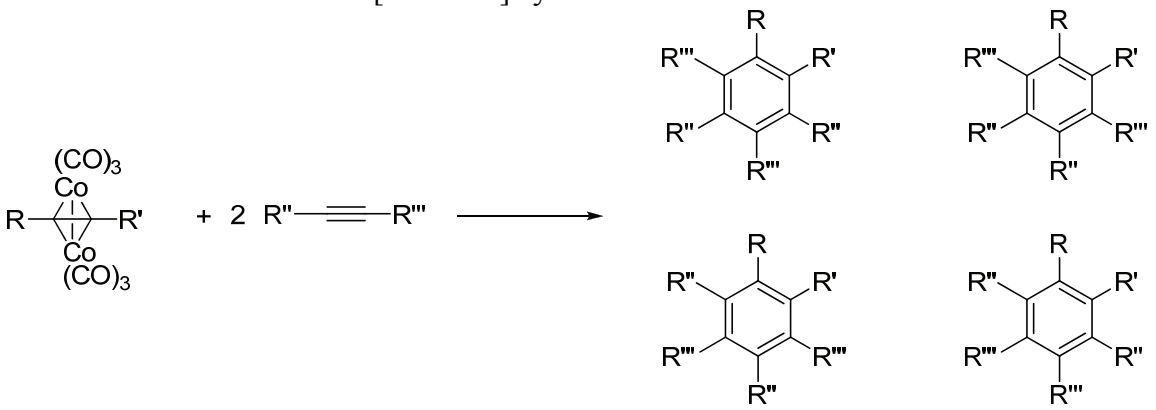

In addition to the above options, it was hoped that, if nitroalkyne complexes could be made, they would prove sufficiently stable to allow for functional group transformations at the ligand, in turn revealing other metal- stabilized fragments of novel composition. Particularly versatile by virtue of its trimethylsilyl substituent, [μ-1-nitro-2-(trimethylsilyl)ethyne-1,2-diyl]bis(tricarbonylcobalt)(*Co–Co*) (**25**) appeared to have potential in electrophilic substitution chemistry. Similarly, [μ-1-nitroethyne-1,2-diyl]bis(tricarbonylcobalt)(*Co–Co*) (**26**) was considered a valuable starting material if it could be deprotonated and exploited as a nucleophile.

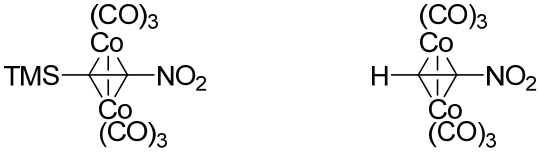

25 **26**

Chapter 2. Preparation and Properties of Nitroacetylenes

2.1 Introduction

The history of nitroacetylenes spans over a hundred years, but is marred by their poor characterization, in part as a result of their reactivity, difficult preparation, and often-cumbersome purification. Inductive and resonance electron withdrawing substituents increase alkyne reactivity.[104] The nitro group has an electronegativity of 3.70, surpassed only by fluorine,[105] and, when attached to an alkynyl *sp*-hybridized carbon with an electronegativity of 3.1,[**106] produces a highly reactive moiety. Electron deficiency is spread over both alkyne carbons through conjugation, shown by the canonical resonance structures in Figure 2.

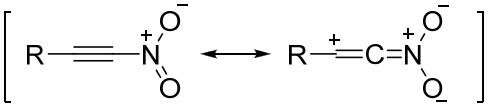

Figure 2. Resonance structures of nitroalkynes.

This reactivity is likely the reason why only fifteen nitroacetylenes have been generated: **16**,[107] **18**,[108,109,110] 3,3-dimethyl-1-nitrobut-1-yne (*t*-butylnitroacetylene) (**27**),[65,111,104,112] 3-methyl-1-nitrobut-1-yne (*iso*-propylnitroacetylene) (**28**),[111,104] 1-nitropent-1-yne (propylnitroacetylene) (**29**),[104] 1-nitro-2-tris(*iso*-propylsilyl)ethyne (TIPSnitroacetylene) (**30**),[109,110] 1-nitro-2-phenylethyne (phenylnitroacetylene) (**31**),[104,90,114] 1-nitroprop-1-yne (methylnitroacetylene) (**32**),[109,110] 1-nitrohex-1-yne (butylnitroacetylene) (**33**),[111,104] 1-(dimethyl-*iso*-propylsilyl)-2-nitroethyne (**34**),[109,110] 1-(dimethyl-*tert*-butylsilyl)-2-nitroethyne (**35**),[109,110] 1-iodo-2-nitroacetylene (**36**, iodonitroacetylene),[115] 1-nitro-2-[*p*-(trifluoromethyl)phenyl]acetylene (**37**),[115] 1-bromo-2-nitroacetylene (bromonitroacetylene) (**38**),[115] and 1-nitro-2-(*p*-nitrophenyl)acetylene (**39**).[115]

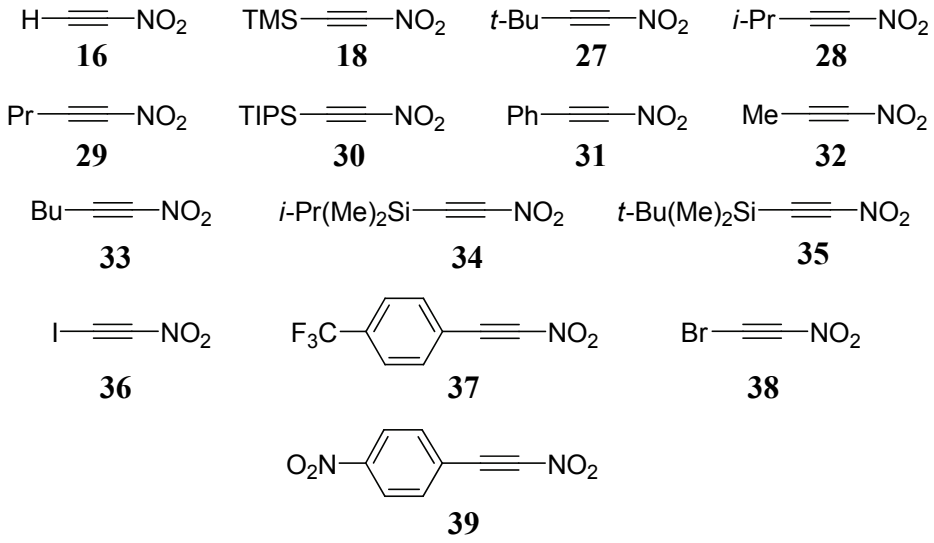

[**] Compare to 2.5 for sp^3 and 2.8 for sp^2.

Of these, **16**,[107] **18**,[108,109] **27**,[65] **28**,[111] **30**,[109] **31**,[114] **32**,[109] **33**,[111] **34**,[109] and **35**[109] have been described in the refereed literature, and only **18**,[108,109] **27**,[65,104,112] **28**,[111,104] **29**,[104] **30**,[109,110] **34**,[109,110] and **35**[109,110] have actually been isolated.[65,116,117,118,119,114,108,109,107] No general synthetic pathway exists; thus, each nitroacetylene presents its own challenges. The following comprehensive overview of properties, histories, and reactions of known nitroacetylenes precedes an account of this investigation in this area.

2.2 General Properties of Nitroacetylenes

Nitroacetylenes are light yellow or light yellow-green, lachrymatory, volatile, thermally unstable liquids.[104,65,117,118,119,114] Their stability increases with increasing steric bulk of substituents on the other terminus, which hinders nucleophilic attack.[104,81] When such substituents are silyl-based, additional electronic stabilization is observed.[120]

At –3 °C, **27** freezes into colorless crystals, thus constituting the only nitroalkyne with a recorded melting point.[65,104] The boiling point of **27** is 55 °C at 15 torr,[65,104] corresponding to a hypothetical value of 167 °C at atmospheric pressure, unattainable because of decomposition. Zhang et al. estimated the boiling point of **16** to be between 60 and 100 °C at atmospheric pressure.[107] Compounds **27**, **28**, and **29** all distill between 0 and 10 °C at 0.1 torr.[104] Jäger, in his PhD thesis, observed that **27** underwent reactions in nonpolar solution at 110–120 °C without polymerization, and aggressive heating, contact with a glowing hot iron nail, and impact all failed to cause detonation.[104,65]

Nitroacetylenes have half-lives that correlate directly with their steric bulk. At room temperature, **27** has a half-life of 2–3 days, **28** about 10 hours, and **29** about 1–2 hours.[104] In toluene solution at 80–85 °C, this value for **27** decreases to 30 minutes.[104] Compound **27** passes through a GC unchanged at 107 °C when measured against a standard, compared to 50–70 % survival of **28** at 104 °C and only 10–20 % of **29** at the same temperature.[104] Schmitt et al. claimed that **30** was the most stable nitroalkyne yet to be discovered, based only on the qualitative observation that it did not decompose upon standing in neat form at room temperature for several hours.[81] However, **27** appears to behave similarly.[104]

In 1992, Schmitt et al. measured the gas phase acidity of **16**, deduced by generating nitroacetylide anion (**16a**) inside a mass spectrometer by reaction of **30** with fluoride ion and subsequent deprotonation of acids of known acidity.[69]

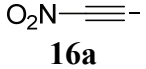

16a

A value of $\Delta H°_{acid}$ = 354 ± 4 kcal/mol was determined, more acidic than acetylene, and about equal to nitromethane (356.4 kcal/mol), trifluoromethylacetylene (355.2 kcal/mol), and cyanoacetylene (350.8 kcal/mol).[69] The electron affinity of the nitroacetylide ion was found to be greater than 2.55 eV.[69]

Nitroacetylenes have been characterized most extensively by IR spectroscopy (Table 1, next page). Data for some molecules, such as **18**, have been collected both neat and in the gas phase, illustrating the difference between conditions. One common characteristic of all solvated or liquid phase nitroacetylene IR spectra is the C–N stretching vibration that appears markedly lower than nitroalkanes and nitroaromatics, at

Table 1. IR data of nitroacetylenes.

Compound	Nitroacetylene	$\tilde{\nu}_{C\equiv C}$ (cm^{-1})	$\tilde{\nu}_{NO2}$ asym./sym. (cm^{-1})	Other (cm^{-1})	Ref.
16	H—≡—NO_2	2132			107
18	TMS—≡—NO_2	2250[a] 2167[124]	1520/1348[a,108] (1531/ N.A.)[a,109] 1551,1514/1339[124]	1260;[b] 860[a,108] (1265, 895, 865, 795)[a,109] 1256,[b] 960, 851, 803, 763; 729[f,124]	108,109,124
27	*t*-Bu—≡—NO_2	2231 s 2270 w	1513–1512/1352[104] (1512/1368, 1350)[65]	2981, 2939, 2913, 2876, 2835;[c] 1481, 1468, 1388, 1370;[d] 1254, 1205;[e] 935, 844, 737; 730.5;[f] 530	104,65
28	*i*-Pr—≡—NO_2	2245 s 2210 w	1510/1345	2980, 2940 sh, 2880 sh;[g] 1466, 1388;[d] 878, 780;[h] 730[f]	104
29	Pr—≡—NO_2	2260 s, 2200 sh	1515/1358	2980, 2960, 2890;[g] 2450 vw; 1465, 1425 sh, 1389 sh;[d] 835, 826, 770; 730[f]	104
30	TIPS—≡—NO_2	2150	1520/1325	950, 880, 680	109[a]
31[i]	Ph—≡—NO_2	2240 w[104,125] 2219[a,90]	1542/1353[a,90] 1535/1355[114] 1300/560[125]	1701,1249, 701[a,90] 3070[g,125]	104[i]
32	Me—≡—NO_2	2264	1543, 1526/1342	822, 833	109[a]
33	Bu—≡—NO_2	2265 s			104
34	*i*-Pr$(Me)_2$Si—≡—NO_2	2160	1533/1325	1251, 880, 810	109[a]
35	*t*-Bu$(Me)_2$Si—≡—NO_2	2175	1531/1327	1261, 961, 829, 783	109[a]

[a]Gas phase measurement. [b]Si–C symmetric deformation. [c]C–H stretch of ^{t}Bu. [d]C–H deformation. [e]C–H vibration of ^{t}Bu. [f]C–N vibration. [g]C–H stretching. [h]C–H vibration of ^{i}Pr. [i]See Section 2.3 for discussion of this compound.

Note: Where conflicting data on the same compound is reported, both are provided and marked with their respective references.

730 cm^{-1}.[121] The nitro group shows a characteristic asymmetric stretching frequency around 1535–1510 cm^{-1}, with its symmetric counterpart at 1355–1330 cm^{-1}.[122,121] In many nitroacetylenes, the triple bond absorption is split into one strong and one weak band, about 35–60 wave numbers apart, a phenomenon sometimes seen in acetylenes bearing substituents of first row elements.[104] In his thesis, Jäger predicted that this band would be weaker, unsplit, and shifted to lower wave numbers for substituents of second or third row elements.[104] Indeed, Schmitt et al. confirmed this prediction by observing only a single peak for silyl-substituted nitroacetylenes.[108,109] Monoalkylated acetylenes typically exhibit $\tilde{\nu}_{C\equiv C}$ = 2140–2100 cm^{-1} and internal alkynes at 2260–2210 cm^{-1}.[123] The nitro group causes a shift to higher wave numbers: that of **16** appears at 2132 cm^{-1} and those of the alkylnitroalkynes range from 2265 to 2231 cm^{-1}.[65,109]

The only recorded UV-Vis spectra of nitroacetylenes appear in Jäger's doctoral thesis.[104] They are characterized by π–π* absorption between λ_{max} = 235 and 239 nm with a log ε of ~ 3.9 and a second, weaker absorption band (sh) at λ_{max} = 290 nm (log ε = 1.5–2.7),[104] which was ascribed to an *n*–π* transition (Table 2).[104]

Table 2. UV-Vis data for **27**, **28,** and **29**.[104]

Compound	Nitroacetylene	Wavelength (nm)	log ε
27	*t*-Bu—≡—NO_2	238	3.9
		290	1.5
28	*i*-Pr—≡—NO_2	239	3.81
		290	2.2
29	Pr—≡—NO_2	235	3.88
		290	2.7

Comparison of these data with those of the *trans*-nitroalkene analogs revealed typical bathochromic shifts of the π→π* transition of the triple bond of ~ 10 nm, and the *n*→π* transition[113] ~ 20 nm, both with slightly smaller ε values.[104]

The mass spectra of several silylnitroalkynes and **31** have been recorded.[108,109,114,90]

Ph—≡—NO_2

31

While the molecular ion is not always visible for the former, a large (M^+ – alkyl) peak can be observed, a consequence of the easy fragmentation of the trialkylsilyl group.[126] The spectra share the well-defined loss of NO_2, but not of oxygen, as sometimes seen with more stable nitro compounds, such as nitroarenes.[108,109,126] Loss of NO followed by elimination of CO was observed by Kashin et al. in the case of **31**,[114,126] but Woltermann's reinvestigation of this compound did not detect the second process.[90] Loss of NO requires prior rearrangement to the nitrite.[126] Since no other nitroacetylenes fragment in this manner, this process appears unique for **31**, if indeed it was not misassigned.

Proton NMR data are published for only five nitroalkynes: **16**, **27**, **28**, **29**, and **31**.[107,65,104,125] The ^1H NMR spectrum of **27** in CCl_4 contains a characteristic *t*-butyl

singlet at δ 1.34 ppm, relatively deshielded compared to other *t*-butyl substituted acetylenes. The same relative deshielding is found in the proton spectra of **28** [δ 1.30 (6 H, d, CH_3), 2.8 ppm (1 H septet, CH)] and **29** [δ 0.85–1.25 (3 H, m, CH_3), 1.35–1.95 (2 H, m, CH_2), 2.3–2.6 ppm (2 H, t, propargylic CH_2)].[104] In **16**, a diagnostic triplet appears at δ 3.37 ppm ($^2J_{NH}$ = 1.6 Hz), again downfield relative to other terminal alkynyl hydrogens.[107,65] This triplet is due to coupling of the proton to the ^{14}N nucleus through the acetylenic bond, a coupling usually too broad to be observed because of the electric quadrupole moment of ^{14}N.[127] However, if the electric field gradient is symmetric about the ^{14}N nucleus (which occurs when atoms with similar electronegativities are attached to the nitrogen nucleus in a symmetric fashion), the quadrupole coupling constant is near zero and the relaxation time becomes long enough to detect the ^{14}N signal.[127,128] In **16**, the *sp*-hybridized acetylenic carbon bound to the nitro group matches the electronegativity of the oxygen atoms, thus allowing observation of ^1H–^{14}N coupling as a triplet in the proton spectrum.[107]

In addition to long range ^1H–^{14}N coupling, ^{13}C–^{14}N coupling can also be seen in the ^{13}C NMR spectrum of **16**, as evidenced by the triplet at δ 82.3 ppm with J_{CN} = 32.2 Hz.[107] The terminal carbon appears as a triplet at δ 55.6 ppm and exhibits a long-range ^{13}C–^{14}N coupling of $^2J_{CN}$ = 4.5 Hz. This coupling is indicative of the nitroacetylene bond and is present in the ^{13}C NMR spectra of all nitroacetylenes.

Because most nitroacetylenes are liquids, no X-ray crystal structures are known, including **27**, for which crystallization at low temperature was reported.[104]

2.3 The Synthesis of Nitroacetylenes

Prior efforts to generate nitroacetylenes, both successful and unsuccessful, are presented in this section. The unsuccessful direct nitrations and eliminations appear first, followed by the various successful methods, each ordered chronologically.

2.3.1 Unsuccessful Strategies

A first attempt to make a nitroalkyne by direct nitration of acetylene (**41**) was made over a century ago by Baschieri, who used a traditional nitrating agent, fuming nitric acid.[88] The results were inconclusive, but later investigators found 3-isoxazolecarboxylic acid (**42**) and **9**, in addition to unidentified explosive byproducts (Scheme 7).[129,130,131,132]

Scheme 7. Reaction of nitric acid with acetylene.

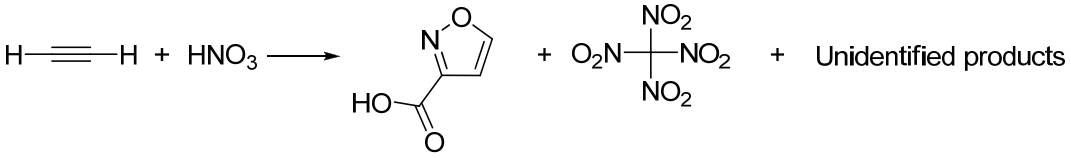

41 **42** **9**

In 1903, Wieland obtained a small amount of yellow crystals from the reaction of cinnamaldehyde with nitric oxide, exhibiting a melting point of 143 °C and a molecular

formula of $C_8H_4N_2O_4$.[133] Among the structures proposed was **39**, a suggestion that was not corroborated due to lack of material.[133]

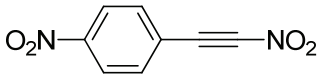

39

This molecule resurfaced in 1960, when Novikov et al. claimed its formation in the reaction of 1-nitro-2-phenylethylene (**42**) with N_2O_4 (Scheme 8).[134]

Scheme 8. Proposed preparation of **39**.[134]

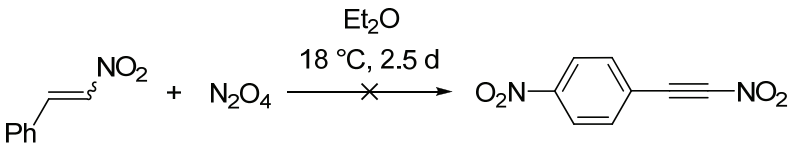

42 **39**

Yellow crystals were obtained in low yield (2.1 %), whose elemental analysis and melting point matched those of Wieland's compound. In addition, the composition was confirmed by the molecular weight analysis. Kerber and Chick repeated this reaction in 1967, but showed that the structural assignment of the product as being **39** was incorrect.[104] In 1969, Jäger and coworkers put the issue to rest by identifying the product as 3-nitro-4*H*-1,2-benzoxazin-4-one (**43**).[66,104]

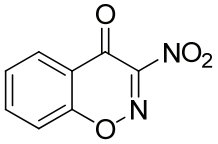

43

In 1968, Robson, Tedder, and Woodcock obtained nitrosoacetylenes by action of nitrosonium chloride on alkynyl mercury(II) or Grignard reagents (Scheme 9).[135]

Scheme 9. Nitrosoacetylene formation.

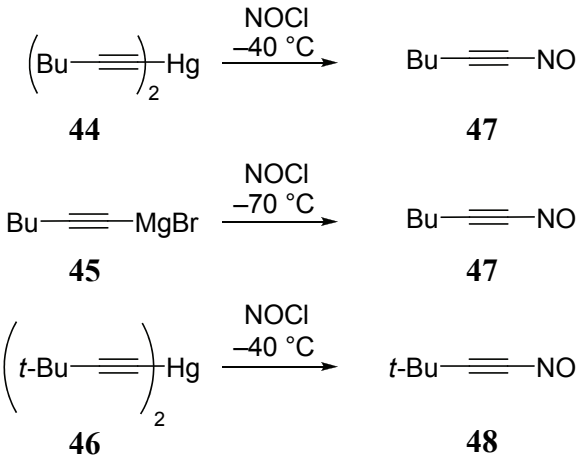

Through a private communication with Tedder, Jäger learned that they had extended their methodology to an analogous reaction with nitronium chloride in order to achieve nitroalkynes, but were unsuccessful (Scheme 10).[104]

Scheme 10. Nitronium chloride nitrations of Tedder.[135]

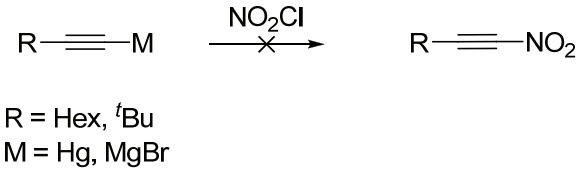

In this same communication, Tedder also stated that they had attempted to oxidize nitrosoacetylenes unsuccessfully, but no details were provided.[104] Only a few years later, Motte et al. and Jäger et al. would oxidize nitrosoacetylenes to the corresponding nitroacetylenes.[116,111]

Woltermann treated a host of phenylacetylides with various nitrating agents in an attempt to generate **31** (Scheme 11).[90,136]

Scheme 11. Failed nitration of various phenylacetylides.

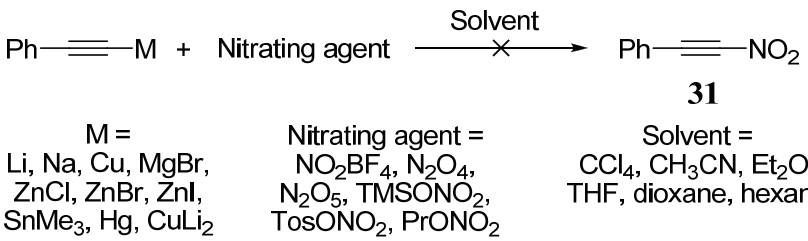

Schmitt et al. had earlier alluded to the fact that lithium acetylides could not be nitrated with nitronium salts without offering any experimental detail.[109] None of Woltermann's

reactions resulted in nitroacetylenes, but a study was made of the reaction between phenyl metal acetylides and N_2O_4 that showed an interesting oxidative coupling (see Section 2.5).

Concurrent with direct nitrations, eliminations began to be explored as routes to nitroacetylenes. In 1930, Loevenich et al. treated (*Z*)-1-bromo-1-nitro-but-1-ene (**49**) with dimethylamine and obtained a thin, pungent, red oil, which they claimed to be 1-nitro-but-1-yne (**50**, Scheme 12).[137]

Scheme 12. Proposed formation of **50**.[137]

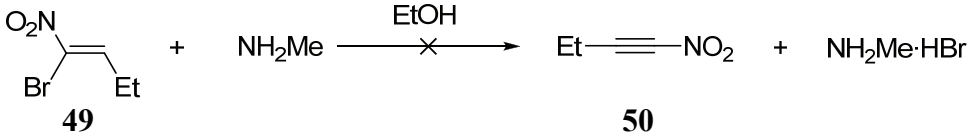

49 **50**

An analogous dehydrobromination employing diethylamine and (*Z*)-1-bromo-1-nitropent-1-ene (**51**) gave a similar material, assigned structure **29** (Scheme 13).[137]

Scheme 13. Proposed production of **29**.

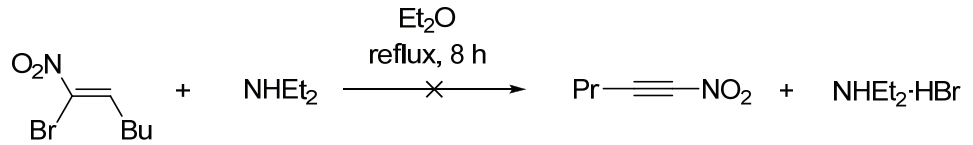

51 **29**

These oils exploded upon heating or attempted vacuum distillation, reacted instantly with Baeyer's reagent (alkaline potassium permanganate), and decolorized bromine solution upon heating.[137] The positive Baeyer test proved unsaturation, and the relatively forcing conditions required to decolorize a bromine solution suggested the presence of a deactivated double or triple bond. Nitrogen analysis of the compound purported as **50** showed 13.51 % nitrogen, less than the expected value of 14.14 %. Similarly, the corresponding values for proposed **29** were 11.46 % and 12.39 %.[137] On standing, these materials turned into viscous, resinous substances, which Loevenich et al. attributed to polymerization.[137] That same year, Loevenich and another coworker produced an oil from (*Z*)-1-bromo-1-nitro-2-phenylethene (**52**) by the same methodology, which they characterized as **31** (Scheme 14).[138]

Scheme 14. Desired preparation of **31**.

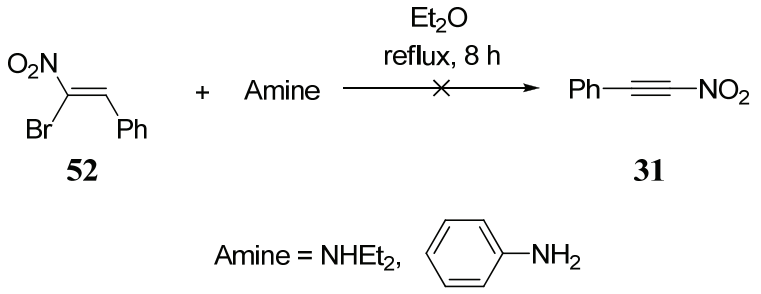

As for purported **29** and **31**, this material exploded when heated, reacted with Baeyer's reagent, was deficient in nitrogen by quantitative analysis, and showed a close molecular weight, but did not decolorize bromine solution.[138] Decades later, analytical instrumentation allowed for a more thorough investigation of this reaction, and Jäger reproduced Loevenich's results, however found that only 50 % of the theoretical amount of dimethylammonium bromide was generated. Acetylenic IR bands were absent in the reaction mixture, and NMR analysis showed only starting material.[104] Given this evidence and Jäger's study of amine addition to nitroacetylenes (Section 2.5), it is reasonable to assume that any nitroalkynes that may have formed in solution would not have survived the reaction conditions and that Loevenich's structural assignments were erroneous.

Not deterred by this failure, Jäger tried forcing elimination from a mixture of both isomers of **52** with methanolic potassium hydroxide and anhydrous sodium methoxide, but found only the addition products (Scheme 15), suggesting that nucleophilic addition was preferred over dehydrobromination.[104]

Scheme 15. Nucleophilic addition to **52**.[104]

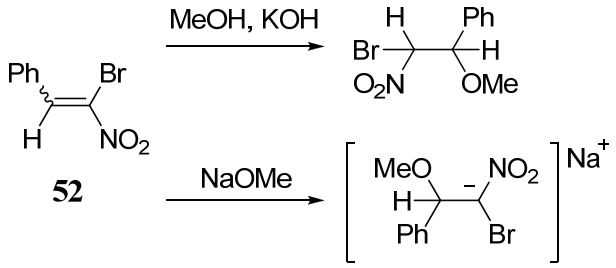

Jäger's thesis makes interesting reading, because, in addition to searching the literature for references to nitroacetylenes, he contacted many authors whose pursuits of nitroacetylenes were unpublished. He learned that, in 1965, Viehe and Reinstein ventured unsuccessfully to dehydrohalogenate 1-bromo-3,3-dimethyl-1-nitrobutene (**53**).[104] The alkene was passed over potassium hydroxide in the gas phase under vacuum at 130 °C (Scheme 16), a method that previously yielded base-sensitive fluoroacetylenes.[139]

Scheme 16. Unsuccessful dehydrohalogenation of **53**.

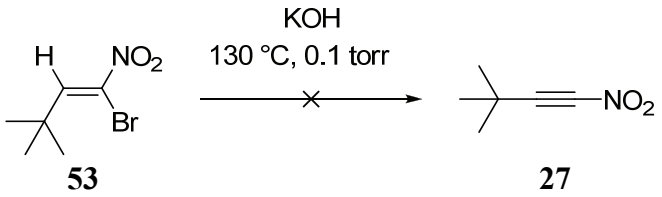

53 **27**

Notwithstanding this lack of success, the investigation served as the basis for elimination experiments by Gompper, which focused on dehydrobromination of 1-bromo-1-nitro-2-(N,N-dimethyl)aminoethene (**54**) to 2-(N,N-dimethylamino)-1-nitroacetylene (**55**) (Scheme 17).[104]

Scheme 17. Desired preparation of **55**.

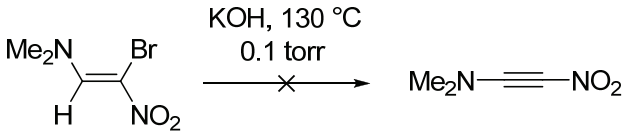

54 **55**

Compound **55** was mentioned the next year in a paper by Gais et al. on 'push-pull' acetylenic systems.[140] The precursor **54** is described in detail and **55** included in a general synthetic scheme (reproduced in Scheme 18), but the experimental makes no reference to it.[140]

Scheme 18. General method of Gais et al. for ynamine production.[140]

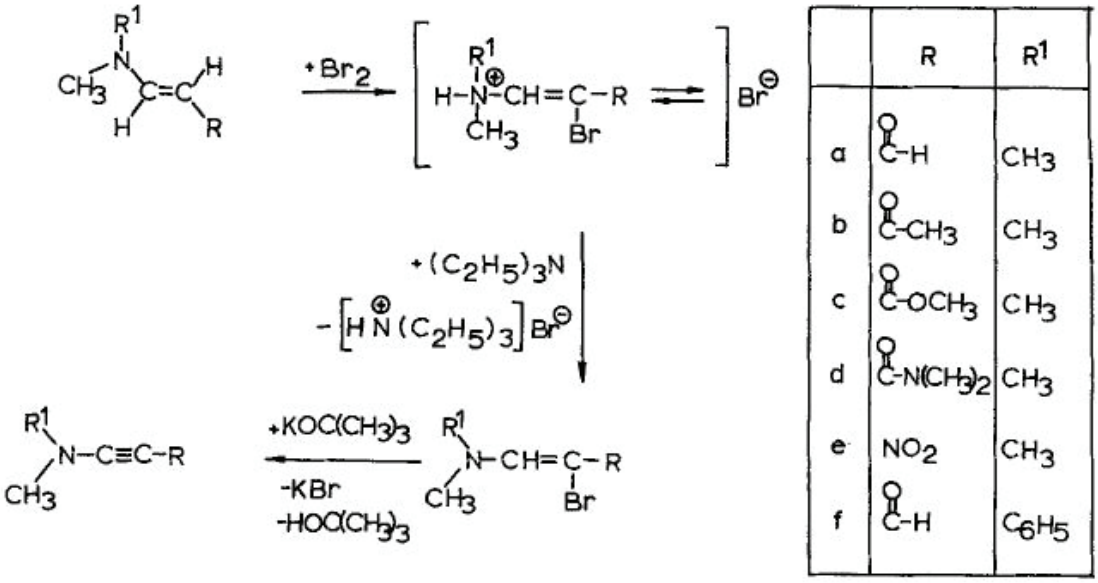

When Jäger repeated Viehe and Reinstein's attempted gas phase elimination of both isomers of **53**, he obtained only pivalic acid and unidentified products.[104] Because the same conditions later yielded nitroacetylenes from 1-nitro-2-haloalkenes, he concluded that nucleophilic addition was favored over elimination in the case of the 1-bromo-1-nitroalkenes and attributed this to the diminished acidity of their protons, compared to those of the 2-halo-1-nitro isomers.

Although successful in the gas phase, when hydrodehalogenation of both isomers of 2-chloro-1-nitro-2-phenylethene (**56**) and 2-iodo-1-nitro-2-phenylethene (**57**), respectively, was attempted by Jäger using trimethylamine, potassium *t*-butoxide, sodium acetate, or silver oxide in solution, acetylenic bands failed to appear in the IR spectrum (Scheme 19).[104]

Scheme 19. Failed eliminations from 1-nitro-2-haloethenes.[104]

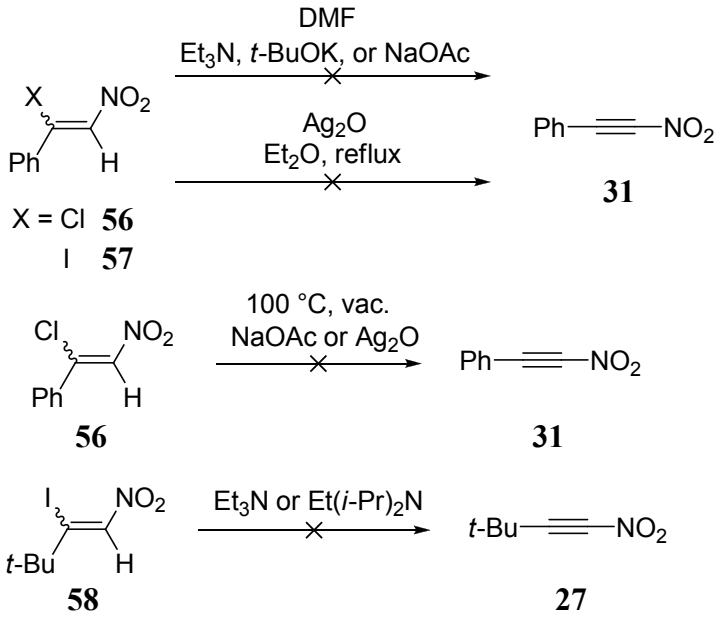

No reaction occurred when **56** was vacuum distilled from sodium acetate or silver oxide at 100 °C. Even the starting material that eventually produced **27** by another method, 3,3-dimethyl-2-iodo-1-nitrobutene (**58**), showed only a trace of an alkyne band in the IR spectrum when reacted in solution with trimethylamine or (di-*iso*-propyl)ethylamine.[104] These results, summarized in Scheme 19, are not surprising when viewed in light of our current knowledge of the rapid reaction of nitroacetylenes with nucleophiles.

Dewar pursued the dehydrobromination of the new (*E*)-1-bromo-1-nitro-2-trifluoromethylethene (**59**) in 1983,[86] which resulted in a red oil similar to that obtained by Loevenich et al. (Scheme 20).[137,138]

Scheme 20. Elimination envisaged by Dewar.[86]

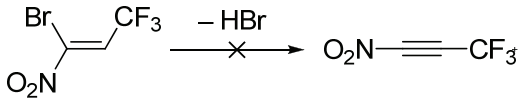

59 **60**

Unfortunately, this report lacks experimental details, so no further information is available.

Woltermann applied the addition-elimination that generated substituted acetylenes from **61**[141] to nitroalkyne synthesis in 1996 (Scheme 21).[90]

Scheme 21. Addition-elimination mechanism of **61** with nucleophiles.

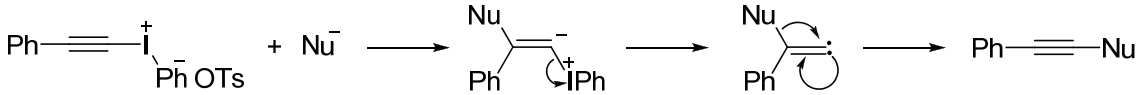

61

When the nucleophile was sodium nitrite, only benzonitrile and carbon dioxide resulted. There was no evidence of nitro- or nitrosoalkynes in solution, and no intermediates were trapped.[90]

2.3.2 Successful Strategies

The first reproducible synthesis of a definitively-characterized nitroacetylene came in 1969, when Jäger and co-workers prepared **27** through a gas-phase hydrodehalogenation of a mixture of the *E* and *Z* isomers of **58** (94 % yield in the 1969 paper, 96 % yield in Jäger's 1970 thesis) (Scheme 22).[65,104]

Scheme 22. Preparation of **27**.

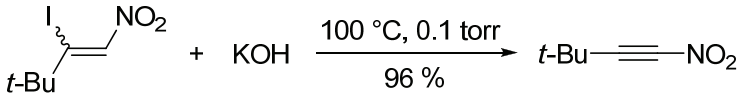

58 **27**

A year later, the effort that went into this synthesis became apparent in Jäger's doctoral thesis, which details his experiments with **27**, **28**, **29**, **31**, and **33**.[104] Because elimination reactions had not afforded nitroacetylenes in solution, he performed his reactions in the gas phase with heterogeneous catalyst, a procedure that previously rendered access to base- and polymerization-sensitive alkynes.[139] Conditions had to be optimized since only a narrow window existed for formation of each nitroacetylene. Higher reaction temperatures favored elimination, but also lowered yields through decomposition, and the distillation rate had to be adjusted to avoid co-distillation of starting material on the one hand, or decomposition of product on the hot potassium hydroxide on the other. Of the

new nitroalkynes generated, **27**, **28**, **29**, **31**, and **33**, the first three were isolated and well characterized (Scheme 23).

Scheme 23. Gas-phase syntheses of various nitroacetylenes.[104]

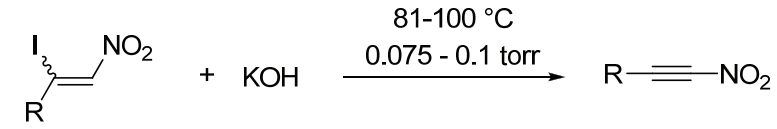

R = Ph	**57**	R = Ph	**31**
^{t}Bu	**58**	^{t}Bu	**27**
^{i}Pr	**62**	^{i}Pr	**28**
Pr	**63**	Pr	**29**
Bu	**64**	Bu	**33**

Jäger noted that greater steric bulk of the substituents led to greater stability. Compound **27** was the most stable, showing no decomposition when formed at 100 °C. The less bulky **28** and **29** required lower reaction temperatures for their generation to avoid complete decomposition, some of which was noted by coloration of the potassium hydroxide. The butyl and phenyl derivatives were formed in satisfactory yield, but were not volatile enough to be separated from the starting materials. The details of the preparation of **27**–**29** are provided in Table 3.

Table 3. Conditions for nitroalkyne formation.[104]

Compound	Structure	*t* (°C)	P (torr)	Dist'n rate (g/h)	Yield (%)
27	*t*-Bu—≡—NO_2	100	0.1	1	96
28	*i*-Pr—≡—NO_2	86–88	0.075	0.5	74
29	Pr—≡—NO_2	81–83	0.075	0.5	28

Jäger's eliminations remained the only ones to successfully afford nitroalkynes until almost thirty-six years later when Eaton et al. made several new nitroacetylenes in this way, including **36**, **37**, **38**, and **39**.[115]

36 **37** **38** **39**

A general reaction scheme of their approach is provided below (Scheme 24).[115] In addition to these new nitroacetylenes, their method also produced the known **29**[104] and **32**.[109,115]

Scheme 24. Eaton's preparation of nitroacetylenes from nitroalkenes.[115]

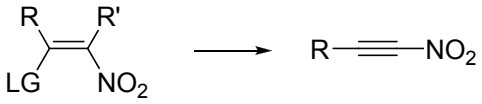

LG = leaving group

R =	Pr	**29**
	Me	**32**
	I	**36**
	p-CF_3Ph	**37**
	Br	**38**
	p-NO_2Ph	**39**

Although **36**–**39** could not be isolated, **36** and **37** were directly observed by ^{13}C NMR, in which they exhibited the diagnostic ^{13}C–^{14}N coupling, and all could be identified as their Diels-Alder adducts to cyclopentadiene.

In 1975 Motte et al. and Jäger et al. formed nitroacetylenes from alkynes for the first time by oxidizing **48** to **27** with either hydrogen peroxide or peracetic acid, in up to 40 % yield (Scheme 25).[116,111]

Scheme 25. Oxidation of **48** to **27**.

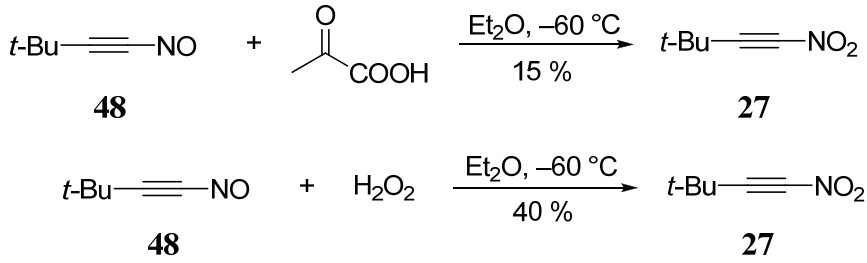

The nitrosoacetylene was made by the action of N_2O_4 on 3,3-dimethyl-1-(trimethylstannyl)butyne (**65**) (Scheme 26).

Scheme 26. Preparation of **48**.

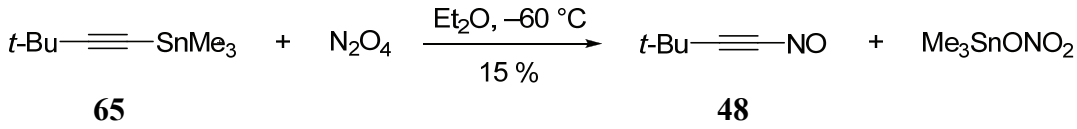

This reaction required low temperatures due to facile rearrangement of nitrosoacetylenes to nitriles above –40 °C,[135,116] a fact Woltermann overlooked while studying the reaction of N_2O_4 with both 2-phenyl-1-(trimethylstannyl)ethyne (**66**) and mercury(II) phenylacetylide (**67**) in search of 2-phenyl-1-nitrosoethyne (**68**) (Scheme 27).[90]

Scheme 27. Reaction of **66** and **67** with N_2O_4.

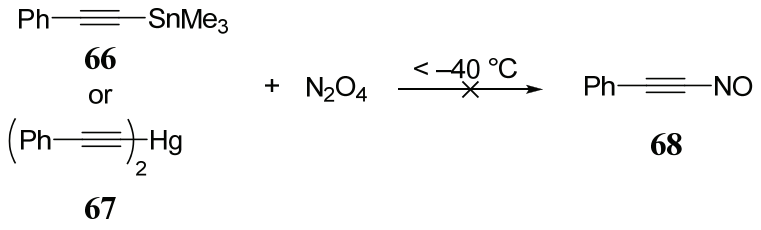

Both processes yielded benzoyl cyanide, the expected decomposition product of **68**.[136,90]

The successful generation of nitrosoacetylenes according to Scheme 26 suggested that, under certain conditions, N_2O_4 may act as $NO^+NO_3^-$ in an electrophilic manner (Scheme 28),[90] rather than as a source of $NO_2^{\bullet}$ radicals.

Scheme 28. Addition-elimination mechanism proposed by Woltermann.[90]

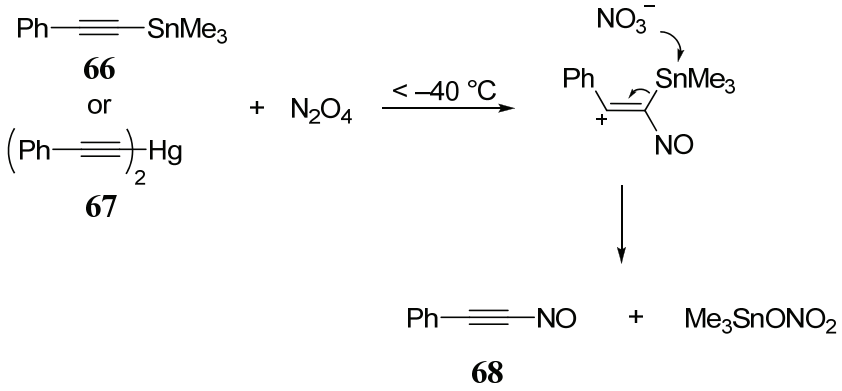

Other nitrations of trialkyltin compounds were observed to take place through radical mechanisms, and both radical and addition-elimination products were found when N_2O_4 reacted with various acetylides, so the nature of the reaction is unclear.[114,142,90]

Petrov et al. added to the confusion when they claimed that nitroacetylenes had formed under conditions similar to those used by Motte et al. and Jäger et al. in the generation of nitrosoacetylenes (Scheme 29).[118,119,111,116]

Scheme 29. Nitrations of (trialkyltin)alkynes with N_2O_4 as described by Petrov et al.[118,119]

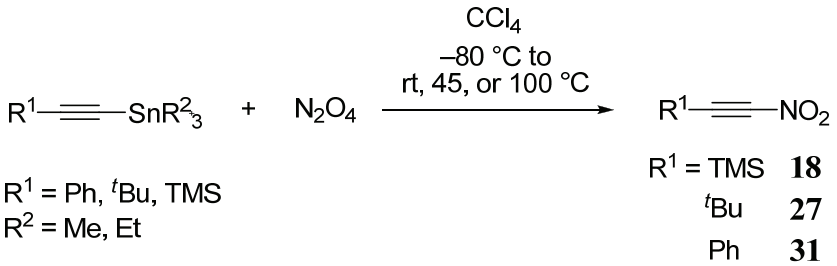

Based on limited IR data and incomplete nitrogen analysis, Petrov et al. assigned structures of **18**, **27**, and **31**.[118] The evidence for competing nitration pathways,[114] the previous results of Motte et al.[116] and Jäger et al. showing addition-elimination of N_2O_4,[111] and more recent studies of low temperature radical nitration with N_2O_4[143] prevent outright dismissal of the claims by Petrov et al., but serious doubts remain. Although **18** and **27** are described as yellow oils, in agreement with the literature,[108,104] **31** is characterized as a red oil, characteristic of nitrosoacetylene decomposition.[135] The nitrogen analyses for the compounds described as **27** and **31** deviated approximately 5 % from the theoretical values, and the IR spectrum of **27**, taken in 5 % CCl_4, was dubious.[119] Jäger recorded the bands for the nitro group of **27** at 1512 and 1352 cm^{-1}, whereas Petrov et al. report peaks of 1544 and 1355 cm^{-1}.[104,119] Similarly, there are discrepancies in the triple bond stretching frequencies: Jäger quotes 2231 cm^{-1}, with a shoulder at 2270 cm^{-1}, Petrov has them at 2214 and 2224 cm^{-1}.[104,119] In addition, for **18** we found disagreements between Petrov's values and ours (see Section 2.7.3). In view of the observations of Robson et al.,[135] it is possible that the trialkylstannylalkynes were nitrosylated and rearrangement products isolated upon warming.

The first successful direct nitration of alkynes appeared in 1975, when Jäger et al. produced nitroacetylenes with either nitronium fluoroborate (NO_2BF_4) or dinitrogen pentoxide (N_2O_5) (Scheme 30).[111]

Scheme 30. Direct nitration of trimethylstannylalkynes.[111]

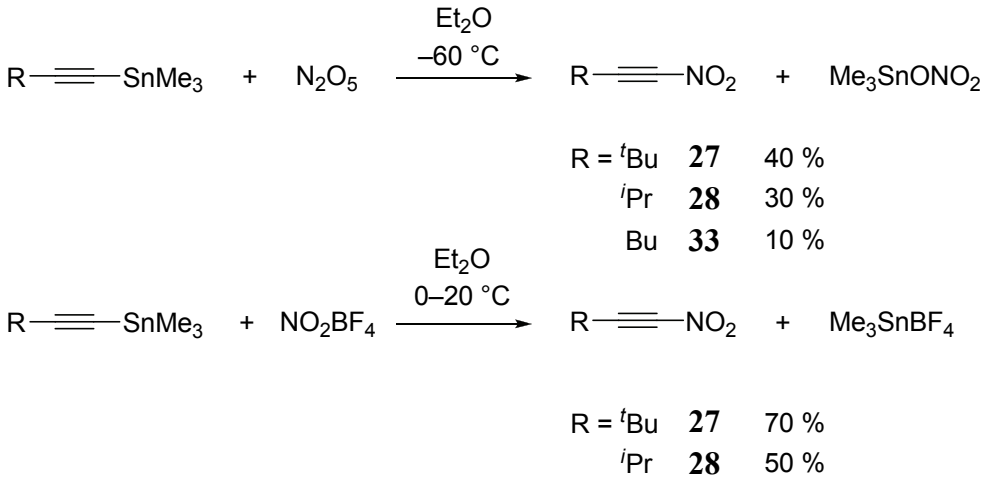

Compounds **27**, **28**, and **33** were presented without characterization.[111] This method afforded good yields of nitroacetylenes previously accessible only by elimination. The nitronium salt proved to be a better nitrating agent than N_2O_5, and in both cases, the reaction was facilitated by decreasing the steric bulk of the trialkylstannyl groups.

In 1980, Kashin and co-workers extended the scope of this nitration by claiming the conversion of **66** to **31** in low (4.5 %) yield (Scheme 31).[114]

Scheme 31. Preparation of **31** according to Kashin et al.[114]

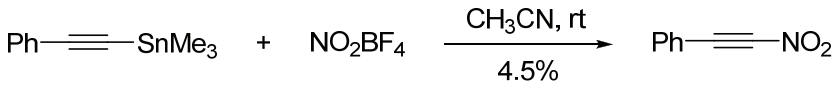

66 **31**

The reaction conditions were nearly identical to those of Jäger et al.,[111] but employed dissolved NO_2BF_4 in acetonitrile at room temperature,[144] rather than suspensions in cold methylene chloride.[111] A parent ion peak *m/z* = 147 and the loss of NO_2 *m/z* – 46 appeared in the MS of **31**, along with loss of NO *m/z* – 30, atypical for nitro compounds, but common for nitrites, suggesting that the nitro group had rearranged (see Section 2.2 for more details).[114,126] The expected phenyl peak *m/z* = 77, did not appear, but a peak at *m/z* = 75 was attributed to a phenyl fragment. The only IR spectral data presented by Kashin et al. were the asymmetric and symmetric stretching of a nitro group at 1535 and 1355 cm^{-1}, respectively.[114] No NMR spectra were collected, and the diagnostic C–N stretch at 730 cm^{-1} was absent in the IR spectrum. Kashin et al. attributed the low yield to the oxidation of **31** by $NO_2^{\bullet}$ radicals or N_2O_4 to give 3-cyano-2,2-dinitro-1-phenyl-1-propanone (**69**) (Scheme 32).

Scheme 32. Formation of **69** from **66** and NO_2BF_4 proposed by Kashin et al.[114]

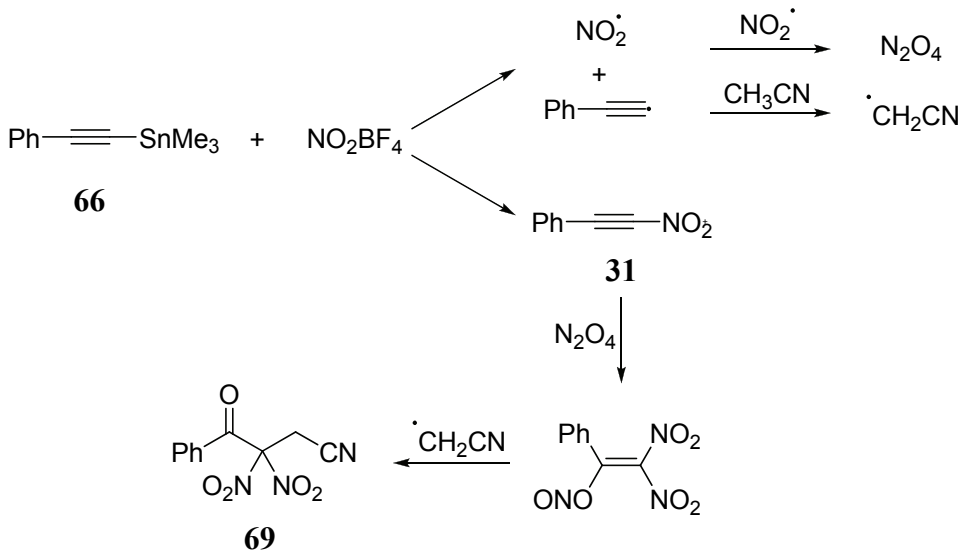

66 **69**

Woltermann reinvestigated this reaction in 1996 and found that phenylethyne (**70**) was the major product, along with a small amount (5 %) of 3-benzoyl-5-phenylisoxazole (**71**), trace quantities of benzoyl cyanide, and what was characterized as **31** (Scheme 33).

Scheme 33. Reinvestigation of Kashin's preparation of **31**.[90]

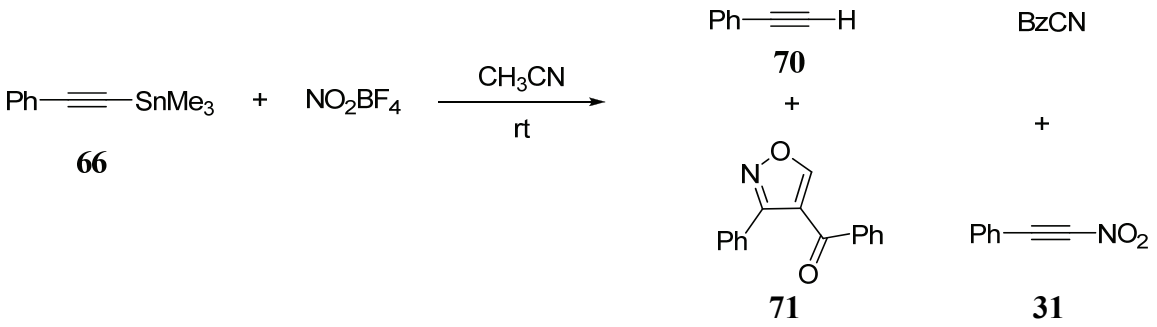

He observed none of side product **69** reported by Kashin et al.,[90,114] but because **69** and **71** have coincidental parent ion peaks of *m/z* = 249) and share a number of similar IR bands, it is probable that the original structure assignment (based on MS and limited IR spectra) was incorrect. Woltermann reported a more complete IR spectrum, including the triple bond stretch at 2219 cm^{-1}[90] and an unidentified peak at 1701 cm^{-1}, but did not record any NMR spectra. Although some of the data of Kashin et al. and Woltermann seem to indicate formation of **31**, without observing the characteristic $^{13}C–^{14}N$ coupling in the ^{13}C NMR spectrum or the diagnostic stretch at 730 cm^{-1} in the IR spectrum, the structure of the compound remains uncertain.

The most convenient direct nitration of acetylenes appeared in 1986, when Schmitt et al. used trialkylsilyl acetylenes instead of their tin counterparts.[108,111] They synthesized **18**, **30**, **34**, and **35** in this manner (Scheme 34).[108,109] Nitronium fluoride was also effective, but gave poorer yields and was more difficult to handle than NO_2BF_4.[108]

Scheme 34. Synthesis of silylnitroacetylenes from trialkylsilylacetylenes.[109]

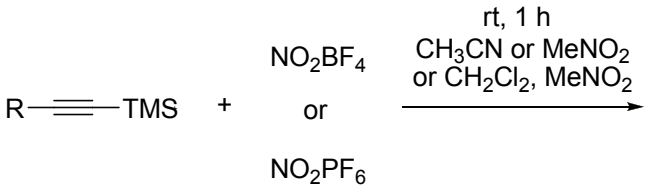

R=			R=			
	TMS	**72**		TMS	**18**	70 %
	$SiMe_2{}^iPr$	**73**		$SiMe_2{}^iPr$	**34**	34 %
	$SiMe_2{}^tBu$	**74**		$SiMe_2{}^tBu$	**35**	59 %
	TIPS	**75**		TIPS	**30**	57 %
	Me	**76**		Me	**32**	trace

This new variation had several advantages: The silylacetylenes were commercially available, the reaction was completed in two hours at room temperature, and toxic tin reagents were avoided. Unfortunately, this method was ineffective for the known **27** and **31** (Scheme 35), and **32** was prepared only in trace quantity.[109]

Scheme 35. Silylacetylenes impervious to NO_2BF_4 and NO_2PF_6.[109]

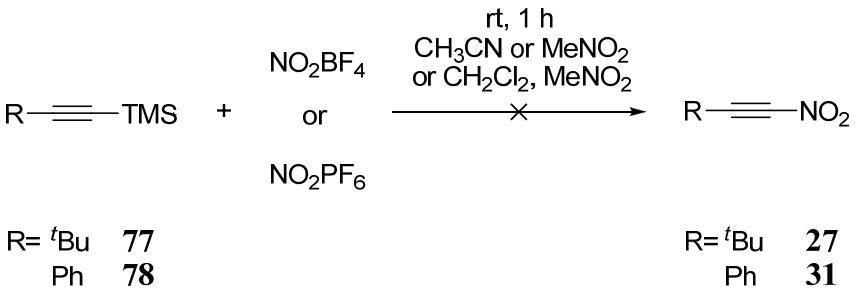

The new nitroacetylenes were characterized by GC-MS, GC-IR, and derivatization by [3 + 2] and [4 + 2] cycloadditions (see Section 2.5 for more details on the cycloadducts).[108,109,81]

In 2002, Zhang et al. modified the method of Schmitt et al. to afford a low yield of **16** from 1-(trimethylsilyl)ethyne (**79**) in solution (Scheme 36).

Scheme 36. Preparation of **16** by modified method of Schmitt et al.[107]

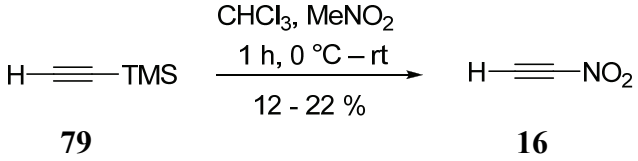

Purification was complicated, and **16** was characterized by ^{1}H NMR, ^{13}C NMR, and limited IR data in solution, but was never concentrated beyond 1 M.[107] It exhibited long range ^{1}H–^{14}N coupling in the ^{1}H NMR spectrum (δ 3.37 ppm, $^2J_{NH}$ = 1.6 Hz) and ^{13}C–^{14}N coupling as a triplet at δ 82.3 ppm (J_{CN} = 32.2 Hz) and δ 55.6 ppm ($^2J_{CN}$ = 4.5 Hz) in the ^{13}C NMR spectrum. It remains the only nitroacetylene with a published ^{13}C NMR spectrum. Further proof of **16** came from addition and cycloaddition products, several of which were unexpected (see Section 2.5).[107]

For the reactions depicted in Scheme 34, Schmitt had proposed a mechanism shown in Scheme 37, based partly on the observation of a side product in the reaction of **72**, assigned as 1-fluoro-2-nitro-1,2-bis(trimethylsilyl)ethene (**80**), which was characterized solely by mass spectral data.[108] The latter contained a peak at *m/z* = 77, corresponding to F–Si–Me_2^+, seemingly at odds with the proposed structure.

Scheme 37. Mechanism proposed by Schmitt et al. for the nitration of **72** to give **80**.[109]

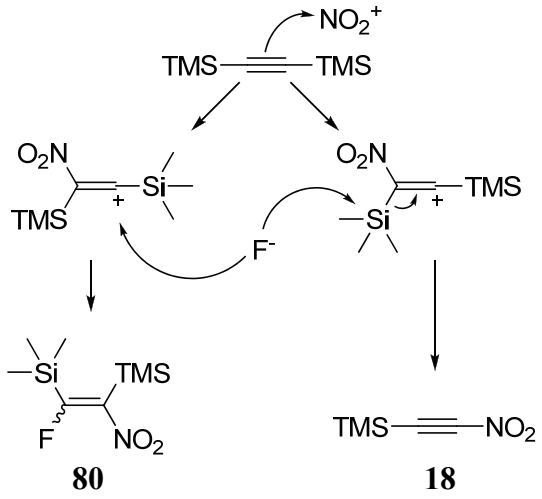

In the corresponding nitration of (trimethylsilyl)acetylene to give **16**, Zhang et al. had isolated a seemingly related side product.[107] However, the detection of two methyl peaks at δ 2.19 and 2.09 ppm in the ^{1}H NMR spectrum, of corresponding signals at δ 14.7 and 18.7 ppm in the ^{13}C spectrum, and of ^{19}F NMR peaks indicative of the presence of F–Si bonds, pointed to the formation of either of the two rearranged isomers: 2-(fluorodimethylsilyl)-1-nitropropene (**81**) or 1-(fluorodimethylsilyl)-2-nitropropene (**82**) (Scheme 38).[107]

Scheme 38. Mechanism of formation of **16**, **81**, and **82**.

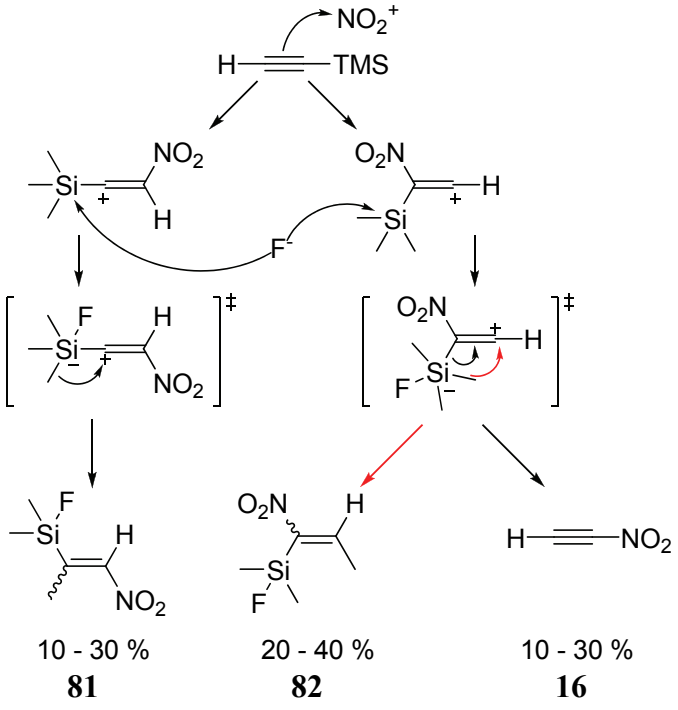

It is possible that such a process (depicted in Scheme 39) also occurred in Schmitt's nitration of **72** (Scheme 37). If so, the structure of **80** might have been misassigned, and its true nature may be 2-(fluorodimethylsilyl)-1-nitro-1-(trimethylsilyl)-propene (**83**) or 1-(fluorodimethylsilyl)-1-nitro-2-(trimethylsilyl)propene (**84**). Either possibility would be consistent with the presence of the mass spectral fragment at *m/z* = 77 noted by Schmitt et al. [108]

Scheme 39. Formation of **18** via pentavalent silicon intermediate.

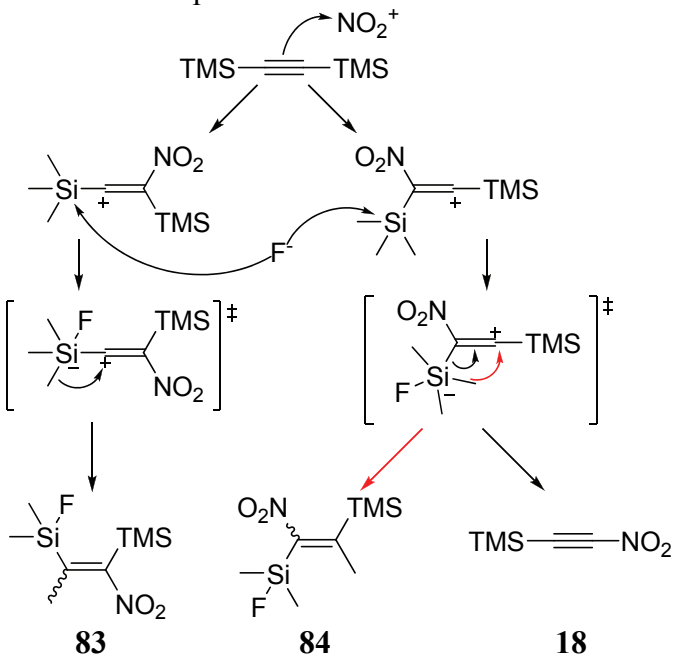

Finally, one notes that the first step in the mechanisms in Scheme 38 and Scheme 39 could also be fluoride ion attack on silicon, as Olah believes (Scheme 40).[145]

Scheme 40. Initiation of trialkylsilylacetylene nitration by fluoride attack on silicon.

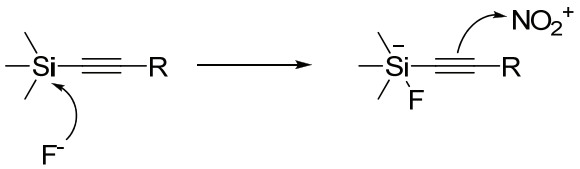

A simple metathesis reaction between 1-phenyl-2-chloroethyne (**85**) and sodium nitrite was described by Yamabe et al. in a 1979 report from the Sasebo College of Technology in Japan (Scheme 41).[125]

Scheme 41. Reaction of **85** with sodium nitrite.[125]

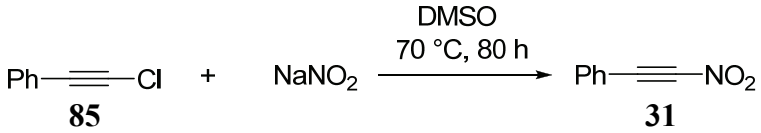

Formation of **31** was claimed in an unquantified "small amount" that could not have exceeded 20 % because after 80 hours, only 20 % of **85** had disappeared. Column chromatography of the reaction mixture on an unspecified solid phase, eluting with hexanes followed by diethyl ether gave unreacted **85** and the compound described as **31**, respectively. It exhibited a single peak on GC (FID), and the ^{1}H NMR spectrum in an unspecified solvent consisted of an AB^2C^2 multiplet at δ 7.75 ppm. The elemental analysis fit: calcd. (C 65.5, H 3.4, N 9.5) %, found (C 65.76, H 3.4, N 9.69) %, but the IR spectrum showed some discrepancies with the corresponding spectrum obtained by Jäger for **31**,[104] most notably the absence of the diagnostic band at 730 cm^{-1}. Considering that the half-life of the *t*-butyl analog **27** is only 30 minutes at 80–85 °C in toluene solution,[104] it seems unlikely that **31** survived the workup conditions. Without a mass spectrum and full NMR data, it is impossible to confirm the structure of **31**.

Two nearly identical government reports surfaced in 2004 and 2006, documenting research into nitroalkyne synthesis by decomposition of nitrogen-rich molecules.[89,146] The abstracts mentioned nitroacetylenes explicitly, but pertinent details were removed from the body of the text before publication in a public government database. What remains are descriptions of the general synthesis of substituted acetylenes in nearly quantitative yield from glyoxaldihydrazones or 1-amino-1,2,3-triazoles with lead tetraacetate in tetramethylguanidine (TMG) and methylene chloride at temperatures between –120 and –80 °C (Scheme 42).

Scheme 42. Decomposition of glyoxaldihydrazones and tetrazoles to give alkynes.

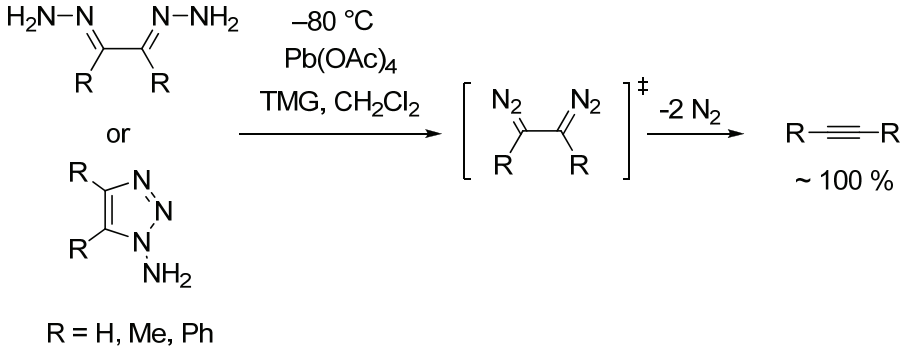

With appropriate starting materials, one can envisage an extension of this method to the preparation of nitroacetylenes.

Many of the methods described in this section by which nitroacetylenes can be made and others have been applied in thus far futile attempts to reach the holy grail of this chemistry, dinitroacetylene (or DNA for short, **22**). These attempts are summarized in the next section.

2.4 Historical Approaches to Dinitroacetylene (DNA)

It is difficult to provide a comprehensive account of the attempts to prepare DNA, because unsuccessful work is rarely disclosed, but by relying on personal communications, theses, and government reports, one may obtain a reasonable picture.

Baschieri was probably the first to seek DNA in 1901 (Scheme 7).[88] Target molecules were not explicitly stated, but his straightforward approach of passing acetylene gas through a traditional nitrating acid implies that direct nitration was the goal.

Jäger's mononitrations of trialkylstannyl acetylenes (Scheme 30), also suggests that he would have attempted dinitration of bis(trimethylstannyl)ethyne (**86**), as indicated in Scheme 43, but no records of such attempts exist.[111]

Scheme 43. Possible dinitration of **75** to DNA, **22**.

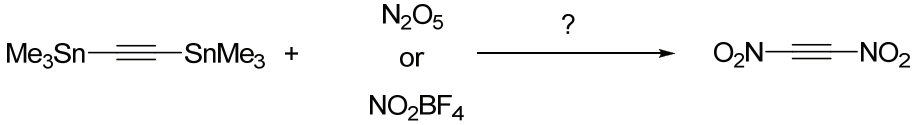

86 **22**

Petrov et al. probably tried the same with N_2O_4,[118,119] and Kashin et al. likely did so again with NO_2BF_4 in 1980.[114] The analogous nitration of **72** was carried out in 1986 by Schmitt et al., rendering **18** (Scheme 34),[108] and it seems plausible that DNA was the goal.[110]

A government report by Dewar from 1983 details the first explicit endeavor aimed at synthesizing DNA.[86] Elimination, cycloreversion, and direct nitration approaches were discussed, but only direct nitration was pursued. The experiments employed **9** (tetranitromethane), NO_2BF_4, N_2O_4, N_2O_5, NO_2Cl, and methyl nitrate as nitrating reagents, which were reacted with alkali metal acetylides (exact metals unspecified), zinc acetylides, cuprous acetylides, silver acetylides, alkynyl Grignard reagents, trimethylsilylalkynes, trimethylstannylalkynes, acetylenecarboxylic acids, acetylenecarboxylic acid salts (unspecified), and triphenylphosphonium acetylene salts (Scheme 44). None of these reactions led to any nitroacetylenes.

Scheme 44. Direct nitrations undertaken by Dewar et al. on attempted routes to DNA.[86]

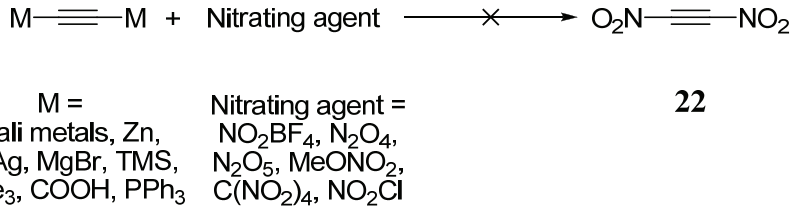

22

No experimental details appeared in the report. The experiments of Kashin et al. with **31**[114] were not cited, and it was incorrectly stated that only two nitroacetylenes were known (six with reasonable characterization were announced by 1983). Two of the unsuccessful methods employed by Dewar had been proven to work eight years earlier,[111] and another was shown to be feasible only three years later,[108,109] calling into question the experimental quality.

The clearly stated purpose of Woltermann's thesis was to make DNA.[90] Many of the methods explored (Scheme 45) were the same as Dewar's, and Woltermann describes

a study of the nitration of phenylacetylide (see Section 2.3) and the identification of a few side products not described by Dewar, but ultimately failed to make DNA.[90]

Scheme 45. Woltermann's attempts to synthesize DNA.[90]

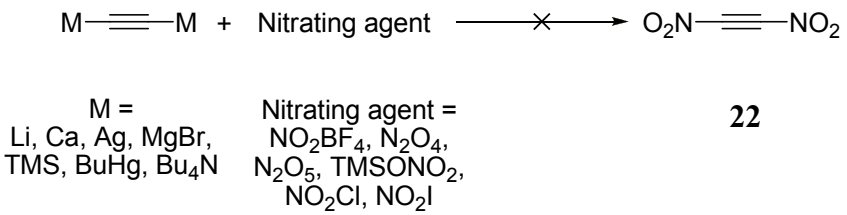

Woltermann also tried desilylating **18** in the presence of nitronium ion (Scheme 46).

Scheme 46. Woltermann's failed nitrodesilylation of **18** to give DNA.[90]

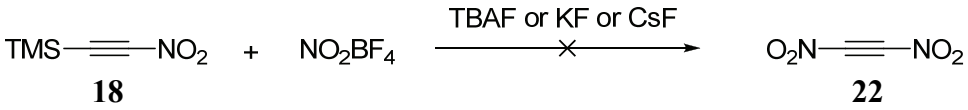

With fluoride ion in solution, **18** was desilylated, but even under forcing conditions, electrophilic addition did not occur and decomposition resulted.[90] Schmitt et al. showed by mass spectroscopy that, in the gas phase, the nitroacetylide anion attacked trimethylsilyl chloride and methyl iodide, suggesting that it could act as a nucleophile, but DNA formation was not reported.[69]

Concurrent with the direct nitrations of Dewar, Baum and Tzeng sought DNA by elimination and thermal cycloreversion approaches. Several alkenes so produced, including **15** and 1,2-dibromo-1,2-dinitroethene (**87**), were potential precursors to DNA by elimination, which was attempted unsuccessfully by Dewar and likely by Baum and Tzeng as well (Scheme 47).[60,55,147,59,57]

Scheme 47. Potential elimination routes to DNA from **15** and **87**.

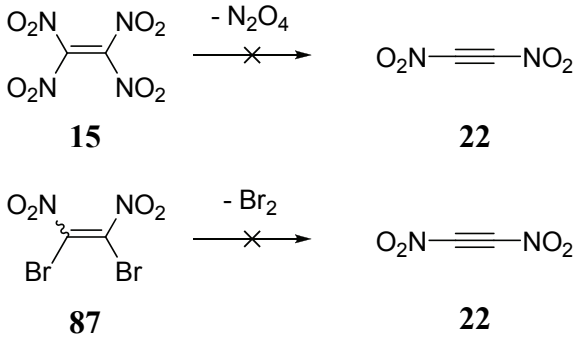

Efforts toward producing DNA through thermal cycloreversion centered around 11,12-dinitro-9,10-dihydro-9,10-ethenoanthracene (**88**) (Scheme 48).[64]

Scheme 48. Potential thermal cycloreversion route to DNA from **88**.

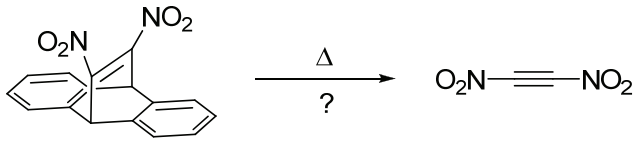

88 **22**

Thermal cycloreversion of acetylenes bearing electron withdrawing substituents from adducts of this type had precedent in the literature.[148,149,150] No published account of Baum and Tzeng's investigation to produce DNA from **88** by a retro Diels-Alder cycloaddition exists, but Nielsen cited a personal communication in his book "Nitrocarbons," that Baum was unable to isolate or trap any material from this reaction.[151] Dewar et al.[85] quotes a personal communication from Baum, in which the synthesis of DNA was claimed, described as a white solid decomposing at 60 °C. He states in the same paper identical properties for **15**. The known **15** does not and DNA likely does not have such properties. Woltermann pursued the same reaction, finding that a temperature of 430 °C was required for thermal cycloreversion at 0.05 torr, a temperature at which DNA is unlikely to survive (see Section 2.6).[90] The expected anthracene (**89**) product was obtained along with stoichiometric amounts of nitrogen and carbon dioxide, possibly derived through decomposition of intermediately generated DNA (Scheme 49).

Scheme 49. Cycloreversion of **88** with decomposition products.

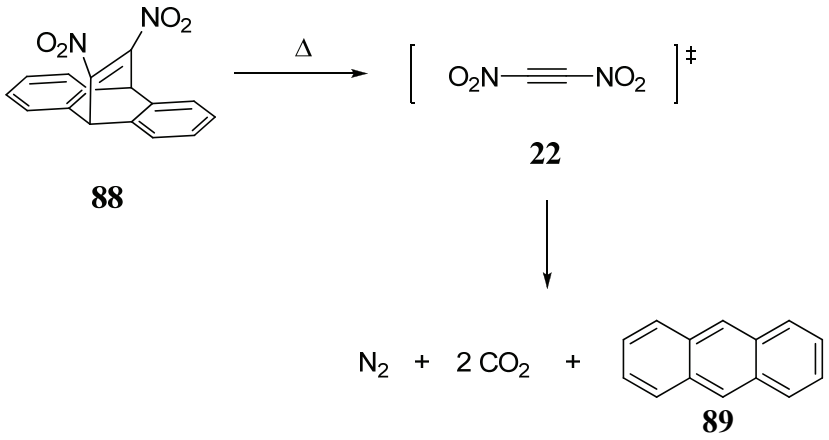

Several derivatives of **88** in which added electron donating substituents were meant to promote the cycloreversion at lower temperatures were sought,[152] but none were successfully prepared.[90]

In a manner similar to that of Yamabe et al.,[125] Woltermann attempted the metathesis of diiodoethyne (**90**) with silver nitrite to furnish DNA (Scheme 50).[90]

Scheme 50. Attempted reaction of **90** with silver nitrite to access DNA.[90]

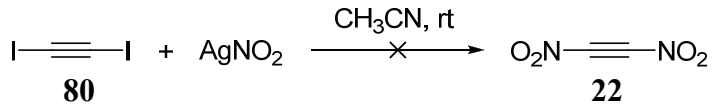

Carbon dioxide, nitrogen and nitrogen(II) oxide formed immediately upon mixing, along with an unidentified, white precipitate that decomposed to silver iodide.

In another approach, Woltermann tried to obtain DNA through oxidation of **91**.[153] A number of oxidizing agents led to either polymerized material or decomposition (Scheme 51).

Scheme 51. Unsuccessful oxidation of **91**.

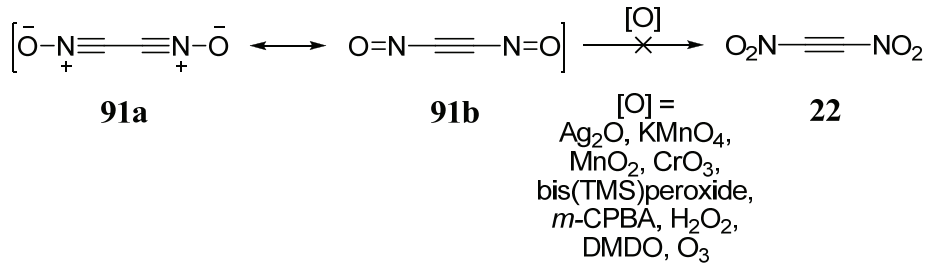

Calculations suggest that **91b** is only a minor contributor to the ground electronic state of **91**, a possible rationale for this failure.[92,153]

As discussed in Section 2.3.2 (Scheme 42), it is likely that DNA was also targeted via the decomposition of glyoxaldihydrazones or amino-1,2,3-triazoles, although there is no public record of such attempts (Scheme 52).[89,146]

Scheme 52. An unsubstantiated possible approach to DNA.

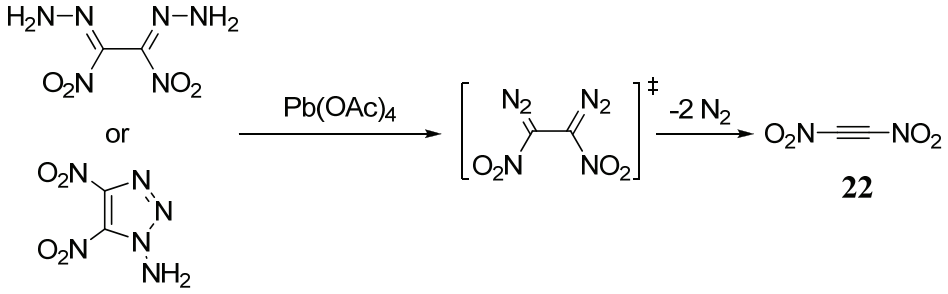

The most promising synthetic effort toward DNA to date came from eliminations similar to those that yielded new nitroacetylenes (Section 2.3, e.g., Scheme 24).[154] The free species was not directly observed, but the cyclopentadiene (**95**) adduct of DNA was isolated in low yield by Zhang et al. (Scheme 53).[154]

Scheme 53. Formation of **93**, the Cp adduct of DNA.[154]

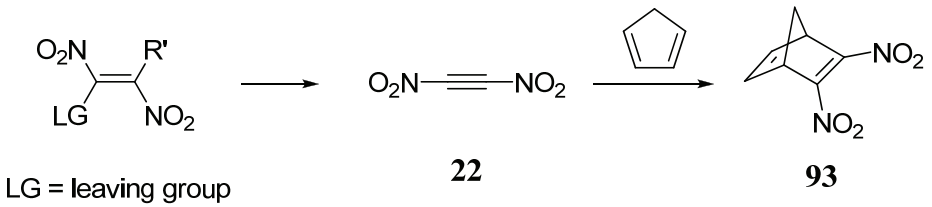

However, the reaction conditions left open the possibility that **93** was generated from the starting alkene or other species in the mixture, and without more evidence, the formation of DNA cannot be confirmed.[154]

2.5 Reactions of Nitroacetylenes

Nitroacetylenes are similar to nitroalkenes in their chemistry: Both are electron deficient and contain unsaturated carbon-carbon π bonds, and both have a canonical resonance structure that leaves a positive charge on the *β*-carbon, rendering it subject to nucleophilic attack (Figure 3).

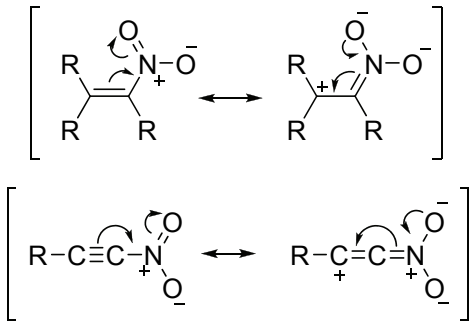

Figure 3. Resonance structures of nitroalkenes and nitroacetylenes.

However, as first noted by Jäger,[104] nitroacetylenes are more reactive. Thus, addition or cycloaddition reactions that require elevated temperatures or catalysts in the case of nitroalkenes take place with nitroacetylenes between –30 and 20 °C and without added catalyst. Moreover, bulky substituents, such as *t*-butyl, markedly inhibit reactions of the former, whereas **27** converts smoothly at room temperature.[104]

Nitroacetylenes decompose slowly upon standing, even when cold, and faster at higher concentrations.[108,107] They are sensitive to base[104,108] and water,[104] decomposing rapidly when exposed to aqueous sodium chloride or sodium bicarbonate solutions,[108] likely through nucleophilic addition pathways. During its slow decomposition at room temperature, 3,3-dimethyl-1-fluoropropyne (**94**) forms arenes and oligomers (Scheme 54).[139,155] In contrast, **27**, after a month of standing, produces only an unidentifiable, inseparable mixture.[104]

Scheme 54. Thermal conversion of **94** into **95** and oligomers as reported by Viehe et al.[139,155]

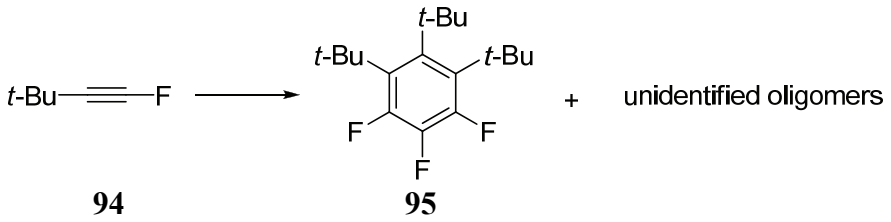

94 **95**

Compound **30** pyrolyzed at 200 °C in an open test tube to 1,4-bis(tri-*iso*-propylsilyl)butadiyne (**96**) in 50 % yield (Scheme 55).[81]

Scheme 55. Pyrolysis of **30** to **96**.

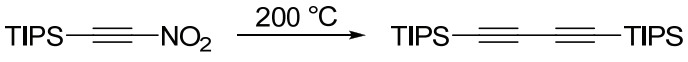

30 **96**

Schmitt et al. assumed that this process occurred by bond homolysis and alkynyl radical coupling.[81] Such coupling products are absent in the nitration of trialkyltin compounds with NO_2BF_4 (Scheme 31),[114] but Woltermann obtained 1,4-bis(phenyl)butadiyne (**97**) from reaction of N_2O_4 with lithium phenyl acetylide (Scheme 56).[90]

Scheme 56. Alkynyl coupling of **98** to **97**.[90]

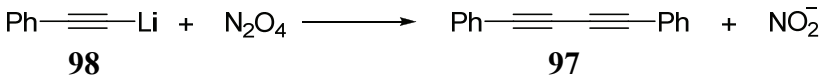

98 **97**

Oxidative coupling of acetylides to butadiynes has been known for over a century and it appears that N_2O_4 acts as a one electron oxidant in these reactions.[156] Woltermann (see also Scheme 11) explored counter ions other than lithium in the reaction with N_2O_4, successful with zinc chloride and bromide, but not the Grignard analogs, which abstracted H from solvent to give **70** (Scheme 57, next page).[90]

Scheme 57. Reactions of metal phenylacetylides with N_2O_4.[90]

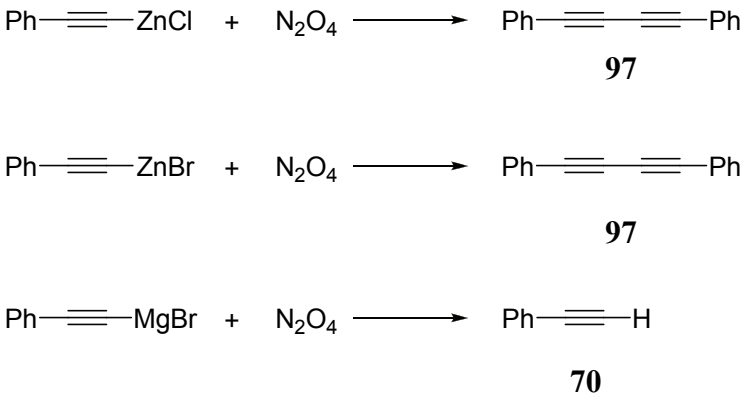

Both lithium aluminum hydride (LAH) and H_2/Pt reduce **27** to 3,3-dimethylbutamine (**99**) (Scheme 58).[104]

Scheme 58. Reduction of **27** to **99** with LAH.[104]

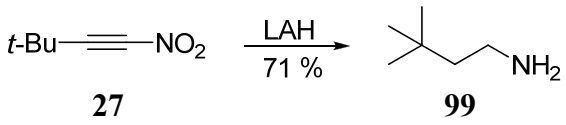

As indicated by the resonance picture in Figure 3, nucleophilic addition to nitroacetylenes is facile. Jäger observed that bromination of **27** in chloroform gave one (unspecified) isomer of 1,2-dibromo-3,3-dimethyl-1-nitropropene (**100**) in 95 % yield (Scheme 59).[104]

Scheme 59. Bromination of **27** to **100**.[104]

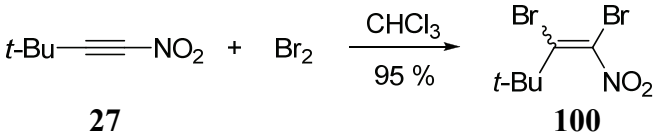

Water attacks just as easily, yet, unlike the hydrolysis of nitroalkenes, no polymerization occurs. Thus, compound **27** was treated with wet THF overnight at room temperature to afford 74 % of 3,3-dimethyl-1-nitro-2-butanone (**101a**) (Scheme 60).[104]

Scheme 60. Hydrolysis of **27** to **101a**.[104]

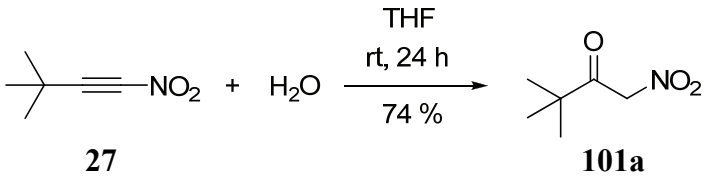

Compound **101a** did not form a hydrazone, as is common for α-nitroketones, but instead tautomerized in 15–17 % yield (Scheme 61).[104]

Scheme 61. Keto-enol tautomerization of **101a** to **101b**.[104]

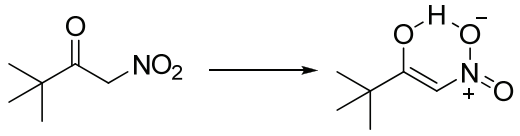

101a **101b**

Alcohol addition also proceeds cleanly without a basic catalyst, unlike nitroalkenes. By letting **27** stand in methanol or ethanol, good conversion to the (*Z*)-nitrovinyl ether occurred at room temperature in 24 hours (Scheme 63).[104]

Scheme 62. Alcohol addition to **27**.[104]

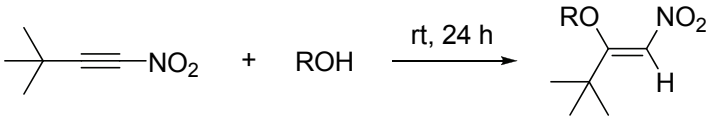

27

R = Me **102** 86 %
Et **103** 78 %

Zhang et al. found that ethanol added to **16** quantitatively in 15 minutes at 0 °C in nitromethane solution to produce both isomers of 2-methoxy-1-nitroethene, which thermally equilibrated upon warming (Scheme 63).[107]

Scheme 63. Ethanol addition to **16**.[107]

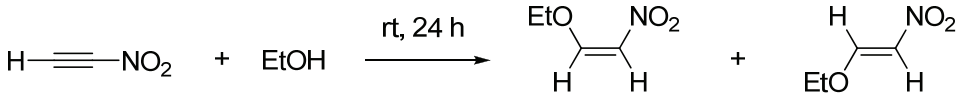

16 **104** **105**

Nitroacetylenes undergo trans addition with dry hydrogen chloride, to the Z isomers of **106** and **107** (Scheme 64).[104]

Scheme 64. HCl addition to nitroacetylenes.[104]

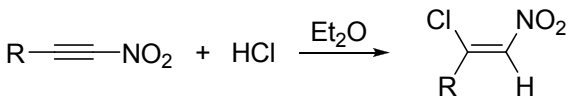

R = ^{t}Bu, 94 % **106**
^{i}Pr, 50 % **107**

While acids add to alkynes normally by initial protonation, electron withdrawing substituents, such as methoxycarbonyl, appear to enable initial nucleophilic attack, followed by protontaion,[157] and such may be the case also with nitroacetylenes.

Aminations are quite exothermic, requiring cold dilute solutions of reagents. Jäger noted that 100 mg of **27** would pop violently and inflame upon contact with a drop of a secondary amine.[104] When dilute solutions of an amine and **27** were combined at 0 °C, reaction was immediate, affording only the corresponding (*Z*)-enamine (Scheme 65).

Scheme 65. Amine addition to **27**.[104]

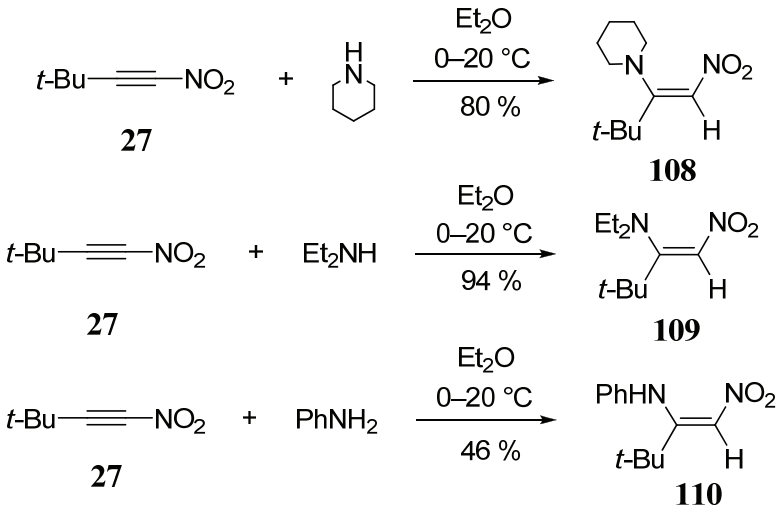

Zhang et al. noted that the reaction of piperidine with **16** gave the trans nitroenamine **111** as the major product, which equilibrated with the cis isomer **112** over time (Scheme 66).[107]

Scheme 66. Piperidine addition to **16**.[107]

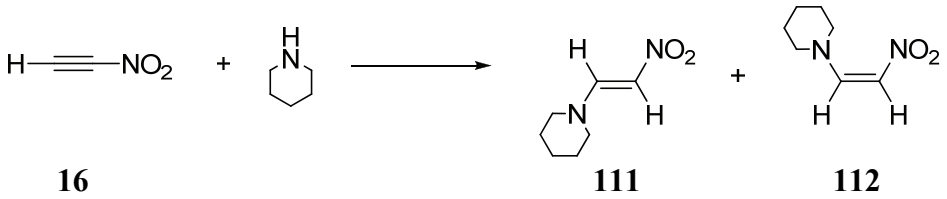

Nitroacetylenes undergo a plethora of cycloaddition reactions. For example, [2 + 2] cyclizations are prevalent in the presence of enamines. The resulting cyclobutenes undergo thermal ring opening, usually at elevated temperatures (Scheme 67).

Scheme 67. [2 + 2] cycloadditions of enamines to nitroalkynes.

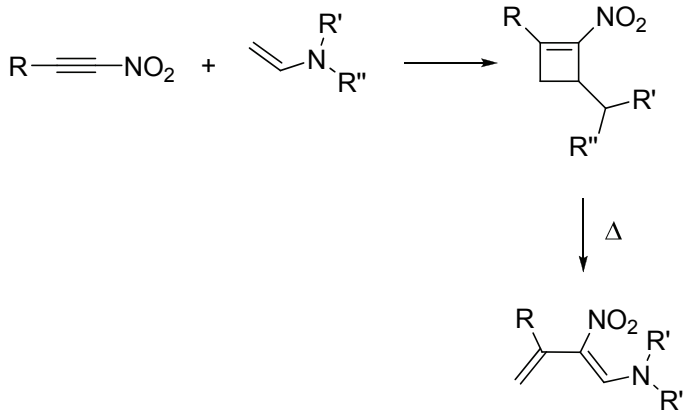

Interestingly, exposure of **27** to **113** at room temperature gave **115** directly via **102** (Scheme 68).

Scheme 68. Reaction of **27** with enamine **111** to give diene **113**.[104]

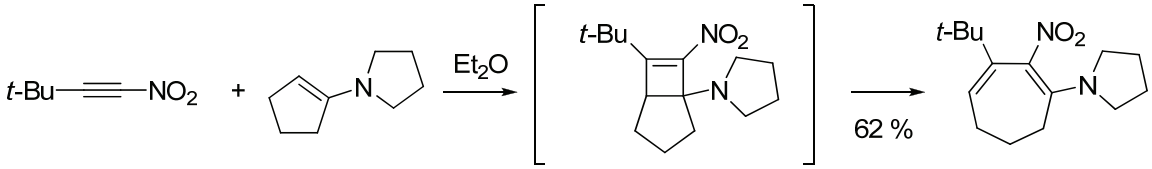

27 **113** **114** **115**

Jäger wished to extend this reaction to ynamines, hoping to achieve cyclobutadiene **116** by causing **27** to react with 3,3-dimethyl-2-(N,N-dimethylamino)-1-nitrobutyne (**117**) (Scheme 69).[104]

Scheme 69. Proposed formation of **116** from **27** and **117**.[104]

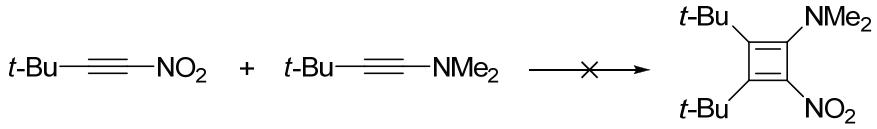

27 **117** **116**

Such [2 + 2] cycloadditions had been employed previously in the synthesis of 'push-pull' cyclobutadienes (Scheme 70).[158,159,160,161]

Scheme 70. Formation of cyclobutadiene **119** from the 'push-pull' acetylene **118**.[104]

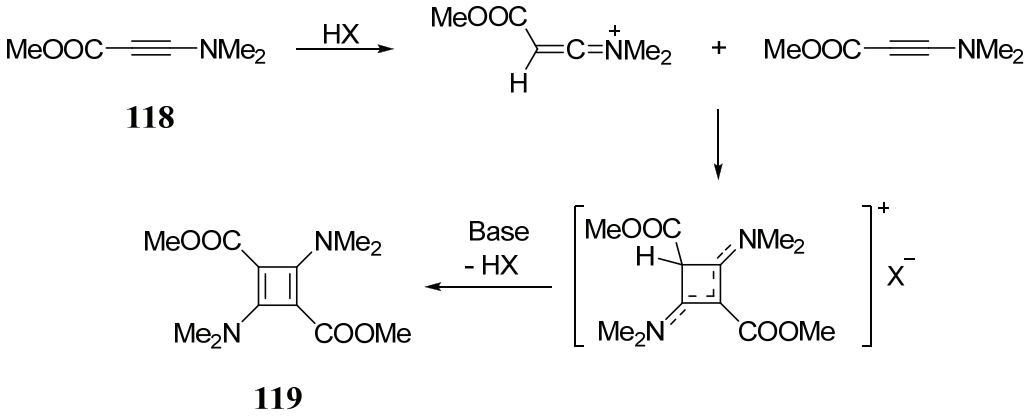

Unexpectedly, a cycloaddition cascade took place, resulting in **120** (Scheme 71).

Scheme 71. Reaction of **27** with **117** to furnish **120**.[104]

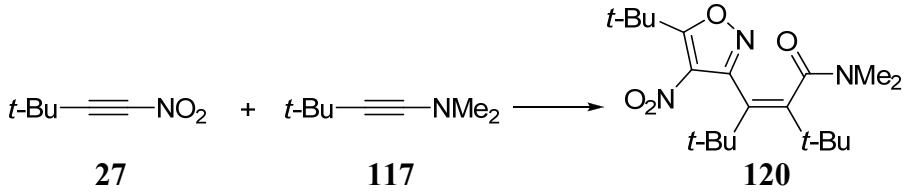

Instead of [2 + 2] cycloaddition, a [3 + 2] cycloaddition had taken place between **27** and nitrile oxide **121** (later isolated), the mechanism for which was postulated by Jäger (Scheme 72, next page).

Scheme 72. Mechanism for formation of **121** from **27** and **117** proposed by Jäger.[104]

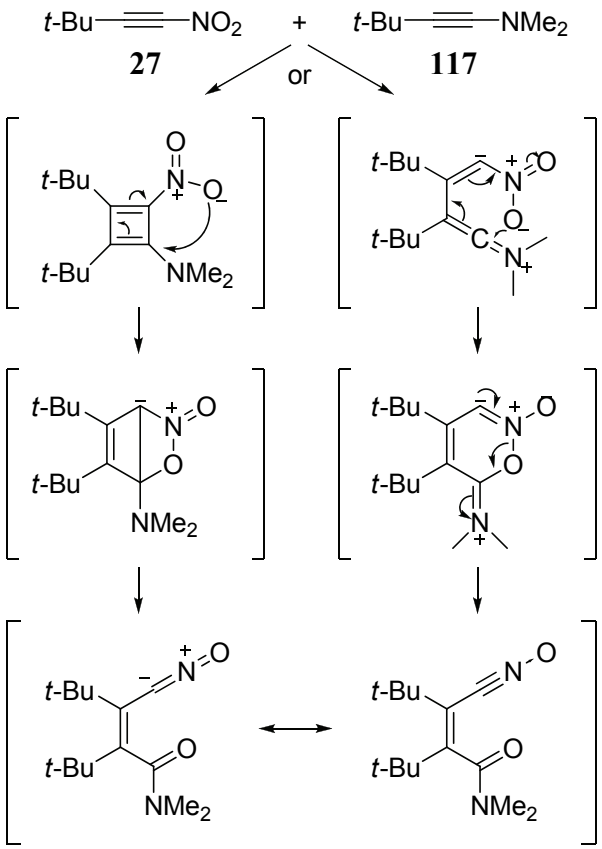

121

Like other acetylenes, nitroacetylenes undergo dioplar [3 + 2] cycloadditions with nitrile oxides.[162,163,164] For example, Jäger treated **27** with 9-anthracene-nitrile oxide (**122**) to give 3-anthracene-4-*t*-butyl-5-nitroisoxazole (**123**) regioselectively (Scheme 73).[104]

Scheme 73. Reaction of **27** with **122**.[104]

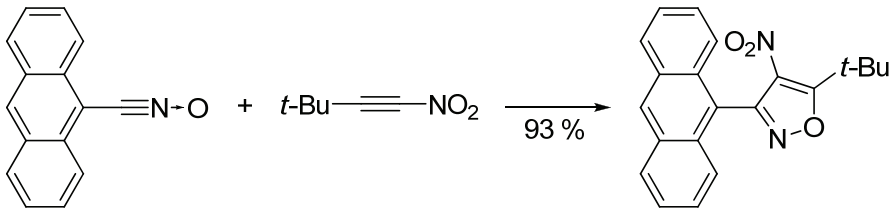

122 **27** **123**

This regioselectivity is dictated by the powerful polarity of **27**.

Decades later, Zhang et al. found similar cascades involving nitrile oxides in the reactions of **16** with enol ethers.[107] While trying to effect a Diels-Alder cycloaddition with furan, they isolated 3-{2-[3-oxo-(*E*)-propenyloxy]-(*E*)-vinyl}-5-nitroisoxazole (**124**)

and 3-{2-[3-oxo-(*E*)-propenyloxy]-(*E*)-vinyl}-5-nitroisoxazole (**125**), instead of the expected 2-nitro-7-oxabicyclo[2.2.1]hepta-2,5-diene (**126**) (Scheme 74).[107]

Scheme 74. Addition of **16** to furan.[107]

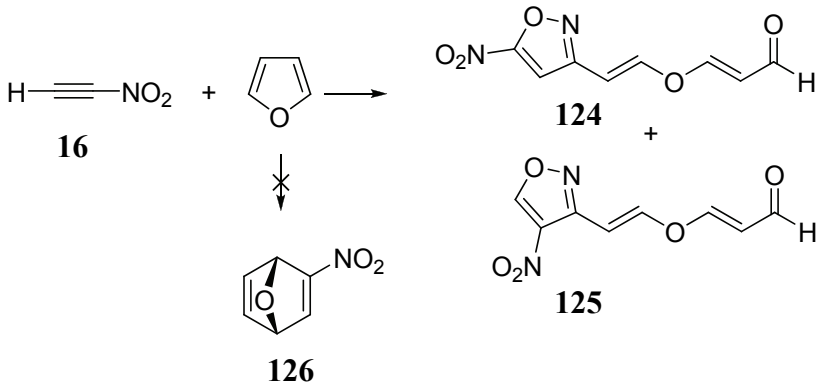

Both vinyl butyl ether and 2-methoxypropene gave related products (Scheme 75).

Scheme 75. Addition of **16** to vinyl butyl ether and 2-methoxypropene.[107]

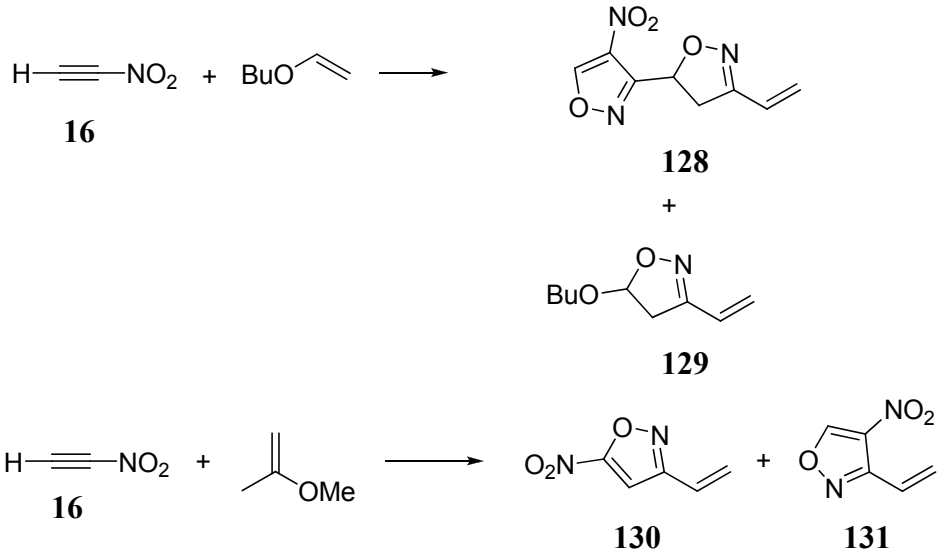

Unlike the reactions with enamines, these vinyl ethers do not undergo [2 + 2] cycloadditions, but rather involve the oxygen on the nitro group as a nucleophile. Zhang et al. proposed that highly reactive unsaturated analogs of nitronates would form,[107] in the same way that nitroalkenes react with electron rich alkenes to give nitronates, as shown for **16** in Scheme 76.[165] These molecules could undergo Cope fragmentation, yielding intermediate nitrile oxide **132** and an ester.[107]

Scheme 76. Proposed mechanism of **16** and a vinyl ether to nitrile oxide **132**.

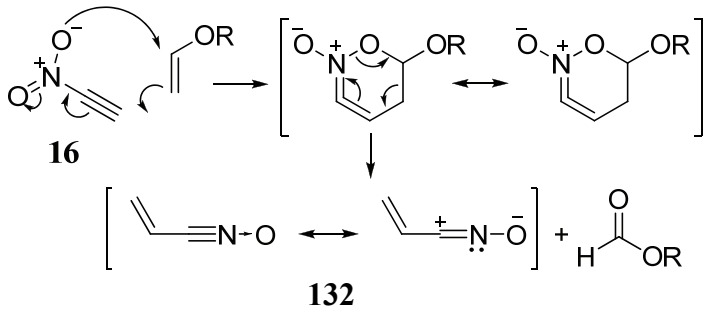

Species **132** was envisaged to be trapped either by an additional molecule of enol ether to give **129**, or by **16** to give intermediate vinyl nitroisoxazoles **130** and **131**. The latter would cyclize with a second molecule of nitrile oxide to give **127** and **128** (Scheme 77). In the case of furan, this mechanism would engender the products **124** and **125**, in which the second enol ether function is rendered unreactive by the appended formyl group.

Scheme 77. Consecutive reactions of **130** with **16**, **132**, and vinyl butyl ether to give **127**, **128**, **129**, **130**, and **131**.[107]

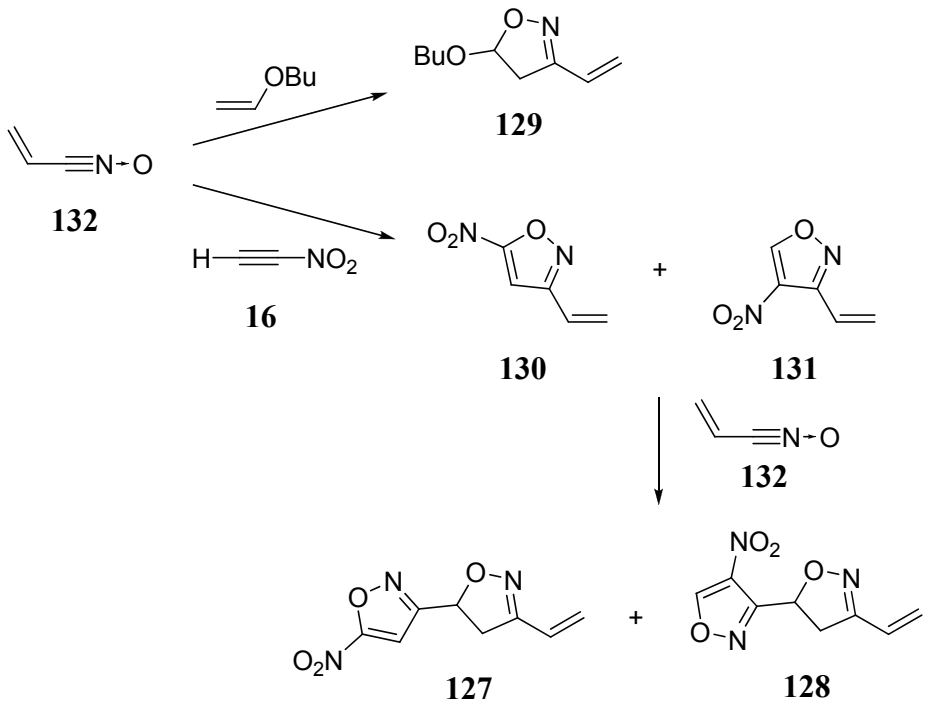

Isoxazoles have also been isolated from failed reactions aimed at generating nitroacetylenes, and it is possible that the latter were intermediates. For example, as described earlier, Baschieri found **41** from the reaction of nitric acid with acetylene (Scheme 7),[88] and Woltermann isolated isoxazoles from the reaction of alkali phenylacetylides with N_2O_4 (Scheme 11), from the addition of N_2O_4 to phenylacetylene,

and from the nitration of **66** (Scheme 32).[90] These presumably originated from an intermediate nitrile oxide.[136]

Schmitt et al. observed [3 + 2] cycloadditions of **18** with diazomethane and trimethylsilylazide, yielding 4-nitro-5-(trimethylsilyl)pyrazole (**133**) and 4-nitro-3,5-bis(trimethylsilyl)-1,2,3-triazole (**134**), respectively, (Scheme 78).[81] Both of these are excellent energetic materials because of the large amount of nitrogen by weight, and the triazole is particularly valuable because 1,2,3-triazole cannot be directly nitrated at the 4 or 5 positions.[81]

Scheme 78. Synthesis of **133** and **134** from **18** by [3 + 2] cycloaddition.[81]

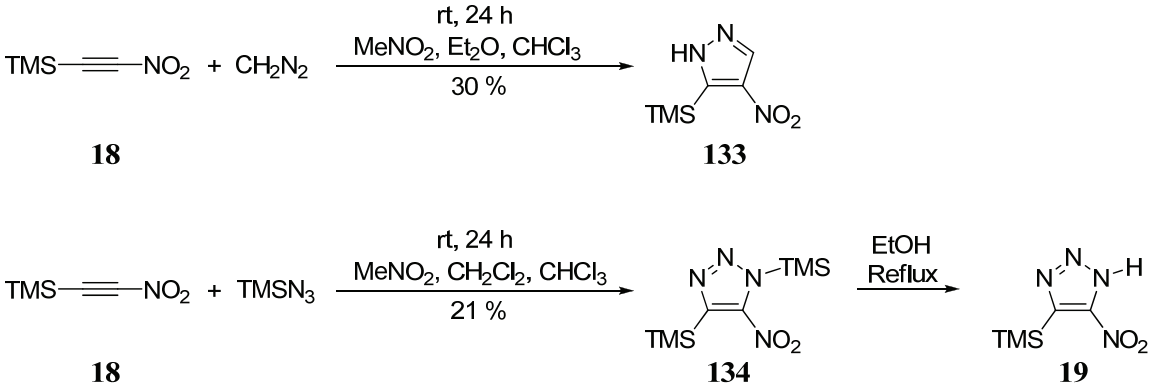

Not surprisingly, the Diels-Alder [4 + 2] cycloaddition features dominantly in the chemistry of nitroacetylenes. While some dienes were unreactive (Table 4), several underwent cycloaddition, as outlined in Table 5.[104,81,115,65,109,107]

Table 4. Dienes unreactive toward the Diels-Alder cycloaddition with nitroalkynes.

Compound	Name	Structure
135	2,4-dimethyl-1,3-butadiene	
136	1,3-cycloheptadiene	
137	1,3-cyclooctadiene	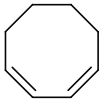
138	cyclooctatetraene	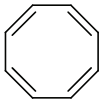
139	tetracyclon	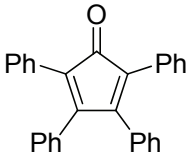
140	2,5-dimethylfuran	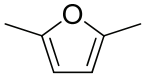
141	diphenylbenzylfuran (DPBF)	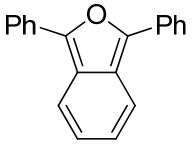

Table 5. Dienes undergoing the [4 + 2] Diels-Alder cycloaddition with nitroacetylenes.

Compound	Name	Structure	Nitroalkyne	Structure
92	cyclopentadiene (Cp)		See Table 6	See Table 6
142	1,3-cyclohexadiene		**18** **28**	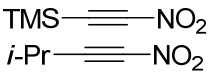
143	furan		**18**	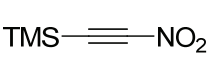

Cp has been most widely used, namely with **16**,[107] **18**,[81] **28**,[104] **29**,[104,115] **30**,[81] **32**,[115] **36**,[115] and **37**[115] (Table 6), and, as mentioned earlier (Scheme 53), there is even some evidence to suggest that DNA may have been trapped by Cp.[154]

Table 6. Diels-Alder reactions of Cp with nitroacetylenes.

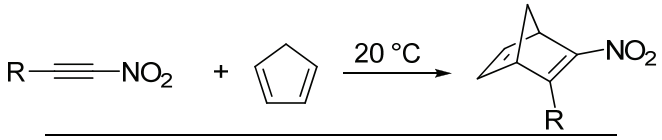

R =	Reactant	Product	Yield (%)
H	**16**	**144**	50
TMS	**18**	**145**	50
^{t}Bu	**27**	**146**	89
^{i}Pr	**28**	**147**	47
Pr	**29**	**148**	24
TIPS	**30**	**149**	75
Me	**32**	**150**	[a]
I	**36**	**151**	[a]
p-CF_3Ph	**37**	**152**	[a]
Br	**38**	**153**	[a]
p-NO_2Ph	**39**	**154**	[a]

[a] Unpublished data.[115]

Jäger compared nitroalkynes with alkynes and alkenes bearing similar electron withdrawing substituents in the [4 + 2] cycloaddition to Cp (Scheme 79).[104]

Scheme 79. Competitive reaction between Cp and **27**, **155**, **156**, or **157**.[104]

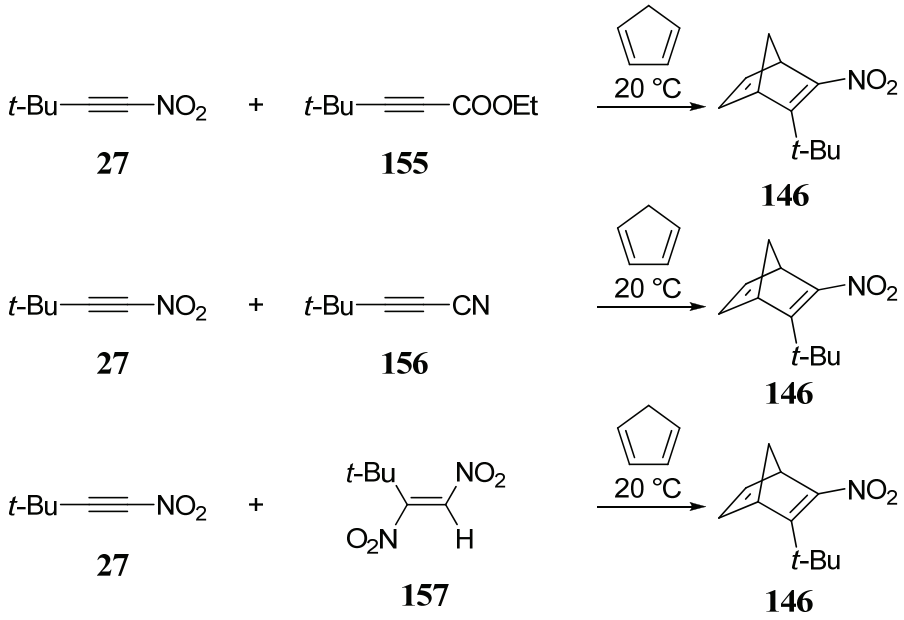

A 1:1 ratio of **27** with ethyl 3,3-dimethylbut-1-yncarboxylate (**155**), 4,4-dimethylpent-2-ynenitrile (**156**), or *trans*-3,3-dimethylnitrobutene (**157**), mixed with excess Cp furnished only **146** after 1.5–two hours at room temperature.[104] From these data, Jäger estimated

that the rate constant for the reaction of **27** with Cp was 10^4 greater than that with the other dienophiles.[104]

Surprisingly, no metal complexes of nitroacetylenes have been described. Moreover, aside from the platinum catalyzed hydrogenation of **27**, no metal mediated or catalyzed reactions with nitroacetylenes have appeared. This thesis will present the first nitroalkyne metal complexes (Chapter 3) and metal-mediated nitroalkyne cyclizations (Chapter 4).

2.6 Theoretical Studies of Nitroacetylenes

A number of theoretical studies of alkynes include nitroacetylenes, but are not focused on this functionality.[166,167,168,169,170,171,172,173,174,175] More relevant to the present discussion are the investigations discussed below.

Because X-ray crystallographic determinations of nitroalkyne structures do not exist, their calculated geometries are of interest. A Density Functional Theory (DFT) derived structure of DNA showed no imaginary vibrational frequencies, implying the plausibility of its existence. Prior to its synthesis, **16** was similarly computed to be stable, suggesting that such estimations may hold predictive value.[93,107] The nitro groups of DNA were found to lie perpendicular to one another, allowing each one to interact with one of the two orthogonal π bonds (Figure 4).[93,92]

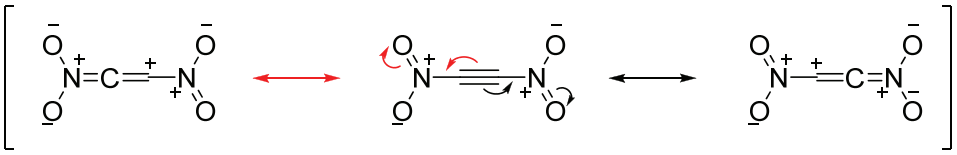

22

Figure 4. Resonance interaction of the nitro groups of DNA with orthogonal acetylenic π bonds.

Similarly, **32**, **55** (2-amino-1-nitroethyne), and 2-(N,N-difluoroamino)-1-nitroethyne (**158**) were each predicted to exist, and the nitro and N,N-difluoroamino groups of **158** were predicted to be perpendicular.[93,92]

55 **158**

Compound **55** was computed to be co-planar, which allows for resonance donation from the amino group into the π orbital made electron poor by interaction with the nitro group (Figure 5).[93]

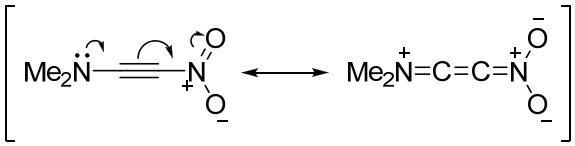

55

Figure 5. Resonance structures of **55**.

The preference of the nitro group to interact with electron rich π orbitals was also evident in later studies.[176,177]

Predictions of enthalpies of formation for unknown nitroacetylenes are also of interest because a positive ΔH_f° contributes to explosive energy output.[††] One of the first contributions to this area was by Dewar et al. using the MINDO/3 method, who arrived at a value of 0.3 kcal/mol for DNA.[85] A Hartree-Fock (HF) approach by Politzer et al. afforded a value of 89 kcal/mol,[92] while Golovin et al. reached a value of 52 kcal/mol (448 cal/g) by similar methods.[178] Golovin et al. also calculated the ΔH_f° for **16** to be 48.5 kcal/mol, or 683 cal/g, more than three times that of RDX (206 cal/g).[178] Politzer's value of 89 kcal/mol for DNA corresponds to 763 cal/g.[92] Clearly, nitroacetylenes are high energy-density materials. Although not directly comparable because they are not all isomeric, the enthalpies of formation of all nitroacetylenes calculated by Golovin et al.[178] appear in Table 7 below for completeness.

Table 7. Calculated standard enthalpies of formation of nitroacetylenes.[178]

Compound	Structure	ΔH_f° (kcal/mol)
60	$F_3C-C\equiv C-NO_2$	–109.5
159	$F-C\equiv C-NO_2$	9.5
160	$ONO-C\equiv C-NO_2$	34
161	$MeO-C\equiv C-NO_2$	34
32	$Me-C\equiv C-NO_2$	36
55	$Me_2N-C\equiv C-NO_2$	41
162	$H_2N-C\equiv C-NO_2$	43
158	$F_2N-C\equiv C-NO_2$	47.5
16	$H-C\equiv C-NO_2$	48.5
22	$O_2N-C\equiv C-NO_2$	52
16a	$^-C\equiv C-NO_2$	115.91

Politzer et al. also estimated the bond order in several nitroacetylenes to investigate the effect of the nitro group on the strength of the acetylenic bond.[93] Although the number computed for **40** (2.42)[93] was less than that measured by Mulliken et al. (3.0),[179] the effect of alkynyl substituents remained comparable. One nitro group was found to strengthen the acetylenic bond relative to **40** (acetylene) (bond order of 2.47 vs. 2.42, respectively); the second further raised the bond order to 2.54.[93] Juxtaposing amino with nitro had the opposite effect (bond order 2.38), the result of resonance donation, as shown in Figure 5.

Vijayakumar et al. calculated the dipole moments and polarizabilities of **55** and other nitroalkynes by HF and Density Functional Theory (DFT) methods,[180] both furnishing relatively large values. It is instructive to compare **32** with 1-fluoropropyne (**163**) in these respects.

$Me_2N-C\equiv C-NO_2$ **55** $\quad$ $Me-C\equiv C-NO_2$ **32** $\quad$ $Me-C\equiv C-F$ **163**

[††] See Appendix A, section A4.

Considering only inductive effects, one would expect **163** (electronegativity of F ≈ 3.96) to have a greater dipole moment than **32** (electronegativity of NO_2 ≈ 3.70). However, resonance in the latter causes more effective electron withdrawal and hence polarization of the molecule. Consequently, **32** has dipole moment and static electric polarizabilities three times larger than **163**.[180]

Electrostatic potential maps of DNA reveal it to be highly electron deficient and hence impervious to electrophilic attack.[93] Schmitt et al. and Woltermann have shown that reaction of nitroacetylenes with electrophiles is indeed unproductive.[109,90] Instead, nucleophilic attack is prevalent.[93,104,108,90,107]

In this vein, the hydride affinities of nitroacetylenes **16** and **32** were calculated by Vianello et al. and compared with those of their fluorine analogs, 1-fluoroethyne (**164**) and **163**, respectively. Relative to acetylene = 0.0 kcal/mol, **16** gives a value of 61.7 kcal/mol and **32** a value of 54.4 kcal/mol. The corresponding numbers for their fluorine analogs **164** and **163** are 34.4 kcal/mol and 29.6 kcal/mol, respectively.[177] These data are summarized in Table 8.

Table 8. Hydride affinities of nitroacetylenes **16** and **32** and their fluorine analogs **164** and **163**.[177]

Compound	Structure	H^- affinity (kcal/mol)
41	H—≡—H	0.0
16	H—≡—NO_2	61.7
164	H—≡—F	34.4
32	Me—≡—NO_2	54.4
163	Me—≡—F	29.6

They confirm the dominance of the nitro group over fluorine that had been computed by Vijayakumar et al. (*vide supra*). In fact, nitroacetylenes had the greatest hydride affinities of all the acetylenes surveyed, including those bearing trifluoromethyl and nitrile groups.

The [4+2] cycloaddition of DNA to furan was computed by Jursic, who found the activation energy to be 8.1 kcal/mol,[181] indicating its relative facility. Whether this result is of practical importance is doubtful in view of the fact that **16** forms isoxazoles when exposed to furan.[107]

Finally, the thermal decomposition of nitroalkanes, nitroalkenes, and nitroalkynes was modeled by Dewar et al. with the MINDO/3 method.[85] Three assumptions were made: that thermolysis involved generation of $NO^{\bullet}$ or $NO_2^{\bullet}$ radicals, that direct homolytic cleavage of the C–N or O–N bond was not likely, and that rearrangement of the nitro group would occur prior to bond cleavage.[85] The last of these assumptions was predicted by the first. Thus, Dewar et al. suggested an initial rearrangement of nitro into a nitrite (Scheme 80).[85]

Scheme 80. Rearrangement of a nitro group to a nitrite during decomposition of a nitroalkyne, as suggested by Dewar et al.[85]

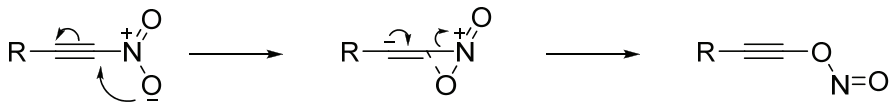

The nitrite would then undergo homolytic bond cleavage at one of two sites, as illustrated by Scheme 81.

Scheme 81. Mechanism for rearrangement and thermal homolysis of alkynyl nitrites calculated by Dewar et al.[85]

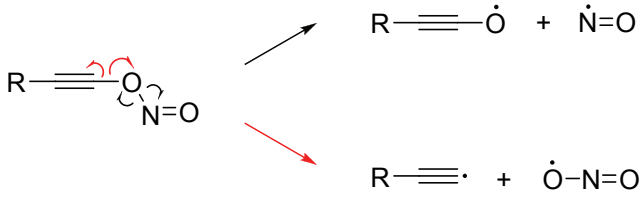

This rearrangement was calculated to have an E_a = 20 kcal/mol, which would make it facile, but the only evidence of its occurrence in nitroacetylenes is found in the mass spectrum of **31** (Section 2.3.2, Scheme 31), a molecule whose structure is suspect.[114,90]

The conclusion of this review sets the stage for our work in this area. It is clear that nitroacetylenes, in particular dinitroacetylene, are formidable targets. Not only are they difficult to synthesize, but they are also difficult to handle and store. As outlined in Section 1.3, our aim was to address these problems by transition metal complexation. As a first step toward this goal, reliable preparations of suitable nitroacetylenes had to be developed. The remainder of this chapter will describe efforts along these lines.

2.7 Results and Discussion

As stated above and in Section 1.3, the goal of this thesis was to produce **24** from suitable precursors, such as **25** and **26**. During the course of this work, the list was expanded to include also **165**, **166**, and **167**.

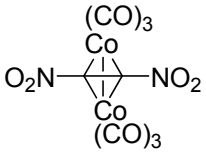

24

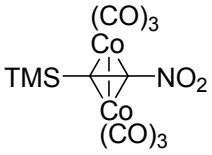

25

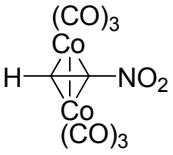

26

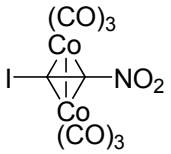

165

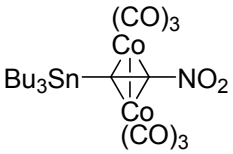

166

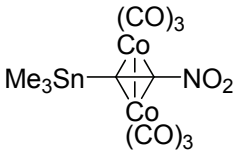

167

This task required reliable and scalable preparations of the corresponding alkyne ligands, **18**, **16**, **36**, 1-nitro-2-(tributylstannyl)acetylene (**168**), and 1-nitro-2-(trimethylstannyl)acetylene (**169**).

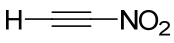

16

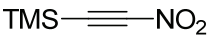

18

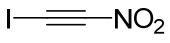

36

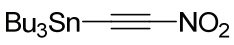

168

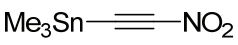

169

As described in Section 2.3.2, **16** and **18** had been made previously, but only in small amounts. Moreover, **16** had been accessed solely in solution and the characterization of **18** was incomplete. Finally, isolated **36**, **168**, and **169** were unknown. Apart from adequate characterization of all compounds, we planned explosive safety testing of **18**.

2.7.1 Iodonitroacetylene, (Tributylstannyl)nitroacetylene, and (Trimethylstannyl)nitroacetylene

In unpublished work, Eaton et al. generated a species by a complicated elimination sequence (as in Section 2.3.2) at low temperature, whose NMR data pointed to the presence of **36**.[115] Therefore, it was hoped that **36** would form at low temperature through direct nitration of 1-iodo-2-(trimethylsilyl)ethyne (**170**),[182,183] to be trapped subsequently by **23**. Hence, **170** was treated with NO_2BF_4 at –78 °C (Scheme 82).

Scheme 82. Reaction of **170** with NO_2BF_4.

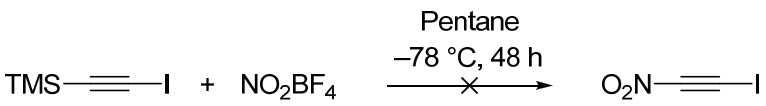

170 **36**

The clear, colorless solution changed over two days to a light yellow color (usually indicative of nitration), but ^{13}C NMR analysis failed to detect **36**. Addition of **23** to the mixture was unsuccessful in providing **165**. Equally futile attempts to construct **165** from the dicobalt hexacarbonyl complex of **170** are found in Chapter 3. Consequently, **36** was not pursued further as a precursor to **24**.

Turning to **168** and **169**, the class of (trialkylstannyl)nitroalkynes is unknown. We hoped to synthesize its first members by mononitration of distannylalkynes, in analogy to Scheme 30. In a first foray, bis(tributylstannyl)acetylene (**171**) was exposed to NO_2BF_4 in pentane. Instead of nitration, destannylation occurred to give (tributylstannyl)acetylene (**172**) (Scheme 83). We suspect that acidic impurities in the nitrating species are responsible for this outcome. Careful analysis of the reaction mixture showed no sign of **168**, and addition of **23** did not provide any **166**.

Scheme 83. Formation of **172** from **171** and NO_2BF_4.

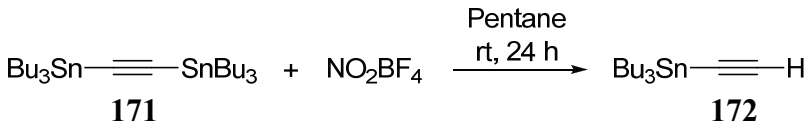

Changing the tin reagent to **86** in methylene chloride-pentane to reach **169** also failed (Scheme 84), even though protodestannylation did not occur. ^1H NMR analysis of the crude product revealed a low intensity trimethylstannyl peak at δ 0.50 ppm, corresponding to a singlet at δ –9.6 ppm in the ^{13}C NMR spectrum.

Scheme 84. Reaction of **86** with NO_2BF_4.

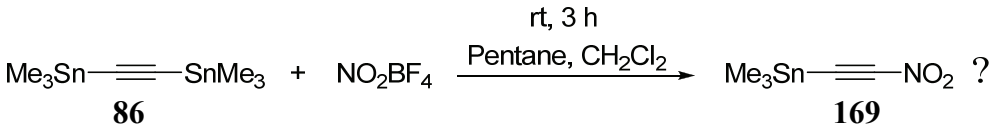

Relative to starting material, these signals were deshielded by about the same amount as those of **72** compared to **18** (Table 9), suggesting the possible generation of traces of **169**.

Table 9. ^1H and ^{13}C NMR chemical shifts of **18**, **72**, **86**, and tentative **169**.

Compound	Structure	^1H δ(ppm)	Δ (ppm)	^{13}C δ(ppm)	Δ (ppm)
72	TMS—≡—TMS	0.15	0.19	0.0	–1.3
18	TMS—≡—NO_2	0.34		–1.3	
86	Me_3Sn—≡—$SnMe_3$	0.28	0.22	–7.8	–1.8
169	Me_3Sn—≡—NO_2	0.50		–9.6	

However, we could not detect the diagnostic ^{13}C–^{14}N coupling in the ^{13}C NMR spectrum, nor could we trap **169** as **167**. Further attempts to improve the yield of this reaction failed, and this approach was also abandoned.

2.7.2 Nitroacetylene

Nitroacetylene (**16**) had been made in 2002 (Scheme 36) by Zhang et al. by the nitration of **79** in nitromethane-chloroform.[107] Guided by a solvent screen performed to find optimal conditions for the preparation of **18** (to be described in Section 2.2.3), we initially attempted this reaction with a suspension of NO_2BF_4 in pentane solution on small scale (0.5 mmol). This procedure gave traces of **16**, as evidenced by the triplet at δ 3.37 ppm in the ^{1}H NMR spectrum, arising from the alkynyl proton (Scheme 85).

Scheme 85. Small-scale synthesis of **16**.

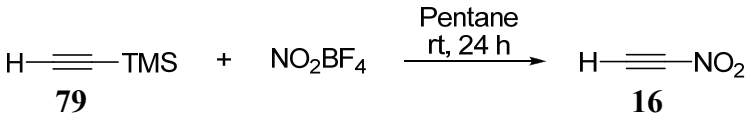

79 **16**

This reaction was not complete even after 24 hours and engendered a host of side products. Compound **16** decomposes upon concentration, and chromatography is deleterious, so it could not be purified with the quantity at hand. Attempts to trap **16** from the crude reaction mixture with **23** to give **26** afforded only complexed **79** (Chapter 3). Having confirmed the sensitivity of **16** as documented,[107] attention was turned to scaling up the original preparation to afford **16** in gram quantity (Scheme 86). This work benefited from collaboration with Dr. Mao-Xi Zhang at Lawrence Livermore National Laboratory (LLNL).

Scheme 86. Formation of **16** from **79** and NO_2BF_4.

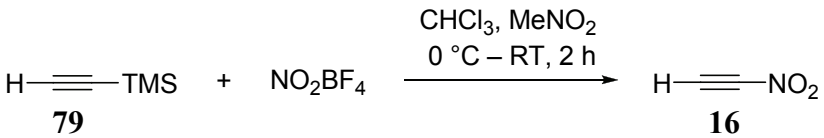

79 **16**

In a mixture of chloroform and nitromethane, approximately 10 % of **16** was obtained (as estimated by integrating the alkynyl proton in the ^{1}H NMR spectrum against a standard), accompanied by several alkenyl side products. Zhang had previously observed that **16** is stabilized by nitromethane,[115] which posed a difficulty to our goal of **26**, because we found that nitromethane decomposes **23**. However, nitromethane does not affect dicobalthexacarbonyl alkynes, so we hoped that **26** would form before **23** decomposed. Unfortunately, this was not the case, and treatment of the crude reaction mixture with **23** resulted only in decomposition and no formation of **26**.

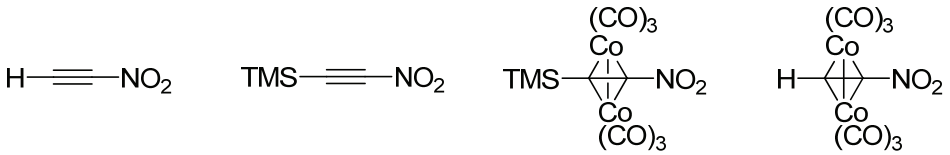

16 **18** **25** **26**

These difficulties discouraged further investigation of this compound in favor of the more stable **18**.

2.7.3 (Trimethylsilyl)nitroacetylene

Three synthetic pathways to **18** have been reported: Petrov's reaction of N_2O_4 with 2-(trimethylsilyl)-1-(trimethylstannyl)ethyne (**173**) (Scheme 29),[118,119] Schmitt's nitration of **72** with NO_2BF_4, cesium fluoride, and tetrabutylammonium tetrafluoroborate in methylene chloride,[108] and Schmitt's nitration of **72** with either NO_2BF_4 or NO_2PF_6 in acetonitrile, nitromethane, or a mixture of methylene chloride and nitromethane (Scheme 34).[109] All three are summarized in Scheme 87.

Scheme 87. Reported preparations of **18** by various methods.

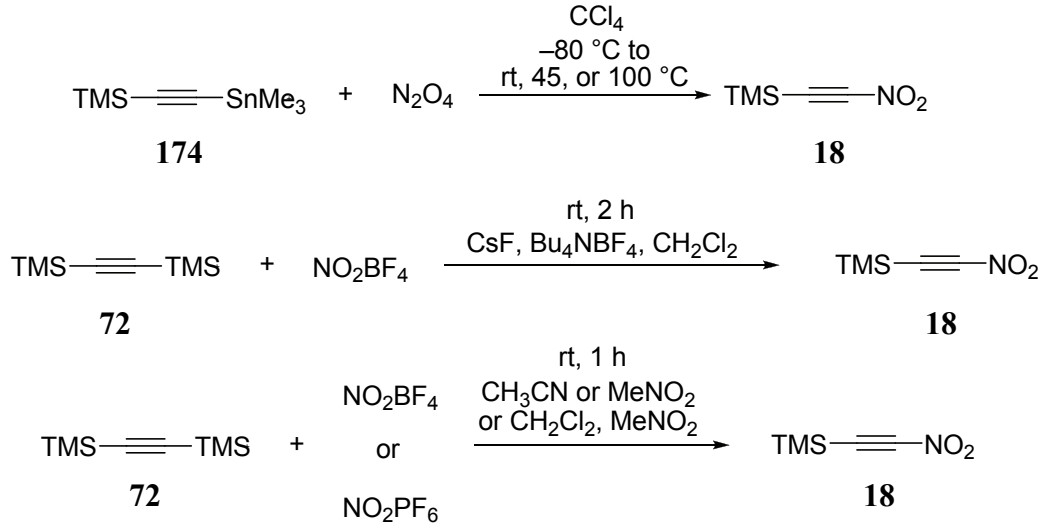

We discounted the Petrov approach, because the purported **18** had been poorly characterized,[118,119] the difficulty of handling N_2O_4, and the toxicity of the tin reagent compared to its silyl counterpart. The two preparations of Schmitt et al. appear similar on first glance, but differ significantly with respect to solvents, reagents, and workup procedures. The first calls for methylene chloride as a solvent and specifically notes acetonitrile as being poor,[108] whereas the second lists acetonitrile, nitromethane, or a mixture of nitromethane and methylene chloride as appropriate solvents.[109] The second procedure also makes no mention of the fluoride or tetrafluoroborate salts employed in the first, and lists another nitrating agent, NO_2PF_6.[109] Astonishingly, the first preparation recommended an aqueous workup, which Jäger had previously shown to hydrate **27**.[108,104] We chose the second Schmitt procedure for our investigations, because it employed less reagents and an anhydrous workup. A series of small scale (1 mmol) experiments were undertaken to establish a protocol for purifying NO_2BF_4 and to find appropriate solvent(s) that maximize the yield of **18**.

The impurities present in NO_2BF_4 as received from commercial sources (Acros or Custom Chem Lab) are thought to be excess fluoride salts or hydrofluoric acid.[108,109,154]

To remove them, Ciaccio et al. recommend subliming NO_2BF_4 and then heating it to 150 °C,[144] while Schmitt et al. triturated the salt with nitromethane.[109] In our hands, the first treatment left a white powder that did not fume when exposed to air and gave very poor yields of **18**.[144] The second furnished free-flowing, clear crystals that resulted in acceptable yields of **18**.[109] Crude NO_2BF_4 proved less effective than purified material, as shown in Table 10.

Table 10. Effects of NO_2BF_4 purification on yields of **18**.

Solvent	NO_2BF_4	*t* (h)	Yield by NMR (%)
Pentane	Crude	24	20-25[a]
Pentane	Purified	24	62-65
CH_2Cl_2	Crude	2	10–11
CH_2Cl_2	Purified	2	28

[a] Yield based on isolation of subsequent reaction products.

The best results were obtained when NO_2BF_4 was triturated once with nitromethane, washed briefly with a small amount of methylene chloride, and then vacuum dried to leave clear, free-flowing crystals.

Turning to the screening for an optimal solvent, solubility (or lack thereof) of the nitrating agent, as well as polarity appear to be of little predictive value. Thus, the good solvents acetonitrile and sulfolane, as well as the bad solvent methylene chloride, gave poor yields of **18**. Nitromethane, in which NO_2BF_4 dissolves slightly (0.5 %),[184] was better, and when mixed with methylene chloride was optimal, rendering 65 % of **18** on a 40 mmolar scale. On a smaller scale (1 mmol) pentane (which does not solvate NO_2BF_4 at all) proved equally effective, but, unfortunately, its performance deteriorated on scale up (10 mmol), when the yield decreased to 26 %. A picture of the reaction in progress in this solvent is shown in Figure 6 and a yield profile versus time is shown in Figure 7.

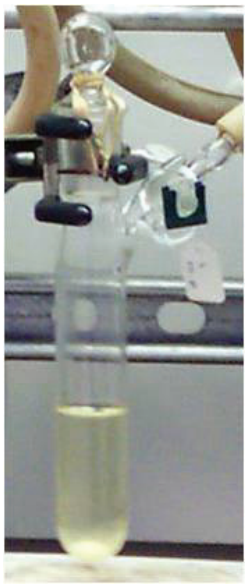

Figure 6. Formation of yellow **18** in pentane solution.

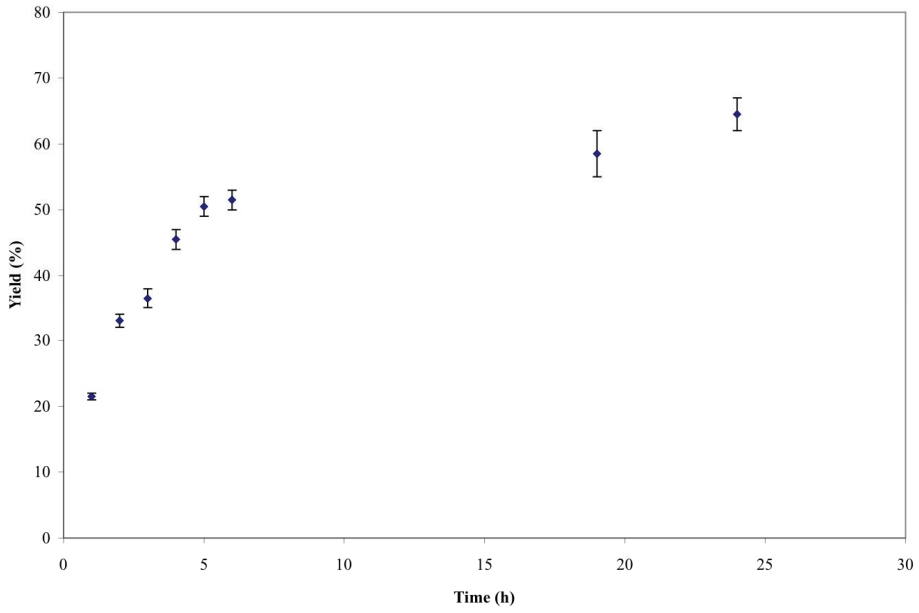

Figure 7. Yield of **18** in pentane solution vs. time as estimated by ^{1}H NMR spectra.

Because side products constitute approximately 20–30 % of the weight of crude **18**, as analyzed by GC-MS, we had to develop a method for purifying **18**. Schmitt's original procedure does not go beyond simple filtration of the crude reaction mixture through a plug of silica gel. Therefore, the crude product was distilled *in vacuo* at 0 °C / 0.1 torr and then subjected to column chromatography. We discovered that alumina is completely deleterious, while silica gel decomposes **18** more slowly, allowing satisfactory pure product recovery when eluted quickly (< 30 seconds). Compound **18** is a bright lemon-yellow, mobile liquid, its purity evidenced by its ^{1}H and ^{13}C NMR spectra (Figures 8 and 9, next pages).

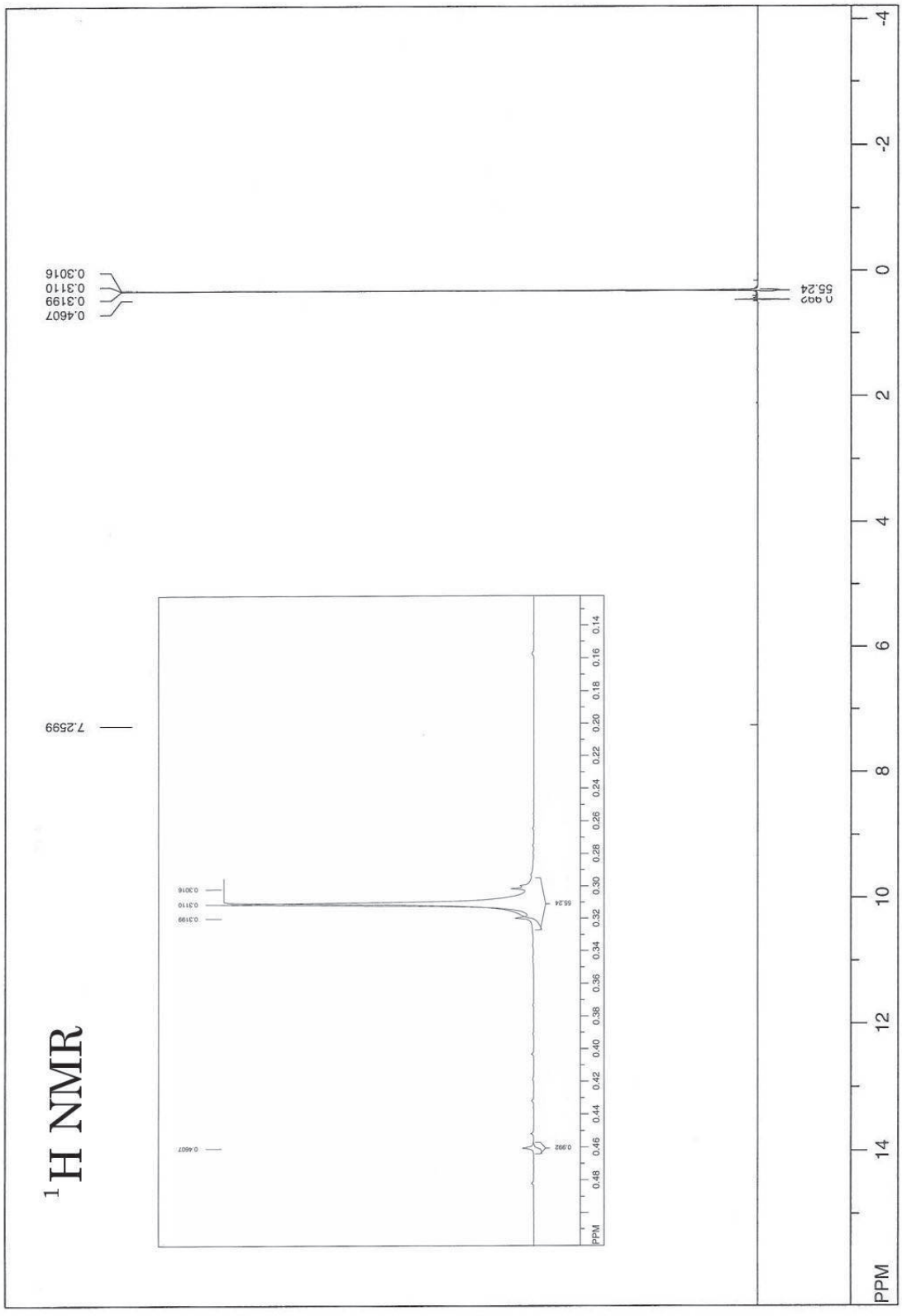

Figure 8. ^{1}H NMR spectrum of high-purity **18** in $CDCl_3$.

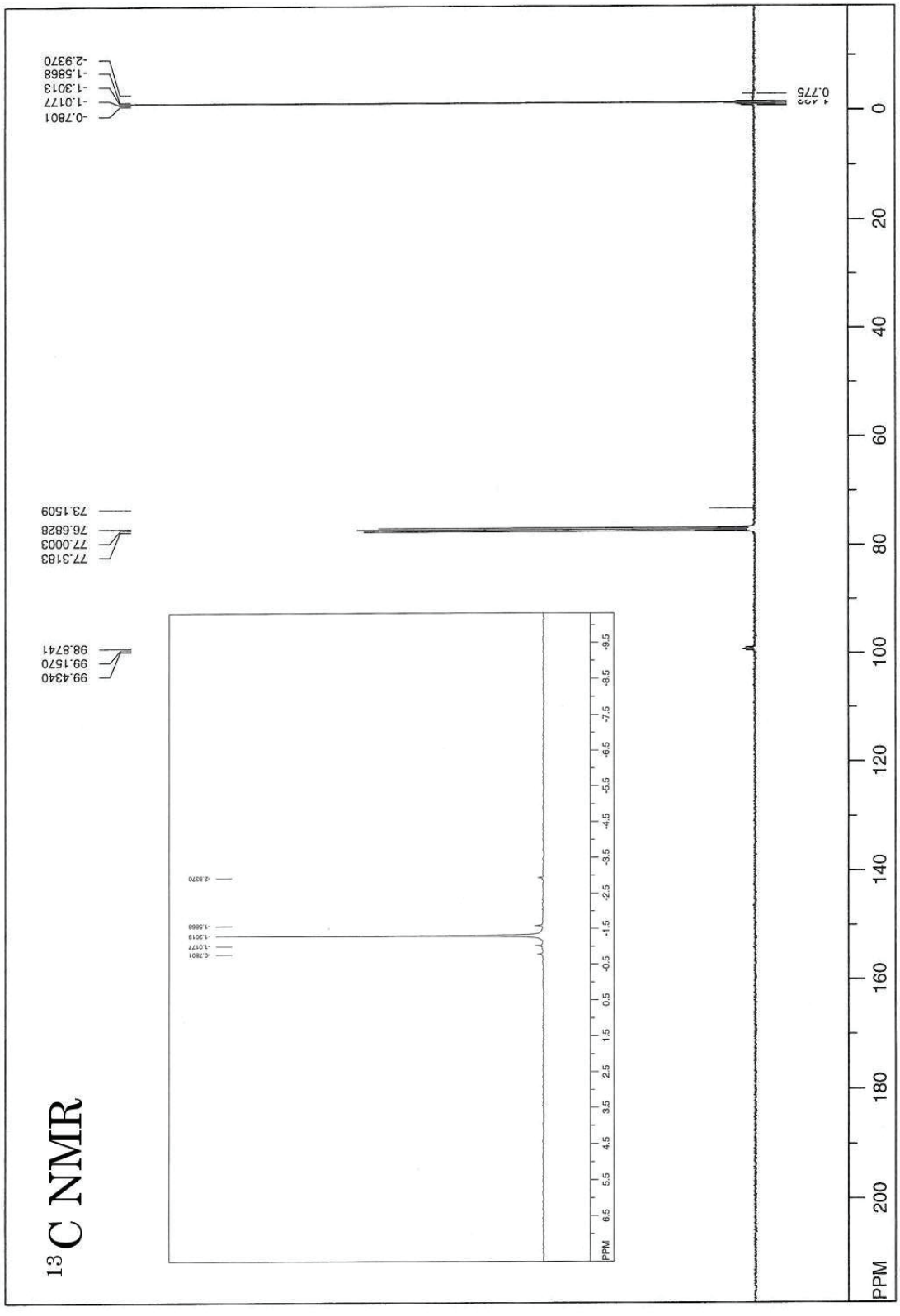

Figure 9. ^{13}C NMR spectrum of high-purity **18** in $CDCl_3$.

Previous reports characterized the contaminants in this preparation as **80**[108] and 1,4-bis(trimethylsilyl)butadiyne (**174**).[107] Our investigation evidenced unreacted **72** and dissolved trimethylsilylfluoride by NMR spectroscopy. The GC-MS spectrum showed what appeared to be **81** and **82** (which may be from desilylated **83** and **84**, see discussion in Section 2.3.2), several unidentified compounds bearing a TMS group, and **174**, in an approximate 18 : 7 : 1 ratio. When the reaction was conducted or worked up in chloroform, we discovered that a new compound appears, the hydrogen chloride addition product to **18**, to which we tentatively assign the structure (*Z*)-2-chloro-2-(trimethylsilyl)-1-nitroethene (**175**).

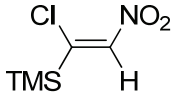

175

A small amount of hydrogen chloride is usually present in chloroform, accounting for the formation of **175**. Addition occurs in a trans fashion as shown by Jäger for other nitroalkynes,[104] and because only one isomer is observed, it is assumed to have the Z configuration. This molecule elutes with only a slightly lower R_f value than **18**, making separation difficult. Compound **175** has a distinctive isoprene-like odor that contrasts with the lachrymatory **18**; solutions of each can be differentiated by smell alone. A parent ion of **175** appears at *m/z* = 166/164 (1:3) in the mass spectrum, followed by the base peak for TMS at *m/z* = 73. The proton NMR spectrum in $CDCl_3$ exhibits two singlets in the ratio 1:9, one for the alkenyl hydrogen at δ 7.71 ppm and the other for TMS at δ 0.36 ppm. The former δ value compares well with those of similar alkenes (measured in CCl_4), such as **56**, **105**, and **106** (δ 7.15–7.42 ppm).[104]

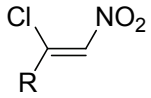

R = Ph **55**
^{t}Bu **102**
^{i}Pr **103**

The carbon spectrum consists of two alkenyl carbon signals at δ 159.4 and 147.8 ppm, along with that for TMS at δ –1.4 ppm. The IR spectrum shows absorptions for the alkenyl C–H (3082 cm^{-1}),[185,186] C–H stretching from the TMS group (2960, 2903, 2855 cm^{-1}),[187,188] C=C (1583 cm^{-1}),[104,186] nitro (1519 cm^{-1} and 1349 cm^{-1}),[189] Si–CH_3 deformation (1254 cm^{-1}),[188] methyl rocking on TMS (851 cm^{-1}),[188] and C–N stretching (725 cm^{-1}).[121,104] These data agree well with the IR spectra of **105** and **106**, which exhibit each of these bands in the same regions.[104]

Pure **18** freezes into an amorphous glass between –75 and –72 °C, but a crystalline solid could not be attained. At atmospheric pressure, a boiling point of 99 °C for **18** was observed, which decreased to 0–10 °C at 0.1 torr, consistent with boiling points of other nitroacetylenes.[65,107,104] The expected singlet for TMS appeared at δ 0.34

ppm in the ^{1}H NMR spectrum and at δ –1.3 ppm in the ^{13}C spectrum. The ^{13}C–^{14}N coupling indicative of the acetylenic carbon bearing the nitro group was observed as a triplet at δ 99.2 ppm with J_{CN} = 28.2 Hz, downfield from the corresponding signal for **16** at δ 82.3 ppm (J_{CN} = 32.2 Hz).[107] No long range ^{13}C–^{14}N coupling is evident in the TMS-bearing carbon, which manifests as a singlet at δ 73.2 ppm. The mass spectrum agrees with the literature values, including peaks at $M^+ - 15$ (–CH_3), $M^+ - 46$ (–NO_2), and $M^+ - 73$ (–TMS). The IR spectrum cannot be compared to that of Schmitt et al., because of different recording conditions (Table 1, Section 2.2),[108] and it differs from that previously disclosed by Petrov et al.[118,119] In particular, the nitro absorptions found at 1514 and 1339 cm^{-1} disagree with those of Petrov et al. at 1528 and 1355 cm^{-1}. However, they are similar to those of alkylnitroalkynes **27**, **28**, and **29**, which lie between 1515–1510 cm^{-1} and 1358–1345 cm^{-1}, respectively. The C≡C stretching peak also differs, 2167 cm^{-1} versus 2215 cm^{-1} (Petrov et al.).[‡‡] The alkyl C–H stretching band of **18** was observed at 2964 cm^{-1} (unreported by Petrov et al.). Most TMS substituents have very strong Si–C symmetric deformation and rocking bands at ~ 1250 and ~ 840 cm^{-1}, respectively, both of which are observed for **18**.[187] Perhaps the most diagnostic IR band, due to C–N vibration, was found at 729 cm^{-1}, consistent with the same band in the spectra of **27**, **28**, and **29**,[104] and absent in the work of Petrov et al.[118,119]

Subjecting **18** to a drop hammer test returned positive initiation with a 2.5 kg weight for a DH_{50} = 174 cm, showing a low sensitivity to initiation. By comparison, many commercially available explosives are more sensitive, including PETN, RDX, and TNT (Table 11).[190] The data show that **18** is explosive. This is unexpected because of its extremely deficient oxygen balance (–139 %), and suggests that **27** (with the same oxygen balance) may be explosive as well. The results underscore the need for care when handling nitroacetylenes, especially those with more favorable oxygen balances, such as **16** (–56 %) or DNA (0 %, or perfect).

Table 11. Drop hammer heights of explosive standards and **18**.[190]

Compound	Structure	DH_{50} (cm)
3	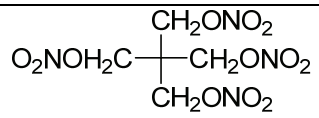	14–20
11	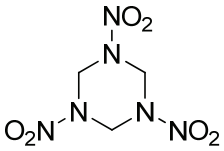	32
5	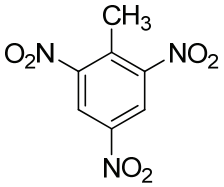	100
18	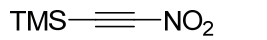	174

[‡‡] Curiously, Jäger states in a footnote that the acetylenic band of **18** appears at 2165 cm^{-1}, with no further discussion.[104]

2.8 Conclusion

This chapter has described the general physical and chemical properties of nitroacetylenes, historical attempts to make nitroacetylenes, syntheses of known nitroacetylenes, known reactions of nitroacetylenes, and our synthetic efforts in this area. A large-scale preparation and purification of **18** was established, and a new alkenyl contaminant identified. Compound **18** was shown to be explosive and was characterized by previously unreported physical and spectral properties, including ^{1}H and ^{13}C NMR spectra and a complete IR spectrum that corrects deficient literature data.

Chapter 3. Hexacarbonyldicobalt Nitroalkyne Complexes

3.1 Introduction

Organic π-systems coordinate to transition metals by "forward" donation of electron density from filled π orbitals to low-lying empty *d* orbitals on the metal, and similar "back" donation from filled *d* orbitals to π* orbitals of the ligand.[94] Such coordination alters the electronic structure of the organic ligand, and with it, its physical properties and reactivity. In some cases, it is transformed into a new species after demetallation, while in other cases intact recovery is possible.

We planned to generate a transition metal complex of DNA that would be sufficiently stable to permit isolation and to yield free DNA upon demetallation. In the form of a dinuclear hexacarbonyl alkyne complex, cobalt had been shown to stabilize reactive alkynes bearing electron withdrawing groups[95,191] and to return them on demetallation.[97] Such complexes are prepared from the commercially available **23**.

In principle, compound **24** could be made by direct ligation of DNA or manipulation of a suitable precursor. Ligation is a simple one-step process (Scheme 88), but requires the unknown DNA.

Scheme 88. Proposed ligation of DNA.

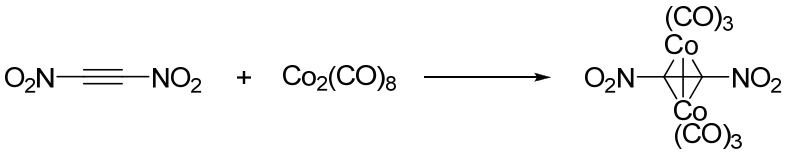

22 **23** **24**

Functional group interconversion of an appropriately substituted alkyne (Scheme 89) would require the judicious choice of R.

Scheme 89. Functional group transformation of R to furnish **24**.

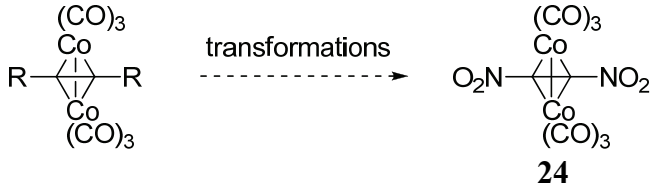

24

Acetylation of [μ-1,2-bis(trimethylstannyl)ethyne-1,2-diyl]bis(tricarbonylcobalt)(*Co–Co*) (**176**) (Scheme 90),[98] desilylation of [μ-1-(trimethylsilyl)-2-(*p*-tolylsulfonyl)ethyne-1,2-diyl]bis(tricarbonylcobalt)(*Co–Co*) (**177**) (Scheme 91),[192] and transformation of [μ-1-(isocyanato)hept-1-yne-1,2-diyl]bis(tricarbonylcobalt)(*Co–Co*) (**178**) into the corresponding carbamate and amine (Scheme 92),[100] provide a glimpse of the potential of such a strategy.

Scheme 90. Reported acetylation of **176** with acetyl chloride and $AlCl_3$.[98]

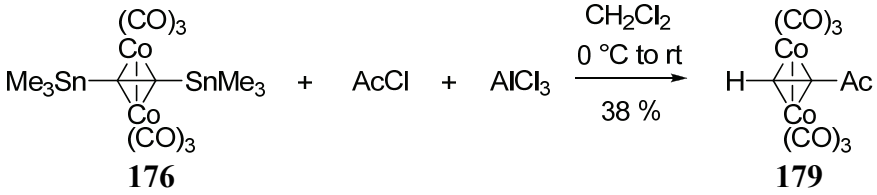

176 **179**

Scheme 91. Desilylation of **177**.[192]

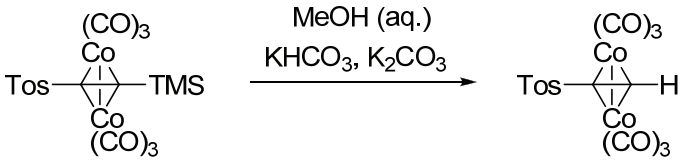

177 **180**

Scheme 92. Transformation of **178** into the amine and carbamate derivatives.[100]

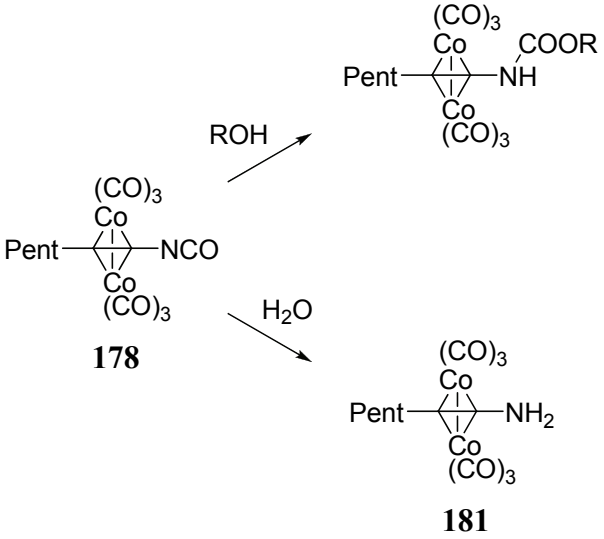

178 **181**

Finally, nitration of an appropriate complex might lead to **24** (Scheme 93).

Scheme 93. Nitration route to **24**.

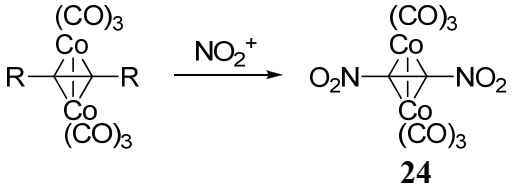

24

The next section begins with a brief summary of the properties of hexacarbonyldicobalt alkyne complexes, and subsequent sections describe our efforts to prepare a complex of DNA by the methods described above, including the successful syntheses of **25** and **26**.

3.2 General Properties of Hexacarbonyldicobalt Alkyne Complexes

The first example of a hexacarbonyldicobalt alkyne complex was obtained in 1954 from the reaction of 1,2-diphenylethyne (**182**) with **23**.[193] Numerous analogs have been synthesized since then, and all are red to purple, volatile, crystalline solids or oils.[67,95,98,194,195,196,96,197] These compounds decompose very slowly in air at room temperature,[95] and more quickly in solution.[198] Alkyne substituents affect the ease of formation and stability of the corresponding complexes.[96,95] Electron donating substituents accelerate coordination because they trap the intermediate $Co_2(CO)_7$ more effectively.[198,94] Electron withdrawing groups have the opposite effect, but form more stable compounds because of strong back bonding from the metal centers.[96] The enforced ligation of unreactive alkynes is limited to temperatures below 50 °C, above which cobalt clusters appear.[199,200] The coordinated alkyne has characteristics of both an alkyne excited state and an alkene: π^* orbitals are partially filled by back bonding, substituents are bent out of linearity with the alkyne carbons in a *cis* fashion, and the triple bond character of the alkyne is diminished, changing the hybridization of the ligated carbons toward sp^3.[201,185,95] These generalities are supported by spectroscopic observation, detailed below.

Ultraviolet-Visible (UV-Vis) spectra are reported for only a handful of complexes, mostly bearing aryl substituents,[202,203,204,205] and are not well defined, featuring a maximum absorption at the solvent cutoff (~ 218 nm), followed by several shoulders, in the range of 275–290 nm ($\log \varepsilon = 4.3$) for some systems,[202] around 435–450 nm ($\log \varepsilon$ = 3.1–3.3) for all.[202] This latter absorption, sometimes accompanied by a weaker signal between 550–565 nm ($\log \varepsilon = 2.8$–2.9), colors these complexes red.[202]

Infrared spectra are principally characterized by very strong carbonyl absorptions around 2100–2000 cm^{-1}. Depending on symmetry, five or six bands appear [$\tilde{\nu}_1$(A1), $\tilde{\nu}_2$(A1), $\tilde{\nu}_4$(B1), $\tilde{\nu}_5$(B1), $\tilde{\nu}_6$(B2), and sometimes $\tilde{\nu}_3$(A2)],[198,202] although $\tilde{\nu}_2$(A1) and $\tilde{\nu}_6$(B2) often overlap, and only $\tilde{\nu}_1$(A1), $\tilde{\nu}_2$(A1), $\tilde{\nu}_4$(B1), and $\tilde{\nu}_6$(B2) are strong, resulting in the observation of only three bands in lower resolution spectra.[193] Electronegative substituents on the coordinated alkyne draw electron density away from the cobalt centers, decreasing the back bonding to the carbonyl groups, in turn shifting these bands to higher wavenumbers (typically ~ 5–15 cm^{-1}), while electron donating groups effect the opposite.[198,205,96,206,95] Similarly, substitution of more electron rich ligands, such as phosphines or arsines, for carbonyls decreases the carbonyl bands ~ 20–40 cm^{-1}. Alkyne C–H stretching vibrations occur around 3100 cm^{-1},[98] close to the value of free terminal alkenes, signaling that the hybridization of the alkyne carbon has pronounced sp^2 character.[185] This change is also evident in the triple bond absorption, which changes from ~ 2200–2100 cm^{-1} in free alkynes to ~ 1630–1480 cm^{-1} when coordinated.[185] At the low energy end of the spectrum, cobalt-carbonyl bending is observed around 570–510 cm^{-1},[207,208] cobalt-carbonyl stretching around 510–420 cm^{-1},[207] and cobalt-alkyne vibrations at 610–550 and 400 cm^{-1}.[207,208,209,185,202] Cobalt-cobalt

bonds are unobservable on most instruments, producing bands in the far IR around 200 cm^{-1}.[209]

By analyzing the effects of coordination on the carbonyl and alkyne absorptions, Meyer et al. were able to calculate a rough estimate of the relative strengths of forward (σ) and back (π) donation to and from the acetylene ligand:[207]

> "Indeed, the generally accepted structure for metal-alkyne bonding involves σ-donation from the alkyne π-electron density to an empty metal *p* or *d* orbital and back donation from a filled metal *d* (or *dp* hybrid) orbital to an alkyne π^* orbital. σ-donation reduces the π-electron density of the acetylenic triple bond and thus lowers the IR frequency. Back donation into the π^*-level also weakens the triple bond. Thus, both σ- and π-coordination lower $\tilde{\nu}_{C\equiv C}$; their effect is additive ($\sigma + \pi$)."[207]

When coordinated, the alkyne appears to be a double bond by IR frequency (~ 1560 cm^{-1}), a shift of ~ 650 cm^{-1} from a triple bond. Because the bond order is decreased by one, coordination is assumed to be the equivalent of a two electron transfer, and thus: $(\sigma + \pi) = (\Delta\tilde{\nu}_{C\equiv C} / 650\ cm^{-1}) \times 2$ electrons.[207]

At the same time, the carbonyl absorptions describe the difference between forward and back donation:

> "Turning to the metal-CO interaction, the $\tilde{\nu}_{CO}$ frequency is a good indicator of the net charge on the metal. Previous work permits a quantitative estimate of this charge as a function of the decrease of $\tilde{\nu}_{CO}$: in the monoanion $Co(CO)_4^-$ the decrease is about 100 cm^{-1} with respect to $\tilde{\nu}_{CO}$ in the neutral compound $Co_2(CO)_8$. A similar result is obtained when one or more carbonyl ligands are replaced by strong donor ligands. It is thus possible to calculate the net charge transferred from the alkyne to the metal in the complexes $(RC\equiv CR')Co_2(CO)_6$. This quantity is given by the difference between σ-donation from and back-donation to the alkyne ($\sigma - \pi$)."[207]

Comparison of average[§§] $\Delta\tilde{\nu}_{CO}$ of a specific compound to the $Co(CO)_4^-$ / $Co_2(CO)_8$ system gives: $\sigma - \pi = \Delta\tilde{\nu}_{CO} / 100\ cm^{-1}$.[207] With values for both $(\sigma + \pi)$ and $(\sigma - \pi)$, both σ and π are realized by solving for a system of equations.

For example, [μ-3,3,3-trimethyl-prop-1-yne-1,2-diyl]bis(tricarbonylcobalt)(*Co–Co*) (**183**) has an average $\tilde{\nu}_{CO}$ of 2051 cm^{-1}, 17 cm^{-1} less than that of $Co_2(CO)_8$ (2068 cm^{-1}), which leads to $\sigma - \pi = 0.17$.[207] For the alkyne absorptions, $\Delta\tilde{\nu}_{C\equiv C}$ is 583 cm^{-1}, yielding $\sigma + \pi = 1.79$.[207] Solving the system produces: $\sigma = 0.98$ and $\pi = 0.81$. Alone, each number is meaningless, but together, they show that forward donation is greater than back donation in this complex. When compared with the results of the more electron withdrawing CF_3 substituents of [μ-1,1,1,3,3,3-hexafluoro-but-2-yne-1,2-

---

[§§] For higher resolution spectra, average $\Delta\tilde{\nu}_{CO}$ is calculated by the following equation: average $\Delta\tilde{\nu}_{CO} = \{[(\tilde{\nu}_2 + \tilde{\nu}_6) / 2] + \tilde{\nu}_1 + \tilde{\nu}_4\} / 3$.

diyl]bis(tricarbonylcobalt)(*Co–Co*) (**184**) (σ = 0.985 and π = 1.205),[207] forward donation appears to be similar in magnitude, but the back donation to the alkyne ligand is much greater in **184**.

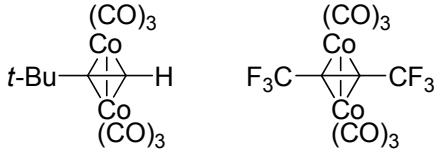

183 **184**

From their survey, Meyer et al. found that $\sigma > \pi$ for alkynes bearing electron donating or poorly withdrawing substituents, $\sigma \approx \pi$ for alkynes with one electron withdrawing substituent, and $\sigma < \pi$ for alkynes substituted with two electronegative groups.[210]

The mass spectra of these complexes contain weak molecular ions, sometimes unobservable,[211,202] and carbonyl loss is facile.[202] A peak for $[Co(alkyne)]^+$ is usually found, as are free alkyne and its fragments.[202] Recombination products are noted, and for long ion dwell times, substituted benzene peaks corresponding to cyclotrimerization have been observed.[202]

Hexacarbonyldicobalt alkyne complexes are diamagnetic and thus conveniently observed by NMR spectroscopy. Counterintuitively, coordination to the electron rich cobalt atoms deshields acetylenes, shifting terminal alkyne hydrogens ~ 4 ppm to δ 6.0–6.5 ppm, and alkyne carbon signals ~ 5–20 ppm to δ 70–115 ppm.[212,95] Forward donation of the alkyne π system to the empty *d* orbitals on cobalt disrupts the cylindrical distribution of electrons around the alkyne responsible for significant shielding.[95] This severely decreases inductive transmission through the alkyne π bonds, noted by the effect of substituents on free and coordinated acetylenes.[201] For example, phenyl substitution of acetylene (δ 1.80 ppm) causes deshielding of the terminal hydrogen by $\Delta\ \delta$ 1.13 ppm.[201] The corresponding signals of their complexes (δ 5.97 and 6.28 ppm, respectively), differ by only $\Delta\ \delta$ 0.31 ppm.[201] Both deshielding and hindered induction are more pronounced in the ^{13}C NMR spectra. For example, the signal for the terminal carbon of propyne (**185**) (δ 67.6 ppm) is upfield from its internal alkyne counterpart (δ 80.1 ppm).[95] On coordination, both alkyne carbons are deshielded, the terminal carbon by δ 5.4 ppm, and the internal by δ 10.7 ppm.[95] Alkyne substituents affect magnitude and direction of chemical shifts on coordination, but examination of the data shows multiple factors at work that preclude simple generalizations. Happ et al. tried correlating chemical shifts of free and coordinated alkyne carbons, as shown in Figure 10.

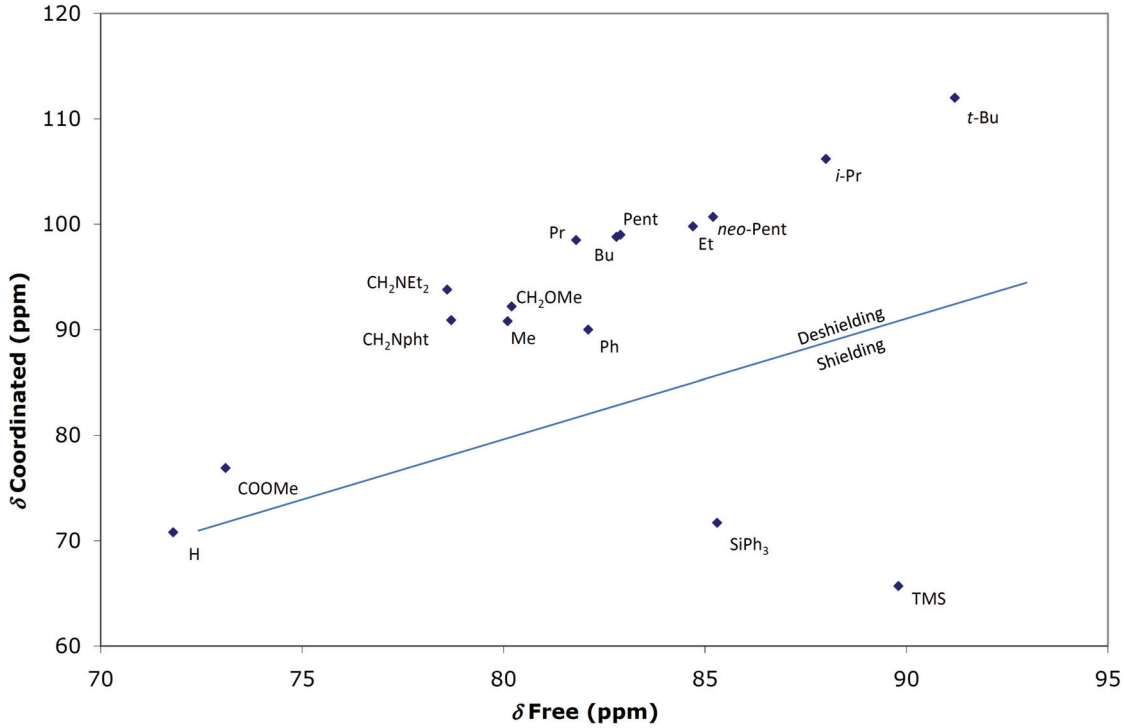

Figure 10. Comparison of free and coordinated ^{13}C NMR chemical shifts of internal alkyne carbon as originally presented by Happ et al.[95] Vertical distance from line denotes magnitude of shielding.

The line drawn through the center represents no change on coordination. Points above it are deshielded, those below shielded by coordination, and the vertical distance from the line indicates the magnitude of this change. While the alkyl groups approximate a line correlating to electronegativity, silyl substituents and heteroatom substituted alkyl groups are outliers. Poor correlation of change in chemical shift with substituent electronegativity is also evident in the proton spectra as seen in Figure 11.

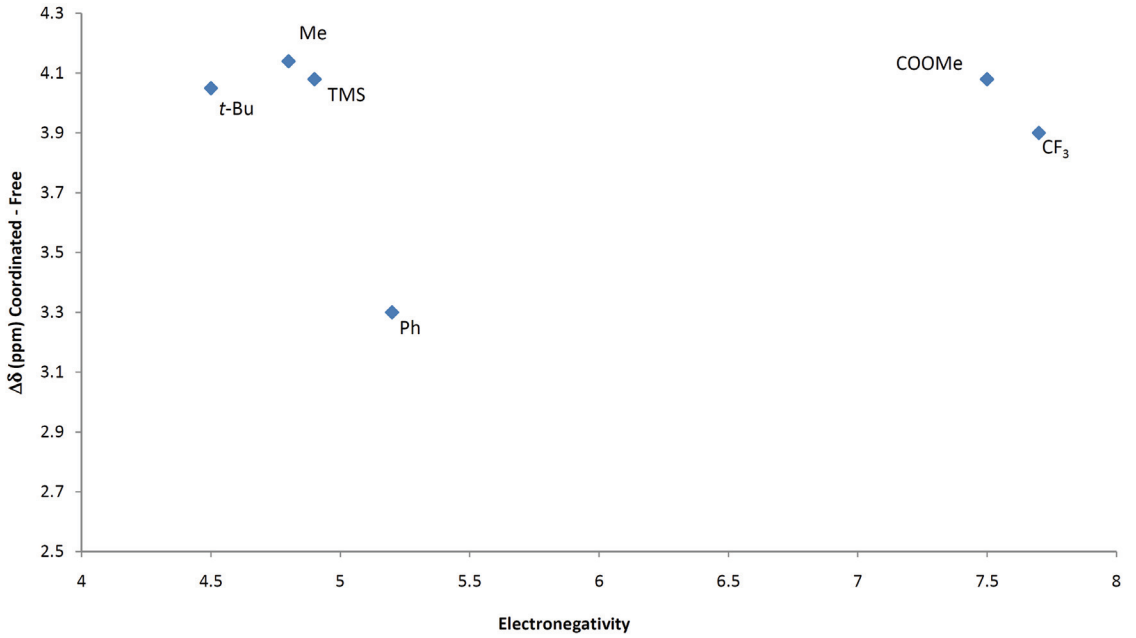

Figure 11. Lack of correlation between electronegativity and change in ^{1}H NMR chemical shift on alkyne coordination.[95,201,211] Electronegativity values taken from Golovin et al.[178] for consistency.

These data underscore the complexity of the changes in the NMR spectra brought about by ligation. Prediction of these changes is not possible based on our current knowledge of these systems.

The hybridization of coordinated alkyne carbons is not clear from NMR data. Proton NMR spectra of terminal alkyne complexes show signals in the alkene region, suggesting an sp^2 hybridization, while carbon NMR signals and C–H coupling constants (J_{CH} = 220–225 Hz)[185] place hybridization between sp and sp^2. No correlation between substituents and coupling constant has been observed.[185]

Carbonyl ligands appear at ~ δ 200 ppm in the ^{13}C NMR spectrum, usually as a single broad signal at room temperature due to spin-spin coupling with cobalt (I = 7/2), an absorption which resolves at –80 °C to either two resonances in a 1:2 ratio for symmetric or three resonances for asymmetric alkyne systems.[201] Experiments with trialkylphosphine pentacarbonyldicobalt alkyne derivatives indicate the occurrence of carbonyl fluxionality, as seen in isoelectronic relatives.[201]

X-ray crystallography shows that alkyne carbons form a tetrahedron with the cobalt atoms of such complexes.[215] The cobalt-cobalt bond is shortened compared to **23**, and the carbon-carbon bond is lengthened relative to the free alkyne. For example, in the case of (μ-1,2-diphenylethyne-1,2-diyl)bis(tricarbonylcobalt)(*Co–Co*) (**186**), the former is shortened to 2.47 Å from 2.52 Å[73] and the latter lengthened to 1.36 Å from 1.19 Å. Thus, on this basis, the coordinated alkyne carbons adopt a hybridization close to sp^2 (sp^2 = 1.33 Å, sp^3 = 1.54 Å).[213] These distances are typical of Co–Co and alkyne C–C bonds, between 2.445–2.489 Å and 1.28–1.37 Å, respectively.[95] These bond lengths do not correlate with each other, nor do they correlate to a single factor, such as substituent size, substituent electronegativity, or $\tilde{\nu}_{C\equiv C}$. As a result of coordination, substituents are bent

away from the metal centers, out of co-linearity with the acetylenic bond.[214] The angle of deformation is approximately 130–150 °,[214] which, in contrast to the bond distances, suggests that the acetylenic carbons are between *sp* and sp^2-hybridized.[215] The bond angles between the alkyne and substituent exhibit an trend inversely proportional to the electronegativity of the latter, as shown in Figure 12.

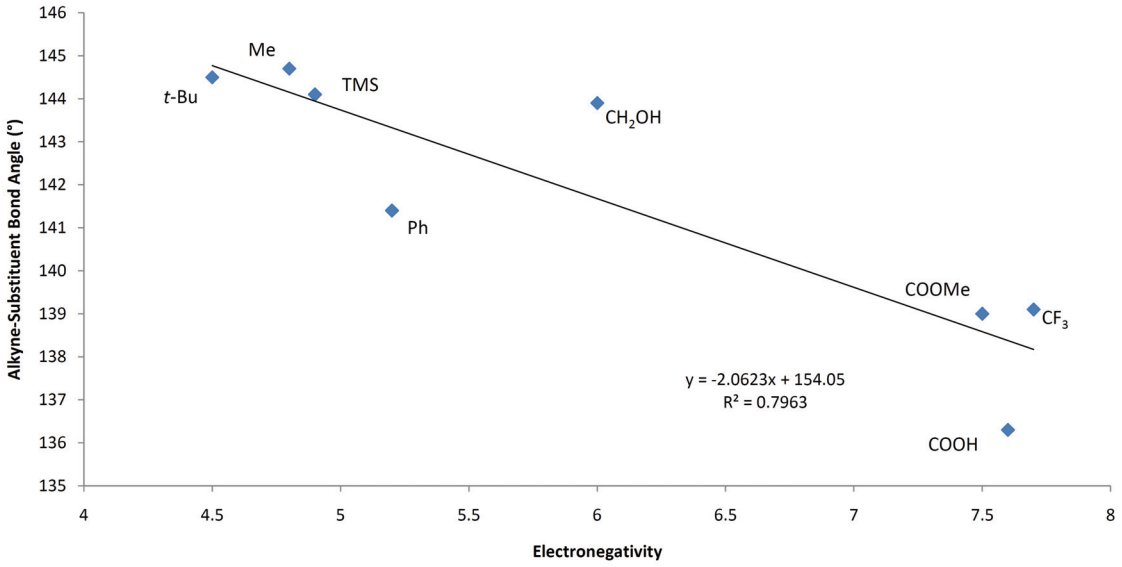

Figure 12. Correlation of substituent electronegativity with alkyne-substituent bond angle.[216,95,217,218,219,220,221,222,223,225,224,226,227,228,229,230,231,232,233,234,235,236] Electronegativities taken from Golovin et al.[178] for consistency.

This trend indicates a shortening of cobalt-alkyne carbon bond lengths with increasing substituent electronegativity. Such groups increase electron demand by the alkyne and thus promote stronger back donation from the cobalt centers, in effect 'pulling' them closer to the alkyne carbon to which they are attached. Cobalt-alkyne carbon distances range from ~ 1.92–2.05 Å (Figure 13). No trend could be discerned when these distances were compared with ^{13}C NMR chemical shifts for the relevant carbons.

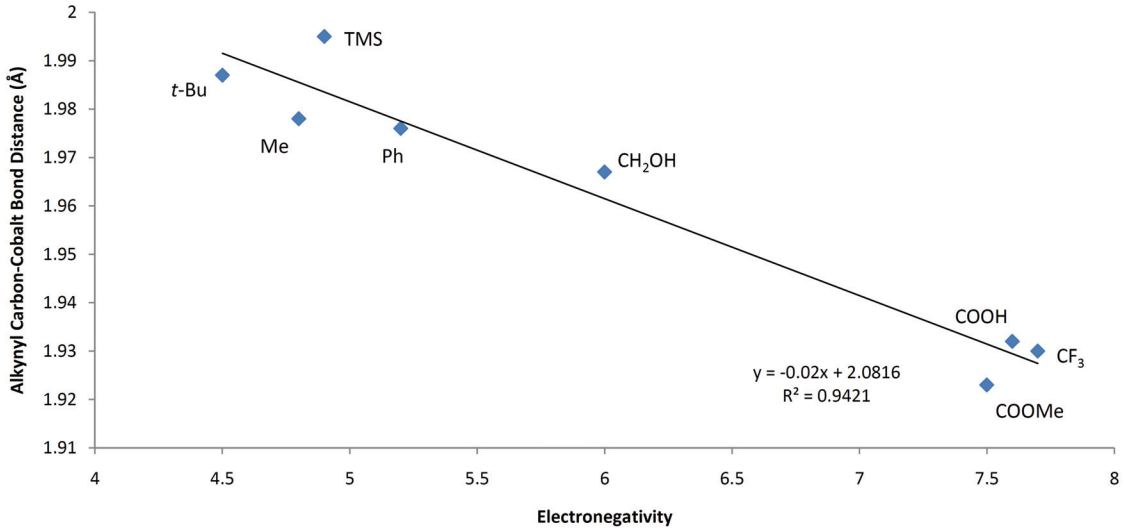

Figure 13. Effect of substituent electronegativity on alkyne carbon to cobalt bond distance for selected complexes.[216,95,217,218,219,220,221,222,223,225,224,226,227,228,229,230,231,232,233,234,235,236] Electronegativities taken from Golovin et al.[178] for consistency.

X-ray data provide the simplest correlation with substituent electronegativity of all the spectroscopy known for hexacarbonyl dicobalt alkyne complexes.

Only a few cyclic voltammetry (CV) studies of such complexes have been reported,[237,238,239,240,236] and many focus on those partially substituted by phosphine ligands. Most undergo irreversible reduction at room temperature, even at fast scan rates. Reactions reversible only at lower temperatures or faster scan rates are considered quasi-reversible. Electron withdrawing substituents help increase the stability of the radical anion formed by delocalizing the negative charge and, thus, also increase the $E_{1/2}$. Substituent electronegativity cannot be the only factor affecting stability of the radical anion, because [μ-3,3,3-trifluoro-1-(trimethylsilyl)-prop-1-yne-1,2-diyl]bis(tricarbonylcobalt)(*Co–Co*) (**189**), which bears an electropositive TMS group, has a greater $E_{1/2}$ than [μ-3,3,3-trifluoro-prop-1-yne-1,2-diyl]bis(tricarbonylcobalt)(*Co–Co*) (**190**), without it (Table 12).

Table 12. $E_{1/2}$ reduction potentials for selected hexacarbonyldicobalt alkynes.[237,238,239,240,236]

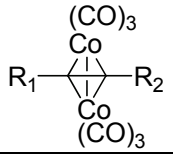

Compound	R_1	R_2	$E_{1/2}$ (V)
187	*t*-Bu	*t*-Bu	–1.03
183	*t*-Bu	H	–1.03
188	Ph	H	–0.90
186	Ph	Ph	–0.82
190	CF_3	H	–0.76
189	TMS	CF_3	–0.68
184	CF_3	CF_3	–0.51

Very little information about the thermal analysis of cobalt complexes is available.[241,236] Differential scanning calorimetry (DSC) and thermogravimetric analysis (TGA) have shown an initial brief exotherm followed by an endotherm, thought to indicate exothermic polymerization followed by complete carbonyl loss.[241]

With the preceding brief description of the general properties of hexacarbonyldicobalt complexes in mind, the following section describes our efforts toward producing complexes **24**, **25**, and **26**.

3.3 Results and Discussion

3.3.1 Trapping Strategy

The simplest approach to ligating a reactive organic molecule is by *in situ* trapping. This method was deemed advantageous for nitroalkynes, because it avoided their isolation, and we planned to use **23** to trap DNA directly, since efforts to do so in the case of **16**, **36**, and **169** as potential precursors to **24** had failed (Chapter 2, Section 2.7.1 and 2.7.2). Our efforts in this area are detailed below.

Analogous to the nitrations of Petrov et al.[118,119] (Chapter 2, Section 2.3.1), **171** was treated with N_2O_4, then transferred to a solution of **23** (Scheme 94).

Scheme 94. Attempted nitration of **171** with N_2O_4.

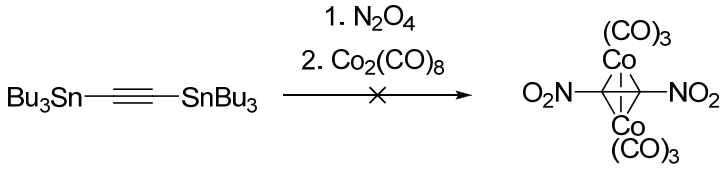

171 **24**

Following workup, only unreacted **23** remained. Similar to the results of Loevenich et al.[137,138] and Petrov et al.[118,119] (Chapter 2, Sections 2.3.1 and 2.3.2), a red oil, which

showed no acetylenic bands in the IR spectrum, had precipitated in the reaction flask prior to transfer of the mother liquor, implying that nitration had not occurred. These negative results deterred subsequent nitrations of trialkyltin acetylenes with N_2O_4.

Schmitt et al. and Woltermann failed to isolate nitration products from the reaction of NO_2BF_4 with **18**.[109,90] With the thought that some DNA might exist in solution, the crude reaction mixture of **18** with NO_2BF_4 was exposed to **23** (Scheme 95).

Scheme 95. Attempted nitration of **18** and trapping of products.

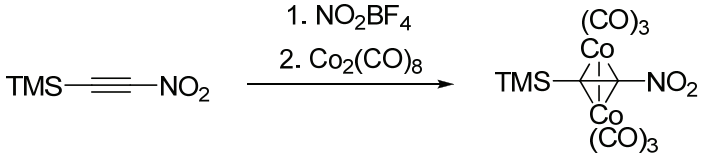

18 **25**

Only complex **25** was obtained (the synthesis of which is described in Section 3.3.4), supporting the claims of Schmitt et al. and Woltermann that **18** did not react with NO_2BF_4.

Our final efforts toward trapping DNA were based on the elimination protocol of Eaton et al.,[115] shown previously in Chapter 2, Section 2.4 (Scheme 53). This procedure had been conducted in the presence of Cp, which ostensibly trapped DNA as a Diels-Alder adduct. We substituted **23** for Cp to trap DNA as **24** (Scheme 96).

Scheme 96. Attempted elimination trapping of DNA with **23**.

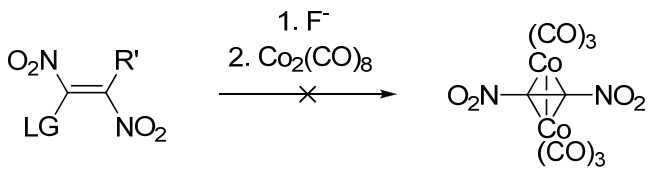

LG = leaving group **24**

No alkyne complexes were detected and unreacted **23** was evidenced by TLC. The procedure was repeated at 50 °C, but the results were the same. None of the starting alkene was recovered, indicating that it had reacted with fluoride ion. Control experiments showed tolerance of **23** to the solvent system, fluoride source, and the starting alkene. These observations suggest that alkynes failed to form or decomposed prior to attack by **23**.

The failure of the preceding attempts prompted the exploration of a functional group transformation strategy, involving what was hoped to be more readily accessible alkyne complexes bearing functions that were deemed to be precursors to the nitro group.

3.3.2 Functional Group Transformation Strategy

Two potential direct precursors to **24** are the unknown (μ-1,2-diaminoethyne-1,2-diyl)bis(tricarbonylcobalt)(*Co–Co*) (**191**) and [μ-1,2-bis(isocyanato)ethyne-1,2-diyl]bis(tricarbonylcobalt)(*Co–Co*) (**192**). Because of spectroscopic evidence of similar complexes in solution[100] and proven oxidation of amines[242] and isocyanates[243] to nitro groups by dimethyldioxirane (DMDO), we hoped that **191** and **192** might be oxidized to **24** without demetallation, as is the case for certain combinations of oxidizing agents and complexes (Scheme 97).[97,244]

Scheme 97. Proposed oxidation of **191** or **192** to **24**.

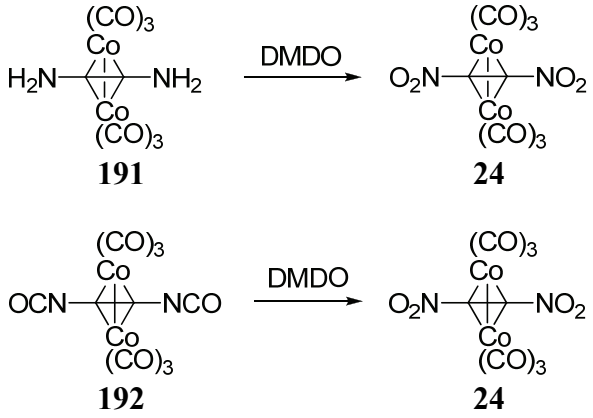

This section explores our efforts at their synthesis, which involved various approaches to harnessing the inherent reactivity of acetylenedicarboxylic acid and its derivatives. As will be seen in the following summary, these attempts proved futile.

We began our investigation by exploring the preparation of amine **191**. The desired ligand, 1,2-diaminoethyne (**193**), is unknown, because it is unstable with respect to ketenimine tautomerization,[245] precluding the synthesis of **191** by the trapping approach. However, Schottelius et al. have provided evidence for a related 1-heptynyl-1-amine complex, made in solution by hydrolysis of the corresponding isocyanate,[100] providing encouragement for a ligand modification route to **191**. Accessing **191** would require three steps from the known 1,2-bis(amido)ethyne (**194**),[246] and include [μ-1,2-bis(amido)ethyne-1,2-diyl]bis(tricarbonylcobalt)(*Co–Co*) (**195**), its conversion[247] to {μ-1,2-bis[*N*-(*t*-butoxycarbonyl)amino]ethyne-1,2-diyl}bis(tricarbonylcobalt)(*Co–Co*) (**196**), followed by hydrolysis (Scheme 98).

Scheme 98. Proposed synthetic path to **191** from **194**.

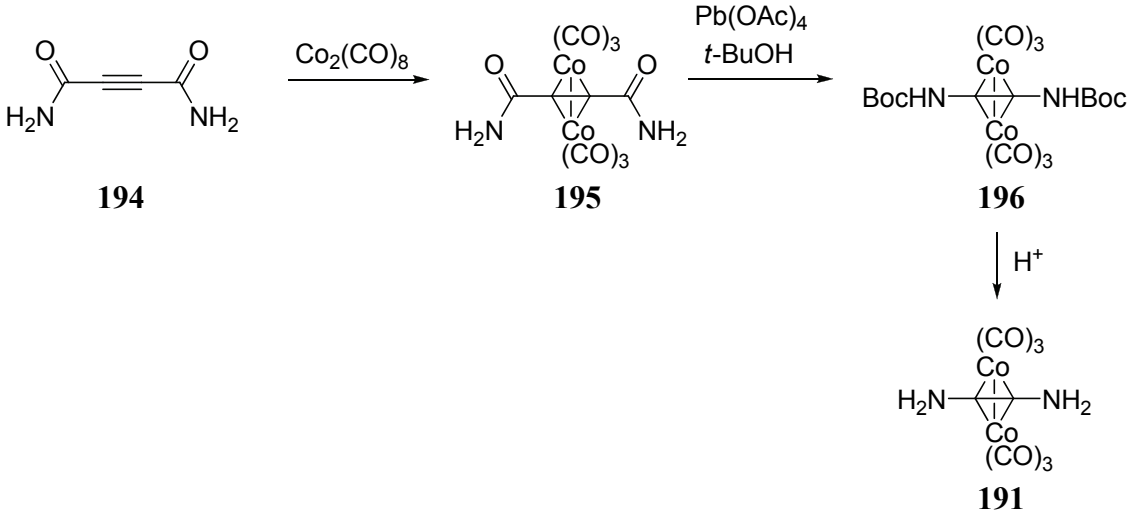

Low temperature reaction of the commercially available dimethyl acetylenedicarboxylate (**197**) with ammonium hydroxide was reported to have produced **194** (Scheme 99).[246]

Scheme 99. Bisamidation of **197** with ammonium hydroxide.[246]

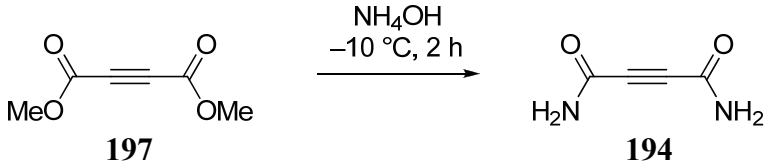

In accordance with the literature procedure, a tan precipitate quickly formed. However, ^{1}H NMR spectroscopy revealed contaminants, and the melting point after recrystallization (168–170 °C) conflicted with the incongruous literature values of 190–192 °C[246] and 290–292 °C.[248] Subsequent recrystallizations did not change the melting point or clarify the ^{1}H NMR spectrum. The mass spectrum revealed a molecular ion of m/z = 144, confirming that **194** (m/z = 112) had not formed.

Stymied by these difficulties, we pursued an alternative approach to **196** in Scheme 96 from the known [μ-(but-2-ynedioic acid)-1,2-diyl]bis(tricarbonylcobalt)(*Co–Co*) (**198**) and diphenylphosphoryl azide (DPPA) (Scheme 100).

Scheme 100. Proposed synthesis of **196** from **198**.

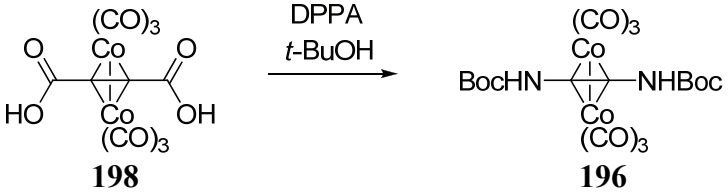

Complex **198** had been accessed from but-2-ynedioic acid (**199**) and **23** under forcing conditions in a carbon monoxide atmosphere (Scheme 101).[96]

Scheme 101. Formation of **198** from **199** and **23**.[96]

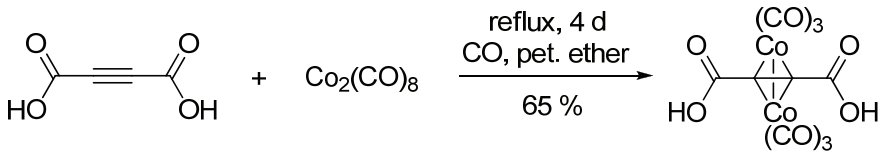

199 **23** **198**

Before engaging in this challenging preparation, we sought [μ-(prop-2-yne carboxylic acid)-1,2-diyl]bis(tricarbonylcobalt)(*Co–Co*) (**200**) as a test case to probe its reactivity. To this end, we treated 2-propynoic acid (**201**) with **23** (Scheme 102).

Scheme 102. Unsuccessful ligation of **201** by **23**.

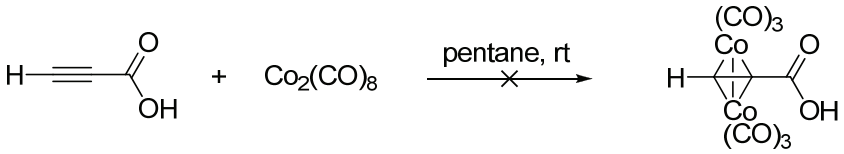

201 **23** **200**

Vigorous gas evolution, usually an indicator of successful ligation, was noted, and, after workup, bright red crystals with a sublimation point of 82–84 °C were obtained. These crystals enjoyed solubility in toluene and diethyl ether, along with moderate solubility in pentane, unlike **198.**[96] Carbonyl peaks in the IR spectrum at 2106, 2068 and 2033 cm^{-1} were similar to literature values (2107, 2065, and 2031 cm^{-1}),[236] as were two weaker bands (1664 and 1476 cm^{-1}), most likely corresponding to the acid carbonyl and the coordinated alkyne bond (1661 and 1474 cm^{-1} lit.).[236] Addition of deuterated chloroform caused the red crystals to become gummy and paramagnetic, preventing collection of NMR data. Although the IR spectrum was consistent with reported values for **200**, the behavior of the product in deuterated chloroform was not. Similar IR frequencies are noted for $Co_3(CO)_9$(alkyne) complexes, known to form with terminal alkynes in the presence of acid,[198,236] raising questions of its composition. Without further spectra, insufficient data exist to assign this structure conclusively.

Unable to prepare **200**, we turned to **199** (Scheme 103).

Scheme 103. Attempted reaction of **199** with **23**.

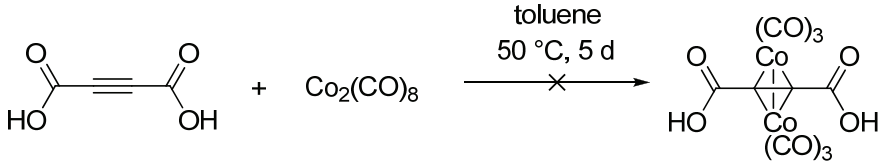

199 **23** **198**

Conditions were similar to the literature,[96] but avoided the dangerous carbon monoxide, and after five days, no reaction was observed. Sonication failed to promote it and decomposed the starting material. Discouraged by the problems with **195** and **198**, we turned to **192**.

Our approach to **192** was inspired by the multistep transformation of oct-2-ynoic acid (**202**) into **178** by Schottelius et al. (Scheme 104).[100]

Scheme 104. Schottelius' transformation of **202** into **178**.[100]

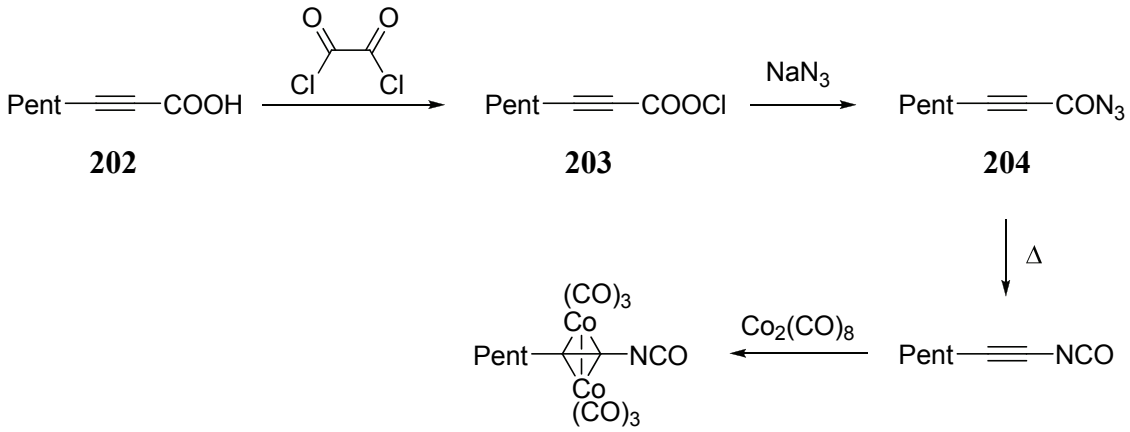

The route planned to **192** was similar (Scheme 105), but applied the cobalt reagent before acyl azide formation to mitigate friction sensitivity[249] and avoid [3 + 2] cycloaddition of the azide to the free alkyne bond.[78]

Scheme 105. Proposed transformation of **199** into **192**.

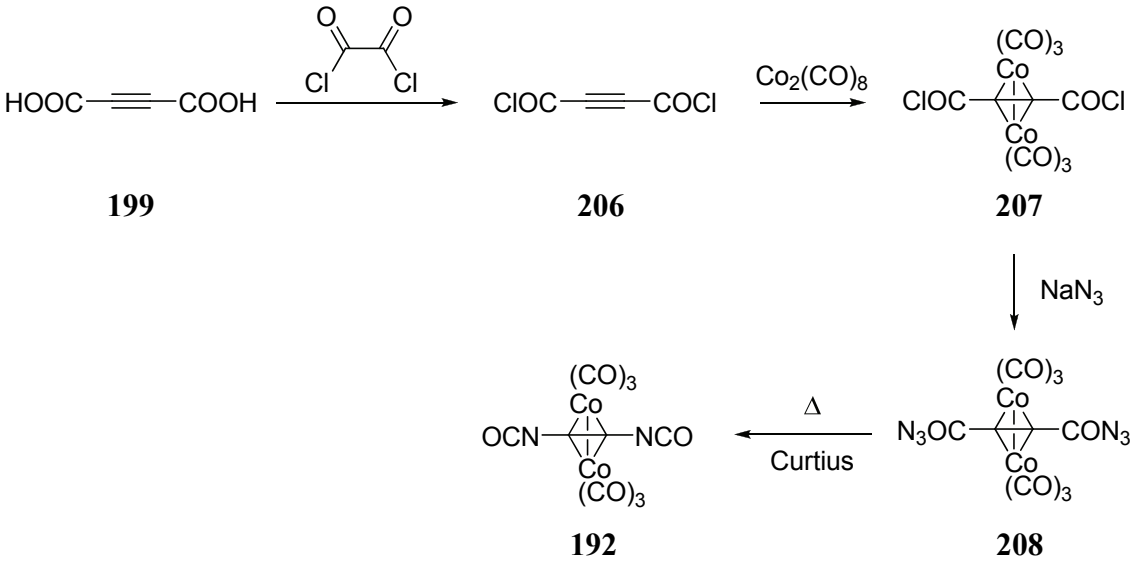

Acyl azides are commonly prepared from acid chlorides and azides,[251] so [μ-1,2-bis(acid chloride)ethyne-1,2-diyl]bis(tricarbonylcobalt)(*Co–Co*) (**207**) was chosen as the precursor to [μ-1,2-bis(acylazido)ethyne-1,2-diyl]bis(tricarbonylcobalt)(*Co–Co*) (**208**), which could provide access to **192** by a Curtius rearrangement.[250] The key steps, however, were the synthesis and coordination of the known acyl chloride **206**.

Two preparations for **206** exist: reaction of 11,12-bis(acid chloride)-9,10-dihydro-9,10-ethenoanthracene (**209**) with maleic anhydride (**210**) (Scheme 106), and treatment of **198** with PCl_5 (Scheme 107).

Scheme 106. Diels' reaction of **209** with **210** to form **206**.

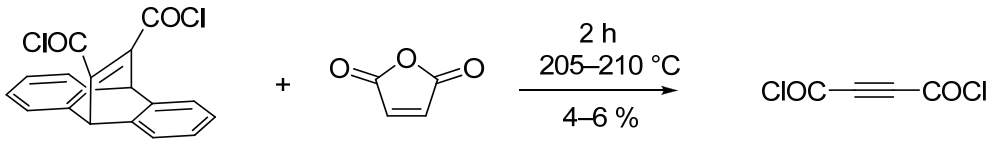

209 **210** **206**

Scheme 107. Preparation of **206** from **199** and PCl_5.

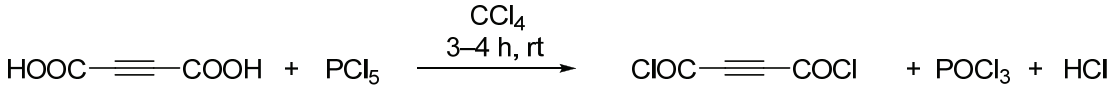

199 **206**

The former, reported by Diels in 1938, furnished pure **206** in poor yield (4–6 %),[252] while the latter method afforded **206** contaminated with $POCl_3$ and HCl, two compounds incompatible with **23**.[253] To avoid these problems, we modified the Vilsmeier reaction[254] of Schottelius[100] to give **206** (Scheme 108). Immediate gas evolution and darkening was noted on addition of DMF to a mixture of oxalyl chloride and **199**, indicating formation of the Vilsmeier-Haack reagent.

Scheme 108. Unsuccessful Vilsmeier reaction to form **206**.

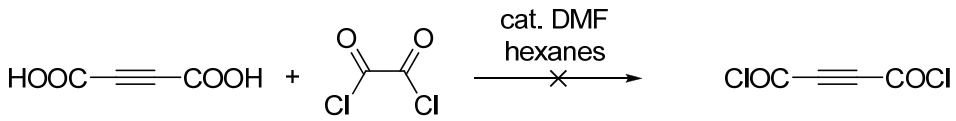

199 **206**

The IR spectrum of the product did not match the literature,[255] and reaction with methanol did not provide any **197**, as evidenced by ^{1}H NMR spectroscopy. With simpler options to **209** yet unexplored, we did not pursue **206** by Diels's method, leaving this project to future researchers.

The unknown [μ-1,2-bis(hydrazido)ethyne-1,2-diyl]bis(tricarbonylcobalt)(*Co–Co*) (**211**) is an alternative starting material for **208** via treatment with nitrous acid (Scheme 109).

Scheme 109. Proposed reaction of **211** with nitrous acid to give **208**.

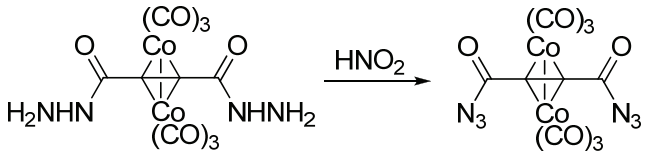

211 **208**

Because 1,2-bis(hydrazido)ethyne (**212**) had been reported previously from the commercially available diethyl acetylenedicarboxylate (**213**),[256,257,258,259] we planned to synthesize and treat it with **23** to afford **211**, as shown in Scheme 110.

Scheme 110. Proposed synthesis of **211** via **212**.[259]

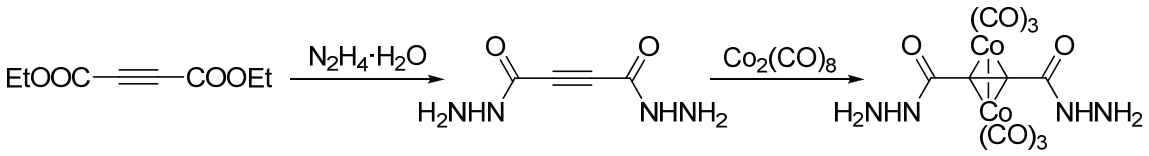

213 **212** **211**

The literature procedure called for **213** and hydrazine in ethanol heated to reflux (Scheme 111).[259]

Scheme 111. Reported formation of **212** from **213**.

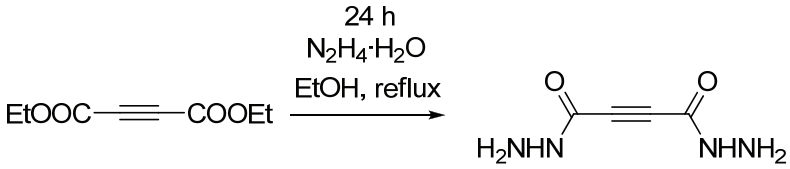

213 **212**

The off-white crude product had a similar melting point (188–190 °C vs. 187–189 °C lit.)[259] and IR spectrum to those reported by Mikroyannidis et al.,[259] but contained an extra signal at δ 5.8 ppm in the ^{1}H NMR spectrum. Recrystallization from hot water afforded translucent walnut-brown crystals, identified as 5-oxo-3-pyrazoline-3-carboxhydrazide (**214**) by their spectral characteristics.[260]

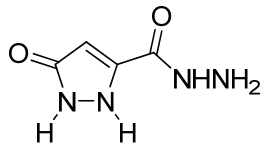

214

The proton NMR spectrum of **214** consisted of one sharp singlet at δ 5.96 ppm (lit. δ 6.03 ppm),[260] and four broad singlets. Signals for ring carbons appeared at δ 88.8 and 135.8

ppm in the ^{13}C NMR spectrum, along with two carbonyl peaks at δ 159.2 and 160.7 ppm (Patterson et al. reported one carbonyl signal at δ 160.08 on a low field instrument).[260] Differential scanning calorimetry (DSC) shows an endotherm at 201 °C prior to melting and decomposition at 236–240 °C, supporting the literature assertion that **214** exists as a hydrate.[260] The similarities of these data to those of Mikroyannidis et al.[259] call into question their structure assignment of **212**.

To probe the reactivity of a substituted hydrazine toward **213**, *N*-(*t*-butoxycarbonyl)hydrazide (**215**) was exposed to **213**. Instead of the sterically protected 1,2-[bis-*N*-(*t*-butoxycarbonyl)hydrazido]ethyne (**216**), however, a plethora of inseparable alkenes resulted (Scheme 112).

Scheme 112. Attempted production of **216** from **213**.

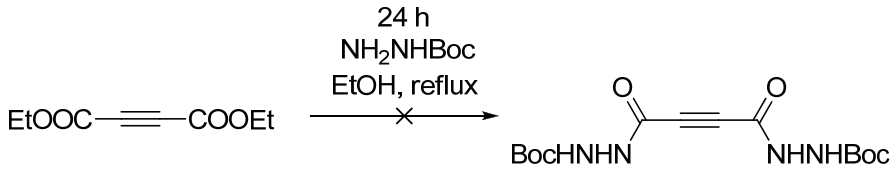

213 **216**

To circumvent evident nucleophilic attack, the triple bond of **197** was protected with **23**[67] and the resulting [μ-1,2-bis(dimethyl carboxylate)ethyne-1,2-diyl]bis(tricarbonylcobalt)(*Co–Co*) (**217**) was treated with hydrazine (Scheme 113).

Scheme 113. Deleterious addition of hydrazine to **217**.

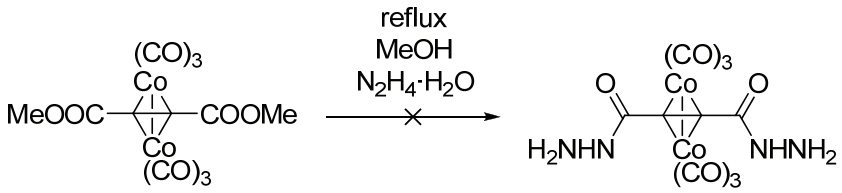

217 **211**

Nucleophiles sometimes attack the substituents on the alkyne ligand in preference to the carbonyls in such complexes,[253,100,261,262] but in this case, hydrazine was deleterious and only decomposition resulted.

In conclusion, our pursuit of **24** by functional group transformations of acetylenedicarboxylic acid and its derivatives failed. Future investigations along these lines should benefit from sterically protected hydrazide functionalities to prevent intramolecular and intermolecular nucleophilic attack. The next section details attempts to effect the nitrations of various alkyne[$Co_2(CO)_6$] complexes toward the same goal.

3.3.3 Strategy of Nitration of Alkyne[$Co_2(CO)_6$] Complexes

The simplest way to add a nitro group to a compound is by nitration. Many nitrating agents also oxidize, and, like nucleophiles, oxidizing agents can react selectively with certain substituents without demetallating cobalt complexes.[262,97] We sought to determine the reactivity of silyl, stannyl, and iodo complexes toward nitrating reagents on route to **24**. This section describes our efforts in that area.

Our inquiry began with the readily prepared silyl derivatives. [μ-1,2-Bis(trimethylsilyl)ethyne-1,2-diyl]bis(tricarbonylcobalt)(*Co–Co*) (**218**) was made from **72** and **23** in 92 % yield (Scheme 114).[67]

Scheme 114. Preparation of **218** from **72** and **23**.

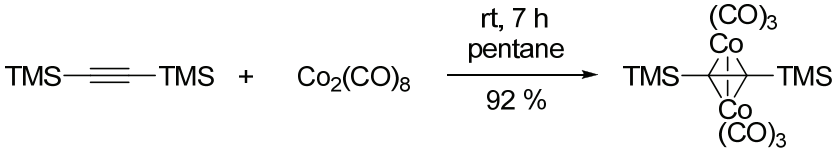

72 **23** **218**

Based on the success of prior desilylative nitrations,[263,109,108] **218** was exposed to NO_2BF_4 (Scheme 115).

Scheme 115. Destruction of **218** by NO_2BF_4.

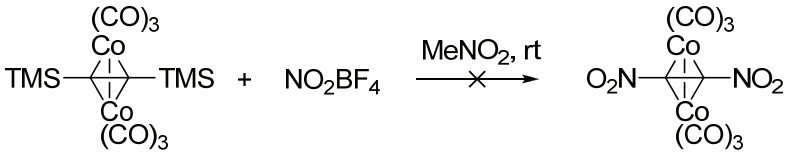

218 **24**

A pink, paramagnetic, intractable residue was resulted, indicating that oxidation was preferred over nitration. To mitigate this oxidation problem, we sought a more compatible nitrating agent.

Transfer nitrating agents are typically not powerful oxidizers, because they contain a NO_2^+-equivalent bound to a heteroatom as a neutral species, which is attacked by an anion of a suitable substrate.[264] Our attention turned to desilylation of **218** with fluoride to the corresponding anion **218a** and its subsequent nitration with **3** (PETN). Repetition of this scheme would lead to **24** (Scheme 116). We chose **3** because it is the most stable and least sensitive nitric ester, a class of compounds suitable for transfer nitration.[248]

Scheme 116. Strategy toward **24** via complexed alkyne anions.

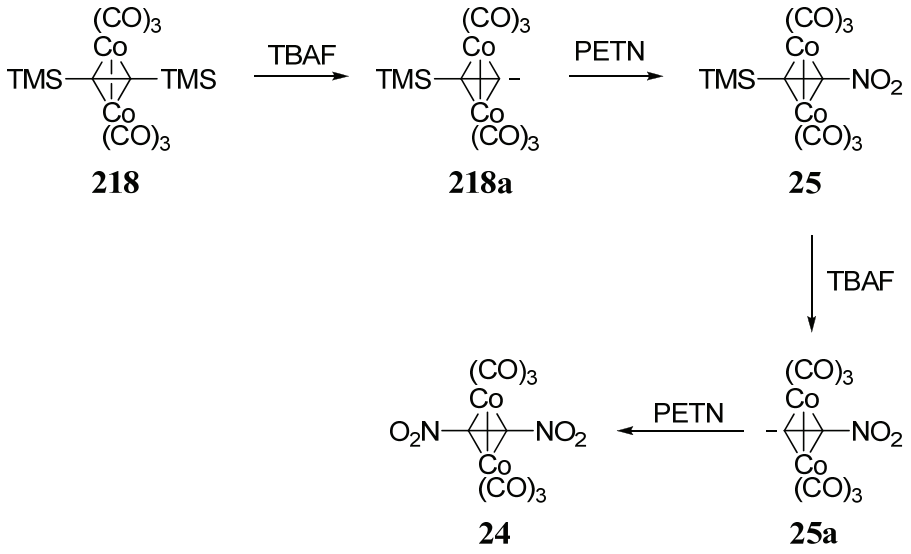

There was some indication in the literature that this scheme might be workable. In 1985, Magnus et al. subjected [μ-(trimethylsilyl)ethyne-1,2-diyl]bis(tricarbonylcobalt)(*Co–Co*) (**219**) to strong base.[99] The resulting species, purported **218a**, not only generated products of oxidative coupling, but could also be trimethylsilylated and benzylated[99] Unfortunately, addition of TBAF to **218** immediately decomposed it (Scheme 117).

Scheme 117. Attempted transfer nitration of **218** with TBAF and **3**.

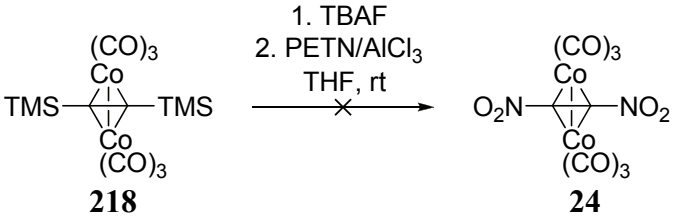

Destruction of **218** also occurred with potassium fluoride in protic solvent without formation of **219** or [μ-ethyne-1,2-diyl]bis(tricarbonylcobalt)(*Co–Co*) (**220**) (Scheme 118).

Scheme 118. Attempted protodesilylation of **218** with KF.

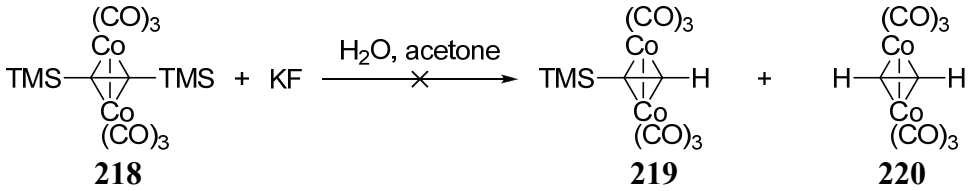

That fluoride attacked the metal rather than silyl moieties was confirmed by subjecting **188**, a compound containing no silyl groups, to TBAF (Scheme 119).

Scheme 119. Destruction of **188** by TBAF.

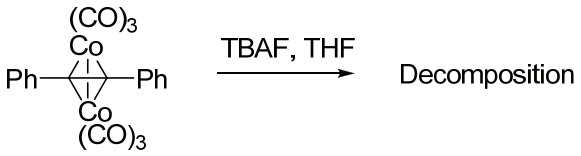

188

Reaction was immediate, leaving only a light orange paramagnetic residue. These results do not conclusively show that desilylation of **218** is untenable, but do imply that fluoride ion is deleterious.

To probe whether simple protodesilylation was possible, **218** was treated with trifluoroacetic acid (TFA) (Scheme 120).

Scheme 120. Attempted protodesilylation of **218** with TFA.

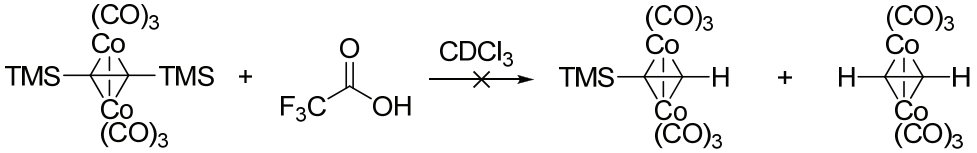

218 **219** **220**

Demetallation was quick but incomplete even with a 10-fold molar excess of TFA. Unreacted **218** and freed **72** were noted by ^{1}H NMR spectroscopy, but there was no evidence for the formation of **219** and/or **220**.

Desilylation of **218** was also attempted with potassium carbonate in methanol (Scheme 121).

Scheme 121. Attempted reaction of **218** with methanolic K_2CO_3.

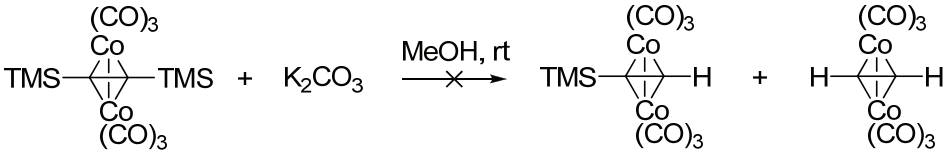

218 **219** **220**

This procedure destroyed **218** in fifteen minutes, without a trace of **219** or **220**. Destruction of such complexes by base is not without precedent,[205] but is puzzling in view of the successful protodesilylations of related mono(trilethylsilyls) complexes executed by Dickson,[206] and our later success with **26** (see Section 3.3.5).

Having failed to create anion **218a** from **218**, we repeated Magnus's deprotonation protocol for **219**,[99] followed by addition of **6** (tetryl) (Scheme 122).

Scheme 122. Attempted transfer nitration of **219** with **6**.

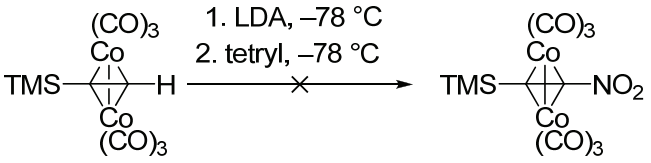

219 **25**

Comparison of the resulting material with an authentic sample of **25** (see Section 3.3.4) revealed that nitration had not taken place. In a second attempt, **6** was replaced with N_2O_4 (cf. Scheme 44). Two red compounds ensued, which were separated by column chromatography. The first was [μ-1,4-bis(trimethylsilyl)butadiyne-1,2-diyl]bis(tricarbonylcobalt)(*Co–Co*) (**221**), as observed by Magnus[99] (Scheme 123).

Scheme 123. Attempted low temperature nitration of **219** with N_2O_4.

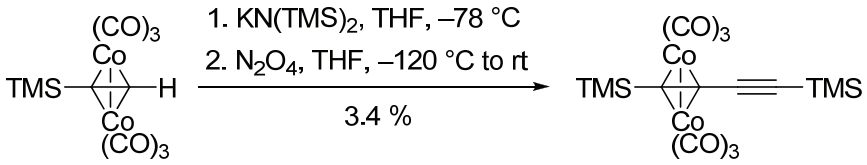

219 **221**

The presence of the two trimethylsilyl groups were confirmed by two signals in a 1:1 ratio in the ^{1}H NMR spectrum at δ 0.21 and 0.33 ppm, and an absorption for the Si–C deformation mode at 1250 cm^{-1} in the IR spectrum. The carbonyl stretching signals were found at 2092, 2054, and 2025 cm^{-1}, and a weak absorption at 2130 cm^{-1} was assigned to the uncoordinated triple bond. Finally, the mass spectrum showed a weak molecular ion at *m/z* = 480, a peak for TMS (*m/z* = 73), and fragmentation involving the loss of six carbonyls.

We were unable to identify the second compound, because of the small amounts obtained in this experiment. There were two TMS signals at δ 0.23 and 0.36 ppm (1:1) in the ^{1}H NMR spectrum. A molecular ion of *m/z* = 654 and loss of nine carbonyl groups in the mass spectrum implied the presence of a cobalt cluster, but those with bridging carbonyls were ruled out by IR spectroscopy. No alkynes were detected by IR spectroscopy, but strong carbonyl absorption at 2101, 2092, 2062, and 2029 cm^{-1} could have masked a signal near 2100 cm^{-1}. The lack of absorptions at 1550 and 1350 cm^{-1}, combined with the absence of the loss of a mass spectral fragment *m/z* = 46, established the absence of the nitro group. These data show that **219** was not nitrated and suggest that the second compound may be a product of oxidative coupling like **221**.

Unable to remove a proton from **219**, we turned to potential hydride abstraction, which might generate cation **218b**, in turn to be trapped with NO_2^-. We chose triphenylcarbonium tetrafluoroborate (**222**) as a reagent, but it did not react with **219** (Scheme 124).

Scheme 124. Attempted hydride abstraction from **219** with **222**.

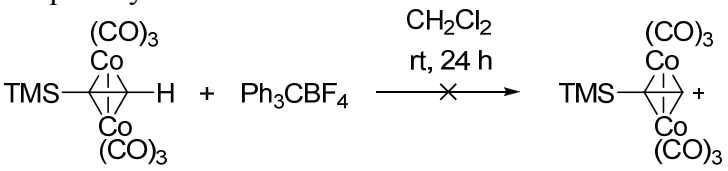

219 **222** **218b**

Having failed to nitrate, desilylate, or deprotonate the silyl-substituted **218** or **219**, we sought recourse in stannyl derivatives **176** and [(tributylstannyl)ethyne-1,2-diyl]bis(tricarbonylcobalt)(*Co–Co*) (**223**).[98] Substitution of tin for silicon can enhance reactivity, as demonstrated by Jäger et al.[111] and Schmitt et al.[109] (Chapter 2, Schemes 30 and 35).

Attempted nitration of **223** with NO_2BF_4 or N_2O_4 proved deleterious, paralleling the experiences with **218** (Scheme 125).

Scheme 125. Attempted reaction of **223** with NO_2BF_4 or N_2O_4.

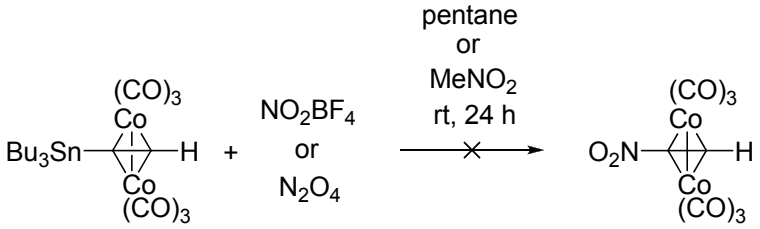

223 **26**

Corey et al. had reported that **9** (tetranitromethane) in DMSO nitrated alkene trialkyl tin compounds,[265] but this reagent also failed (Scheme 126).

Scheme 126. Destruction of **223** by **9** in DMSO.

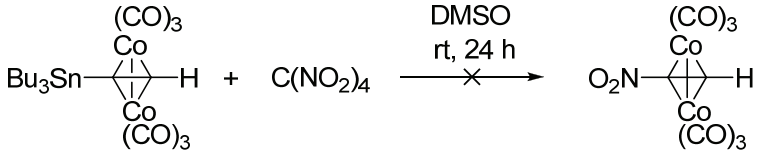

223 **9** **26**

Since direct nitrations proved unsuccessful, transfer nitration of **223** was explored. Tin compounds are readily transmetallated, so BuLi was chosen to lithiodestannylate or perhaps deprotonate **223**, to be followed by treatment with **6** (tetryl) to complete the nitration (Scheme 127).

Scheme 127. Attempted transfer nitration of **223** with BuLi and **6**.

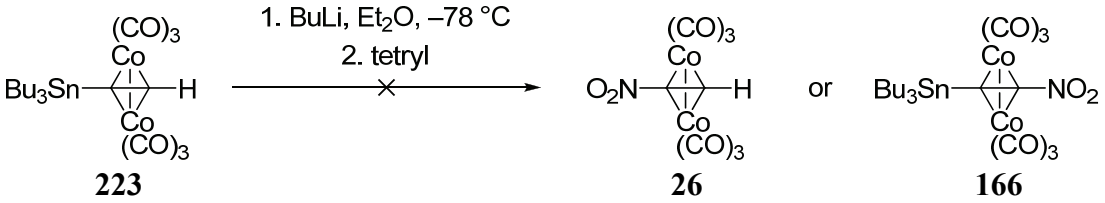

223 **26** **166**

Over 30–60 seconds, BuLi changed the red solution to orange, and subsequent addition of **6** darkened it to brown, leaving only unreacted **223** after workup. With the thought that the less sterically hindered proton may provide more facile reaction with an anion, triflic acid was substituted for **6**. This afforded a scant amount of unidentified dark purple oil (Scheme 128).

Scheme 128. Decomposition of **223** with BuLi and triflic acid.

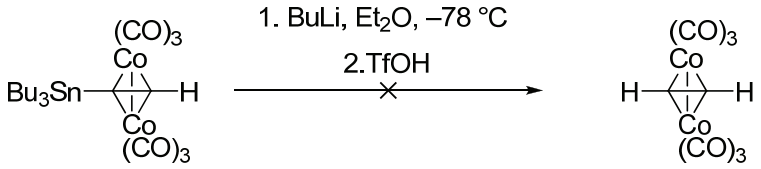

223 **219**

Insufficient sample existed for full characterization. The proton NMR spectrum reveals a butyl group and contains no free or complexed terminal alkyne proton signals. Very strong carbonyl stretching bands at 2050, 2036, 2015, and 1983 cm^{-1}, but none around 1800 cm^{-1}, indicate that the unknown is a cobalt carbonyl complex without bridging carbonyls. A weak absorption at 2101 cm^{-1} could be from an alkyne bond, hinting at a structure akin to **221**. Isotopic patterns in the EI-MS attest to the presence of tin. While the molecular ion of *m/z* = 401 appears to be inconsistent with **221** this peak is likely due to a fragmentation ion. Without further data, we could not assign a structure to this compound.

Destruction of **223** by deprotonation prompted us to test simple protodesilylation by adding triflic acid alone to **223** (Scheme 129).

Scheme 129. Ineffective protodesilylation of **223** by triflic acid.

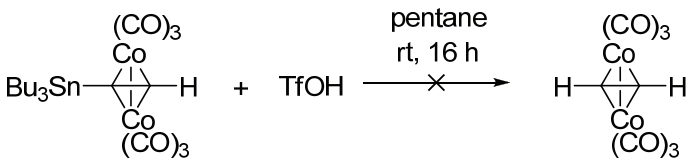

223 **219**

The acid left the metal centers unmolested, as seen with other such complexes,[266] and also did not react with the tin, leaving only starting material after sixteen hours.

We then examined *in situ* anion generation. By heating **176** with a stoichiometric amount of tributylstannyl fluoride (**224**) in a fifty-fold excess of dry propyl nitrate (**225**), we sought to effect transfer nitration to **24** (Scheme 130).

Scheme 130. Reaction of **176**, **224**, and **225** to form possible **167**.

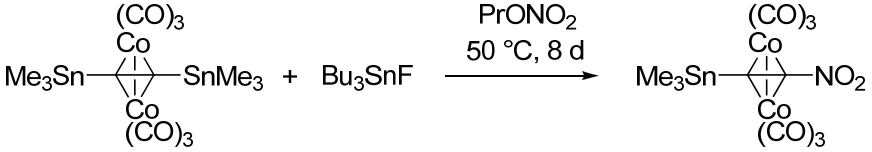

176 **224** **167**

After eight days, this reaction produced a trace of a red material that exhibited a singlet at δ 0.42 ppm with satellites from long range tin coupling in the ^{1}H NMR spectrum, and carbonyl absorptions at 2093, 2056, and 2029 cm^{-1} in the IR spectrum. The proton NMR signal is shifted downfield, and the carbonyl absorptions are at higher wavenumber relative to **176**, similar to the difference between **25** and **218** (Table 13), hinting at a structure of **167**. The region of the IR spectrum containing nitro absorptions was masked by absorptions of Nujol, making detection of an already weak signal impossible.

Table 13. Spectral data for **25**, **176**, **218**, and possible **167**.

Compound	Structure	NMR ^{1}H δ(ppm)	NMR $\Delta\delta$(ppm)	IR CO (cm^{-1})
218	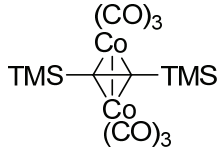	0.30		2047, 2022, 2014
			0.04	
25[a]	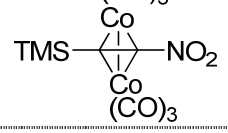	0.34		2109, 2075, 2046
176	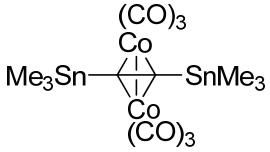	0.38		2060, 2040, 2015
			0.04	
167	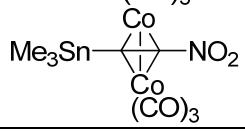	0.42		2093, 2056, 2029

[a] The preparation and properties of **25** are described in detail in Section 3.3.4.

Definitive characterization, including ^{13}C NMR and mass spectra, was prevented by insufficient sample, and attempts to increase the reaction scale were unsuccessful. Without conclusive spectroscopic evidence, we can only state that the compound is a

cobalt carbonyl complex bearing a trimethyltin substituent, leaving an opportunity for further investigation.

Stymied by these failures, we turned to one of the few successful electrophilic substitutions of a complexed alkyne: Seyferth's 1971 acylation of **176** to **179** (Scheme 90).[98] This experiment was repeated successfully, for calibration (Scheme 131).

Scheme 131. Acylation of **176** with acetyl chloride and $AlCl_3$.

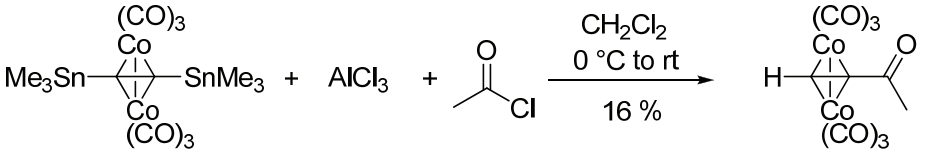

176 **179**

Next, we replaced the electrophile with *N*-nitropyrazole (**226**) as a non-oxidative source of nitronium ion.[264] Lewis acids such as $AlCl_3$ form charge separated nitronium salts with nitric esters or nitramines, activating the latter for nitration.[267] Unfortunately, compound **176** was destroyed by **226** and $AlCl_3$ (Scheme 132).

Scheme 132. Attempted nitration of **176** with **226**.

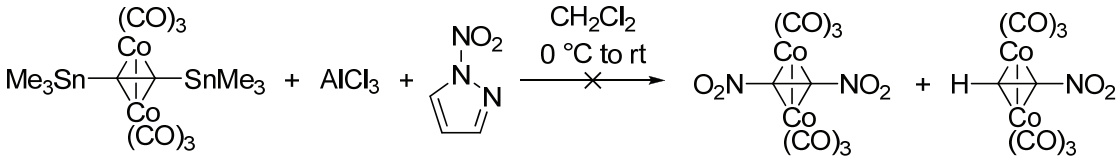

176 **226** **24** **26**

Incorporating a better leaving group in the potential nitrating agent by employing *N*-3,4-trinitropyrazole (**227**) was equally unsuccessful (Scheme 133), as was the use of **225** and $AlCl_3$ (Scheme 134).

Scheme 133. Attempted nitration of **176** with **227**.

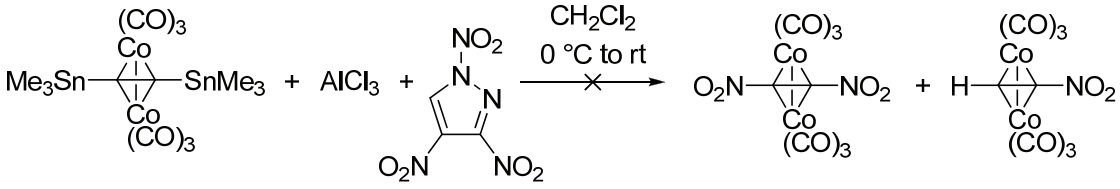

176 **227** **24** **26**

Scheme 134. Attempted nitration of **176** with **225**.

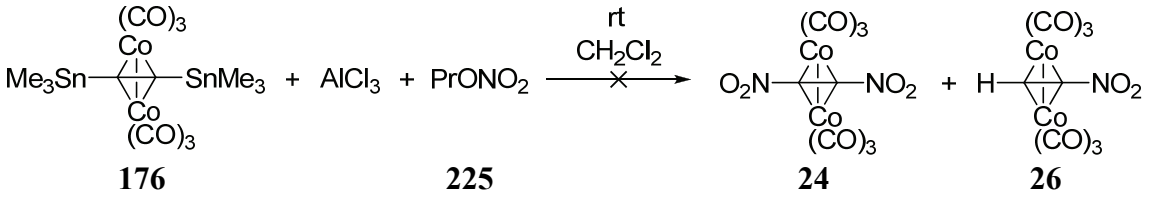

The closest nitronium analog of acetyl chloride, NO_2Cl, instantly decomposed **176** at temperatures from –78 °C to 0 °C, regardless of the presence or absence of $AlCl_3$ catalyst (Scheme 135).

Scheme 135. Destruction of **176** by NO_2Cl.

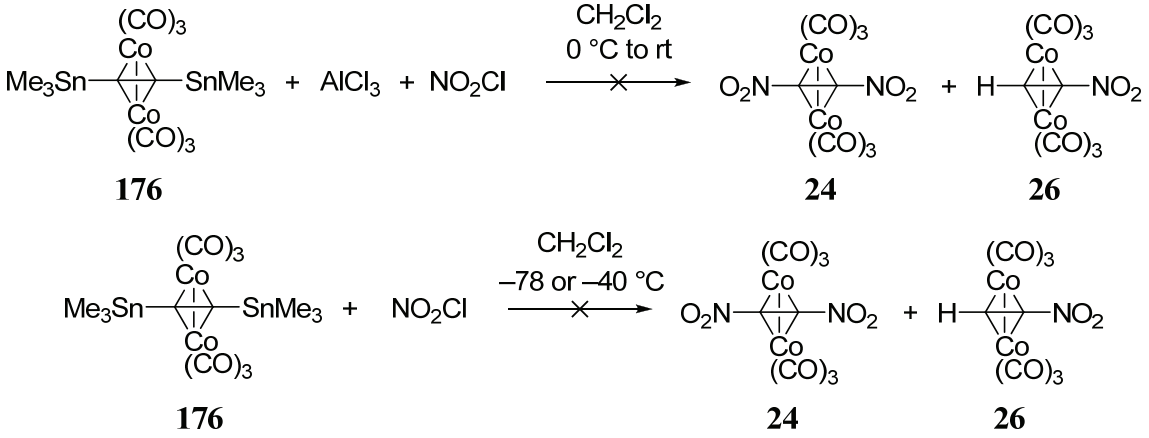

Unable to produce a nitration analogous to Seyferth's acylation, we considered whether a novel palladium-catalyzed coupling with a labile nitro group might provide the desired **24**. Tributylstannyl substituted alkyne cobalt complexes were proven substrates for Stille-type reactions,[268,269] but treatment of **176** with **226** in the presence of tetrakis(triphenylphosphine)palladium(0) (**228**) was ineffective (Scheme 136).

Scheme 136. Unsuccessful palladium catalyzed reaction of **176** with **226**.

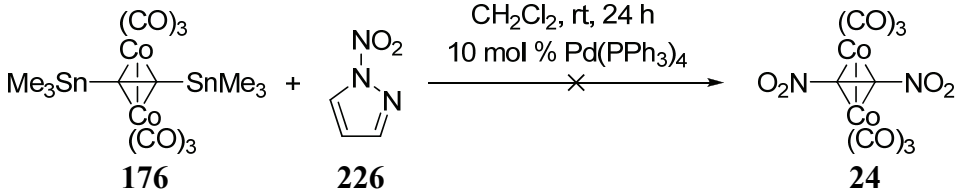

The more traditional Stille reagent, iodobenzene (**229**) also did not react (Scheme 137).

Scheme 137. Ineffective palladium catalyzed coupling of **176** with **229**.

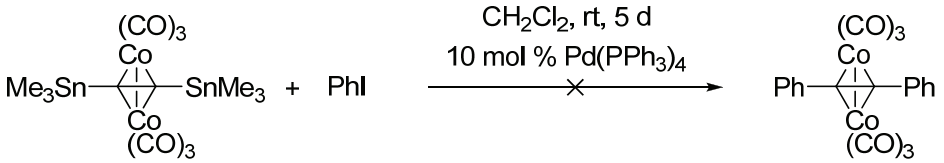

176 **229** **186**

The failure of this normally straightforward coupling boded poorly for further variations of this approach, so we redirected our efforts to iodo substituted complexes.[***]

Nucleophilic substitution of iodoalkanes with silver nitrite[271,272] was dubbed the Viktor Meyer reaction, after its discoverer in 1872,[273,274,275,276,277] and has since expanded to include iodoaromatics.[278] We were curious how it would fare with the ambiguously hybridized cobalt complexes, specifically the unknown [μ-1-iodo-2-(trimethylsilyl)ethyne-1,2-diyl]bis(tricarbonylcobalt)(*Co–Co*) (**230**). With silver nitrite, this reaction could potentially lead to **25** (Scheme 138), a compound whose spectral properties we had identified (see Section 3.3.4).

Scheme 138. Desired Viktor Meyer reaction of **230**.

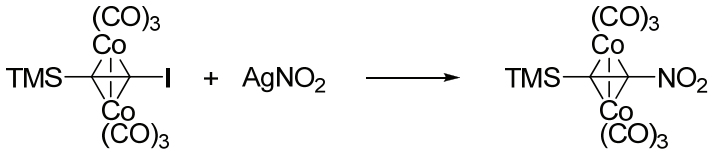

230 **25**

We first had to prepare **170**, which was accomplished in 30 % yield by treating **79** with BuLi, followed by iodine (Scheme 139), a modification of a previous iodination.[279]

Scheme 139. Preparation of **170** from **79** and iodine.

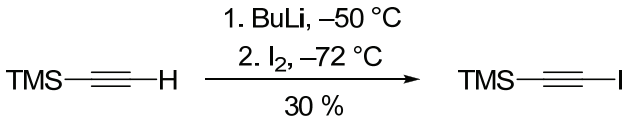

79 **170**

Alkyne **170** coordinated to **23** in 32 % yield (Scheme 140).

[***] Palladium catalyzed nitration of an aromatic system has recently been reported.[270]

Scheme 140. Reaction of **170** with **23**.

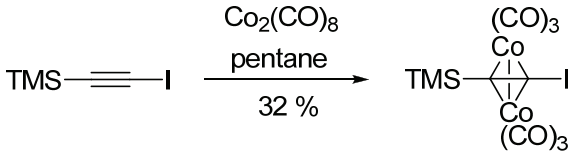

170 **230**

The previously unreported dark red **230** exhibited a molecular ion of *m/z* = 510 and loss of six carbonyls in the mass spectrum, as well as a TMS fragment (*m/z* = 73). The IR spectrum contained three very strong metal carbonyl absorptions at 2094, 2058, and 2032 cm^{-1}, and the proton NMR spectrum consisted of a lone singlet at δ 0.35 ppm. The ^{13}C NMR spectrum showed a signal at δ 0.12 ppm for the TMS carbon, two alkyne peaks at δ 50.7 and 83.5 ppm, and a broad carbonyl resonance at δ 198 ppm. The diagnostic shielding effect of iodine[280] was manifest in the chemical shift of the alkyne carbon at δ 50.7 ppm. The compound underwent slow decomposition, as indicated by the appearance of a singlet at δ 0.19 ppm for free **170**.

With **230** in hand, we mixed it with silver nitrite. In diethyl ether, only slight decomposition was noted after twenty days (Scheme 141).

Scheme 141. Lack of reaction between **230** and silver nitrite in diethyl ether.

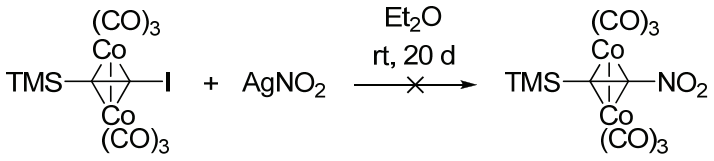

230 **25**

Acetonitrile increased the solubility of the silver nitrite and, after two days, TLC confirmed complete consumption of the starting material without formation of **25** (Scheme 142).

Scheme 142. Attempted reaction of **230** and silver nitrite in acetonitrile.

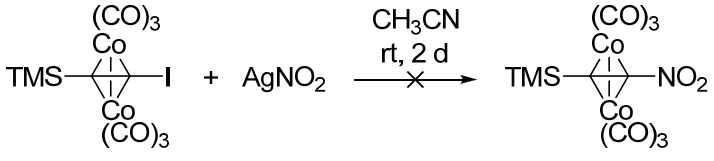

230 **25**

Mild oxidizing agents, such as iron(III) (standard reduction potential of + 0.77 V), can demetallate such complexes, so it is likely that silver(I), with a standard reduction potential of + 0.80 V, oxidized **230**. These results imply that the Viktor Meyer reaction is not tenable with readily oxidized complexes, such as **230**, but similar reagents with lower oxidation potentials, such as mercury(I) nitrite or lead(II) nitrite, might still hold promise.

In conclusion of this section, it is clear that manipulation of the complexed alkyne carbons in the dinuclear cobalt complexes is difficult, and all attempts to elicit nucleophilic and electrophilic reactivity failed. Indeed, the disappointing results called into question the entire strategy of stabilizing nitroalkyne by metal complexation. Fortunately, as the next section shows, this assessment turned out to be overly pessimistic.

3.3.4 A Milestone: Hexacarbonyldicobalt (Trimethylsilyl)nitroacetylene

The major goal of our work was to stabilize nitroalkynes by coordination to transition metals. This section provides the proof of this concept by the synthesis of **25**. It will include a description its physical properties and its preliminary reactivity, particularly with respect to its potential to function as a precursor to **24**. Cyclization reactions with other alkynes of relevance to organic synthesis will appear in Chapter 4.

Considering the litany of frustrations recorded in the previous sections, the synthesis of the first nitroalkyne metal complex was remarkably simple, namely direct coordination of **18** to **23** (Scheme 143).

Scheme 143. Reaction of **18** with **23** to form **25**.

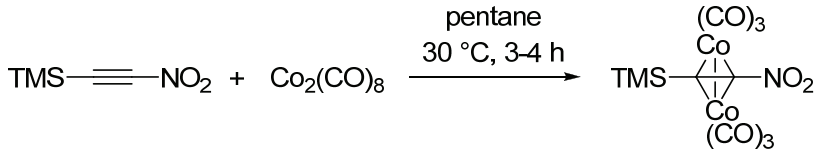

18 **23** **25**

This reaction was unhindered by alkenes and alkanes, ligating only the alkyne, and was neither hindered nor promoted by white light. Higher temperature accelerated the formation of **25**, but was limited by the generation of larger cobalt clusters above 50 °C. Purification was readily accomplished by column chromatography, which allowed the elution of **25** as a blood-red band.

Complex **25** is a dark-red, air-stable, crystalline solid, viewed on the end of a cold finger in Figure 14. It melts with decomposition at 104 °C in an open capillary, and sublimes at 45 °C at 0.1 torr pressure, a feature common for such complexes.[95,98]

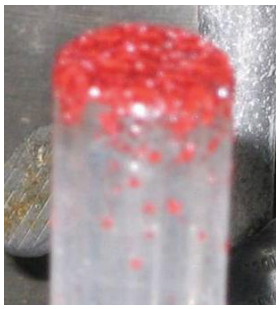

Figure 14. Crystals of **25** after sublimation (photograph by the author).

The melting point exceeds that of **219** (28–29 °C), [μ-1-(trimethylsilyl)prop-1-yne-1,2-diyl]bis(tricarbonylcobalt)(*Co–Co*) (**231**) (61–62 °C), and [μ-1-phenyl-2-(trimethylsilyl)ethyne-1,2-diyl]bis(tricarbonylcobalt)(*Co–Co*) (**232**) (62–64 °C), and is only slightly less than two complexes bearing substituents with much greater bulk, **218** (110–113 °C) and **187** [(μ-1,1,6,6-tetramethylhex-3-yne-3,4-diyl)bis(tricarbonylcobalt)(*Co–Co*)] (115–117 °C).[95]

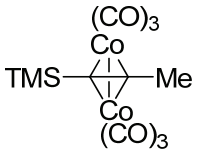

231

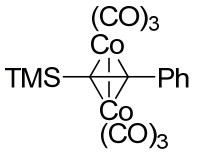

232

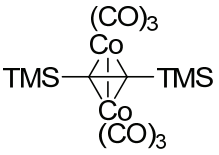

218

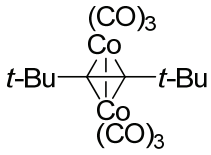

187

Organic solvents of polarity between pentane and methanol dissolve **25** immediately. It is insoluble in, but not decomposed by, water. Solvents deleterious to **23**, such as DMSO, NMP, and DMF, do not affect **25** at room temperature, but decompose it with the formation of refractory cobalt solids at elevated temperatures. Compound **25** oxidizes very slowly in solution when exposed to air, most notably at the solution-air interface, enjoying greater longevity than similar complexes.[198]

Similar to the UV-Vis spectra of known complexes, that of **25** consists of a maximum absorbance at the solvent cutoff (~ 218 nm), followed by several shoulders. The π→π* transitions of the conjugated nitroalkynes or nitroalkenes observed at λ_{max} ~ 235–240 nm or 225–230 nm, respectively,[104] are conspicuously absent, revealing a profound change in the electronic system. The color-producing absorption occurs at λ_{max} ~ 430 nm (log ε = 2.99), similar to other complexes and apparently uninfluenced by the nitro group.[205,202] No shoulder appears in the range of 275–290 nm, but an absorbance is noticed at ~ 255 nm (log ε = 4.33). While this hypsochromic shift may be due to the nitro group, comparison to similar shoulders in the UV-Vis spectra of complexes bearing electron withdrawing substituents, such as **26** (λ_{max} ~ 270 nm) (see Section 3.3.5) and [μ-1,2-bis(pentafluorophenyl)ethyne-1,2-diyl]bis(tricarbonylcobalt)(*Co–Co*) (**233**)[205] (λ_{max} 270 nm), suggest another influence, possibly steric crowding of the TMS group.[202]

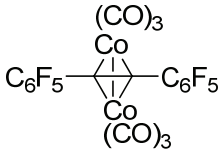

233

The presence of the nitro group in **25** appears to be indicated by a shoulder at λ_{max} ~ 300 nm (log ε = 4.02), absent in the electronic spectra of other (non-nitro) systems. Only **26** exhibits a similar absorption (λ_{max} ~ 325–330 nm) (see Section 3.3.5). These peaks are typical of the n→π* transition around 290 nm found for nitro derivatives.[113] Jäger observed λ_{max} 295–320 nm for nitroalkenes.[104]

The most prominent feature in the IR spectrum of **25** is the region of the carbonyl absorptions (Table 14).

Table 14. Carbonyl IR bands of selected complexes. Values in red indicate bands included in average $\tilde{\nu}_{CO}$ ($\tilde{\nu}_1$, $\tilde{\nu}_4$, $\tilde{\nu}_6$, and $\tilde{\nu}_2$).

Compound	Structure	Primary $\tilde{\nu}_{CO}$ (cm^{-1})	Avg. $\tilde{\nu}_{CO}$ (cm^{-1})
220[95]	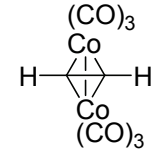	2099, 2059, 2034, 2028, 2017	2063
219[95]	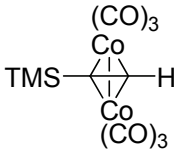	2092, 2054, 2029, 2021, 2011	2057
218[95]	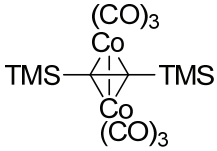	2085, 2047, 2022, 2014, 2002	2050
189[206]	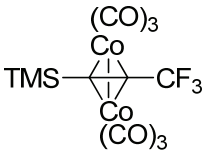	2108, 2070, 2046, 2040, 2001	2074
25[124]	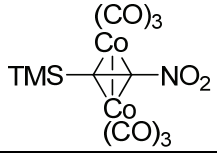	2110, 2075, 2046	2077

Resolution of our spectrometer permitted the observation of only three bands, at 2110 ($\tilde{\nu}_1$), 2075 ($\tilde{\nu}_4$), and 2046 cm^{-1} ($\tilde{\nu}_6$ and $\tilde{\nu}_2$), with an average value of 2077 cm^{-1}. Compared to the respective average $\tilde{\nu}_{CO}$ values of **218** (2050 cm^{-1}), **219** (2057 cm^{-1}), and **220** (2063 cm^{-1}),[95] that of **25** is shifted to higher wavenumbers by 14–27 cm^{-1}, evidently due to the presence of the nitro group.[198,205,96,206] Its electron withdrawing power appears even larger than that of trifluoromethyl by this criterion.[206] For example, the average $\tilde{\nu}_{CO}$ value of **189** is 2074 cm^{-1}.[206] These numbers are compared in Table 14 above.

Complex **25** shares several absorption bands with the free ligand **18**, most obviously those of the methyl groups on TMS, which are largely unaffected by coordination. The C–H stretching bands of **18** and **25** appear at 2964 cm^{-1}. Symmetric deformation of the methyl groups bound to silicon appear at 1256 cm^{-1} in the spectrum of **18** and 1253 cm^{-1} in that of **25**. Typically, such bands are "remarkably constant in position"[188] unless the silicon is directly connected to a highly electropositive atom, and we observed these between 1257 and 1248 cm^{-1} for all TMS-bearing complexes. The Si–CH_3 vibrations of the methyl group are nearly as constant, at 850 cm^{-1} in the IR spectrum of **18** and at 841 cm^{-1} in that of **25**, and always absorbing between 858 and 841 cm^{-1}, irrespective of substrate.

The asymmetric and symmetric stretching of the nitro group on **25** appear at 1503 cm^{-1} and 1323 cm^{-1}, at lower wavenumber than in the corresponding spectrum of **18** (1514 and 1339 cm^{-1}). These data place the nitro group of **25** within the range expected

for nitroaromatics (1555–1487 cm^{-1} and 1357–1318 cm^{-1}),[189] but below the region for nitroalkenes (1540–1510 cm^{-1} and 1360–1335 cm^{-1}),[104,189] nitroalkynes (1515–1510 cm^{-1} and 1358–1345 cm^{-1}),[104] and various nitroalkanes (1560–1534 cm^{-1} and 1388–1344 cm^{-1}).[189] Because IR frequencies of nitro groups reveal information about the chemical environment of the atom to which they are attached, one could deduce that the hybridization of the alkyne carbon of **25** is closest to aromatic sp^2.[189]

This notion is supported by coordinated alkyne $\tilde{\nu}_{C\equiv C}$ at 1609 cm^{-1} in the IR spectrum of **25**, near the high end of the expected range for such complexes[207] and comparable to $\tilde{\nu}_{C=C}$ of nitroalkenes studied by Jäger (1647–1595 cm^{-1}).[104] Meyer's work indicated that strongly electronegative alkyne substituents gave a $\Delta\tilde{\nu}_{C\equiv C}$ above the average ~ 650 cm^{-1}, but **25** exhibited a difference of only 559 wavenumbers from the alkyne absorption of **18** (2168 cm^{-1}). Some explanation might be found in the alkene resonance structures of nitroacetylenes (Figure 2, Chapter 2, Section 2.1), which decrease the triple bond character of the alkyne, thus lowering the $\tilde{\nu}_{C\equiv C}$ for **18** compared to similar molecules without resonance, such as the trifluoromethyl analogs of **16** and **18**, 3,3,3-trifluoroprop-1-yne (**234**) and 3,3,3-trifluoro-1-(trimethylsilyl)prop-1-yne (**235**), shown in Table 15.[207,281]

Table 15. Alkyne IR absorption bands for selected nitroalkynes and their trifluoromethyl analogs.

Compound	Structure	$\tilde{\nu}_{C\equiv C}$ (cm^{-1})	Ref.
16	H—≡—NO_2	2132	107
234	H—≡—CF_3	2160	282,283
18	TMS—≡—NO_2	2167	124
235	TMS—≡—CF_3	2205	281

Coordination to cobalt disrupts conjugation of the nitro group to the alkyne π system (seen clearly in UV-Vis spectra), and the alkene resonance structure of the free ligand is of little consequence to $\tilde{\nu}_{C\equiv C}$ in the complex. Thus, the $\Delta\tilde{\nu}_{C\equiv C}$ observed on coordination is smaller than similar complexes.[207]

Absent from the spectrum of **25** is the typical C–N vibration at 730 cm^{-1} for all nitroalkynes (Table 16 contains assigned IR absorptions of **18** and **25**).[104] The same band in the spectra of nitroalkenes is between 743–722 cm^{-1}, while that in nitro aromatics shifts to higher wavenumber (875–830 cm^{-1}).[104,189] No signals appear consistently between 743–722 cm^{-1} or 875–830 cm^{-1} in all four known nitroalkyne complexes, but the spectra of **26** (see Section 3.3.5) and phosphine-substituted derivatives of **25** (see below) exhibit absorptions around 739–732 cm^{-1}, in the nitroalkene $\tilde{\nu}_{C-N}$ range. While it is possible that this weak band is masked by neighboring peaks in the spectrum of **25**, more examples of coordinated nitroalkynes are needed to confirm this assignment.

Table 16. IR absorption assignments of **18** and **25**.

Compound and $\tilde{\nu}$ (cm^{-1})		
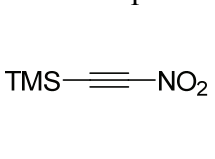	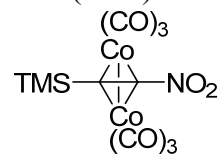	
18	**25**	Assignment
	3044	methyl C–H stretch
2964	2964	
2168	–	free C≡C stretch
–	2110	CO stretch
	2075	
	2046	
–	1609	coordinated C≡C stretch
1514	1503	asym. NO_2 stretch
1339	1323	sym. NO_2 stretch
1256	1253	Si–CH_3 deformation
851	845	Si–CH_3 rocking
729		C–N stretch
–	715	Co–C_{ac} stretch
	512	
–	493	Co–CO bending
	447	

Two signals are thought to belong to cobalt-alkyne carbon stretching motions (715 and 512 cm^{-1}),[185,284,209] and two absorptions at 493 and 447 cm^{-1} are attributed to cobalt-carbonyl bending.[185,202] Table 16 contains assigned IR absorptions of **18** and **25**.

Estimation of the relative strengths of forward (σ) and back (π) donation by the method of Meyer et al.[207] provided further insight into the effect of the nitro group on the complex. For **25**, $\Delta\tilde{\nu}_{CO}$ = –9 cm^{-1}, and $\Delta\tilde{\nu}_{C\equiv C}$ = 559 cm^{-1}, leading to values of σ = 0.885 and π = 0.975.[207] These data indicate that back bonding plays a greater role than forward donation in the ligation of **18**, a phenomenon usually observed for an alkyne substituted with two electron withdrawing groups.[207] Although the data necessary to calculate σ and π values for **189** are unavailable, comparison of the values of **25** with those of **190** (σ = 0.93, π = 1.00) shows a greater π:σ ratio in **25** (1.10 for **25**, 1.08 for **190**),[207] indicating a greater degree of back bonding in **25**.

The mass spectrum exhibited a weak molecular ion at *m/z* = 429 (30 %) and fragment ions due to the sequential loss of six carbonyls [*m/z* = 401 (25 %), 373 (40 %), 345 (22 %), 317 (14 %), 289 (32 %), and 261 (70 %)]. Peaks at *m/z* = 271 (70 %), 243 (70 %), and 215 (72 %) correspond to loss of four, five, and six carbonyls, respectively, and nitro. In contrast to prior observations that found complete decarbonylation and demetallation prior to fragmentation of the alkyne,[202] the signal at *m/z* = 271 is of approximately the same abundance (70 %) as that at *m/z* = 261. These data indicate that nitro-carbon bonds rupture more easily than their silicon-carbon counterparts, and with

the same facility as a cobalt-carbonyl linkage. A moderate abundance ion count is noted at *m/z* = 179 (45 %), which is $M^+ - 15$ for **174**, the recombination product of two fragments of **18**. The signal at *m/z* = 231 (70 %) stems from carbonyl loss from *m/z* = 287 (20 %) and 259 (12 %). The initial fragment, *m/z* = 287, corresponds to NO loss (*m/z* = 30) from the *m/z* = 317 ($M^+ - 4$ CO). Usually seen only in nitroarenes, NO loss occurs after rearrangement of the nitro group into a nitrite.[126] This rearrangement, predicted by Dewar,[85] was observed for the purported nitroalkyne **31**,[114,90] but not found in the mass spectra of any other nitroalkynes.[109,107,108,124] Sometimes CO elimination occurs after NO loss,[126] and was reported for **31** by Kashin,[114] but the absence of a signal at *m/z* = 203 suggests that this was not the case for **25**. The occurrence of nitrite rearrangement in nitroarenes, and the IR bands of the nitro group appearing in the range expected for nitroarenes, hint that the electron density on the alkyne carbon may be close to that of an aromatic system. Whereas **18** shows rupture of the silicon-methyl bond on electron impact, common for TMS derivatives,[126] this mode is not visible for **25**, presumably because it is masked by the dominant other fragmentations. At the low mass end of the spectrum, a peak for TMS [*m/z* = 73 (46 %)] is observed, along with two unidentified peaks at *m/z* = 75 (100 %) and 84 (58 %). The presence of what appears to be recombination products containing oxygen in the mass spectrum of derivatives of **25** (see below) leaves open the possibility that the peak at *m/z* = 75 is due to combination of cobalt and oxygen, CoO^+. The peak corresponding to cyclotrimerization of **18** coincidentally overlaps with the molecular ion at *m/z* = 429, but comparison with authentic spectra (see Chapter 4) confirms that this product is not present. The cyclotrimerization product of **174** (*m/z* = 582) is also unobserved.

NMR spectra of **25** were anticipated to reveal some information about the electronic nature of the coordinated alkyne. Without a terminal alkyne proton, a direct estimation of hybridization by chemical shift was impossible, but comparison of the TMS signal with those of similar complexes and their parent compounds was made. As expected, only one singlet, attributed to TMS, appeared in the proton NMR spectrum of **25**. This signal had the same chemical shift as the TMS signal for **18**, δ 0.34 ppm, not experiencing the usual slight downfield shift of other TMS-bearing alkynes (Table 17). By contrast, coordination deshields the TMS signal of **235**.

Table 17. ^{1}H NMR chemical shifts of TMS for selected compounds in $CDCl_3$.[124]

		δ ^{1}H NMR Shift of TMS (ppm)		
Compound	**Structure**	**Free**	**Coordinated**	**$\Delta\delta$**
18	TMS—≡—NO_2	0.34	0.34	0.00
79	TMS—≡—H	0.18	0.30	0.12
235	TMS—≡—CF_3	0.20[a]	0.34[b]	0.14
72	TMS—≡—TMS	0.15	0.30	0.15
170	TMS—≡—I	0.034	0.35	0.32

[a] Ref. 281. [b] Ref. 206.

Although it is difficult to draw conclusions from such limited data, the effect of substituent electronegativity on the change in the chemical shift of the terminal proton on coordination was not apparent (Figure 15).

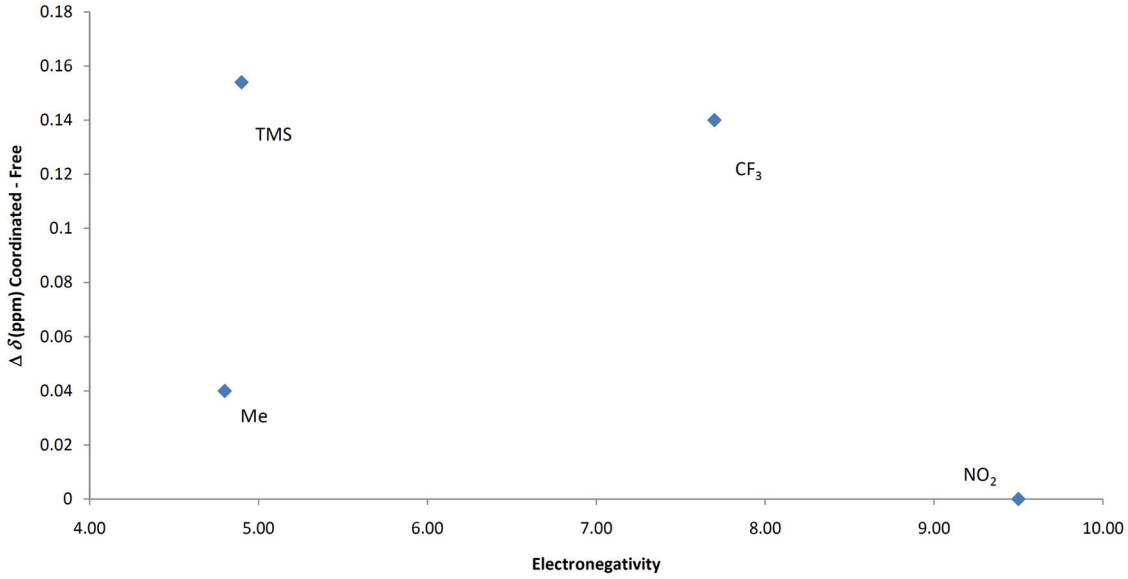

Figure 15. Lack of correlation between electronegativity and ^{1}H NMR shift of TMS. Electronegativities taken from Golovin et al.[178] for consistency.

Since the proton spectra were uninformative, we turned to the ^{13}C NMR spectra of **18** and **25**. Compounds **18** and **25** again stood out amongst similar compounds when comparing chemical shifts of the TMS-bearing alkyne carbon in the ^{13}C NMR spectrum (Table 18).

Table 18. ^{13}C NMR chemical shifts of TMS-bearing alkyne carbons for selected compounds.

		δ^{13}C NMR Shift of TMS-bearing carbon (ppm)		
Compound	**Structure**	**Free**	**Coordinated**	**Δ δ**
18[a]	TMS—≡—NO_2	73.2	73.4	0.2
75[b]	TMS—≡—Me	83.1	79.7	–3.4
77[b]	TMS—≡—Ph	94.2	79.9	–14.3
169[a]	TMS—≡—I	103.7	83.5	–20.2
71[b]	TMS—≡—TMS	113.4	92.8	–20.6
79[b]	TMS—≡—H	89.8	65.7	–24.1

[a] Ref. 124. [b] Ref. 95.

Whereas most TMS-substituted alkyne carbons experience an upfield shift upon coordination, that of **18** remains nearly constant. This is consistent with the unchanged TMS signal in the proton spectrum, but it raised a question: Why did the chemical shift of the TMS bearing carbon not change when coordinated, particularly when the nitro bearing carbon was shifted downfield dramatically, from δ 99.2 ppm in **18** to δ 125.8 ppm in **25**? Assuming that polar effects predominate, we believe that this might be due to the familiar resonance structure made possible by the nitro group, shown in Figure 16.

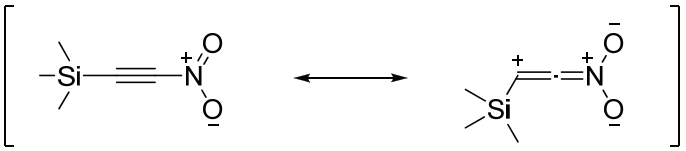

18a **18b**

Figure 16. Resonance structures of **18**.

Silicon can help stabilize the TMS-substituted alkyne carbon in structure **18b** through an α-effect, resulting in more alkene character. Alkyne carbon signals of **18** (δ 73.2 and 99.2 ppm) are observed downfield of those of **16** (δ 55.6 and 81.6 ppm), closer to the range expected for alkenes (δ 100–160 ppm), supporting this theory. When complexed as **25**, the contribution of resonance structure **18b** is severely curtailed or eliminated by coordination to cobalt and its deshielding effect is lost. At the same time, coordination deshields the carbon, and by coincidence, the peaks are nearly identical. The large deshielding of the nitro bearing carbon on ligation (Δ δ 26.6 ppm), surpassed only by those of **230** (see Section 3.3.3) and **26** (see Section 3.3.5), also supports this theory: Attenuation of resonance structure **18b**, in conjunction with decreased inductive transmission through the coordinated alkyne π system, would deshield the nitro bearing carbon. This theory might also explain the smaller difference between the free and coordinated nitro-bearing carbons of **18** and **25** (Δ δ 26.6 ppm), compared to **16** and **26** (Δ δ 30.1 ppm). Without resonance structure **18b** to impart alkene character, the nitro bearing carbon of **16** might experience greater deshielding on coordination from the loss of the cylindrical π system of electrons. Alternatively, β-stabilization (and thus shielding) of the electron poor nitro-bearing carbon by the silicon-carbon bond might be enhanced by the bent structure of the ligated alkyne in **25**, whereas it is not present in **26**. Preparation of **27** and its complex, inductively stabilized but not as effectively so as **18**, might provide further clues.

The triplet arising from ^{14}N–^{13}C coupling of the nitro-bearing carbon that featured so prominently in the spectrum of **18** is absent in that of **25**. This indicates loss of a symmetric electric field gradient around nitrogen (i.e., the alkyne carbon is no longer as electronegative as the two oxygen atoms to which nitrogen is attached) and thus a great reduction in triple bond character. The methyl carbons of TMS appear at δ 0.00 ppm, slightly downfield from the δ –1.02 ppm signal of those in **18**, agreeing with the slight deshielding observed for its alkyne carbon. A broad carbonyl peak manifests itself at δ 197 ppm, in the narrow range of other known complexes, but too broad to be diagnostic.

A single crystal suitable for X-ray diffraction was obtained by sublimation (Figure 17).

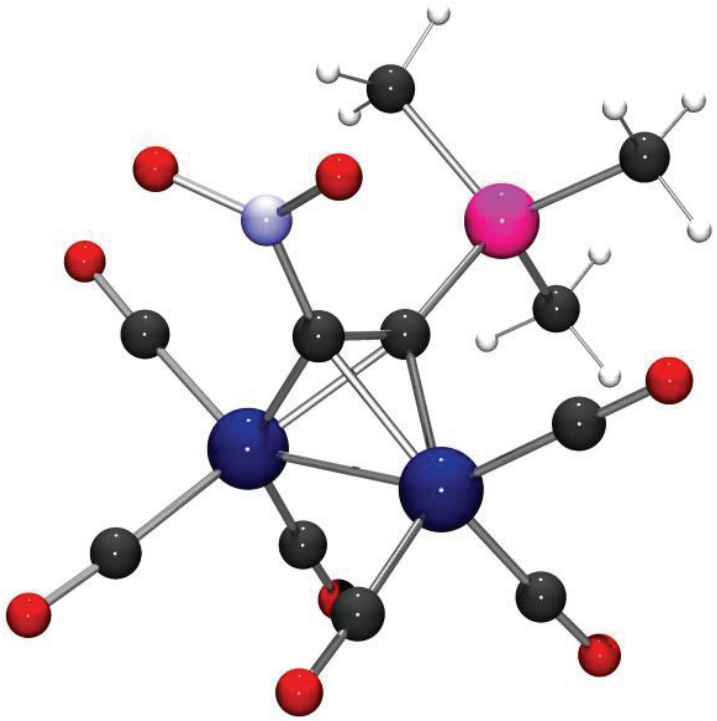

Figure 17. ORTEP plot of **25** projected in POV-Ray. Carbon (black), nitrogen (light blue), oxygen (red), silicon (pink), and cobalt (dark blue), are represented as spheres at the 50 % probability level. Protons (white) are represented as arbitrary sized spheres.

As expected, the alkyne bond is perpendicular to the line drawn by the two cobalt atoms, forming a tetrahedron, and both substituents were bent out of colinearity with the coordinated triple bond. Compared to similar complexes, the carbon-carbon bond distance of 1.359 Å is within range (~ 1.28–1.37 Å), and does not correlate to any obvious substituent characteristics. Other complexes with powerful electron withdrawing substituents,[236,235,217] such as **184**,[234] have carbon atoms 1.36 Å apart, but so does the much less electronegative **186**.[215,285,198] Steric bulk does not appear to influence this distance.[286,216,287,288] Similarly, the cobalt-cobalt bond of **25**, 2.4834 Å, is long for such complexes, but is not an outlier.[219,220,221,222,223,224,226,227,228,229,230,231,232,233,289,290] No correlation to simple substituent parameters or alkyne carbon-carbon lengths can be found.

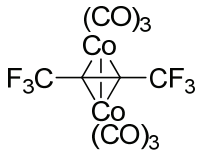

184

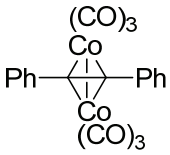

186

The alkyne carbon-silicon interval was 1.857 Å, only 0.003 Å higher than the average for such bonds.[219,220,221,222,223,224,226,227,228,229,230,231,232,233,289,290] The inverse relationship between substituent electronegativity and alkyne carbon-cobalt distance previously noted (see Section 3.2) continues to hold true in the case of **25**, as seen in Figure 18.

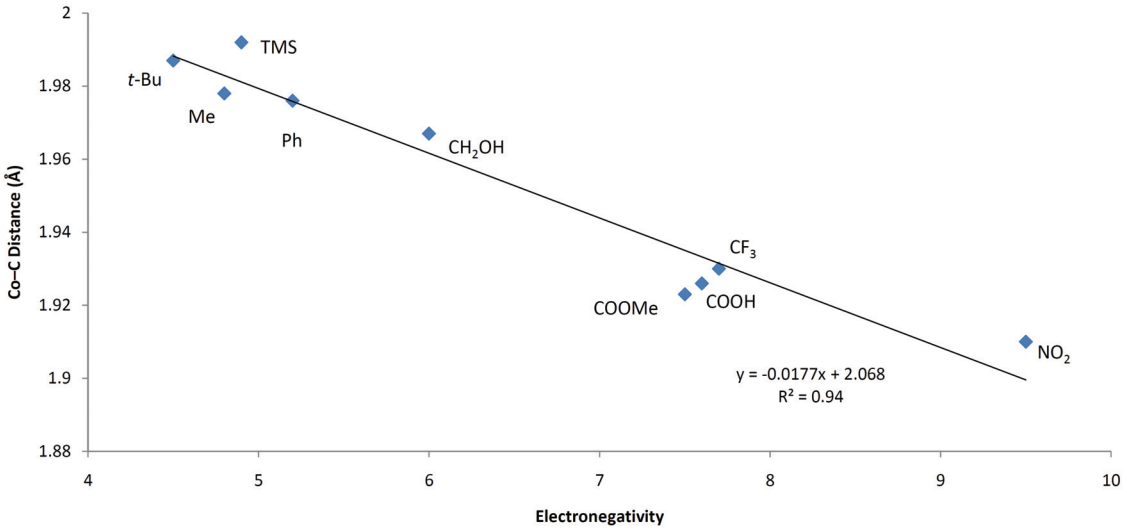

Figure 18. Relationship between substituent electronegativity and cobalt-alkyne bond distance.[216,95,217,218,219,220,221,222,223,224,225,226,227,228,229,230,231,232,233,234,235,236] For NO_2, the value is averaged over **25** and **26**. Electronegativity values from Golovin et al.[178] for consistency.

The nitro-bearing alkyne carbon of **25** is closer on average to the attached cobalt atoms (1.908 Å) than the corresponding distances of any known complex, indicating strong back donation from cobalt to the alkyne. The short alkyne carbon-cobalt distances distort the tetrahedron formed by the alkyne and two cobalt atoms from its usual symmetric shape.[95] The bonds of the TMS-bearing carbon to the two cobalt centers (1.981 and 1.984 Å) are slightly shorter than the average for known TMS-bearing carbons of such complexes (1.995 Å).[219,220,221,222,223,224,226,227,228,229,230,231,232,233,289,290] This finding hints at the occurrence of an inductive effect of the nitro group on the neighboring carbon.

A smaller bond angle between the alkyne and its substituent indicates greater substituent electronegativity, and we predicted that of **25** to be one of the steepest observed. Complexes exhibit values ranging from ~ 128.65 ° for **200**[236] to almost 150 ° for a tungsten-substituted species.[291]

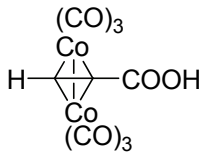

200

The nitro group forms an angle with the coordinated alkyne of 129.53 °, the second most acute ever recorded for such a complex, only behind **200**.[236] This value fits the previously established relationship between substituent electronegativity and bond angle (Figure 19). Full crystallographic data for **25** can be found in Appendix B.

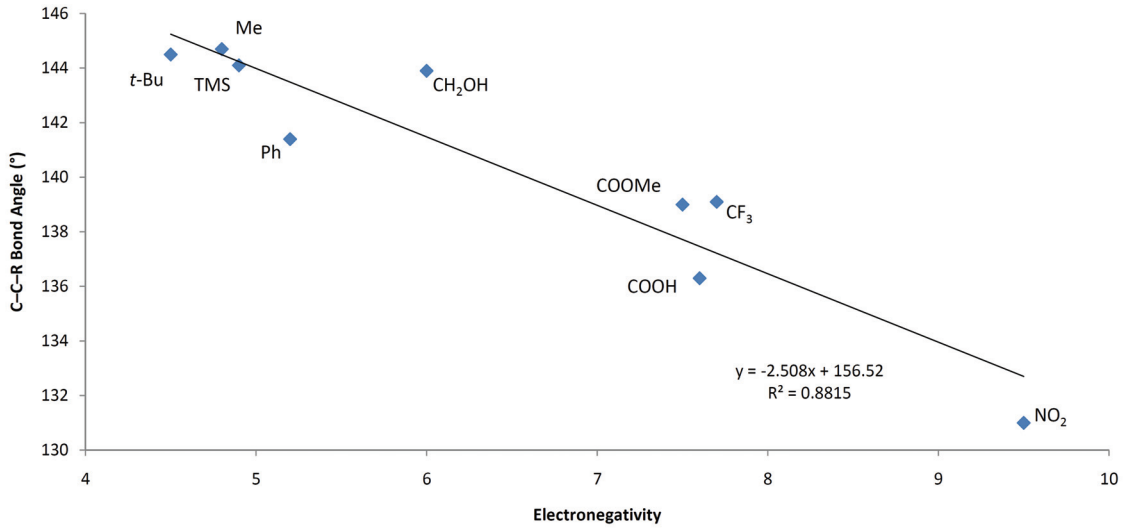

Figure 19. Correlation of substituent electronegativity and alkyne-substituent bond angle.[216,95,217,218,219,220,221,222,223,224,225,226,227,228,229,230,231,232,233,234,235,236] Data point for NO_2 is the average of the relevant angles in **25** and **26**. Electronegativities taken from Golovin et al.[178] for consistency.

Cyclic voltammetry of hexacarbonyldicobalt alkyne complexes reveals that reduction to the radical anion is typically irreversible or quasi-reversible at room temperature. Substitution of the alkyne with electronegative groups increases the longevity of the product. For example, reduction of **187** ($E_{1/2}$ = –1.03 V) is irreversible, but the more electronegative substituents on **184** ($E_{1/2}$ = –0.51 V) allow for re-oxidation. Based on this information and the trends found in the IR and X-ray data, we initially predicted that the nitro group on **25** would permit reversible reduction at room temperature and place the $E_{1/2}$ of **25** close to that of **184**. However, the radical anion of **25** survived only at fast scan rates (100 mV/s or greater), and exhibited $E_{1/2}$ = –0.885 V at room temperature. The $E_{1/2}$ value agrees with its quasi-reversibility, similar to other complexes (Table 19).

Table 19. $E_{1/2}$ reduction potentials for selected hexacarbonyldicobalt alkynes.[237]

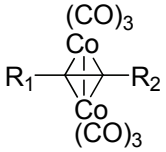

Compound	R_1	R_2	$E_{1/2}$ (V)
187	*t*-Bu	*t*-Bu	–1.03
183	*t*-Bu	H	–1.03
188	Ph	H	–0.90
25	TMS	NO_2	–0.89
186	Ph	Ph	–0.82
190	CF_3	H	–0.76
189	TMS	CF_3	–0.68
184	CF_3	CF_3	–0.51

The magnitude of $E_{1/2}$ places the stability of the radical anion of **25** not near that of **184** or even **189**, but rather closer to **188**.[237] Although one would expect the more electronegative nitro group to cause **25** to have a greater $E_{1/2}$, the trifluoromethyl analog of **25**, **189**, actually has a significantly greater $E_{1/2}$ (–0.68 V). As noted earlier, substituent electronegativity is not the only contributor to the value of $E_{1/2}$, seen first by comparing **189** and **190**, and now with **25** and **189**. The limited present set of data precludes analysis.

Examination of **25** by DSC and thermogravimetric analysis (TGA) in a closed pan evidenced a slight endotherm at 62 °C, possibly signaling some CO loss or melting, followed immediately by exothermic decomposition (398 J/g) peaking at 83 °C (Figure 20).

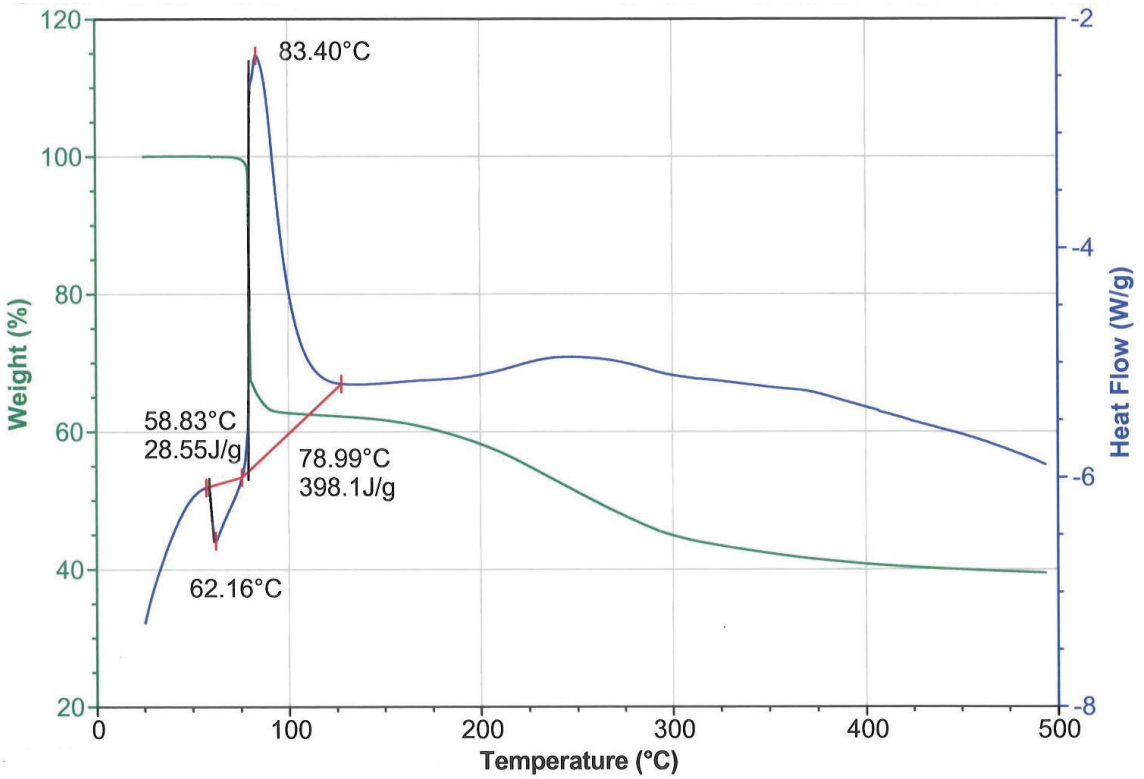

Figure 20. DSC-TGA spectrum of **25**.

Decomposition was accompanied by a weight loss of 37 %, approximating the 39 % weight of the carbonyl groups in the complex. Some hexacarbonyldicobalt alkyne complexes reveal a distinct exotherm followed by an endotherm, thought to arise from exothermic polymerization followed by carbonyl loss.[241] By these criterion, complex **25** appears to polymerize with concomitant carbonyl loss, resulting in an apparent exotherm. Continued heating caused gradual weight loss, thought to be the slow sintering of remaining elements.[241] The activation energy for decomposition was estimated by the Ozawa method using DSC.[292,293,294] The data for this experiment are shown below in Table 20.

Table 20. Values for the determination of the activation energy for decomposition of **25** by DSC.

β (K/min)	T (K)
1	378.33
2	389.43
5	394.90
7	399.45
10	403.82

Traditionally, this energy is the slope of the line derived by an Arrhenius plot (ln k vs. 1/T, where k is the rate constant and T is temperature in Kelvin).[292] For irreversible, uninhibited, exothermic reactions, a varying temperature of decomposition can be measured at a given rate of heating (β), such that a plot of $-\ln(\beta/T^2)$ vs. 1/T gives a rough estimate of the same information. The product of the slope of the line and the universal gas constant (8.314 J/mol·K), in this case 13,600 K × 8.314 J/mol·K = 113.1 kJ/mol, leads to E_a = 27.0 kcal/mol for **25**, shown in Figure 21.

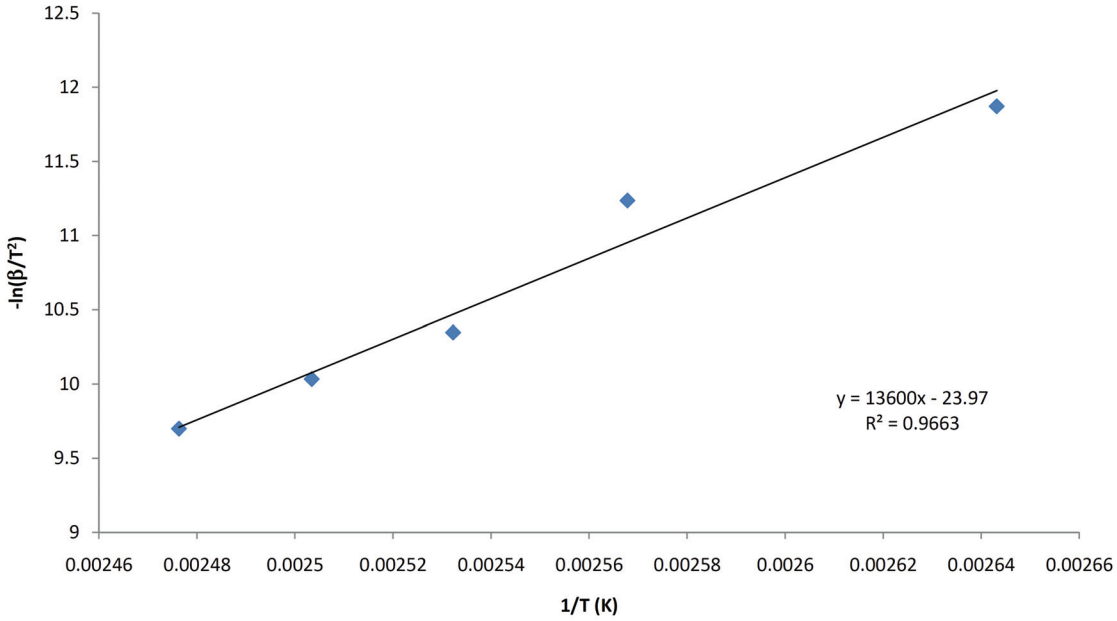

Figure 21. Plot of $-\ln(\beta/T^2)$ vs. 1/T for calculating E_a of decomposition of **25**.

This value is slightly greater than the Co–Co BDE of **23** (19 kcal/mol), supporting the theory that such complexes decompose with polymerization brought about by cleavage of the weak Co–Co bond.[241]

The ready access to **25**, with one nitro group in place, and its remarkable robustness refueled our efforts toward **24** from this complex, a target that we now believe to be a stable entity. These investigations entailed revisiting several of the approaches described in prior sections, notably exchange of the TMS group for nitro and functional group interconversions, in particular nitro group reduction. In addition, the presence of the $Co_2(CO)_6$ moiety provided another handle for modifying the electronic properties of

25 such as to make it potentially more conducive to nitrodesilylation, and this avenue was also explored. Finally, and in a different vein, the ability of **25** to function as a protected form of **18**, from which the ligand would be regenerated by oxidative demetallation, was explored.

To start, the obvious "jackpot" experiment was direct electrophilic nitrodesilylation of **25** along the lines described in Section 3.3.3, notwithstanding the realization that the nitro substituent might reduce the nucleophilic capabilities of the ligand. Indeed, stoichiometric combination of **25** with NO_2BF_4 in acetonitrile did not cause a noticeable change, even at elevated temperatures or in the presence of potassium fluoride (Scheme 144).

Scheme 144. Attempted nitration of **25** with NO_2BF_4.

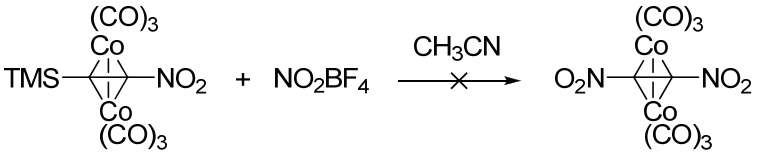

25 **24**

Excess NO_2BF_4 destroyed **25** in 1–2 minutes at –30 °C and immediately at room temperature.

Seeking to turn the presence of the nitro group to our advantage, transfer nitration of **25a** was considered, an entity that appeared to be more stable than the previously scrutinized anion **218a**, because the nitro group should delocalize the negative charge by induction.[295]

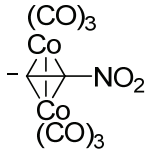

25a

Unfortunately, treatment of **25** with TBAF and **6** (tetryl) between –100 °C and room temperature failed to furnish **24** (Scheme 145).

Scheme 145. Attempted transfer nitration of **25** with TBAF and tetryl.

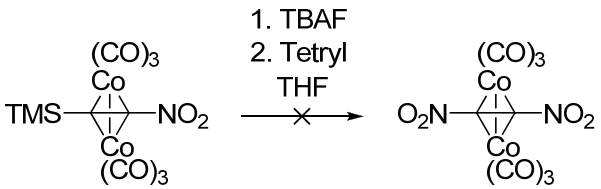

25 **24**

Metallation[296] with BuLi followed by addition of **6** was equally unproductive, immediately forming a black precipitate (Scheme 146).

Scheme 146. Attempted transmetallation and nitration of **25** with BuLi and tetryl.

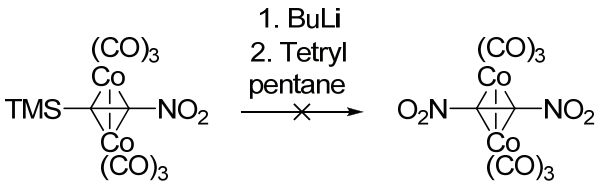

25 **24**

These difficulties led us to try an *in situ* transfer nitration analogous to that of **218** (see Scheme 116), in which **25** was treated with **224** in **225** solvent (Scheme 147).

Scheme 147. Attempted reaction of **25** with **224** in **225** (propyl nitrate).

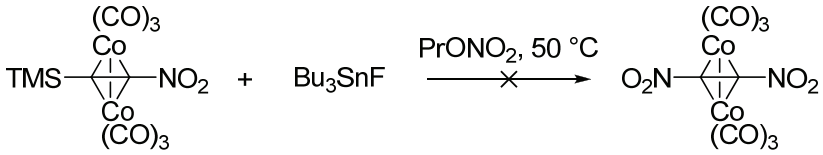

25 **224** **24**

After 24 hours, most of **25** had decomposed, leaving an intractable brown material, and no spots besides starting material were evident by TLC. Sodium methoxide was substituted for tributyl tin fluoride in the hopes that transfer nitration might occur (Scheme 148).

Scheme 148. Unsuccessful transfer nitration of **25** with sodium methoxide in **225**.

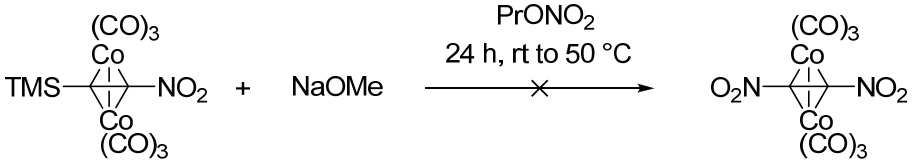

25 **24**

After prolonged heating, a small amount of insoluble dark precipitate had formed, and the only complex observed by TLC was **25**. Together, these attempts to generate **25a** suggested that its reactivity was no less than that of **218a**. Without even a trace of promising material from this reaction, we examined **25** as part of an indirect route to **24**. Specifically, it was thought that if the nitro group could be reduced to amino, the resulting complex might be more nucleophilic.

Reduction of **25** would afford [μ-1-amino-2-(trimethylsilyl)ethyne-1,2-diyl]bis(tricarbonylcobalt)(*Co–Co*) (**236**), a primary amine. Precedent of an amino alkyne complex exists in the form of **181**, which was reported to exist in solution.[100]

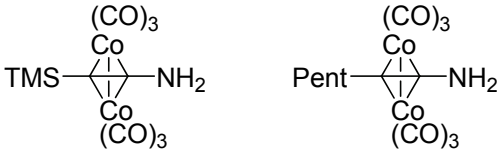

236 **181**

Such complexes are of interest because free primary and secondary ynamines are unknown, presumably due to tautomerization to the more thermodynamically favorable ketenimine, as shown in Scheme 149.[245]

Scheme 149. Tautomerization of an aminoalkyne to a ketenimine.

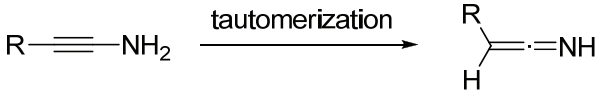

Coordination would prevent tautomerization, and could provide a synthetic equivalent to an aminoalkyne. We planned to reach **236** with the help of reagents known to reduce the nitro moiety.

We began with sodium borohydride in ethanol in the presence of copper sulfate catalyst.[297] This mixture did not change at 0 °C, but became dark brown on warming to room temperature, yielding a trace of a red oil comprised of two components (Scheme 150): starting material and protodesilylated species **26** (the synthesis of which will be described in Section 3.3.5). The presence of the latter was indicated by the presence of the diagnostic singlet at δ6.14 ppm in the proton NMR spectrum.

Scheme 150. Attempted reduction of **25** with $NaBH_4$ leading to **26**.

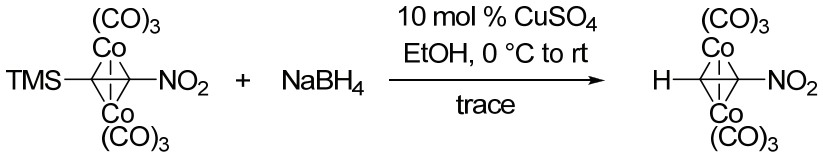

25 **26**

We assume that $NaBH_4$ deprotonated solvent to form a catalytic amount of ethoxide which desilylated **25** to **26**. Because no amines were observed, we elected to switch to a more powerful reducing agent.

Rapid nitro group reduction with $LiAlH_4$ was reported already in 1948.[298] Addition of this reagent to **25** in THF led to an instant darkening of the red color of the starting material and the detection of an unmistakable amine odor (Scheme 151).

Scheme 151. Attempted reduction of **25** with $LiAlH_4$ in THF.

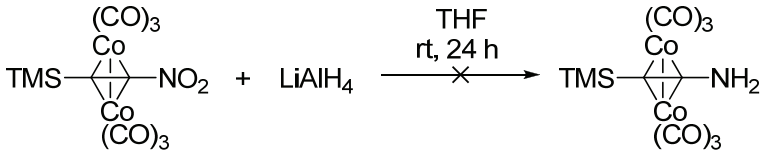

25 **236**

After workup, however, no cobalt complexes remained, suggesting that **236** had decomposed and that the odor originated from a volatile side product, possibly ethanamine or its TMS derivative. When the reaction was conducted in diethyl ether, the solution turned black, usually a sign of decomposition. The only product detectable by NMR was **219**, as evidenced by two singlets at δ 6.36 and 0.30 ppm with an integrated ratio of 1:9 (Scheme 152).[95]

Scheme 152. Reaction of **25** with $LiAlH_4$ in diethyl ether.

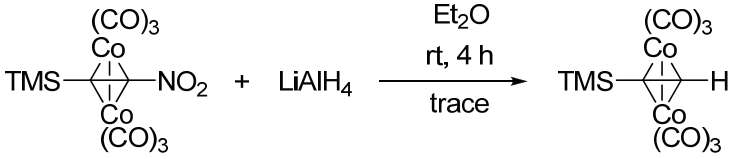

25 **219**

The poor yield and lack of amine products discouraged this line of investigation, and we began to examine derivatives of **25** for desilylation.

An alternative was to render **25** more nucleophilic by replacing carbonyls with phosphines. Up to four carbonyl groups had been substituted by Group V based ligands on similar complexes[299,300,301,302,253,303,196,304,305,201,192,306,197,307,237] by simple displacement, each adding electron density by greater σ donation than the carbonyl groups.[253] This reasoning prompted the preparation of the mono- and bis-trimethylphosphine derivatives of **25**, [μ-1-nitro-2-(trimethylsilyl)ethyne-1,2-diyl](dicarbonyltrimethylphosphanylcobalt)(tricarbonylcobalt)(*Co–Co*) (**237**) and [μ-1-nitro-2-(trimethylsilyl)ethyne-1,2-diyl]bis(dicarbonyltrimethylphosphanylcobalt)(*Co–Co*) (**238**), by reaction with trimethylphosphine (PMe_3) (Scheme 153).

Scheme 153. Preparation of **237** and **238** from **25**.

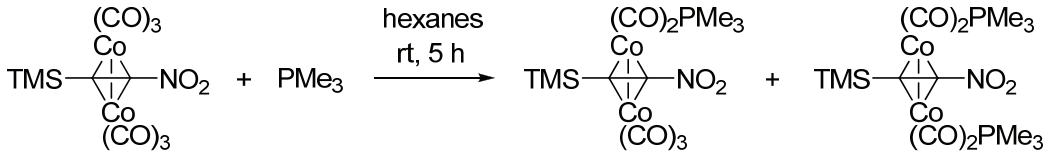

25 **237** **238**

The first and second substitutions replace the axial ligands in similar complexes, leaving only one signal for the phosphine groups in the ^1H NMR spectrum.[300,307,299] Addition of

PMe_3 to **25** led to two distinct bands on the TLC plate, separated by silica gel chromatography to give **237** and **238**. A single PMe_3 signal in the proton NMR spectrum confirmed that the two PMe_3 ligands on **238** were attached to separate cobalt atoms; unsymmetrical substitution causes distinct signals.[300,302] Although X-ray analysis would be required to confirm that substitution occurred axially and not equatorially, a hint of a more complex proton pattern appears in the PMe_3 signal of **238**, indicative of the same virtual coupling seen in diaxially bis(phosphite) substituted complexes.[300]

Each phosphine adds electron density, most evident in the lower energy carbonyl stretching bands in the IR spectra (Table 21).

Table 21. Major carbonyl IR bands for **25**, **237**, and **238**.

Compound	Structure	Primary $\tilde{\nu}_{CO}$ (cm^{-1})	Avg. $\tilde{\nu}_{CO}$ (cm^{-1})
25	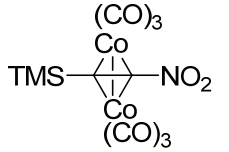	2110, 2075, 2046	2077
237	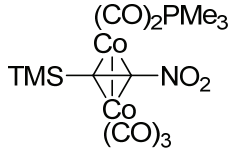	2076, 2026, 1976	2026
238	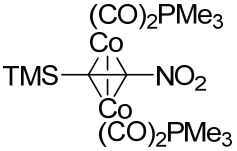	2030, 1978, 1953	1987

The average $\tilde{\nu}_{CO}$ is shifted approximately 40–50 cm^{-1} to lower wavenumber with successive phosphine additions, in agreement with changes observed for such complexes.[300] Phosphines are better σ donors than carbonyls, thus increasing electron density on cobalt and enabling it to better back donate to the carbonyls, lowering their $\tilde{\nu}_{CO}$.[198,300,207] The increased electron density on cobalt simultaneously improves back bonding to the alkyne, lowering the $\tilde{\nu}_{C\equiv C}$, and inhibits σ donation of the alkyne, raising the $\tilde{\nu}_{C\equiv C}$. Compared to **25** (1609 cm^{-1}), the net effect in the $\tilde{\nu}_{C\equiv C}$ of both **237** and **238** is a higher $\tilde{\nu}_{C\equiv C,}$ but it appears non-linear, as **237** exhibits a $\tilde{\nu}_{C\equiv C}$ of 1637 cm^{-1}, while that of **238** is 1627 cm^{-1}. The phosphine ligands shift the asymmetric and symmetric stretching absorptions to lower wavenumber in a more linear fashion: 1494 and 1314 cm^{-1} in the spectrum of **237**, compared to 1492 and 1301 cm^{-1} for **238**. Absorptions due to the TMS group are changed little by this substitution. In and out of plane C–H stretching from the methyl groups on TMS in **25** (2964 cm^{-1}) are shifted only 2 cm^{-1} for **237** (2962 cm^{-1}) and 1 cm^{-1} for **238** (2965 cm^{-1}), an insignificant difference. Similarly, the symmetric methyl deformation on TMS[188] change from 1253 cm^{-1} in **25** to only 1249 cm^{-1} in **237**, and 1246 cm^{-1} in **238**. The methyl vibrations around 840 cm^{-1} also changed little from **25** (845 cm^{-1}) to **237** (846 cm^{-1}) and **238** (841 cm^{-1}). Phosphine C–H methyl stretching at occurs at 2917 and 2827 cm^{-1} for **237** and at 2910 cm^{-1} for **238**. The spectra of **237** and **238** contain symmetric methyl deformation from the PMe_3 groups[308] at 1422

and 1421 cm^{-1}, respectively. Similarly, P–C stretching is thought to occur at 677 and 624 cm^{-1} for **237** and 673 and 622 cm^{-1} in the spectrum of **238**.[308] Curiously, the diagnostic C–N band in the spectra of nitroalkynes at 730 cm^{-1},[104] not present in that of **25**, seems to reappear in the spectra of both **237** and **238**, at 739 and 735 cm^{-1}, respectively. These absorptions correlate with those of nitroalkenes (743–722 cm^{-1}), and also agree with that of **26** (see Section 3.3.5), but in the absence of the same datum for **25**, cannot be positively identified as C–N stretching. Signals believed to belong to cobalt alkyne carbon stretching are shifted from 715 cm^{-1} for **25** to 698 cm^{-1} in the spectrum of **237** and further to 692 cm^{-1} for **238**, both to lower energy, as one would expect for weaker bonding.[185,284,209] A second absorption, less sensitive to the substitution of ligands, appears at 514 cm^{-1} and 515 cm^{-1} for **237** and **238**, respectively, and is attributed to cobalt-alkyne stretching as well.[185,284,209] This stretch occurs at 512 cm^{-1} in the spectrum of **25**. Finally, cobalt-carbonyl bending, present in the spectra of **25** (493, 447 cm^{-1}), **26** (491, 468, 451 cm^{-1}), and **238** (498, 468, and 434 cm^{-1}) is absent in that of **237**. These bands, between 400–500 cm^{-1},[185,202] might be shifted to slightly higher wavenumber and thus masked by the band at 515 cm^{-1}, which appears to have several slight shoulders, or could be shifted to lower wavenumber and out or range of the spectrometer. Identified IR signals are compared for **25**, **237**, and **238** in Table 22.

Table 22. IR absorption assignments of **25**, **237**, and **238**.

Compound and $\tilde{\nu}$ (cm^{-1})			
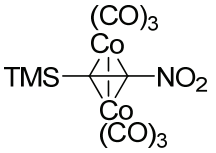	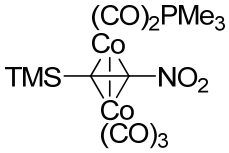	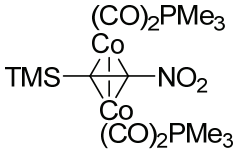	
25	**237**	**238**	Assignment
3044			TMS methyl C–H stretch[188]
2964	2962	2965	
–	2917	2910	PMe_3 methyl C–H stretch[308]
	2827		
2110	2076	2030	CO stretch
		1993	
		1980	
2075	2026	1978	
2046	1976	1953	
		1946	
1609	1637	1627	coordinated C≡C stretch[185]
1503	1494	1492	asym. NO_2 stretch[189]
1323	1314	1301	sym. NO_2 stretch
–	1422	1421	P–CH_3 sym. deformation[308]
1253	1249	1246	Si–CH_3 deformation[188]
845	846	841	Si–CH_3 rocking[188]
	739	735	C–N (?) stretch[104]
715	698	692	Co–C_{ac} stretch[185]
512	514	515	
–	677	673	P–C stretching[308]
	624	622	
493		498	Co–CO bending[207]
		468	
447		434	

The mass spectrum of **237** exhibits a weak molecular ion at *m/z* = 477 (10 %), followed by loss of two carbonyl groups [*m/z* = 449 (24 %), 421 (28 %)]. Subsequent decarbonylation is not observable until *m/z* = 337 (14 %). Some rearrangement of the nitro group and NO loss is indicated by the weak signal at *m/z* = 307 (10 %, 5 CO loss, NO loss), but concomitant CO elimination is not seen (no *m/z* = 279 peak).[126] The first major peak appears at *m/z* = 92 (45 %), the mass of trimethylphosphine oxide, O=PMe_3, an oxidation product. The base signal, at *m/z* = 77 (100 %), is derived from it by loss of methyl. Alone, these fragments would not be easily identified, but together with their absence in the spectrum of **25**, suggest these assignments. Similar fragmentation of methyl is observed with PMe_3 [*m/z* = 76 (56 %)], at *m/z* = 61 (75 %). Present in the mass spectra of **25**, **237**, and **238** is the unidentified ion of *m/z* = 75 (68 %). This corresponds to a mass of the recombination product CoO^+, but its absence in the spectrum of **26** raises doubts about this assignment.

Many of the same features appear in the spectrum of **238**. Carbonyl loss is rapid, but the molecular ion and loss of all four carbonyl groups are observed [*m/z* = 525 (12 %), 497 (10 %), 469 (24 %), 441 (25 %), and 413 (4 %)]. Departure of one PMe_3 ligand leaves a weak signal at *m/z* = 337 (20 %). A second loss of PMe_3 is not seen, suggesting that single substitution by phosphine is more stable than double, a characteristic noted qualitatively in the decomposition of **237** and **238**. Some rearrangement of the nitro group into a nitrite and subsequent loss of NO,[126] also present in the spectra of **25** and **237**, is evidenced by the weak signal at *m/z* = 383 (12 %). Subsequent CO elimination[126] is not observed. As was the case with **237**, the mass spectrum of **238** contained fragments which we attribute to $OPMe_3$ [*m/z* = 92 (27 %)], $OPMe_2^+$ [*m/z* = 77 (66 %)], PMe_3 [*m/z* = 76 (75 %)], and PMe_2^+ [*m/z* = 61 (100 %)]. The possible recombination product CoO^+ [*m/z* = 75 (55 %)] was also present. Peaks for atomic cobalt [*m/z* = 59 (70 %)] and TMS [*m/z* = 73 (15 %)] were also recorded.

The proton NMR spectra of **237** and **238** both contain a singlet for TMS and a doublet for the phosphine methyl groups. The TMS signals of **237** (δ 0.32 ppm) and **238** (δ 0.31 ppm) are slightly upfield from that of **25** (δ 0.34 ppm), revealing the shielding effect of PMe_3. The PMe_3 protons appear at δ 1.44 ppm ($^2J_{PH}$ = 10.2 Hz) for **237** and as only one doublet at δ 1.39 ppm ($^2J_{PH}$ = 8.68 Hz) for **238**, the latter being characteristic of symmetric ligand substitution about the dicobalt center[300,302] and Δ δ 0.05 ppm more shielded than the same peak in the spectrum of **237**, revealing greater electron density imparted by the second PMe_3 group. A small peak in the center of the PMe_3 doublet in the spectrum of **238** might indicate overlap with a more complex signal, and possibly virtual coupling of the methyl protons with the adjacent phosphorus.[300] Such coupling was noted in diaxially substituted trimethylphosphite complexes[300] and suggests diaxial substitution in the case of **238** as well.

The ^{13}C NMR spectra of **237** and **238** also evidence phosphine shielding. The PMe_3 signals appear at δ 19.4 ppm (J_{CP} = 28 Hz) for **237** and slightly upfield at δ 19.2 ppm (J_{CP} = 26 Hz) for **238**. The TMS signals (**237**: δ 1.24 ppm; **238**: δ 2.06 ppm) are increasingly deshielded compared to that in **25** (δ 0.00 ppm), following the counterintuitive trend for **18** and its complexes: More electropositive substrates appear to deshield TMS carbon signals (Table 23, next page). No satisfactory explanation for this trend was found based on polar effects. The alkyne carbon signals of **237** were upfield relative to their counterparts in **25**: The nitro bearing carbon appeared at δ 121.4 ppm (compared to δ 125.8 ppm in **25**) and the TMS-bearing carbon at δ 67.1 ppm (δ 73.4 ppm in **25**). The broad carbonyl signal manifested itself at δ 199 ppm. Quaternary carbon signals in the spectrum of **238** could not be detected because the sample decomposed into paramagnetic material over the required data collection time. This behavior was part of our qualitative observation that stability was inversely proportional to the number of phosphine ligands.

Table 23. ^{13}C NMR TMS signals in **18** and its various complexes.

Compound	Structure	^{13}C NMR TMS Signal (ppm)
18	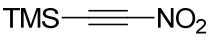	–1.30
25	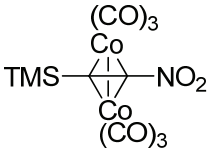	0.00
237	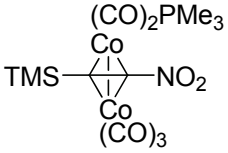	1.2
238	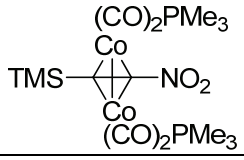	2.1

Complex **237** reacted with NO_2BF_4 at –20 °C to give an intractable red solid upon workup (Scheme 154). This result, coupled with the instability of **238**, discouraged nitration of **237** and **238** as a pathway to **24**.

Scheme 154. Unsuccessful nitration of **237** with NO_2BF_4.

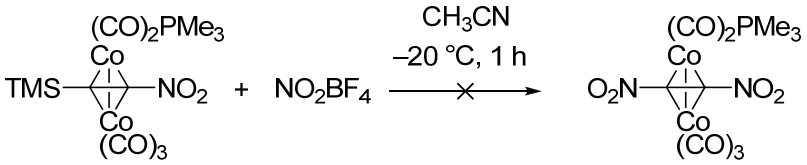

237 **239**

We were left to conclude that nitration of such complexes with NO_2BF_4 was infeasible.

Having proven that nitroalkynes could be stabilized as a cobalt complex, we also sought to show that the free alkyne could be released by oxidative demetallation. Such reactions are known for other alkynes,[97,309,205] and successful recovery of **18** from **25** with traditional reagents would show that **25** is effectively storage for **18**. With a five-fold excess of ceric ammonium nitrate (CAN), quantitative conversion of **25** to **18** (as observed by proton NMR spectroscopy) was achieved in two minutes (Scheme 155).

Scheme 155. Demetallation of **25** with CAN in acetonitrile.

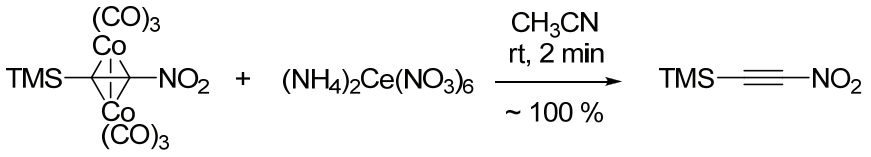

25 **18**

Ligand freed in this manner became starting material for a cyclization (see Chapter 4), confirming the presence of **18** in satisfactory yield. These results are similar to those reported for similar complexes,[97,309,205] and demonstrate proof of our storage concept.

This section has described synthesis, properties, and reactions of the first nitroalkyne transition metal complex, **25**. Complex **25** was proven to be an efficacious storage medium for **18**, permitting its recovery in quantitative yield. Trimethylphosphine derivatives of **25** were also prepared, characterized, and explored as potential precursors to **24**. The following section describes the second nitroalkyne complex, **26**.

3.3.5 Another Milestone: Hexacarbonyldicobalt Nitroacetylene

Having made **25**, we became more ambitious and set our sights on **26**. Although its parent, **16**, was so unstable that it was never isolated,[107] our experience with **25** gave us reason to believe that **26** would be stable at room temperature. In addition to its intrinsic interest, **26** might also be better precursor to **24** because of its terminal proton. This section describes the properties and reactions of **26**, as well as attempts to reclaim **16** by oxidation. Cyclizations of **26** are presented in Chapter 4.

Compound **26** was not accessible by ligation, but rather by protodesilylation from another nitroalkyne complex, **25**. Success was not immediate, however. Desilylation of such cobalt complexes had some precedent,[206] but also included demetallation,[198] and our own results with **218** were not promising (Schemes 115, 116, 118, and 119). Undeterred by these failures, we aggressively pursued protodesilylation of **25** by several routes. Treatment with TBAF in methanol, ethanol, or nitromethane was deleterious to **25** (Scheme 156).

Scheme 156. Failed protodesilylation of **25** with TBAF.

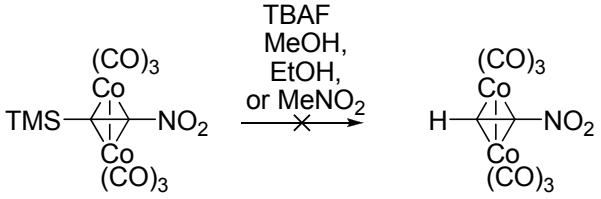

25 **26**

Potassium fluoride also decomposed **25**, leaving only a black precipitate (Scheme 157).

Scheme 157. Attempted reaction of **25** with aqueous KF.

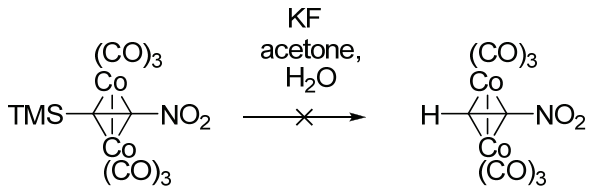

Switching from fluoride to methoxide, we caused **25** to react with potassium carbonate in methanol (Scheme 158).

Scheme 158. Attempted reaction of **25** with potassium carbonate in methanol.

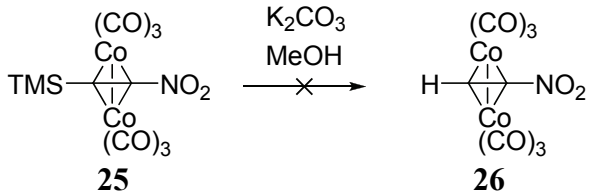

This produced an intractable orange-yellow solid, adding to the list of failures, and beginning to question the viability of protodesilylating **25**.

Success was at last achieved through a modification of the procedure of Solà et al. (Scheme 159).[192] This reaction required specific conditions: a potassium carbonate and potassium bicarbonate buffer solution of low concentration in aqueous methanol maintained at 22–24 °C, affording **26** in 60 % yield.

Scheme 159. Desilylation of **25** to **26**.

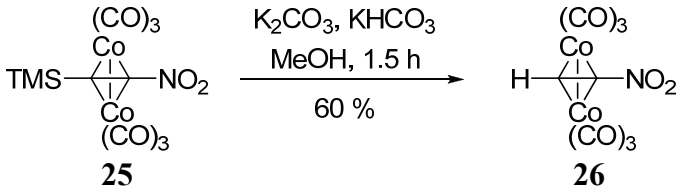

Traces of **25** can be separated by silica gel chromatography, where **25** appears as a red band slightly ahead of the red-orange **26**. Recrystallization from pentane affords flat, dark red needles of **26**, as seen in Figure 22.

Figure 22. Crystals of **26**. (Photograph by the author)

In an open capillary, **26** melts at 49 °C with decomposition, making it one of the highest melting terminal alkyne complexes[95] and indicating relatively strong intermolecular forces for a complex of such molecular weight and steric bulk.[254] Sublimation occurs at room temperature under 0.1 torr pressure and can be used for purification if desired. Compound **26** is soluble in all organic solvents at room temperature except pentane, which solvates **26** slowly, but is almost insoluble at –50 °C. Water neither dissolves nor decomposes **26**.

The UV-Vis spectrum of **26** is similar to that of **25**, containing three shoulders, two of which are affected by the absence of the TMS group. The first, at λ_{max} 270 nm (log $\varepsilon = 4.19$), experiences a bathochromic shift relative to **25** (λ_{max} ~ 255 nm), but is still below the expected range of λ_{max} 275–290 nm for such complexes.[202] The most dramatic effect of removing TMS is noted in the n→π* transition of the nitro group (see Section 3.3.4),[113] where the shoulder experiences a bathochromic shift from that of **25** (λ_{max} ~ 300 nm) to λ_{max} ~ 325–330 nm (log $\varepsilon = 3.91$). X-ray analysis (vida infra) shows the alkyne-TMS and alkyne-proton bond angles to be similar in **25** and **26**, suggesting the n→π* transition is unaffected by sterics. The third shoulder, in the visible portion of the spectrum at λ_{max} ~ 430 nm (log $\varepsilon = 3.04$), is responsible for the red-orange color of **26**.

The IR spectrum shows three absorbances in the carbonyl range, similar to **25**, at 2116 ($\tilde{\nu}_1$), 2083 ($\tilde{\nu}_4$), and 2053 cm^{-1} ($\tilde{\nu}_6$ and $\tilde{\nu}_2$). These are the highest recorded for any complex bearing only one electron withdrawing substituent and even some substituted by two such groups, as seen in Table 24 (next page), attesting to the effect of the nitro group. The asymmetric nitro band (1509 cm^{-1}) is slightly more energetic than that of **25** (1503 cm^{-1}), while the symmetric stretching absorption remains nearly constant (1322 vs. 1323 cm^{-1}), not particularly surprising when considering that the chemical environments of both nitro groups are remarkably similar and that the asymmetric stretching motion is more sensitive to change.[189] This change to higher wavenumber is consistent with the loss of the electron donating TMS group.[189]

Table 24. Carbonyl IR bands of selected complexes. Values in red indicate bands included in average $\tilde{\nu}_{CO}$ ($\tilde{\nu}_1$, $\tilde{\nu}_2$, $\tilde{\nu}_4$, and $\tilde{\nu}_6$).

Compound	Structure	Primary $\tilde{\nu}_{CO}$ (cm^{-1})	Avg. $\tilde{\nu}_{CO}$ (cm^{-1})
220[95]	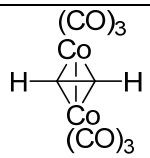	2099, 2059, 2034, 2028, 2017	2063
240[210,204]	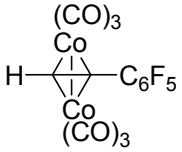	2098, 2061, 2040, 2031, 2025	2065
190[207]	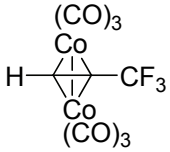	2112, 2072, 2040	2075
25[124]	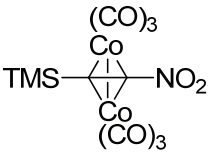	2110, 2075, 2046	2077
241[95]	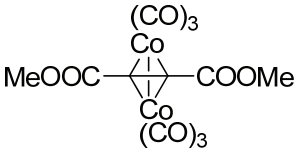	2111, 2080, 2054, 2049, 2025	2080
26[124]	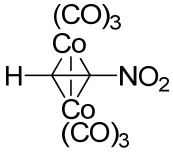	2116, 2083, 2053	2084

The alkyne absorption shifts from 2132 cm^{-1} in **16**[107] to 1618 cm^{-1} in **26**, in the range expected for nitroalkenes as observed by Jäger,[104] and higher than the 1609 cm^{-1} observed for **25** (see Section 3.3.4). Because both electron donating and withdrawing groups decrease coordinated $\tilde{\nu}_{C\equiv C}$, loss of the strongly electron donating TMS group raises the wavenumber of this absorption. The coordinated $\tilde{\nu}_{C\equiv C}$ is one of the higher observed for such complexes, and yet the difference between the free and complexed $\tilde{\nu}_{C\equiv C}$ is only 514 cm^{-1}, smaller than almost any other recorded.[207] As is the case with **18**, we posit that the presence of an alkene resonance form of **16**, no matter how small a contributor, helps to lower $\tilde{\nu}_{C\equiv C}$ in the free alkyne compared to its trifluoromethyl analog (Figure 23).

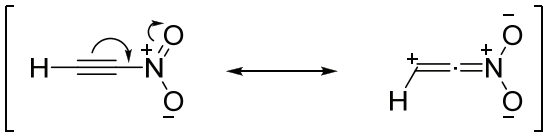

16a **16b**

Figure 23. Resonance structures of **16**.

If this were the only contributor to a low $\Delta\tilde{\nu}_{C\equiv C}$, it would not correlate with the TMS-stabilized resonance structure of **18**, as one would expect a lower $\Delta\tilde{\nu}_{C\equiv C}$ when comparing **18** and **25**. However, terminal alkynes experience a smaller $\tilde{\nu}_{C\equiv C}$ than those substituted because of smaller force constants and less energetic vibrations.[207,209] Alkyne stretching frequencies for alkyl nitroalkynes have values between 2265–2231 cm^{-1},[104] nearly 100 cm^{-1} larger than that of **16**.[107] The $\tilde{\nu}_{C\equiv C}$ of the TMS-stabilized **18** is also relatively large, at 2167 cm^{-1}.[124] Of the compounds surveyed, terminal alkynes have the lowest $\Delta\tilde{\nu}_{C\equiv C}$.[207] The difference of the corresponding values for **16** and **26** appears to be attenuated by resonance in the free ligand, lowering its $\tilde{\nu}_{C\equiv C}$, and the absence of an electron donating group, raising the coordinated $\tilde{\nu}_{C\equiv C}$.

The coordinated alkyne C–H bond resonates at ~3100 cm^{-1} in the spectrum of **26** (partly obscured by the moisture in the KBr pellet), about 200 cm^{-1} lower than the same band in the spectrum of **16** (3284 cm^{-1}), as observed for other alkynes on coordination.[98,207] This signal is similar to those of terminal alkenes,[185] but higher in its value than those of nitroalkenes bearing the alkene hydrogen on the β carbon (3030–3020 cm^{-1}).[104] Other terminal alkynes exhibit this same absorption in a narrow range (3100–3075 cm^{-1}).[207]

Nitroalkynes exhibit C–N stretching in the IR at 730 cm^{-1}, and nitroalkenes at 743–722 cm^{-1}. While no absorptions appear at these values in the spectrum of **25**, one occurs in the spectrum of **26**, at 732 cm^{-1}. The two phosphine derivatives of **25**, **237** and **238**, also show similar signals at 739 cm^{-1} and 735 cm^{-1}, respectively. This band is absent in the spectra of other complexes not bearing a nitro group.[207,208] More IR spectra of nitroalkyne complexes are required to corroborate these assignments.

Cobalt-alkyne stretching is thought to occur at 702 and 509 cm^{-1} in the spectrum of **26**,[185,284,209] while cobalt-carbonyl bending vibrations appear at 491, 468, and 451 cm^{-1}.[185,202] Assignment of the IR bands of **26** appear along with those of **16** in Table 25.

Table 25. IR absorption assignments of **16** and **26**.

Compound and $\tilde{\nu}$ (cm^{-1})		
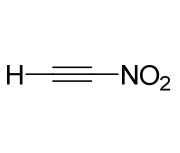	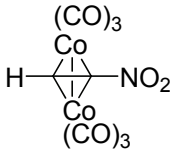	
18	**26**	Assignment
3284	~ 3100	alkyne C–H stretch[185]
2132	–	free C≡C stretch[107]
–	2116	CO stretch
	2083	
	2053	
–	1618	coordinated C≡C stretch[185]
	1509	asym. NO_2 stretch[189]
	1322	sym. NO_2 stretch
	732	C–N (?) stretch[104]
–	702	Co–C_{ac} stretch[185]
	509	
–	491	Co–CO bending[202]
	468	
	451	

The effect of the nitro group on the bonding of **26** is best shown by the estimation of forward (σ) and back (π) donation by the method of Meyer et al.[207] The change in average carbonyl absorption was $\Delta\tilde{\nu}_{CO}$ = –16 cm^{-1}, and $\Delta\tilde{\nu}_{C\equiv C}$ = 514 cm^{-1}, which translates into σ = 0.71 and π = 0.87. As was seen with **25**, back bonding predominates in **26**, noted by π > σ. Also like **25**, the magnitude of σ + π = 1.58 is less than the 1.78 value expected as a minimum for such complexes, again presumably because of the dramatically lower $\Delta\tilde{\nu}_{C\equiv C}$, and thus σ and π values are not directly comparable.

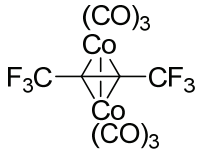

184

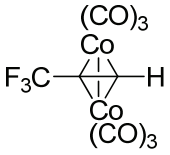

190

The ratio of π:σ, 1.23, is greater than that of **25** (1.10), and the analogous **190** (1.08), and even **184** (1.205),[207] implying that a single nitro group may be more electron withdrawing than two trifluoromethyl groups.

Fragmentation in the mass spectrum of **26** begins with loss of three carbonyls [*m/z* = 329 (65 %), 301 (45 %), and 273 (30 %)] from the weak molecular ion [*m/z* = 357 (5 %)]. Further decarbonylation is less prevalent [*m/z* = 245 (5 %), 217 (17 %), and 189 (17 %)], but prior denitration [*m/z* = 227 (12 %)] yields greater ion counts [*m/z* = 199 (75 %), 171 (75 %), and 143 (90 %)]. As for **25**, **237**, and **238**, rearrangement of the nitro group into nitrite and NO loss is minor, but present, occurring at two points to give ions *m/z* =

215 (15 %) and 159 (25 %). The peak at *m/z* = 84 (17 %) is weak in the spectrum of **26**, unlike those for **25**, **237**, and **238**, and is unaccompanied by *m/z* = 83.

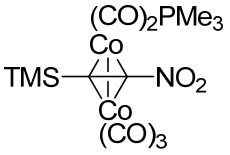

237

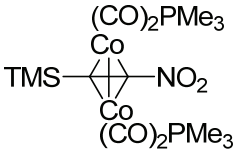

238

More intriguing is the fragment at *m/z* = 97, at 100 % intensity in the spectrum of **26**, but only a minor contributor in the spectra of **25**, **237**, and **238**, where it is attributed to the trimethylsilylethyne ion. Because **26** bears no TMS groups, *m/z* = 97 (100 %) must be a fragment of a larger ion or a recombination product, and remains unidentified. The peak at *m/z* = 78 (65 %) might be due to alkyne cyclization to benzene, observed in the mass spectra of other complexes.[202] Without evidence of cyclotrimerization products in the spectra of other nitroalkyne complexes, however, this assignment is questionable. Finally, cobalt [*m/z* = 59 (55 %)] is also present.

The proton NMR spectrum of **26** consists of a singlet at δ 6.14 ppm from the terminal alkyne proton, slightly upfield from the δ 6.80 ppm signal of **190**, and significantly downfield from the signal of the uncoordinated **16** (δ 3.37 ppm).[107] The change of this shift on coordination, only $\Delta\ \delta$ 2.77 ppm, is the smallest known for any terminal alkyne (Table 26).

Table 26. Difference in chemical shift between selected free and coordinated alkynes.

		δ ^{1}H NMR Chemical Shift in $CDCl_3$		
Compound	Structure	Free (ppm)	Complex (ppm)	$\Delta\ \delta$ (ppm)
16	H—≡—NO_2	3.37[a]	6.14[a]	2.77
70	H—≡—Ph	2.93[b]	6.23[b]	3.30
234	H—≡—CF_3	2.90[c]	6.80[d]	3.90
241	H—≡—*t*-Bu	1.98[b]	6.03[b,e]	4.05
242	H—≡—COOMe	1.74[b]	5.82[b]	4.08
79	H—≡—TMS	2.28[a]	6.36[e]	4.08
185	H—≡—Me	1.88[b]	6.02[b]	4.14
40	H—≡—H	1.80[b]	5.97[b]	4.17

[a]Ref. 124. [b]Ref. 201. [c]Ref. 310 lists this shift as δ 1.88 ppm without solvent in a table of mixed ^{1}H and ^{19}F NMR data. Other perfluoroalkyl acetylenes[311,312,313,314] consistently exhibit a shift of δ 2.90 ppm in $CDCl_3$, which we have adopted for the CF_3 species here. [d]Ref. 206. [e]Ref. 95.

This difference does not correlate with obvious factors such as steric bulk or electronegativity, the latter of which is shown in Figure 24.

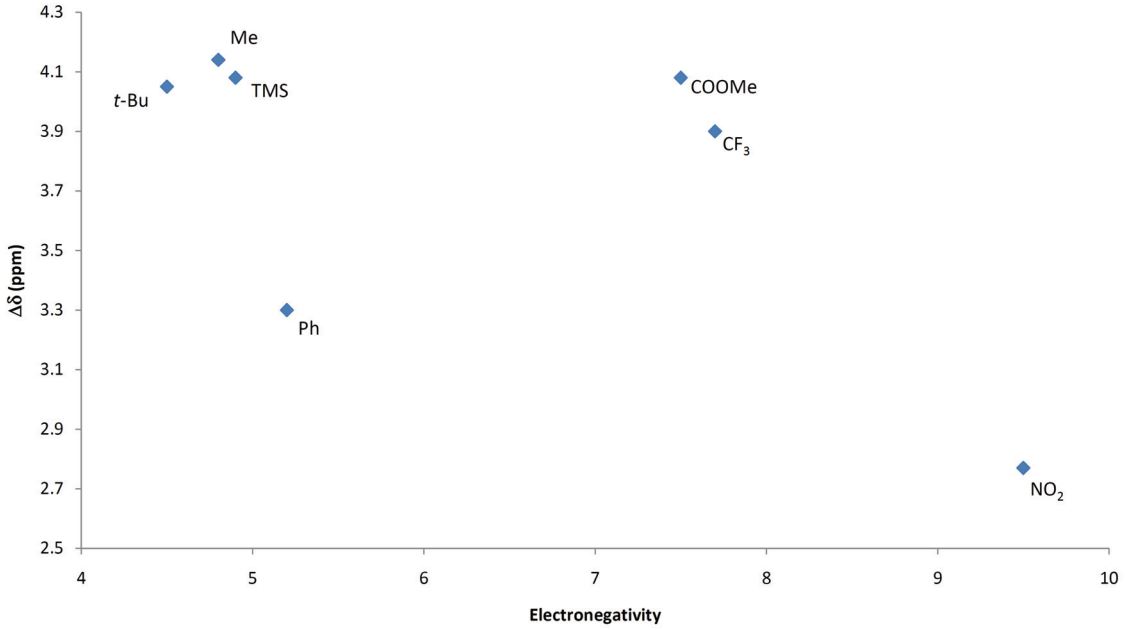

Figure 24. Lack of correlation between substituent electronegativity and change in proton chemical shift upon coordination.[95,124,201,206] Electronegativity values are taken from Golovin et al.[178] for consistency.

Long-range $^{1}H–^{14}N$ coupling is not seen for **26** as it is for **16**, signaling disruption of the highly electron-poor triple bond and an asymmetric electronic field gradient around nitrogen. Likewise, $^{13}C–^{14}N$ coupling is absent in the carbon NMR spectrum of **26**, the relevant carbon signal appearing as a singlet at δ 111.7 ppm. Ligation shifts it downfield by a record $\Delta\delta$ of 30.1 ppm, from δ 81.6 ppm to δ 111.7.[95] The proton bearing carbon of **16** shifts δ 9.6 ppm downfield, from δ 55.6 ppm to δ 65.2 ppm, the largest such downfield terminal carbon shift observed.[95] The magnitudes of these changes are due to the extreme electronegativity of the nitro group and suggest that **24** (the dinitro species) would exhibit an even more dramatic shift. Happ et al. attempted to correlate the amount of shielding contributed by substituents by plotting the chemical shift of an alkyne carbon for free and coordinated terminal alkynes.[95] No trend exists, made even more apparent by adding the data for **26** (Figure 25).

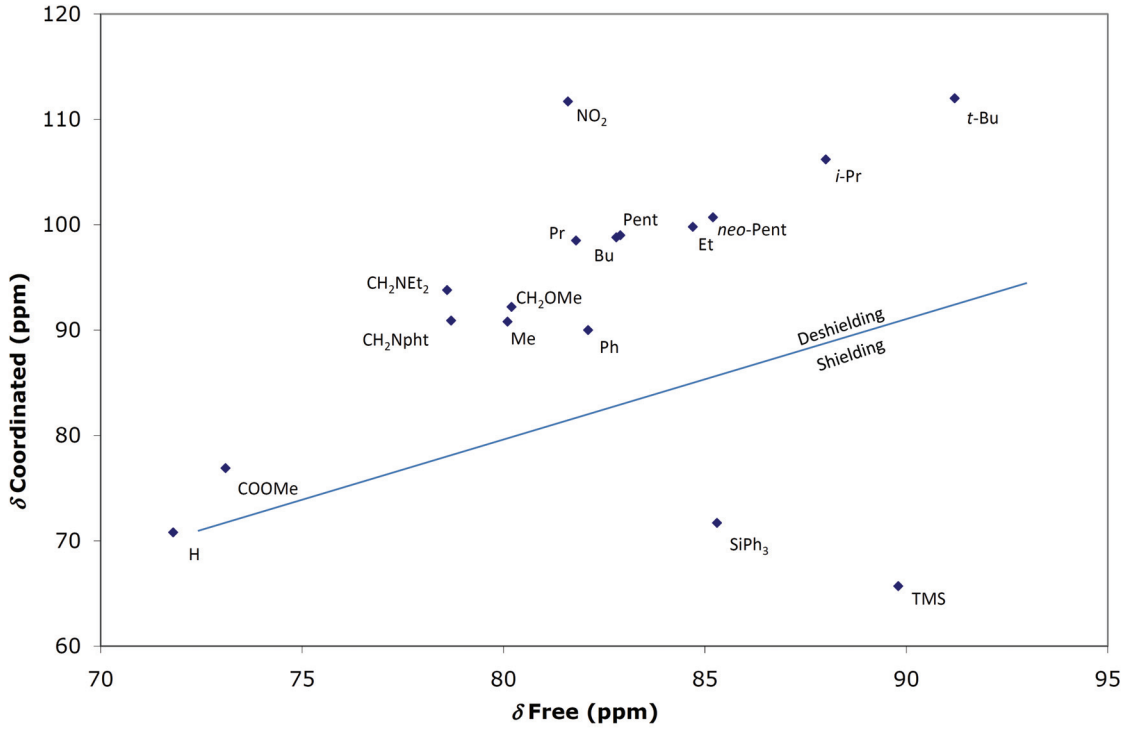

Figure 25. Lack of correlation between free and coordinated alkyne ^{13}C NMR signals including data for **26**.[95,124]

Compound **26** constitutes an outlying data point, exhibiting the greatest deshielding when ligated. No obvious factors, such as steric bulk or electronegativity correlate with free or coordinated alkyne ^{13}C NMR chemical shifts. Both alkyne carbon signals of **26** are upfield from their analogs in the spectrum of **25**. Without the TMS group, back bonding to the alkyne is greater in **26**, as evidenced by the $\tilde{\nu}_{CO}$, which might contribute to greater shielding of the alkyne carbons. The proton-carbon coupling constant of **26** (J_{CH} = 219 Hz) is the lowest of any such reported values for related complexes (albeit marginally so),[201,185] but lack of any apparent correlation with a number of parameters precludes any conclusions about the effect of the nitro group (Table 27, next page). Simple comparison to **40** (acetylene) (J_{CH} = 249 Hz), *cis*-1,2-dichloroethene (**246**) (J_{CH} = 198 Hz), and *trans*-1,2-dibromoethene (**247**) (J_{CH} = 201 Hz) indicate that the alkyne carbons of **26** are somewhere between *sp* and sp^2 hybridization, similar to other complexes.[185,305] Together, these spectra paint a picture of a powerfully electron withdrawing ligand that promotes strong back bonding from cobalt.

Table 27. Observed $^{1}H–^{13}C$ coupling constants for selected hexacarbonyldicobalt alkyne complexes.[201,185]

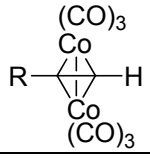

Compound	R	J_{CH} (Hz)	Reference
26	NO_2	219	124
243	Me	220	185
188	Ph	220	201
183	^{t}Bu	221	201
244	^{i}Pent	222	201
220	H	223	201
245	COOMe	225	201

A single crystal of **26** suitable for X-ray diffraction was obtained from pentane (Figure 26).

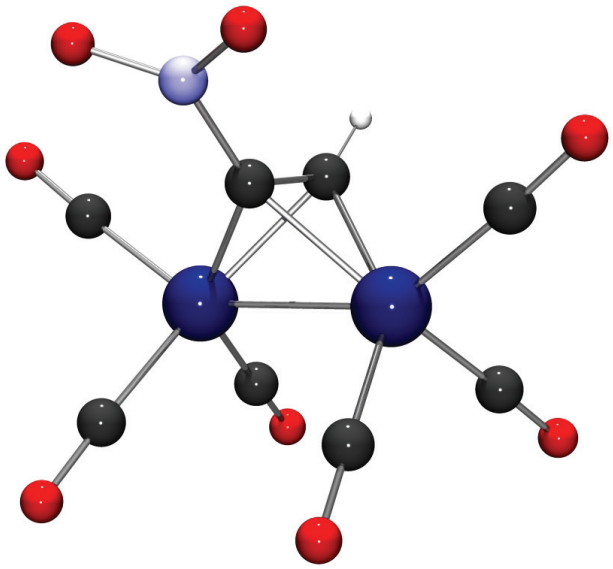

Figure 26. ORTEP plot of **26** projected in POV-Ray. Carbon (black), nitrogen (light blue), oxygen (red), and cobalt (dark blue), are represented as spheres at the 50 % probability level. The proton (white) is represented as an arbitrary sized sphere, but its position is refined.

Similar to **25**, the influence of the nitro group in **26** is evident in the bond distances from the nitro-bearing carbon to the two cobalt centers (1.908 and 1.916 Å, average 1.912 Å), longer only than the corresponding bonds of **25**, and the average bond length of **200** (1.910 Å).

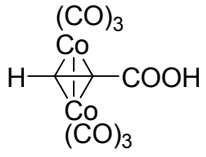

200

Shorter counterparts in **25** suggest that the TMS group might be responsible for this difference, although the origin of its influence is unclear. These close distances evidence strong back bonding, as predicted by IR analysis (see above), and likely impart stability.[96] The closest non-nitro structure to **26** is **200**, which also exhibits this same distortion of the cobalt-alkyne tetrahedron due to the electronegative carboxylic acid substituent.[236] The carbon-nitrogen bond is 1.450 Å, comparable only to **25**, whose C–N bond is 1.455 Å, slightly longer. The carbon-carbon bond (1.344 Å) is longer than the average for terminal complexes (1.325 Å avg., ~ 1.23–1.38 Å range),[227,315,316,317,318,319,320,321,322,323,324,325,326,327,328,329,330,331,332,333,334,335,336,337,338,339,340,284,341,342,343,344,345,346,347,348,349,350,351,352,353,354,355,356,357,358,359,360] but shorter compared to that in **25** (1.359 Å). Similarly, the cobalt-cobalt bond distance, 2.4795 Å, lies in the expected range for similar molecules (~ 2.45–2.51 Å, 2.471 avg.),[227,315,316,317,318,319,320,321,322,323,324,325,326,327,328,329,330,331,332,333,334,335,336,337,338,339,340,284,341,342,343,344,345,346,347,348,349,350,351,352,353,354,355,356,357,358,359,360] and is shorter than that of **25** (2.4834 Å). These values do not correlate with any apparent substituent characteristics. The high quality of the X-ray data for **26** permitted isotropic refinement of the terminal proton, and the C–H bond (0.93 Å) was found to be longer than the average (0.899 Å) of those for the few terminal alkyne complexes for which the proton has been refined,[326,330,333,336,288,284,361,230,354] but still within its range (0.746–1.105 Å). In light of the large scatter, it seems unreasonable to interpret these numbers.

The 132.5 ° angle between the alkyne carbon vector and the nitro group is more obtuse than that of **25** or **200**,[236] but still small for such complexes.[95] This value corresponds to the shorter alkyne carbon-cobalt bond distances and the highly electronegative nitro group, as noted in section 3.3.4, and is also observed for **200** (128.65 °), which bears the electron withdrawing carboxylic acid substituent.[236] The proton-carbon-carbon bond angles in the few terminal complexes for which refined hydrogen data are available range from 132.9–143.6 °,[326,330,333,336,288,284,361,230,354] with an average of 139.6 °, placing the value for **26** (139.2 °) squarely in the middle. On this basis, hybridization of **26** is between *sp* (180 °) and sp^2 (120 °).[73,95] Full crystallographic data can be found in Appendix B.

Cyclic voltammetry of **26** exhibited an irreversible reduction at E_{red} = –0.961 V vs. a ferrocene standard. Without a reversible peak, $E_{1/2}$ is impossible to calculate, but comparison to the reduction peak of **25** (E_{red} = –0.815 V), shows that **26** is more difficult to reduce than **25**. Although it is counterintuitive that a complex bearing an electropositive substituent stabilizes a radical anion better than a complex without, these data agree with those of the trifluoromethyl analogs, **189** and **190**, which exhibited the same stabilization, with $E_{1/2}$ of –0.76 V and –0.68 V, respectively.

The DSC-TGA spectrum for **26** was similar to that of **25** (Figure 27, next page). A slight melting endotherm at 58 °C is followed by a large exothermic decomposition at 102 °C. The asymmetric exotherm has a slight shoulder, corresponding to a 10 % mass

loss, close to the 13 % expected for losing a nitro group, followed by rapid weight diminution of 24 %, corresponding to three COs. The remaining fragment appears relatively stable, undergoing further mass loss of 24 % slowly, between 102 °C and 300 °C. Initial nitro evolution would be unique.[241] This result, coupled with the poor capacity for cyclization of **26** (see Chapter 4) and demetallation of **26** without formation of **16** (see below), might signal that the nitro group is unusually reactive. The more favorable oxygen balance and lower molecular weight of **26** contribute to greater energy release per gram (874 J/g), compared to **25** (398 J/g).

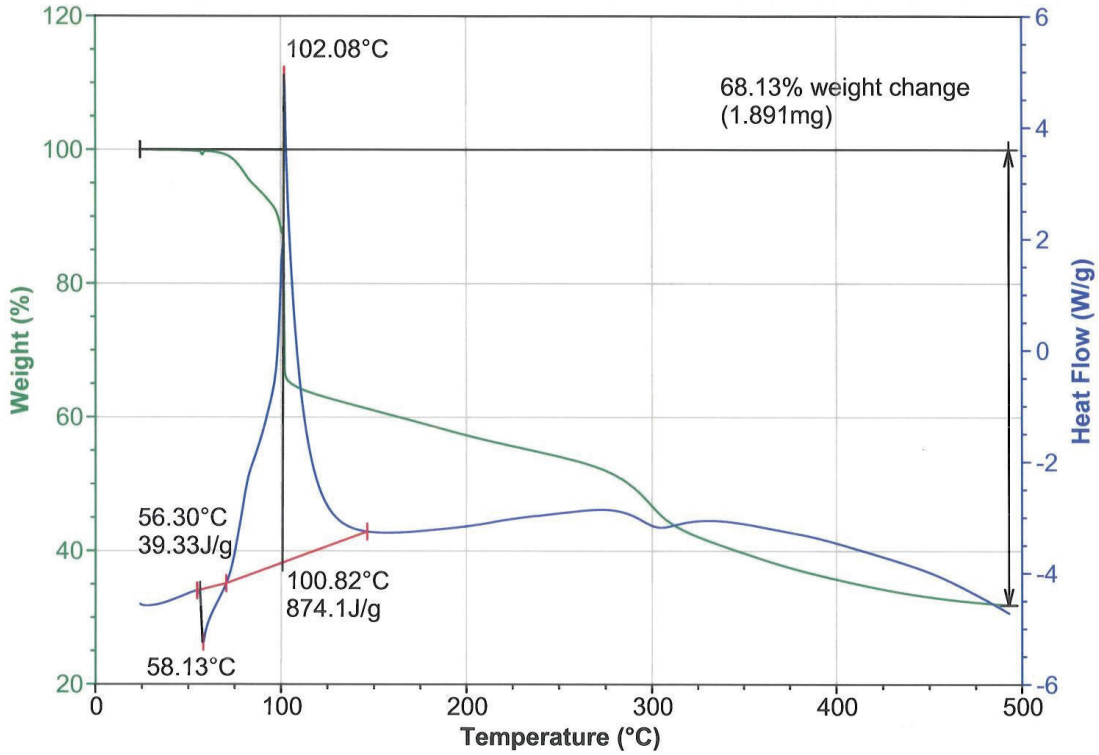

Figure 27. DSC-TGA spectrum of **26**.

With **26** in hand, we probed its reactivity to determine its suitability as a precursor to **24**, various cyclizations, and as storage for **16**. Cyclizations are described in Chapter 4. Attempts at transfer nitration, nucleophilic substitution, and oxidation of **26** are described below.

As noted in Section 3.3.3, deprotonation and nitration of **219** was unsuccessful. Deprotonation of **26** appeared more promising because the electron withdrawing nitro group was known to help stabilize anions by delocalizing negative charge.[295] Once deprotonated, the anion **25a** might be transfer-nitrated to afford **24**. However, one notes that this species was elusive by desilylation of **25** (Schemes 143–146). This scheme was explored by treating **26** with lithium hexamethyldisilazane (LiHMDS), followed by NO_2Cl (Scheme 160).

Scheme 160. Decomposition of **26** with LiHMDS and NO_2Cl.

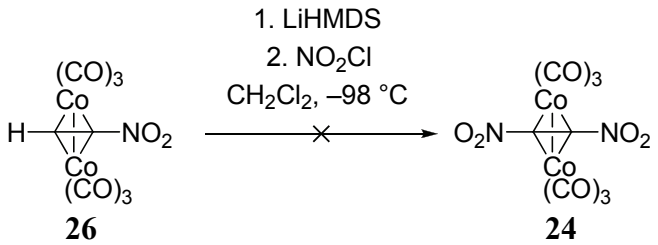

26 **24**

If left to stand, LiHMDS deprotonates methylene chloride, but Zhang found through his work on **10** (octanitrocubane), that this process is prevented by combining LiHMDS with methylene chloride with rapid cooling to –78 °C in under five minutes.[154] Addition of this mixture to a solution of **26** at –78 °C caused a black precipitate to form and immediate loss of all red color, indicating decomposition. Lowering the temperature to –98 °C slowed this process by 1–2 seconds, leaving the possibility that even lower temperature might stabilize the desired anion. These results again underscore the difficulty of producing hexacarbonyldicobalt alkynyl anions.

Attempts to trap **25a** addition of methyl triflate also failed (Scheme 161).

Scheme 161. Attempted reaction of **26** with LiHMDS and methyl triflate.

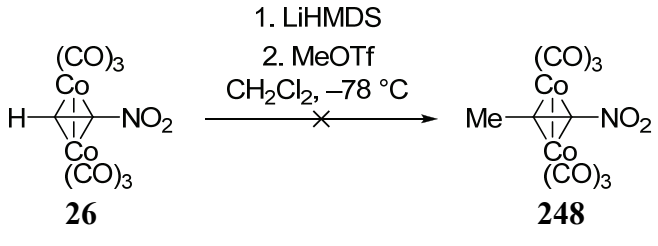

26 **248**

Even at –78 °C, destruction of **26** was immediate, noted by an opaque black color and the absence of any colored spots on TLC, indicative of the presence of cobalt complexes. In the presence of excess methyl triflate, LiHMDS decomposed **26** (Scheme 162), resulting in the same black color.

Scheme 162. Decomposition of **26** with LiHMDS in the presence of methyl triflate.

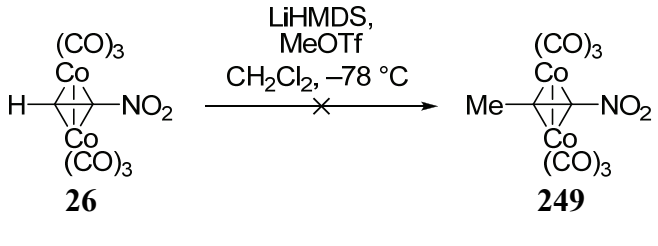

26 **249**

These failures imply that **25a**, if formed, is too reactive to attack an S_N2 acceptor, and might mean that the silylated and benzylated products observed by Magnus[99] originated by another route.[99]

In view of these unsuccessful derivatizations, we returned to the simplest process of recovering the free ligand by oxidative demetallation (Scheme 163), a tranformation that was successful with **25**.

Scheme 163. Attempted demetallation of **26** with CAN.

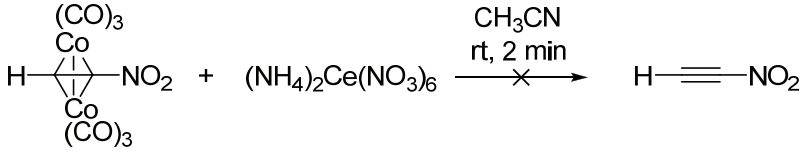

26 **16**

Unfortunately, with a seven-fold molar excess of CAN, **26** was completely consumed within two minutes. ^{1}H NMR spectroscopy confirmed the absence of even traces of **16** or **26**. Similarly, there were no signals in the alkene region, as one would have expected from addition products of **16**. We are left to conclude that either **16** does not form, or it decomposes immediately. The inability to recover **16** from **26** at room temperature limits the storage capacity of **26**, but future research may find suitable conditions for this release.

3.4 Conclusion

This chapter has presented attempts to prepare **24** by trapping, functional group transformation, and nitration of a variety of alkyne and hexacarbonyldicobalt alkyne starting materials. The first two nitroalkyne transition metal complexes, **25** and **26**, were found to be air- and thermally-stable, crystalline solids at room temperature. The nitro moiety appears to be responsible for this stability, and its electron withdrawing effect is evident in the IR, NMR, and CV spectra. The most pronounced effect of the nitro group appears in the X-ray structures of **25** and **26**, where shortened alkyne carbon-cobalt bond lengths suggest strong back donation to the alkyne ligand. Correlation of these distances was found to be inversely proportional to substituent electronegativity. Phosphine adducts of **25** were made, but neither these nor **25** itself could be nitrated. Complex **25** can be viewed as providing effective storage of **18**, from which the latter can be regenerated by oxidative demetallation. The TMS complex is also a precursor to **26**. Deprotonation and nitration of **26** were unsuccessful, as was recovery of **16** by oxidation. Cyclizations of **25** and **26** to furnish nitrobenzenes are described in Chapter 4.

Chapter 4. Nitroalkyne Complexes as Precursors to Organic Compounds

4.1 Introduction

The availability of the novel nitroalkyne complexes **25** and **26** prompted the question of whether they might function as reagents in organic transformations. Of particular interest were cyclization reactions of the alkyne ligand, either on its own or with added unsaturated substrates.

The capacity of hexacarbonyldicobalt alkyne complexes to furnish cyclic organic molecules was recognized as early as 1959, when the carbon monoxide insertion product of a hexacarbonyl dicobalt alkyne complex was observed to thermally decompose into γ-lactones.[362] The next year, substituted benzenes were obtained from [2 + 2 + 2] alkyne cyclotrimerization with such complexes.[363,67] A third relevant reaction was discovered in 1971, when coordinated alkynes were found to combine with alkenes and carbon monoxide to form cyclopentenones (later called the Pauson-Khand reaction).[364,365,366]

Our interest lay in the application of **25** and **26** to the latter two cyclizations. As substrates, these complexes had the potential to form nitrated molecules of interest as synthetic intermediates or as energetic materials. Our efforts to incorporate **25** and **26** into the Pauson-Khand reaction will be detailed first, followed by the [2 + 2 + 2] cyclization.

4.2 Attempted Pauson-Khand Reactions

The transition-metal mediated [2 + 2 + 1] cycloaddition of an alkyne, an alkene, and carbon monoxide to engender cyclopentenones is known as the Pauson-Khand reaction.[364,365,366] Such ketones interest researchers because they are Michael acceptors with a wide variety of synthetic applications. The proposed mechanism[367,368] begins with carbonyl dissociation followed by alkene coordination. The alkene then inserts into a cobalt-carbon bond, and a molecule of carbon monoxide is ligated. Migratory insertion of a carbonyl ligand then sets the stage for successive reductive eliminations of $Co(CO)_3$ fragments to afford the cyclopentenone (Scheme 164).

Scheme 164. Proposed mechanism for the Pauson-Khand reaction.

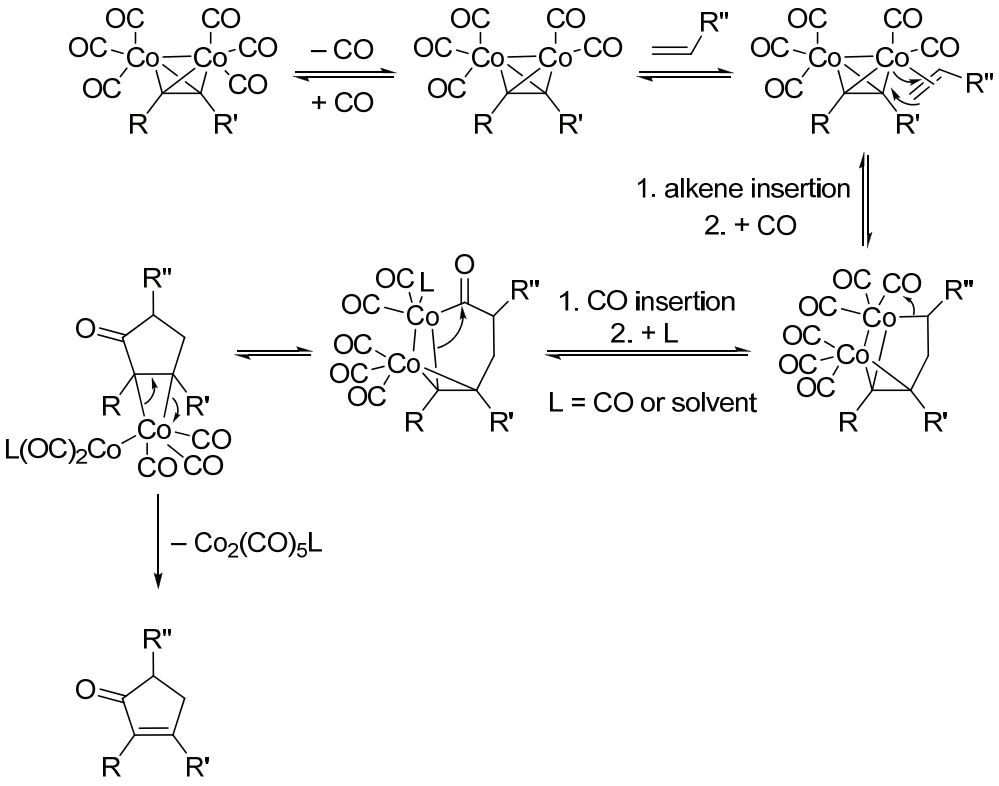

The original conditions for the Pauson-Khand reaction stipulated elevated temperatures, high carbon monoxide pressures, and long reaction times and were often associated with low yields.[364,365,366] Various catalysts later moderated these conditions, but sometimes limited scope.[369,370,371,372,373,304,70,101,374,375,376,377,378,379,380,381,382,383,384,385,386] Currently, the most widely employed initiators are tertiary *N*-amine oxides, which are thought to start the reaction by oxidative removal of CO as CO_2.[380,378,387,70,376]

Substituents affect both the yield and the regioselectivity of the reaction. Most relevant to this section are substituents on the alkyne component. Terminal alkynes are usually the most facile substrates,[388] even when bearing a bulky group.[389,372,390,376,375] Internal alkynes with two sterically demanding substituents do not perform as well, to the point of being unreactive.[372,391] Electron poor alkynes, even terminal ones, also give inferior results.[388]

Both sterics and electronics of substituents influence their eventual position relative to the carbonyl in the cyclopentenone product.[389,392] Large groups appear predominantly α to the carbonyl,[393,394] while electronegative ones prefer β positioning, with a few exceptions,[395,396,392,372,391,397,398] usually associated with the use of transition metal catalysts other than cobalt.[369,399] When competing, steric effects largely trump electronic effects, but as the size difference between the substituents diminishes, the electronic effects play a larger role[389,372,399,393,397,400] (bond polarization has also been proposed as an explanation).[392] For example, the ethyl propynoate (**249**) reacts with norbornene (**250**) to give mainly methyl 5-oxo-tricyclo[5.2.1.0]deca-4-en-3-carboxylate (**251**) (Scheme 165).[396,389]

Scheme 165. Pauson-Khand reaction of **249** with **250**.

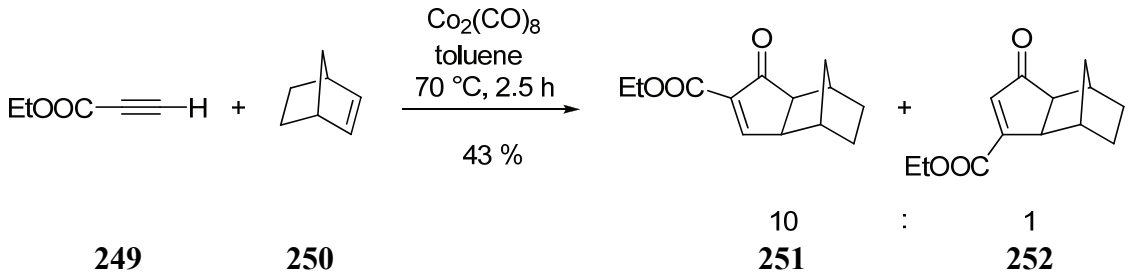

249 **250** **251** **252**

However, replacement of the terminal proton in **249** with methyl, as in ethyl butynoate (**253**) reverses this regioselectivity, rendering a cyclopentenone featuring the ester group β to the carbonyl.[395,401,392,389]

In the case of the potential reaction of **25** with **250**, both steric and electronic effects would seem to conspire to favor 5-nitro-4-(trimethylsilyl)tricyclo[5.2.1.0]deca-4-en-3-one (**254**) over the other regioisomer, 4-nitro-5-(trimethylsilyl)tricyclo[5.2.1.0]deca-4-en-3-one (**255**) (Figure 28).

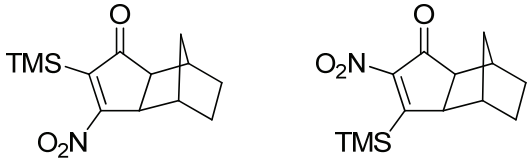

254 major **255** minor

Figure 28. Predicted Pauson-Khand product regioselectivity of **25** with **250**.

While sterically less hindered than **25**, **26** was anticipated to exhibit less regioselection. On the basis of sterics, one would expect the larger nitro group to appear α to the carbonyl, but the electronic factor suggested that it would prefer the β position. One notes that **249** (Scheme 165)[396,389] converts according to the steric criterion. The relatively more strongly electron withdrawing nitro group might make β-selectivity more competitive.

Complexes **25** and **26** were potential precursors to nitrocyclopentenones, only one example of which is known, namely 3-nitro-2-cyclopentenone (**256**), made by Corey et al. in 1981 via the oxidation of an epoxy oxime.[402] Besides being of intrinsic interest, nitrocyclopentenones might be powerful Michael acceptors (with the nitro group α to the carbonyl) or reverse Michael acceptors (with the nitro group in the β position) (Figure 29).

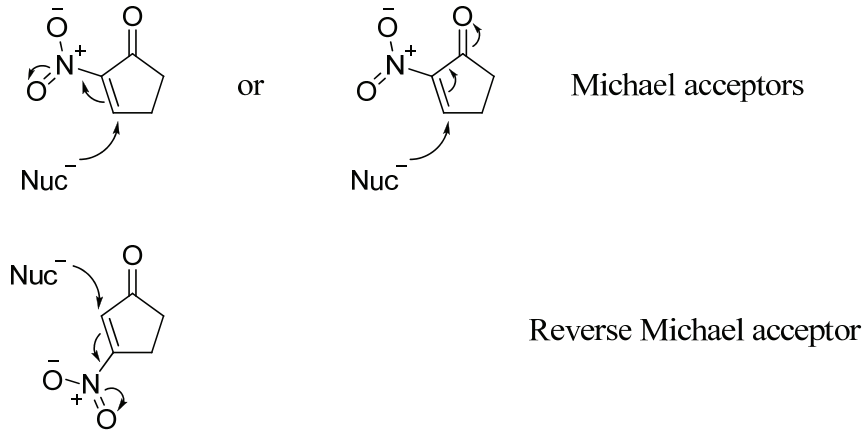

Figure 29. Nitrocyclopentenones as forward or reverse Michael acceptors.

Such molecules would be the first nitrocyclopentenones derived from the Pauson-Khand reaction, and its regiochemistry would provide insight into the effect of powerful electron withdrawing groups on its outcome.

Before committing the valuable **25** or **26** to trial experiments, we sought to calibrate our efforts on the readily available **218** and **219**.

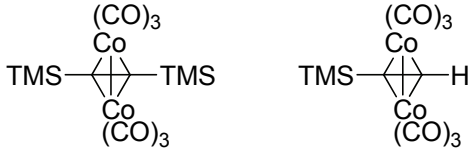

218 **219**

The former had been successful only once in the Pauson-Khand reaction, namely in the cocyclization with allenes.[372] The latter was a well-known substrate in this reaction.[390,372,379,381,380,378,371,383] Our initial attempt with **218** employed Pauson's conditions for the reaction of vinyl benzoate (**257**) with **70** (phenylacetylene) promoted by *N*-methylmorpholine-*N*-oxide (NMO) (**258**) to give 2-phenylcyclopentenone (**259**).[375] In this work, carbon-oxygen cleavage in the (unobserved) initial product was assumed to be effected by some reducing cobalt species, making **257** a useful ethylene equivalent (Scheme 166).

Scheme 166. Failed reaction of **218** with **257**.

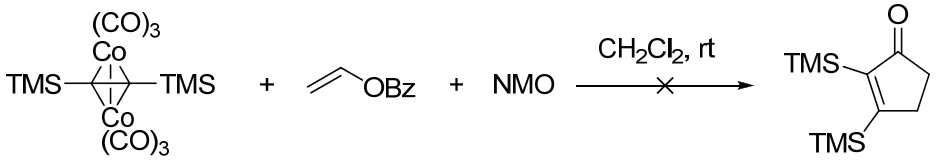

218 **257** **258** **260**

In the event, the starting **218** was consumed, but none of the desired **260** observed. We substituted the more reactive cyclopentene (**261**) for vinyl benzoate and changed the

conditions to those reported by Jeong et al., which included trimethylamine-*N*-oxide (**262**)[387] (Scheme 167).

Scheme 167. Attempted reaction of **25** with **261**.

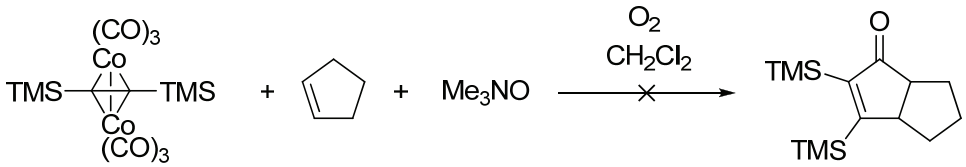

218 **261** **262** **263**

This reaction also met with failure, destroying all of complex **218** without formation of **263**. Evidently, **218** is too bulky a substrate for the reaction. Therefore, attention was turned to **219** and its potential cocylization with **257** (Scheme 168).

Scheme 168. Failed reaction of **219** with **258**.

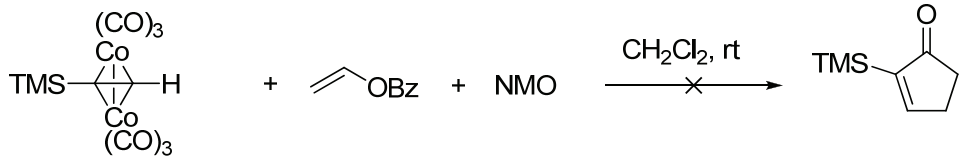

219 **257** **258** **264**

Once again, we were left with no product. As a "reality check," a known reaction was targeted, employing **250**[390] with ammonium hydroxide as the promoter, reported by Sugihara et al. to accelerate the cyclization (Scheme 169).[403]

Scheme 169. Reaction of **219** with **250**.

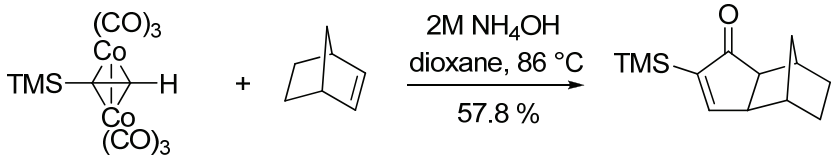

219 **250** **265**

After mixing all the ingredients, heating generated a cloudy black precipitate. Work-up by preparative TLC (Chromatotron) furnished the known 4-(trimethylsilyl)tricyclo[5.2.1.0]deca-4,8-en-3-one (**265**) in 58 % yield. The spectral data of **265** were in accord with literature values.[390]

Having finally ascertained viable conditions, we substituted **25** for **219** (Scheme 170).

Scheme 170. Failed reaction of **25** with **250**.

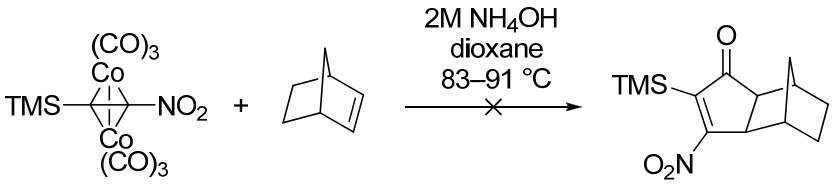

25 **250** **254**

A brown-black precipitate formed, similar to that observed in the reaction of **219**, but the solution was green, typical of oxidation of such complexes. TLC analysis did not reveal any UV-active compounds, including remaining **25**.

This failure prompted us to return to an amine *N*-oxide promoter in an attempt to enhance the reactivity of the electron poor **25** in a manner similar to that of (4*R*)-[3-(trimethylsilyl)prop-2-ynoyl)]-4-phenyloxazolidin-2-one (**266**) (Scheme 171).[400]

Scheme 171. Failed reaction of **25** with **250**.

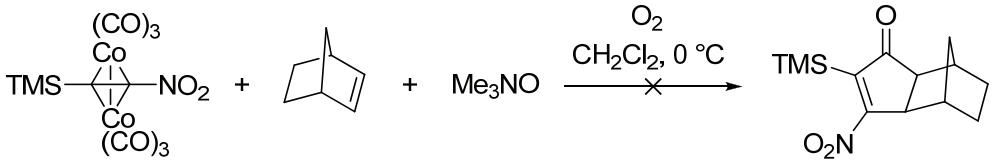

25 **250** **262** **254**

This reaction proved unsuccessful as well, destroying **25** without generating any isolable products.

In a final attempt, we turned to the less sterically hindered **26**, in hopes that it would be more viable than **25**. We employed NH_4OH as a promoter because of its success with **219** (Scheme 172).

Scheme 172. Unsuccessful reaction of **26** with **250** and NH_4OH.

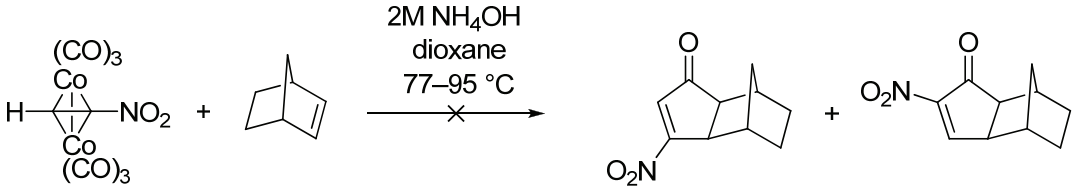

26 **250** **267** **268**

Unfortunately, although **26** disappeared, neither **267** nor **268** were found. Similar to the reaction of **25**, a black precipitate and green solution were observed. In this, as well as all preceding attempts, a search for any amine addition products was fruitless.

What are the reasons for the failure of **25** and **26** to enter Pauson-Khand chemistry? Sterics alone can be discounted, since a number of TMS-substituted alkynes are successful,[372,390,381,383,380,378,379,404] including **266**,[400] but might cause problems in

conjunction with electronics in the case of **25**, considering the failure of the similar (*S*)-2-(trimethylsilyl)ethynyl *p*-tolyl sulfoxide (**269**).[391] Both **25** and **26** bear a powerfully electron withdrawing nitro group that deactivates the alkyne complex toward the Pauson-Khand cyclization. In Chapter 3, we presented evidence of strong backbonding to the alkyne from the metal centers in **25** (Section 3.3.4) and **26** (Section 3.3.5) in the form of shortened carbon-cobalt bond lengths. Such short, strong bonds might make insertions difficult. Indeed, it has been noted that alkene reactivity relates to back donation from *d* orbitals on cobalt to π* orbitals on the alkene.[405,101] In the case of nitroalkynes, cobalt *d* orbitals are already taxed for electron density, and thus unlikely to be good donors to an alkene π* orbital, hampering alkene insertion.

In addition to these electronic arguments, it is possible that the nitroalkyne moiety, in starting materials (especially the sensitive **26**), intermediates, or the desired products, is unstable under the conditions of the Pauson-Khand reaction. The original high temperature, high pressure conditions might be needed to coerce alkene insertion into the reluctant nitroalkyne complexes. In this protocol, nucleophilic catalysts are absent, which might help in preserving any reactive products. The exploration of such alternatives was left in the hands of future researchers.

4.3 [2 + 2 + 2] Cobalt-mediated Cyclotrimerizations

In 1866, Berthelot discovered the first alkyne cyclotrimerization to benzene, using harsh pyrolytic conditions.[71] Nearly a century later, Reppe et al. recognized the capacity of nickel to catalyze or mediate this transformation,[72] and within a few years, a variety of transition metal catalysts appeared, including some based on cobalt.[73,198] Hübel and Hoogzand observed in 1960 that hexacarbonyldicobalt alkyne complexes catalyzed alkyne cyclization,[363] and that a wide variety of substrates, including those with bulky or electronegative substituents, were tolerated.[67]

A possible generic mechanism for this process is shown in Scheme 173 on the next page.[406,407,408] A number of substrates have been investigated, including diynes[409] and unsymmetrical alkynes.[407,408,406,67] The latter give predominantly 1,2,4-trisubstituted arenes.

Scheme 173. Cobalt-mediated [2 + 2 + 2] cyclization mechanism.

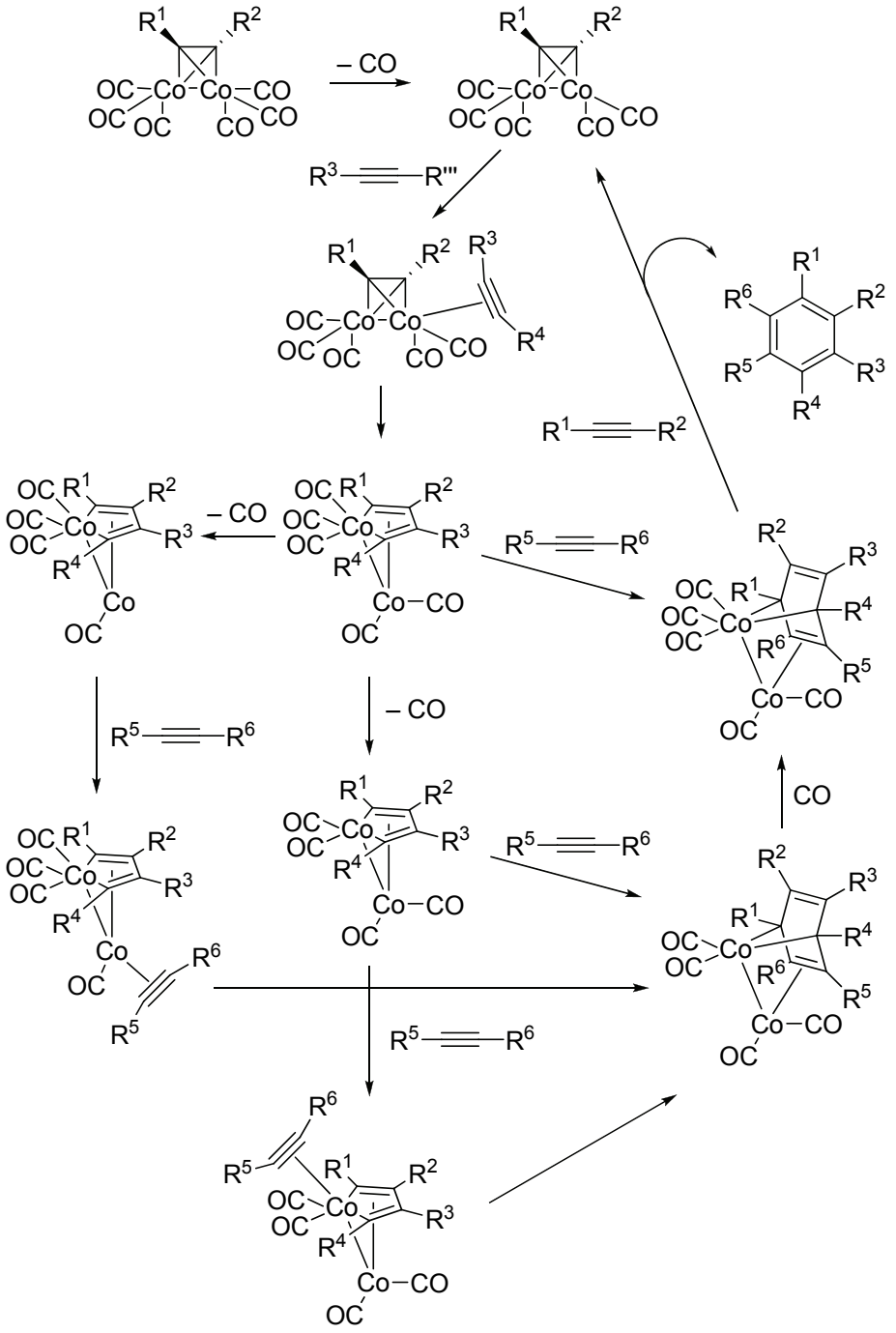

The regioselectivity of such cyclizations is controlled by that of the initial metallacyclopentadiene formation and then further by that of the subsequent third alkyne insertion (Scheme 174).

Scheme 174. Intermediates of the [2 + 2 + 2] cyclization and their products.

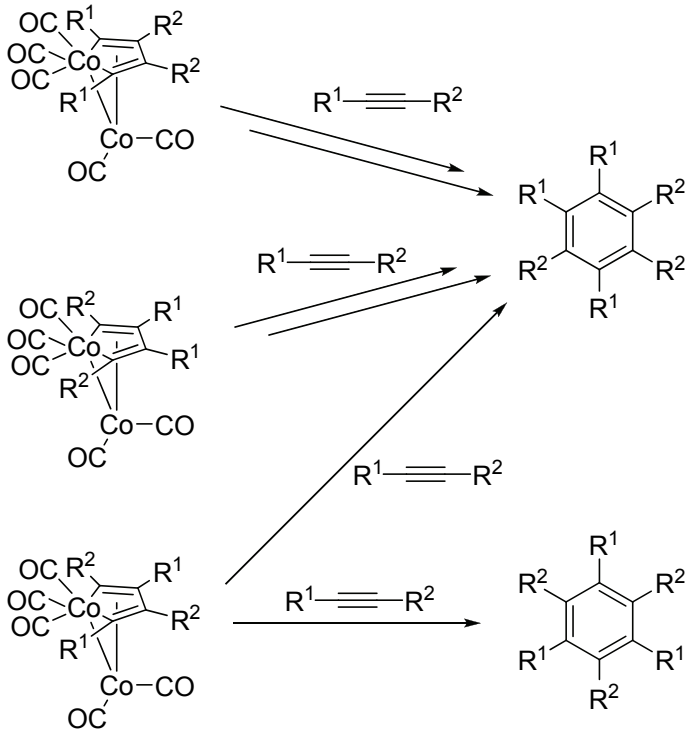

Reactions of α,ω-diynes furnish fused arenes (Scheme 175).[409]

Scheme 175. Cocyclization of alkynes with α,ω-diynes.

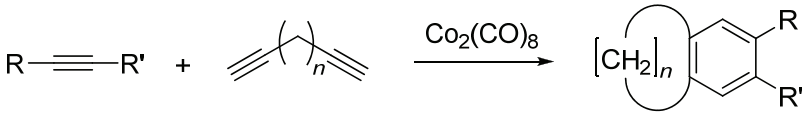

n = 3-5

Specifically, these transformations were run by preforming the monoalkyne cobalt complex in situ, before adding the diyne using syringe pump techniques. Yields were reasonable, even in the case of bulky cocyclization partners.[409] The requisite diynes featuring three to five atom tethers are readily available and lead to five-, six-, and seven-membered ring-fused systems. Shorter carbon chains fail with **23** [$Co_2(CO)_8$],[409] presumably for reasons of strain, although other catalysts, such as [$Co(CO)_4$]Hg,[410] $CpCo(CO)_2$,[411,412] $NbCl_5$,[413] and $TaCl_5$,[413] are successful in accessing four-membered ring compounds. Examples of the power of this strategy using **23** are shown in Scheme 176.[409]

Scheme 176. Reactions of diynes **271**, **273**, and **276** with **23**, **270**, and **275**.[409]

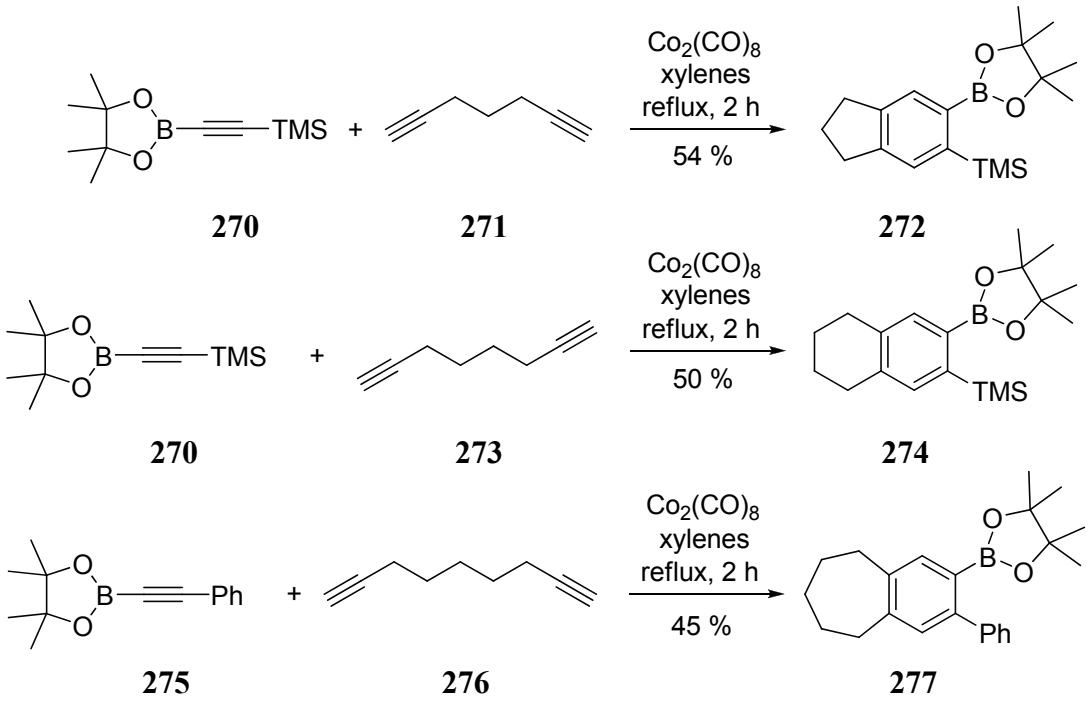

270 **271** **272**

270 **273** **274**

275 **276** **277**

When three discrete alkynes participate in the cyclization, two main factors control reactivity: sterics and electronics. Bulky groups do not necessarily hinder cyclization, as is evident by cyclotrimerization of **79** (Scheme 177).[67,363]

Scheme 177. Cyclotrimerization of **79**.

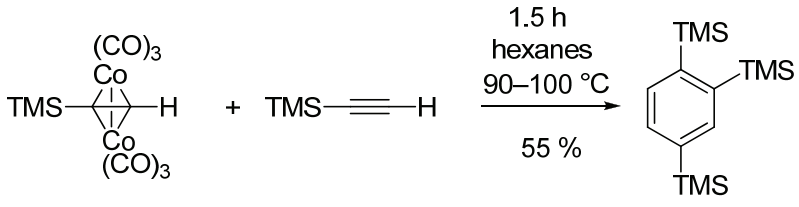

219 **79** **278**

However, two large substituents can diminish yield (e.g., isopropyl[414] or isopropenyl[415]) or prevent reaction altogether (e.g., *t*-butyl,[416] TMS,[67] or *o*-bromophenyl[416]) (Table 28).

Table 28. Steric inhibition of cyclization of **72**, **279**, **280**, **281**, and **282**.

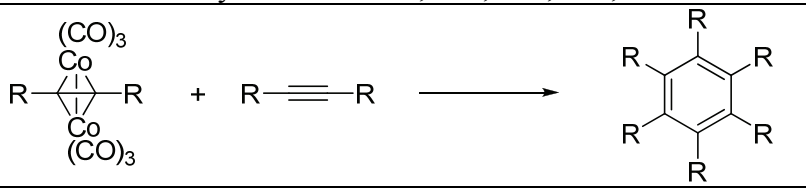

R	Alkyne	Conditions	Yield (%)
i-Pr	**279**[414]	Skellysolve C, reflux, 3 d	12
	**280**[415]	Skellysolve C, reflux[a]	4
t-Bu	**281**[416]	dioxane, 65–100 °C, 2.5–4 h	0
TMS	**72**[67]	hexanes, 100 °C, 3 h	0
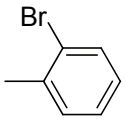	**282**[416]	dioxane, 65–100 °C, 2.5–4 h	0

[a] Reaction time not given.[415]

Some alkynes are viable under specific conditions, such as **78**, which only cyclizes in the presence of **186**.[67] In almost all cases, bulky unsymmetrical alkynes produce unsymmetrically substituted benzenes. Only **78** yields a significant amount of the symmetrical isomer.[67]

The electronic influence on these reactions appears less obvious. Hübel and Hoogzand noted that electron poor acetylenes gave faster cyclizations (but not necessarily increased yields).[416] Alkynes mono-substituted by electron withdrawing groups, including COOMe,[416,406] COOH,[363] CF_3,[417] and CN,[416] all cyclotrimerized, as did the disubstituted **20**[417] and **197**.[406]

20 **70** **182** **197**

However, the corresponding hexacyanobenzene (**283**) failed to form from dicyanoacetylene (**284**).[416] Curiously, Hübel and Hoogzand cited *p*-nitrophenylacetylene (**285**) as an example that "nitroalkynes can't be trimerized at all."[416] Given the context, this is assumed to be an error in translation, having meant to say "nitro-group-containing acetylenes." It is not clear why this function was singled out in this manner. Overall, it appears that electron withdrawing groups do not hinder cyclization, and the few exceptions might have other reasons for failure.

Turning to the issue of regioselectivity, most unsymmetrical acetylenes render only unsymmetrical benzenes via the [2 + 2 + 2] cyclotrimerization, but those bearing strong electron withdrawing groups tend to also produce significant amounts of the symmetrical isomers. For example, **70**,[67,406,418] **79**,[67,363] 1-phenylpropyne (**286**),[418] but-3-yn-1-ol (**287**),[363] 1-methoxyprop-2-yne (**288**),[363] and 2-methylbut-3-yn-2-ol (**289**)[418] all

trimerize exclusively to the corresponding unsymmetrically substituted benzenes (Table 29).

Table 29. Unsymmetrical benzene production from alkynes without strong electrophilic substituents.

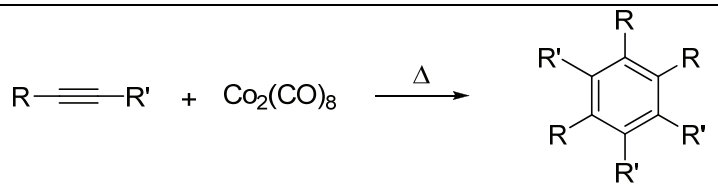

R	R'	Alkyne	Benzene	Yield (%)
Ph	H	**70**[67,406,418]	**290**	90
Ph	Me	**286**[418]	**291**	[a]
TMS	H	**79**[67,363]	**278**	55
CH_2CH_2OH	H	**287**[363]	**292**	14
CH_2OMe	H	**288**[363]	**293**	17
CMe_2OH	H	**289**[418]	**294**	30

[a] Yield not given.

The electron deficient **242**[416] 3-phenylprop-2-ynenitrile (**295**),[416] methyl but-2-ynoate (**296**),[406] and methyl 3-phenylpropynoate (**297**),[406] all give mixtures of isomers. Both isopropenylacetylene (**298**)[418] and 4-phenylbut-3-yn-2-one (**299**)[418] furnish only the symmetrical benzene isomer. These reactions are outlined in Table 30 on the next page. A few exceptions to this trend exist, such as **234** (trifluoromethylacetylene)[417] and 3-phenylpropionic acid (**300**),[363] which both give unsymmetrical benzenes, and **78**[67] (in the presence of **186**) which generates a substantial amount of symmetrical product.

Despite these exceptions and a lack of mechanistic studies on this phenomenon, it seems reasonable to assume that electronegative groups likely polarize the coordinated triple bond in a way that benefits alkyne insertion favoring the symmetrical isomer.

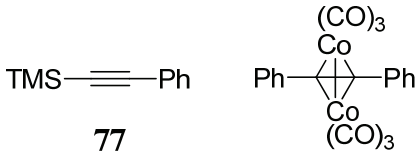

234 **242**

Table 30. Benzene production from electron deficient alkynes.

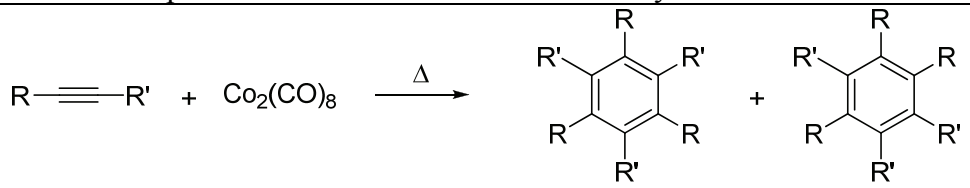

R	R'	Alkyne	Symmetrical Benzene	Yield (%)	Unsymmetrical Benzene	Yield (%)
COOMe	H	**242**[416]	**301**	14	**302**	56
Ph	CN	**295**[416]	**303**	41	**304**	22
COOMe	Me	**296**[406]	**305**	23	**306**	75
COOMe	Ph	**297**[406]	**307**	8	**308**	53
	H	**298**[418]	**309**	10	N/A	0
	Ph	**299**[418]	**310**	[a]	N/A	0

[a] Yield not given.

Nitroalkyne complexes **25** and **26** were anticipated to participate in the [2 + 2 + 2] cyclotrimerization with α,ω-diynes, symmetrical, and unsymmetrical alkynes. Thus, the bulky TMS group had been tolerated in related systems[409] and so had terminal electron deficient alkynes, **234**[417] and **242**.[416] Because the ligated alkynes were electron poor, both **25** and **26** were expected to form regioisomeric mixtures of arenes when treated with an unsymmetrical alkyne.

4.3.1 Reaction of 25 and 26 with α,ω-Diynes

Inspired by the results portrayed in Scheme 176,[409] the potential of **25** and **26** to undergo cocyclotrimerization chemistry was explored using tethered diynes.

4.3.1.1 Cyclization to Indanes

Complex **25** was treated with **271**, affording the unknown 6-nitro-5-(trimethylsilyl)indane (**311**) in 25 % yield and 3 % of a side product thought to be 1,3-bis(2,3-dihydro-1*H*-inden-5-yl)propane (**312**)[410,413,419,348] (based on **25** as a limiting reagent) (Scheme 178).

Scheme 178. Reaction of **25** with **271**.

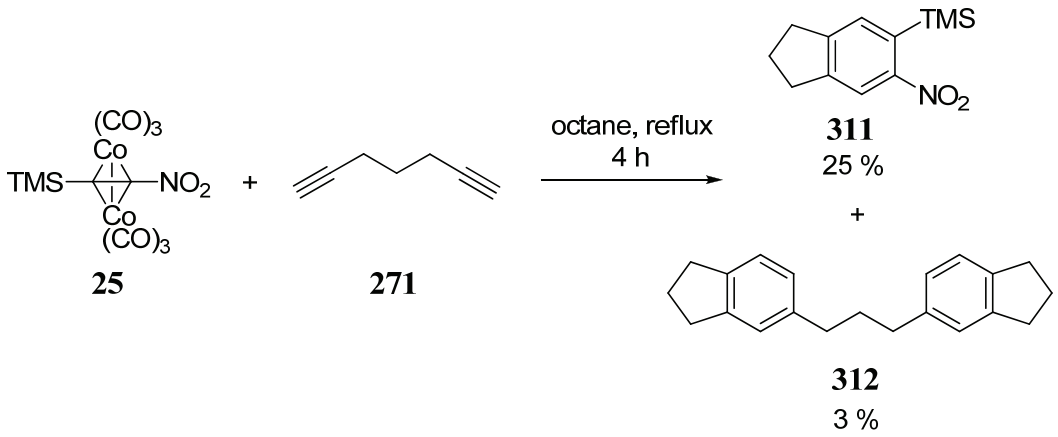

25 **271**

Octane (b.p. 126 ° C) replaced the traditional toluene[407] or xylenes[409] to aid signal detection in the aromatic region of the ^{13}C NMR spectrum of the crude product. The comparatively[409] low yield of **311** is probably due to the sensitivity of **25**. Because **311** was unknown, structural confirmation was obtained by spectral comparison with the closest known analog, 5-nitroindane (**313**).[420,421]

Silicon-methyl vibrations at 1251 and 850 cm^{-1} in the IR spectrum of **311** revealed the presence of the TMS group.[188] The unsymmetrical and symmetrical stretching bands of the nitro group (1519 and 1347 cm^{-1}) were similar to those of **313** (1515 and 1345 cm^{-1}).[420] These absorptions were within the ranges of 1535–1510 cm^{-1} and 1350–1340 cm^{-1} expected for nitrobenzenes.[189] A neighboring peak at 1566 cm^{-1} in **311** corresponds to a similar one in the spectrum of **313** (1588 cm^{-1})[420] and may be due to a carbon-carbon stretching vibration of the aromatic ring. Such vibrations are difficult to assign, because they overlap with those of the nitro group and appear at different wavenumbers and intensities depending on substitution.[123,422] Another absorption, at 1607 cm^{-1}, also had a counterpart in **313** (1611 cm^{-1}),[420] out of range of nitro group stretching, and was easier to attribute to the aromatic skeleton. The aromatic C–H stretching motion in **311** was evident by a peak at 3065 cm^{-1} (vs. 3103, 3072, and 3050 cm^{-1} for **313**) and the corresponding out of plane deformation by one at 891 cm^{-1} (875 and 834 cm^{-1} for **313**[420]).[423] Combined, these C–C and C–H bands provide strong evidence of an aromatic system. Alkyl C–H stretching was observed at 2954, 2901, and 2845 cm^{-1}, similar to **313** (2955 and 2843 cm^{-1}).[420] These bands do not differentiate between cyclic or linear saturated carbons, overlap with the C–H absorption from the TMS methyl groups on **311**, and are therefore not diagnostic.

The mass spectrum of **311** did not exhibit a molecular ion (*m/z* = 235), but rather a fragment parent ion at *m/z* = 220 (100 %), typical of fragmentation of a methyl from the TMS group.[126] Two additional fragment peaks appeared at *m/z* = 190 (23 %) and 189 (23 %). The former is likely due to rearrangement of the nitro group to a nitrite and concomitant loss of NO from the parent ion, the latter to nitro loss from the molecular ion. The former rearrangement, observed for some nitroaromatics,[126] is absent in the mass spectrum of **313** and thus its invocation is tentative.

Of course, most diagnostic were the NMR spectra of **311**. In the ^{1}H NMR spectrum in $CDCl_3$, the TMS group was observed as a singlet at δ 0.33 ppm. Protons from the saturated carbon most distant from the aromatic ring appeared at δ 2.16 ppm as a quintet (J = 7.5 Hz), mimicking their counterparts on **313** in $CDCl_3$, at δ 2.16 ppm (t, J = 7.5 Hz). The remaining four aliphatic protons overlapped at δ 2.98 ppm as a triplet (J = 7.4 Hz). For **313**, these hydrogens are reported as two triplets at δ 2.96 and 2.98 ppm (J = 7.5 Hz each) in one source,[420] and as a broad triplet at δ 3.0 ppm in another.[421] The aromatic hydrogen adjacent to TMS gave rise to a singlet at δ 7.53 ppm, and that next to nitro at δ 8.04 ppm, revealing their para relationship. In the spectrum of **313**, two doublets occurred at δ 7.29 ppm (J = 7.4 Hz) and δ 7.968 ppm (J = 1.4 Hz), revealing vicinal aromatic protons, and the remaining proton between the nitro group and the saturated ring resonated at δ 7.971 ppm.[420]

The ^{13}C NMR spectrum was also largely similar to that of its counterpart **313** (both in $CDCl_3$). The TMS carbons occurred at δ –0.22 ppm. Resonances from the unsaturated ring appeared at δ 25.5, 32.5, and 32.8 ppm, close to those of **313** at δ 25.6, 32.6, and 32.9 ppm.[420] The proton-bearing aromatic carbon adjacent to the nitro group manifested itself as a peak at δ 120.2 ppm (δ 119.4 ppm for **313**). The TMS group shifted both the ipso-carbon signal (δ 134.5 ppm) and that of its neighboring proton-bearing carbon (δ 131.6 ppm) downfield relative to **313** (δ 121.9 and 124.6 ppm, respectively).[420] The bridging quaternary carbons were observed at δ 146.9 and 150.7 ppm, at slightly lower field than those of **313** (δ 145.9 and 147.1 ppm).[420] The nitro-substituted carbon resonated furthest downfield at δ 152.5 ppm, almost identical to the chemical shift of the corresponding carbon of **313** (δ 152.3 ppm).[420] These data are summarized in Table 31.

Table 31. ^{13}C NMR shift assignments of **311** and **313** in $CDCl_3$.

^{13}C NMR signals (δ ppm)		
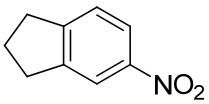	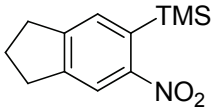	
313[420]	**311**	Assignment
N/A	–0.22	CH_3 on TMS
25.6	25.5	saturated carbons
32.6	32.5	
32.9	32.8	
119.4	120.2	proton-bearing aromatic carbons
121.9	131.6	
124.6		
N/A	134.5	TMS-bearing carbon
145.9	146.9	bridging carbons
147.1	150.7	
152.3	152.5	nitro-bearing carbon

The ^{29}Si NMR of **311** in $CDCl_3$ was recorded at δ –2.32 ppm, normal for TMS.

The successful conversion of **25** to **311** demonstrated that the coordinated alkyne (**18** in this case) can participate in the [2 + 2 + 2] cyclotrimerization reaction.

Repeating this reaction with **26** proved less efficient. Treatment of **26** with **271** in hexanes heated to reflux afforded **313** as a clear oil in only 1.3 % yield (Scheme 179).

Scheme 179. Reaction of **26** with **271**.

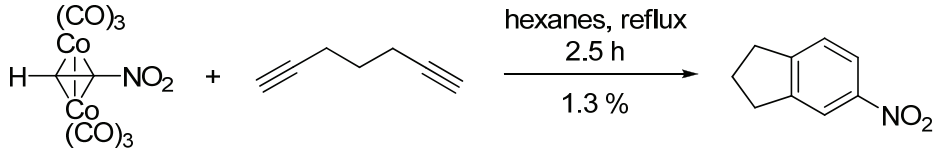

26 **271** **313**

Hexanes replaced octane as the solvent in an attempt to minimize thermal decomposition of **26**. The reaction, monitored by TLC, consumed **26** after 2.5 hours. Unidentified brown and yellow oils, comprised of mixtures of compounds, were separated from the product by preparative TLC (Chromatotron). Compound **313** (vide supra) was identified by comparing its ^{1}H NMR and mass spectra with literature values.[420,421,424,425]

While the yield is poor, the conversion of **26** into **313** indicates that, at least in principle, a stable equivalent of **16** might be useable for synthetic purposes.[426]

4.3.1.2 Cyclization to Tetralins

The second diyne tested with **25** was **273**. Complex **25** was treated with **273** in octane heated to reflux to afford 7-nitro-6-(trimethylsilyl)tetralin (**314**) as a pale yellow oil in 39 % yield. A side product, 1,4-bis(5,6,7,8-tetrahydronaphthalen-2-yl)butane (**315**), derived from trimerization of **273** was also isolated in 21 % yield (based on **25** as the limiting reagent) (Scheme 180).

Scheme 180. Reaction of **25** with **273**.

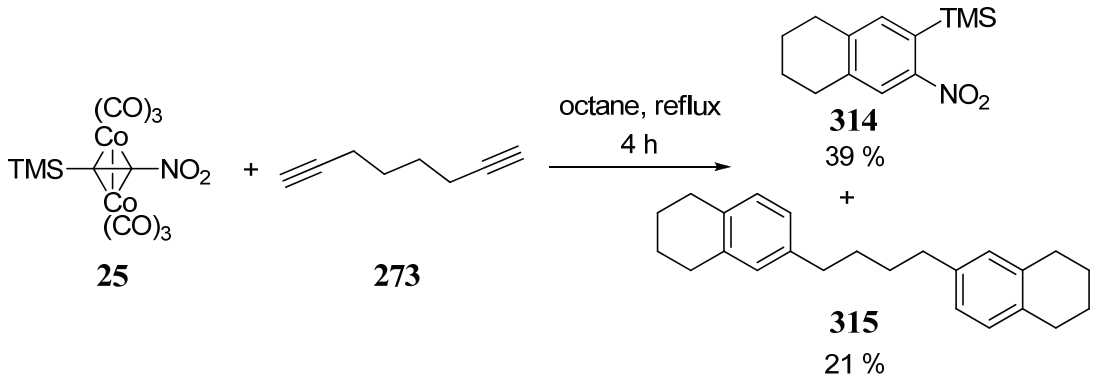

25 **273**

The origin of **315**[410,413] is not certain, but a plausible scenario is shown in Scheme 181. Thus, after release of **314** from putative **316**, **273** is coordinated to form [μ-hepta-1,6-

diyne-1,2-diyl](tricarbonylcobalt)(dicarbonylcobalt)(*Co–Co*) (**317**), the first step in the route to **315** (Scheme 181).

Scheme 181. Mechanism of formation of **317**.

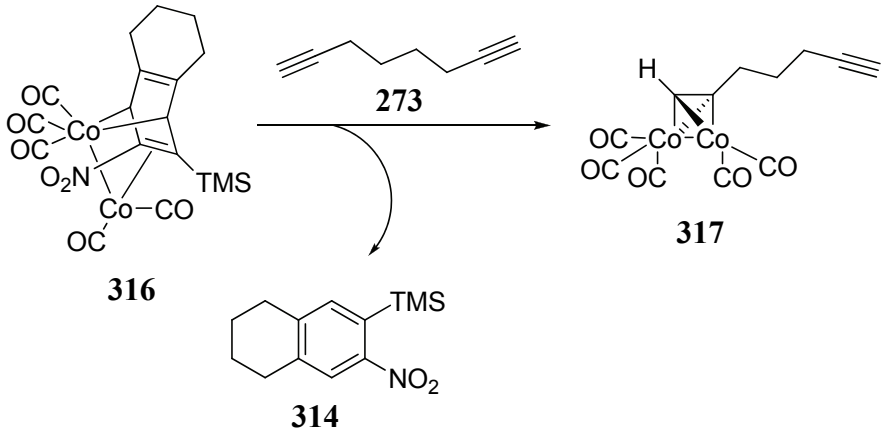

It is unclear why the yield of **314** is greater than that of the slightly smaller **311**. The structural assignment of the unknown **314** was made on the basis of its spectral properties, including IR, MS, and NMR data.

The IR spectrum revealed the presence of the nitro group through its unsymmetrical and symmetrical stretching peaks at 1525 and 1341 cm^{-1},[122,189] similar to those found for **311** (1519 and 1347 cm^{-1}). A weak vibration at 1556 cm^{-1} was again attributed to aromatic C–C ring stretching. The aromatic C–H out of plane bending vibration at 871 cm^{-1} was less energetic than that of **311** (891 cm^{-1}), but such shifts are difficult to predict in heavily substituted ring systems, so its significance is questionable.[189] The aromatic C–H stretching region, partly masked by absorbed moisture, exhibited only one peak, at 3060 cm^{-1}. The C–H stretching vibrations of the saturated ring and the methyl groups on TMS appeared at 2932 and 2858 cm^{-1}. The silicon-methyl deformation vibrations were evident at 1248 and 847 cm^{-1}.[188]

Similar to the mass spectrum of **311**, that of **314** did not contain a molecular ion (*m/z* = 249), but a parent ion at *m/z* = 234 (100 %), due to loss of methyl from the TMS group.[126] The remaining two major peaks in the spectrum [*m/z* = 212 (60 %) and *m/z* = 145 (85 %)] could not be assigned.

As expected, the NMR data in $CDCl_3$ were most useful in confirming the structural assignment of **314**. A singlet at δ 0.33 ppm, in exactly the same position as that of its counterpart **311**, was due to the TMS group. Two aromatic proton singlets were present at δ 7.36 and 7.93 ppm, the latter belonging to the hydrogen ortho to the nitro group, confirming the 1,2-substitution of TMS and nitro. The corresponding proton signals in 6-nitrotetralin (**318**) occur as multiplets at δ 7.2–7.3 ppm and 7.8–8.0 ppm in $CDCl_3$.[425] Two types of saturated proton signals were observed. The benzylic signals were near isochronous and appeared as a broad triplet at δ 2.83 ppm (*J* = 6.4 Hz). The remainder gave rise to a quintet at δ 1.83 ppm (*J* = 3.2 Hz).

The ^{13}C NMR data in $CDCl_3$ had no literature counterpart, but were similar to those of **311**. The TMS signal appeared at δ –0.33 ppm, slightly upfield from that of **311**.

The two homobenzylic carbons were observed at δ 22.6 and 22.7 ppm, while their neighbors resonated at δ 29.1 and 29.5 ppm. The six aromatic carbon peaks could be assigned to the *C*–H (δ 124.7 and 137.1 ppm), C_{fusion} (δ 139.6 and 143.5 ppm), *C*–TMS (δ 132.8 ppm), and *C*–nitro (δ 151.1 ppm) units. These data are summarized in Table 32.

Table 32. ^{13}C NMR shift assignments of **311** and **314** in $CDCl_3$.

^{13}C NMR signals (δ ppm)		
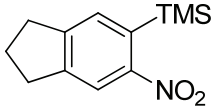	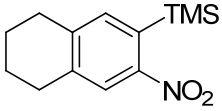	
311	**314**	Assignment
–0.22	–0.33	CH_3 on TMS
25.5	22.6	saturated carbons
32.5	22.7	
32.8	29.1	
	29.5	
120.2	124.7	proton-bearing aromatic carbons
131.6	137.1	
134.5	132.8	TMS-bearing carbon
146.9	139.6	fusion carbons
150.7	143.5	
152.5	151.1	nitro-bearing carbon

The ^{29}Si NMR spectrum in $CDCl_3$ exhibited a peak at δ–3.11 ppm.

Collectively, these data confirm our structural assignment of **314**. Formation of **314** shows that the coordinated alkyne of **25** is incorporated into the cyclization process, as was observed for **25** and **26** with **271**. This demonstrated the synthetic utility of **25** as a stable equivalent of **18**. The reasonable yields of this transformation prompted an investigation of the potential of **25** to cocyclize with nontethered alkynes, described in Section 4.3.2.2.

Encouraged by the above findings, the cocyclization of **273** with nitroacetylene **16**, as embedded in **26** (Scheme 182), was scrutinized, in the hope of rendering **318**.

Scheme 182. Unsuccessful reaction of **26** with **273**.

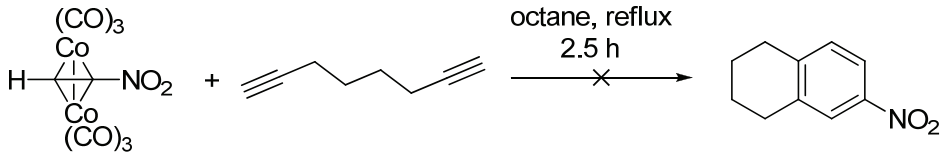

26 **273** **318**

The reaction was monitored by TLC, and **26** was consumed after 2.5 hours. None of the anticipated **318** was detected, although the side product **315** was isolated in 12 % yield (based on **26**). The presence of **315** without concomitant formation of the desired **318** suggested that the more sensitive **26** (see Sections 3.3.4 and 3.3.5) had been destroyed

before the alkyne insertions required for cyclization had occurred. Since a small amount of the corresponding indane **313** had been generated when using boiling hexane (Scheme 179), the relatively higher temperatures associated with Scheme 182 might be to blame, but this aspect was not explored.

This section has described the cobalt-mediated [2 + 2 + 2] cocyclotrimerizations of the ligands in **25** and **26** with α,ω-diynes **271** and **273**, respectively, to form the corresponding nitroindanes and -tetralins. The success, if limited, of these reactions demonstrates that complexes **25** and **26** can act as synthetic equivalents of the free alkynes **18** and **16** in these transformations. These are the first known transition metal mediated cyclizations of nitroalkynes to nitroarenes. The following section describes the reaction of the better behaved **25** with nontethered symmetrical and unsymmetrical alkynes.

4.3.2 All-intermolecular Cyclization of 25 with Symmetrical and Unsymmetrical Alkynes

To expand substrate scope, the reaction of **25** with monoalkynes was probed, specifically its own ligand **18**, **182** (diphenylacetylene), and **197** (DMAD). Both **182** and **197** had been investigated as cocyclization substrates with other alkynes by Hübel in 1960–1961,[363,67] and **197** was further explored by Baxter and co-workers in 1999.[407,406] Compound **18** was, of course, untested, and might furnish substituted trinitrobenzenes, potential energetic materials.

4.3.2.1 Reaction of 25 with Symmetrical Alkynes 182 and 197

In a first foray, we heated **25** with **197** in xylenes at reflux (Scheme 183), in part because the closely related protodesilylated analog of the desired product tetramethyl 5-nitrobenzene-1,2,3,4-tetracarboxylate (**319a**) was known,[427] thus providing a ready route to a chemical structure proof.

Scheme 183. Unsuccessful reaction of **25** with **197**.

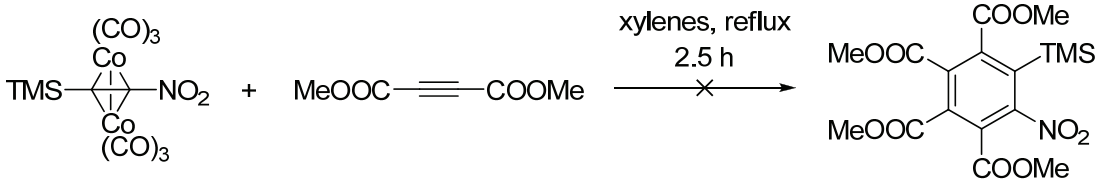

25 **197** **319**

Xylenes were chosen as the solvent, because of the poor solubility of **197** in octane, although this choice had the disadvantage of masking part of the aromatic region in the ^{13}C NMR spectrum of the crude reaction mixture. Analysis by TLC revealed five components that separated into two bands by preparative TLC (Chromatotron), neither of which exhibited a peak in the TMS region of the ^{1}H NMR spectrum. No aromatic proton signals were found near δ 8.8 ppm, the chemical shift of the aromatic hydrogen of **319a**, showing that TMS had not been protodesilylated during chromatography. The spectrum

was also inconsistent with that of the known hexamethyl benzene hexacarboxylate (**320**), a possible side product.[406] These poor results caused us to turn to the less electronegative **182** as the substrate.

Complex **25** was treated with **182**, under the same conditions that were used in the synthesis of **311** and **314** (Scheme 184).

Scheme 184. Failed cyclization of **25** with **182**.

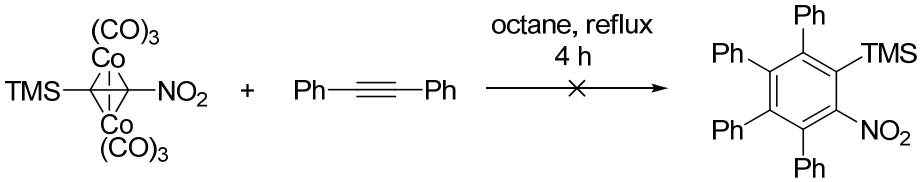

25 **182** **321**

Analysis of the reaction mixture by TLC showed multiple products that could be partly separated by preparative TLC (Chromatotron). The ^{1}H NMR spectrum of the most promising fraction (in $CDCl_3$) contained TMS signals, but also many overlapping peaks in the aromatic region (δ 6.7–6.8 ppm and δ 7.1–7.2 ppm), revealing a mixture that was inseparable by further chromatography. Three peaks appeared in the TMS region, one more intense (δ –0.042 ppm than the other two (δ 0.36 and –0.081 ppm). The peak at δ 0.36 was promising, as its chemical shift was close to that of the TMS signals of **311** (δ 0.33 ppm) and **314** (δ 0.33 ppm). However, the corresponding carbon signals, again one more intense (δ –0.017 ppm) than the other two (δ 0.84 and –0.88 ppm), did not show any correspondence to these models (δ –0.042, 0.36, and –0.081 ppm). The aromatic region contained thirty-four signals between δ 157 and 125 ppm, more than the thirty peaks expected for **321**. One weak signal stood apart at δ 156.5 ppm, hinting at the presence of a nitro carbon by comparison to the corresponding signals of **314** (δ 151.1 ppm), **313** (δ 152.3 ppm), and **311** (δ 152.5 ppm).[420]

Mass spectral data were collected by GC-MS. The largest peak had the longest retention time and exhibited a parent ion of *m/z* = 388 (35 %). This mass was well below that expected for **321** (*m/z* = 499) and does not correspond to any obvious fragment. Other potential fragments, such as *m/z* = 255 (40 %) and 178 (20 %) differed by a phenyl group (*m/z* = 77), but were also inconclusive, although *m/z* = 178 does correspond to diphenylacetylene **182**.

Overall, these data were spurious. If **321** had formed, it was in low yield and admixed with several side products. Adverse steric effects may be the cause of this failure, although similarly crowded molecules had been made by cyclization.[428,429,430,431,432,433] It is possible that with appropriate tinkering this and the preceding reaction might be workable, especially in light of the results to be described next.

4.3.2.2 Reaction of 25 with 18 (Trimethylsilylnitroacetylene)

The autocyclization of **18** appeared very attractive since its products, isomers of tris(trimethylsilyl)trinitrobenzene, were potential precursors to energetic materials. As discussed earlier (Section 4.3), the presence of both a bulky silyl and electron withdrawing nitro group were anticipated to scramble the regioselectivity of intial metallacyclopentadiene formation, thus leading (if successful) to mixtures of symmetrical and unsymmetrical products. In a first attempt to reach such structures, **25** alone was heated to reflux in octane (Scheme 185).

Scheme 185. Thermal decomposition of **25**.

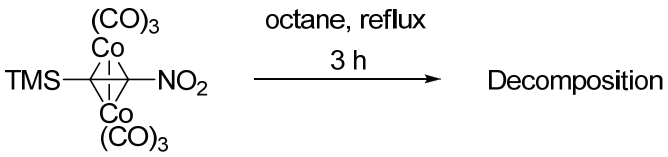

25

The same conditions under which **25** cyclized with **271** and **273** were applied, but no aromatic products were found. Only a trace of unreacted starting material and a purple compound with a high R_f were observed by TLC. On the basis of these data, this product was assumed to be a cobalt cluster. Repeated in xylenes, the reaction gave traces of a few unidentified UV-active compounds along with a green-black fraction, none of which exhibited signals that indicated the presence of cyclization products in the proton NMR or mass spectra.

Undaunted by this failure, we combined **18** and **25**. Gratifyingly, 1,2,4-trinitro-3,5,6-tris(trimethylsilyl)benzene (**322**), 1,3,4-trinitro-1,4-bis(trimethylsilyl)-2,4,5-trinitrobenzene (**323**), 1,2,4-trinitro-3,5-bis(trimethylsilyl)benzene (**324**), and 1,3,5-trinitro-2,4,6-tris(trimethylsilyl)benzene (**325**), along with at least three unidentified compounds, were found (Scheme 186).

Scheme 186. Reaction of **18** with **25**.

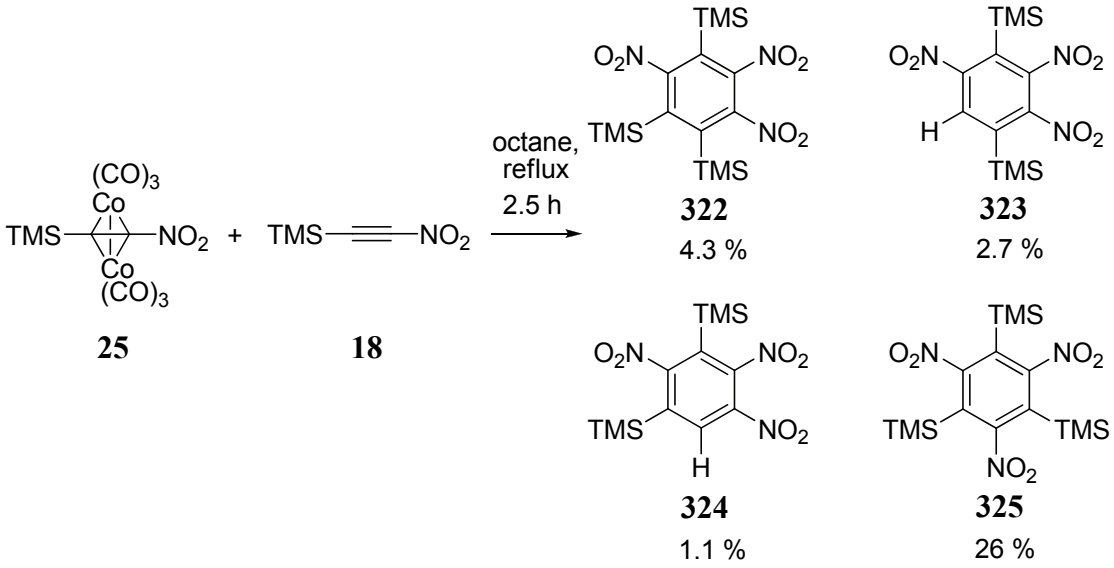

These products were separated by preparative TLC (Chromatotron).

1,2,4-Trinitroisomer **322** was isolated as a thermally unstable, white, amorphous powder in 4.3 % yield. While the molecular ion (*m/z* = 429) could not be observed in the EI-MS, a fairly diagnostic parent fragment signal was detected at *m/z* = 414 (75 %), the result of methyl group fragmentation, as also seen for **18**, **311**, and **314**. There was also a signal at *m/z* = 342 (58 %), possibly due to protodesilylation and loss of methyl (vide infra). A fragment at *m/z* = 223 (25 %) could be derived from *m/z* = 342 by additional loss of nitro and TMS. Other fragments at, 147 (20 %) and 133 (25 %), also observed in the spectrum of **324** (see below), could not be assigned. The base peak was from TMS, at *m/z* = 73 (100 %).

The ^{1}H NMR spectrum of **322** in $CDCl_3$ exhibited three TMS peaks at δ 0.442, 0.438, and 0.35 ppm, clearly indicative of its lack of symmetry. It is likely that the two close-lying signals at ~0.44 ppm originate from the chemically (and hence presumably magnetically) rather similar TMS groups at positions 1 and 2 (Figure 32).

On standing at room temperature, **322** decomposed into a light yellow oil. This sensitivity, in conjunction with the small quantities obtained, unfortunately precluded the recording of a carbon NMR spectrum and a more complete characterization.

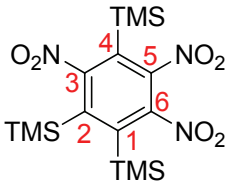

Figure 30. Numbering scheme in **322**.

A second unsymmetrical product, tentatively assigned the structure of the protodesilylated **323**, was isolated as a white-yellow microcrystalline solid in 2.7 % yield.

The IR spectrum of **323** contained several structural clues, but was not as diagnostic as those of the nitroindanes and nitrotetralins. The aromatic C–H stretching region was masked by moisture in the KBr pellet, and the aromatic C–H out of plane deformation was difficult to identify because of multiple substituent effects.[189] Penta-substituted benzene rings can exhibit a C–H deformation band at 875–860 cm^{-1}, but arenes containing three or more nitro groups typically show higher values near 920 cm^{-1}.[189] No absorptions appeared in either region, but a peak at 892 cm^{-1} could be due to this motion. Even the absorptions of the nitro group, usually well-defined, were ambiguous in the case of **323**. Electronic effects appeared to split the unsymmetrical stretching of the ortho nitro groups into three strong bands at 1564, 1550, and 1536 cm^{-1}.[122,189] For example, **17** (TNB) exhibits a single absorption at 1557 cm^{-1},[122] but when nitro groups are adjacent, as in 1,2,3-trinitrobenzene (**326**), two bands appear: 1572 and 1558 cm^{-1}.[122] Substituents have also been observed to split the unsymmetrical nitro stretch, as is the case for picryl chloride (**327**) (1556, 1548, and 1538 cm^{-1}), which also exhibits a strong absorption at 1608 cm^{-1} from aromatic C–C ring stretching. No intense peaks were noted near 1600 cm^{-1} in the spectrum of **323**, raising the question of whether one of the three strong bands centered around 1550 cm^{-1} or a very weak, broad peak at 1640 cm^{-1} could be due to this C–C vibration. Because C–C aromatic ring absorption bands are influenced by substituents and inconsistent in both wavenumber and intensity, they are difficult to assign. Two symmetrical stretching bands at 1381 and 1344 cm^{-1} suggested the presence of nitro groups with different chemical environments, but assignment of any band to a specific nitro group was not feasible. In contrast, the silicon-methyl out of plane deformation was found where expected, at 1254 and 855 cm^{-1}, confirming the presence of the TMS groups.

The EI-MS of **323** again lacked a molecular ion (*m/z* = 357) and exhibited a parent ion at *m/z* = 342 (75 %), due to loss of a methyl fragment. Fragmentation of nitro, TMS, and methyl from the remaining skeleton left *m/z* = 223 (55 %). The largest peak was from TMS, at *m/z* = 73 (100 %). Compound **323** shared two minor fragments with **320**, *m/z* = 147 (25 %) and 133 (35 %).

Only two TMS singlets were observed in the proton NMR spectrum in $CDCl_3$, at δ 0.45 and 0.47 ppm. Similarly, silicon NMR spectroscopy revealed only two signals, at δ 3.61 and 4.74 ppm. Crucial was the presence of an aromatic singlet in the ^1H NMR spectrum at δ 8.46 ppm, integrating for 1 H.

The ^{13}C NMR spectrum in $CDCl_3$ was also highly diagnostic, with two TMS peaks (δ 2.62 and 3.08 ppm) and six distinct resonances in the aromatic region (δ 120.1, 150.0, 151.8, 156.8, 157.8, and 163.8 ppm). The signal at δ 120.1 ppm was assigned to C_{arom}–H, based on its chemical shift and relatively large intensity.

The unsymmetrical nature of **323** was confirmed by these spectra. Its origin therefore had to be the also unsymmetrical **322**, although additional analysis was required to ascertain that it was indeed the TMS group at C-2 that had been lost and not those at either C-1 or even C-4 (vide infra). The latter possibility was discounted, since preferential protodesilylation was expected at C-1 or C-2, because of the mutual steric activation of the adjacent TMS groups.[434]

The structural assignment of **323** was aided by the isolation of a compound to which we tentatively assigned the structure **324**, separated in 1.1 % yield from the

reaction in Scheme 186 as a white microcrystalline solid. The compound exhibited three singlets in the ^{1}H NMR spectrum, at δ0.365, 0.378, and 8.140 ppm, in a 9:9:1 ratio. The position of the aromatic peak is the most diagnostic and was compared to estimates for **323**, **324**, and 1,2-bis(trimethylsilyl)-3,4,6-trinitrobenzene (**327**). These estimates were obtained using the ChemDraw program or using additive incremental subsitutent effects on chemical shifts (+0.95 ppm for *o*-NO_2, +0.33 ppm for *p*-NO_2, +0.17 ppm for *m*-NO_2,[435] +0.18 ppm for *o*-TMS, no change for *m*- and *p*-TMS[436]). As indicated in Table 33, the best match was for the signal at δ8.14 being due to **324**, that at δ8.46 to **323**.

Table 33. Chemical shifts of aromatic protons on isomers of protodesilylated **322** as estimated by ChemDraw and additive benzene substituent effects.

	Estimated and observed aromatic ^{1}H NMR signals (δ ppm)		
	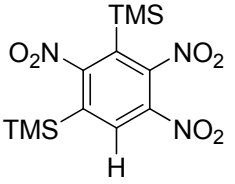	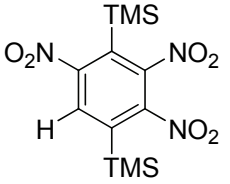	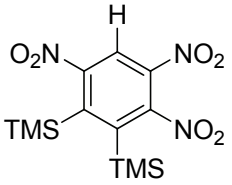
Compound:	**324**	**323**	**327**
ChemDraw:	8.91	9.04	9.14
subs. effects:	8.75	8.90	9.34
observed:	8.14	8.46	N/A

Further evidence in support of these assignments is found in the experimental chemical shifts of models for the arene proton flanked by two nitro groups in **327**. Thus, for **5** (TNT) the corresponding value is δ8.83 ppm,[437] for **328** (picryl chloride) δ8.863 ppm,[438] and for **6** (tetryl) it is δ9.16 ppm.[438] Unfortunately, the limited amounts of **324** prevented a more complete characterization.

The largest fraction collected by chromatography was the first to elute, consisting of the symmetrical **325**. Isolated in 26 % yield, it formed white needles, soluble in most organic solvents at room temperature, including pentane. In an open capillary, crystals of **325** sublimed at 246 °C, surprising for the usually non-volatile trinitrobenzenes,[439,440] and possibly due to the steric bulk of the non-polar TMS groups that disrupt intermolecular polar interactions.

The elemental analysis was satisfactory for the assigned molecular formula of $C_{15}H_{27}N_3O_6Si_3$ (Calcd for $C_{15}H_{27}N_3O_6Si_3$: C, 41.93; H, 6.33; N, 9.78. Found: C, 41.97; H, 6.23; N, 9.41.).

The IR spectrum of **325** was simpler than that of **323**. As expected, there were no absorptions in the aromatic C–H stretching region, but only a peak for the methyl groups of TMS at 2907 cm^{-1}. Two peaks were observed in the unsymmetrical stretching region of the nitro group: 1543 and 1516 cm^{-1}. The occurrence of such multiplicity has been ascribed to steric effects on the conformation of the functional group.[189] The corresponding symmetrical stretching motion gives rise to a signal at 1376 cm^{-1}, at relatively high frequency, signaling that the nitro moiety is not in conjugation with the central ring. It has been noted that bulky substituents can raise the energy of the

symmetrical stretching motion to a maximum of around 1380 cm^{-1}.[122] A weak and somewhat broad peak at 1637 cm^{-1} is probably due to aromatic C–C stretching, in accord with a similar peak at 1640 cm^{-1} in the spectrum of **323**. Finally, the silicon-methyl out of plane deformation bands were found at 1257 and 858 cm^{-1}, both at slightly higher frequency than the corresponding bands in **311**, **314**, and **323**.

The mass spectrum of **325** did not contain a molecular ion (*m/z* = 429), instead exhibiting a peak at *m/z* = 465 (25 %), corresponding to a dihydrate. The base peak was *m/z* = 414 (100 %), [M^+–CH_3], as mentioned above a common fragmentation observed for TMS-bearing compounds, including the similar 1,3,5-triphenyl-2,4,6-tris(trimethylsilyl)benzene (**329**).[431] Another large ion count at *m/z* = 295 (42 %) matches the loss of methyl, TMS, and nitro groups. The final significant peak in the mass spectrum is due to TMS at *m/z* = 73 (66 %).

The ^1H NMR spectrum in $CDCl_3$ contained a single absorption for the TMS groups at δ0.32 ppm, clearly indicative of the symmetry of the molecule.

The ^{13}C NMR spectrum in $CDCl_3$ confirmed the symmetrical substitution of **325**, exhibiting only two aromatic peaks, in addition to that for TMS (δ–0.54 ppm). The first aromatic resonance, belonging to the TMS-bearing carbons, was found at δ126.3 ppm. The second, from the carbons attached to nitro, was at lower field: δ162.7 ppm. These chemical shifts lie near the extremes of the range expected for aromatic carbons.[212]

Definitive structural confirmation was obtained by X-ray crystallography. There is disorder in the TMS and one of the nitro groups, similar to that in the crystal structure of **329**, for which two molecules with differing TMS conformations were found in the unit cell.[431] Only one conformation of **325** is displayed in Figure 31 (next page) for clarity. Several features of the crystal structure of **325** are noteworthy: the orientation of the nitro groups, the planarity of the ring, the internal ring angles, and the interaction of the TMS and nitro groups. Addressing these aspects in sequence, the nitro groups adopt conformations that are close to perpendicular to the plane of the benzene ring, forced out of conjugation with the aromatic system by the sterically demanding TMS groups, as predicted by the unusually high frequency of the symmetrical nitro stretch in the IR spectrum.[189] The phenyl rings of **329** exhibited similar behavior.[431]

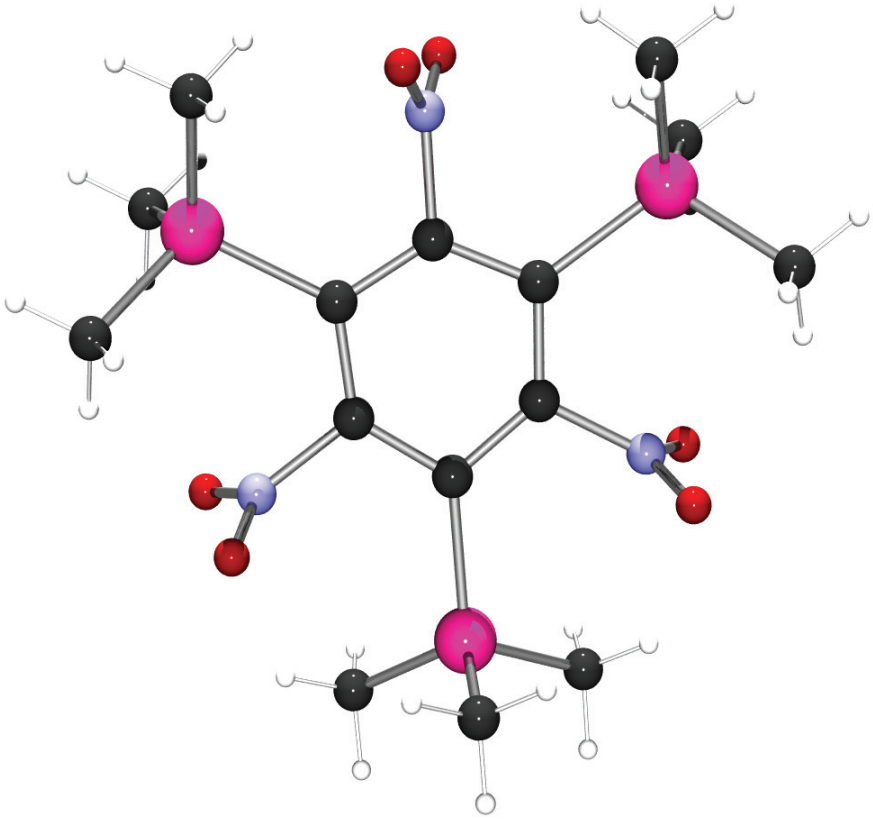

Figure 31. ORTEP plot of **325** as projected in POV-Ray. Carbon (black), nitrogen (light blue), oxygen (red), and silicon (pink) are represented as spheres at the 50 % probability level. Protons (white) are represented as arbitrary sized spheres.

Turning to the encumbered central ring, it maintains planarity, unlike many other crowded benzene rings that are distorted, usually into boat or deformed boat conformations, either as a result of powerful electronic effects, as for 1,3,5-tris(*N*,*N*-diethylamino)-2,4,6-trinitrobenzene (**330**),[441] or simple sterics, as for hexakis(trimethylsilyl)benzene (**331**)[433,432] or hexakis(ferrocenyl)benzene (**332**).[429] These molecules differ from **325**, which contains a nearly perfectly planar central ring. The average deviation of the dihedral angles of the aromatic atoms of several crowded or distorted benzenes from planarity are compared in Table 34.

Table 34. Average deviations of the ring dihedral angles from 180 ° of selected benzenes.

Compound	Structure	Deviation from 180° (°)	Compound	Structure	Deviation from 180° (°)
330[441]	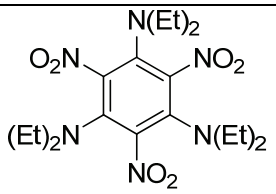	28.7	**7**[20]	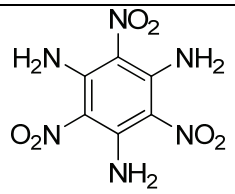	2.9
333[442]	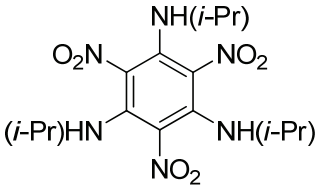	23.5	**329**[431]	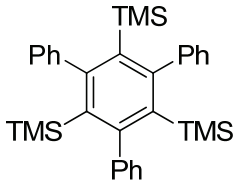	2.7
332[429]	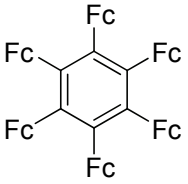	12.0	**335**[444]	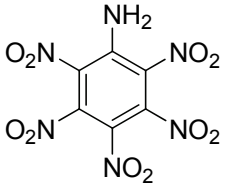	1.8
331[433,432]	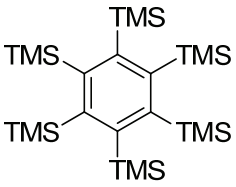	9.8	**336**[445]	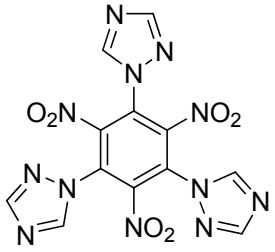	1.6
8[32]	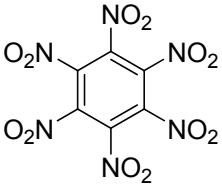	3.7	**325**	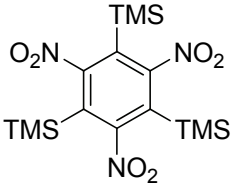	1.2
334[443]	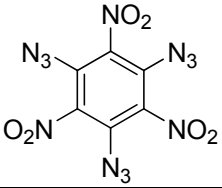	3.4			

Even the less crowded **8** (HNB)[32] and **329**[431] have less planar central rings than **325**. In addition to a flat aromatic core, **325** also exhibits silicon substituents with dihedral angles deviating only 1.2 ° from the plane of the ring, less than the 3.5 ° of the TMS groups of **329**.[431]

In contrast, the core benzene ring is severely distorted from a regular hexagonal array, visible even with the naked eye (Figure 31). While the bond distances alternate somewhat and randomly within experimental error (± 0.01 Å) from their average of 1.388

Å (cf. benzene 1.395 Å), the bond angles alternate regularly between approximately 112 ° at the TMS-bearing carbons and 128 ° at their nitro-bearing neighbors. It appears as if the TMS groups, in order to minimize steric encumbrance, "pull" their ring carbons away from the core. However, a search of the Cambridge Structure Database reveals that angles of such magnitude are actually not uncommon in substituted benzene rings, and **325** follows the general pattern observed for other nitro- and silyl-substituted benzenes.[446,447,431] For instance, 1,3,5-tris(trimethylsilyl)benzene (**337**) has angles of ~117.5 ° centered on the TMS-bearing carbons,[446] while **17** (TNB) exhibits a widening of angles centered on the nitro-bearing carbons to ~124 °.[447] Finally, the X-ray structure of **325** lacks any evidence for coordination of the nitro oxygen to the adjacent silicon centers, a feature dramatically present in hexakis(fluorodimethylsilyl)benzene (**338**)[430] and hexakis(methoxydimethylsilyl)benzene (**339**).[448] Full crystallographic data for **325** can be found in Appendix B.

Inspection of the yields in Scheme 186 reveals that the course of the cyclization favors the symmetrical isomer by ~3:1, a facet that is uncommon in such reactions,[428,417,416] and that has been observed for only a few electron poor alkynes.[418,416] The outcome in the case of **18** indicates the preferential (possibly exclusive) formation of an unsymmetrical cobaltacyclopentadiene intermediate (cf. Scheme 174).

The cyclization was repeated with **18** that had been freed from **25** with CAN just prior to reaction with **25**. This afforded (on small scale) 17.7 % of **325**, demonstrating the ability of **25** to act as an effective storage agent for **18**. This was the first time that a nitroalkyne complex acted as both a reagent and a storage medium in a single synthesis.

As trinitrobenzenes, **322**, **323**, **324**, and **325** are potential precursors to energetic materials. As silylbenzenes, these compounds are also potential subjects to a variety of electrophilic substitutions, opening the door to functionalized trinitrobenzenes that are not readily accessed by classical routes. Exhaustive protodesilylation of **322**, **323**, or **324** would afford 1,2,4-trinitrobenzene (**340**), and all isomers might be nitrated with a suitable reagent, such as nitronium fluoroborate.[263] Compounds **323** and **324** could theoretically render 1,2,3,4,5-pentanitrobenzene (**341**), and **322** and **325** might afford **8** (HNB), which has one of the highest velocities of detonation known.[34] If successful, such schemes would provide greatly simplified routes to these desirable target molecules, compared to the cumbersome, dangerous, multi-step procedures currently employed.[33] Similarly, electrophilic substitution of the TMS groups by bromine, iodine, cyanide, isothiocyanate, sulfate, thioalkyl, acyl, alkyl, or metallic groups[449] might open doors to new functionalized building blocks for more complex energetic materials.

In conclusion, for the first time, nitroalkynes were successfully cyclotrimerized. Complexes **25** and **26** cocylized with diynes to nitroindanes and nitrotetralins. Complex **25** cocyclized with **18** to provide **322**, **323**, **324**, and **325**, all trinitrated benzenes and potential precursors to high-value energetic materials. An X-ray crystal structure of **325** revealed a deformed, yet planar, benzene ring. These results show the potential for coordinated nitroalkynes to act as building blocks for the preparation of polynitrated energetic materials.

4.4 Conclusion

Of the four main goals of this thesis, three were accomplished. Two free nitroacetylenes (**16** and **18**) were produced, and characterization of **18** was completed (Chapter 2). Transition metal complexes of **16** and **18** (**26** and **25**) were synthesized and shown to be stable (Chapter 3). In conjunction with oxidation to recover **18**, this stability showed **25** to be an effective long-term storage medium for **18**. Reactions of **25** and **26** were investigated with the goal of producing a complex of DNA. While this goal remains elusive, transformations of **25** and **26** illuminated the reactivity of such complexes and yielded two phosphine derivatives, **237** and **238**. Use of **25** and **26** as substrates in cycloadditions were unsuccessful in the case of Pauson-Khand cyclizations to nitrocyclopentenones, but successful in [2 + 2 + 2] cobalt-mediated cyclotrimerizations (Chapter 4). Of the two complexes, **25** was shown to be a more versatile reagent, as it combined with **18** to form **322**, **323**, **324**, and **325**, potential precursors to energetic materials. The major product of this reaction, **325**, was characterized by X-ray crystallography and found to have a planar, distorted aromatic ring.

These accomplishments have laid the groundwork for future investigations of nitroacetylenes and their complexes as reagents toward the syntheses of polynitrobenzenes and, hopefully eventually, a complex of DNA and DNA itself.

Chapter 5. Experimental

General

Solvents were dried by distillation over appropriate drying agents: THF (Aldrich), diethyl ether (EMD), and toluene (Aldrich) were distilled from sodium/benzophenone under nitrogen immediately prior to use; methylene chloride (BDH) was distilled from calcium hydride (Aldrich) and stored over 3 Å sieves; DMF (Aldrich) was distilled from $MgSO_4$ and stored over 3 Å sieves; DMSO (Aldrich) was dried over 3 Å sieves; nitromethane (Aldrich) was distilled from anhydrous calcium chloride and stored in a Schlenk flask. Nitronium fluoroborate (Acros or Custom Chem Lab) was washed with nitromethane (1 × 0.5 mL/g), then with methylene chloride (2 × 2 mL/g), and dried under dynamic vacuum for 20 min between washings. Acetic anhydride (JT Baker), acetone (BDH), acetyl chloride (Aldrich), $AgNO_2$ (JT Baker), $AlCl_3$ (Alfa), Argon (Airgas), BuLi (Aldrich), $CaCl_2$ (Fisher), CaH_2 (Aldrich), $(NH_4)_2Ce(NO_3)_6$ (Aldrich), chloroform (BDH), diisopropylamine (Aldrich), 1,4-dioxane (Aldrich), glacial acetic acid (JT Baker), hexamethyldisilizane (Aldrich), hydrazine (Aldrich), hydrazine hydrate (Aldrich), K_2CO_3 (Aldrich), KF (Aldrich), $KHCO_3$ (Spectrum), $LiAlH_4$ (Aldrich), LiHMDS (Alfa), methyl triflate (Aldrich), $MgCl_2$ (Fisher), $MgSO_4$ (Fisher), N_2O_4 (Matheson), $NaBH_4$ (Aldrich), NH_4OH (Fisher), 100 % HNO_3 (Spectrum), nitrogen (Airgas), octane (Aldrich), oxalyl chloride (Aldrich), oxygen (Airgas), pentane (EMD), PMe_3 (Aldrich), potassium hexamethyldisilizane (Alfa), pyrazole (Aldrich), TBAF (Aldrich), TFA (Fisher), triflic acid (Aldrich), **23** (Strem), **72** (GFS), **79** (GFS), **86** (Aldrich), **171** (Aldrich), **182** (Aldrich), **197** (TCI), **199** (Matheson), **201** (Aldrich), **213** (Aldrich), **215** (Aldrich),**222** (Acros), **224** (Aldrich), **225** (Chem Service), **229** (Aldrich), **250** (Aldrich), **257** (Aldrich), **258** (Aldrich), **261** (Aldrich), **262** (Aldrich), **271** (Alfa), and **273** (Aldrich) were used as received. Nitronium chloride,[450] **3**,[451] **6**,[30] **9**,[37] **176**,[98] **186**,[452] **218**,[67] **219**,[67] **226**,[453] and **227**[453] were synthesized according to known methods. All glassware was dried overnight in a 160 °C oven. Unless otherwise noted, all reagents and products were handled using standard Schlenk and glovebox techniques under nitrogen or argon as described by Shriver.[454] Column chromatography was performed using silica gel (mesh 230–400, ICN). Preparative TLC was performed by spinning band (Chromatotron) on silica gel. Solvent mixtures were concentrated using a rotary evaporator operating at 30–40 torr. All reactions were conducted at RT unless otherwise noted.

The identity of products was established using ^{1}H NMR, ^{13}C NMR, ^{29}Si NMR, IR, and mass spectrometry. Purity was confirmed by melting point and elemental analysis; in certain cases, due to small quantities of material or consistency (glassy solids or oils), purity was assessed by NMR. NMR spectra were recorded on Bruker 300, 400, and 500 MHz spectrometers or an Anasazi FT-90 90 MHz spectrometer, and processed using SpinWorks or WinNuts. NMR spectra are reported as the chemical shift in ppm downfield from tetramethylsilane using deuterated solvent as an internal standard ($CDCl_3$ δ –7.26, DMSO-d_6 –2.49, acetone-d_6 –2.05 ppm), or added tetramethylsilane (δ 0.0 ppm). All ^{13}C NMR spectra were recorded with simultaneous ^{1}H decoupling (Waltz 16) unless otherwise noted. Infrared spectra were measured on a Spectronic IR100 IR spectrometer using NaCl plates, NaCl liquid cells, KBr pellets, or a Nujol mull. UV-Vis spectra were recorded on a Hewlett-Packard Model 8453 UV-Vis spectrometer and reported in nm

(log ε). Melting points were taking using a Thomas Hoover Unimelt apparatus in open capillaries. All electrochemical measurements were taken using a BAS 100B cell stand employing a three electrode cell and a silver wire reference electrode. All solutions used 0.1 M NBu_4PF_6 as electrolyte. Electrochemical measurements are reported vs. Fc/Fc^+: For reversible systems as the reduction/oxidation potential ($E_{1/2}$) for irreversible systems as anodic (E_{pa}) or cathodic (E_{pa}) peak potentials using internal standards as a reference.

Mass spectra and combustion analyses were acquired by the Micro Mass Facility of the College of Chemistry, University of California at Berkeley. All mass spectra employed electron impact (EI) ionization. Thermogravimetric and differential calorimetric spectra were collected by Heidi Turner and drop hammer tests were measured by Gary Hust at the High Explosives Application Facility, Lawrence Livermore National Laboratory. X-ray crystallographic data were collected on a Bruker AXS spectrometer at the University of California CHEXRAY facility by Dr. Fred Hollander.

Reaction of 1-iodo-2-(trimethylsilyl)ethyne (170) with NO_2BF_4

To a stirred slurry of purified NO_2BF_4 (310 mg, 2.3 mmol) in pentane (25 mL) at –77 °C was injected **170** (0.38 mL, 480 mg, 2.1 mmol). The reaction mixture became light yellow over 48 h, and was transferred by filter canula to a Schlenk flask containing **23** (1.2 g, 3.6 mmol) at RT. After gas evolution subsided, the mixture was chromatographed on silica gel (450 mL) with pentane, furnishing none of the desired product and only a trace amount of **230**.

Reaction of 1,2-bis(tributylstannyl)ethyne (171) with NO_2BF_4

Into a stirred slurry of purified NO_2BF_4 (148 mg, 1.11 mmol) in pentane (10 mL) was injected **171** (642 mg, 1.06 mmol). A small amount of gas evolution was observed over 15 min. After 24 h, the mixture had darkened to a translucent red color, and was transferred by filter canula to a stirred solution of **23** (409 mg, 1.20 mmol) in pentane (10 mL). Gas evolved vigorously for 15 min, then slowed. The reaction mixture was chromatographed on silica gel (400 mL) with pentane, where **223** eluted as a brown band. The solvent was removed by rotary evaporation to give **223** (360 mg, 56 %) as a viscous, brown oil: ^{1}H NMR (400 MHz, $CDCl_3$) δ 6.28 (s, 1 H), 1.57 (m, 6 H), 1.36 (m, 6 H), 1.12 (m, 6 H), 0.915 ppm (t, J = 7.3 Hz, 9 H); ^{13}C NMR (100 MHz, $CDCl_3$) δ 202 (br), 200 (br), 88.9, 86.7, 27.4 (d, $J_{C–Sn}$ = 12 Hz), 28.8 (d, $J_{C–Sn}$ = 10 Hz), 13.5, 12.8 ppm; IR (film) 2957, 2942, 2872, 2855, 2085, 2072, 2045, 2033, 2009, 1522, 1462, 1376 cm^{-1}.

Attempted synthesis of 1-nitro-2-(trimethylstannyl)ethyne (169)

To a stirred suspension of NO_2BF_4 (61 mg, 0.46 mmol) in pentane (30 mL), was added **86** (154 mg, 0.437 mmol). A red-brown solid formed almost immediately. After 18 h, the cloudy yellow solution was analyzed by NMR spectroscopy and used in a subsequent reaction without effort to isolate a compound that could be **169**: ^{1}H NMR (400 MHz, $CDCl_3$) δ 0.50 ppm (s, 9 H); ^{13}C NMR (400 MHz, $CDCl_3$) (incomplete) δ –9.6 ppm.

Attempted small scale synthesis of nitroethyne (16) from (trimethylsilyl)ethyne (79) and NO_2BF_4

To a stirred slurry of NO_2BF_4 (521 mg, 3.92 mmol) in pentane (10 mL) was added **79** (385 mg, 3.92 mmol). Slow gas evolution was noted, and over 1 h, the solution changed color from clear to light yellow. Aliquots of the solution were analyzed by ^{1}H NMR spectroscopy, which showed only a trace of **16**. No increase in yield was found after 25 h.

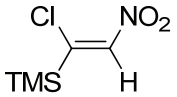

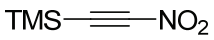

(*Z*)-1-Chloro-2-nitro-1-(trimethylsilyl)ethene (175) and 1-nitro-2-(trimethylsilyl)ethyne (18)

Small scale:

Into a stirred suspension of NO_2BF_4 (410 mg, 3.1 mmol) in pentane (30 mL), was injected **72** (0.64 mL, 480 mg, 2.8 mmol). Small bubbles formed on the surface of the NO_2BF_4. The reaction flask was connected to an oil bubbler, where steady gas evolution was noted. After 24 h, a transparent golden-yellow solution of crude **18** (40–65 %) remained, which was either used directly or purified by column chromatography (see below).

Large scale:

Nitronium tetrafluoroborate (36.74 g, 276.6 mmol) was washed with methylene chloride (3 × 20 mL), dried under dynamic vacuum for 20 min, slurried with nitromethane/methylene chloride (1:1, 110 mL) in a Schlenk flask, and cooled to 0 °C in an ice bath. To this mixture was added a solution of **72** (30.64 g, 179.8 mmol) in methylene chloride (44 mL) by pressure equalized addition funnel at such a rate as to minimize bubbling (approx. 1 h). The solution, now golden orange, was brought to RT over 30 min by exchanging the contents of the cooling bath with warmer water. The reaction mixture was forced through silica gel (50 mL) layered over Na_2SO_4 (50 mL) with argon pressure and eluted with chloroform (700 mL). The solution was stirred over $CaCO_3$ and Na_2SO_4 for 10 min, then gravity filtered. The solvent was removed by rotary evaporation, and the crude **18** dissolved in methylene chloride (150 mL). The solution was again stirred over $CaCO_3$ and Na_2SO_4, filtered, and the solvent removed by rotary evaporation. Residual nitromethane was removed from the crude **18** as an azeotrope by successive addition and evaporation of chloroform (3 × 125 mL) and methylene chloride (1 × 125 mL). Pentane (125 mL) was added to the crude **18**, causing orange-red solids to precipitate, and the resulting yellow solution was vacuum filtered through a plug of glass wool. The solvent was removed by rotary evaporation, and **18** was vacuum distilled at 0 °C / 0.1 torr to leave a yellow liquid (9.83 g, 38.9 %) suitable for reaction with **23**. Higher purity material was obtained by column chromatography (see below).

Purification by column chromatography:

Crude **18** was dissolved in nitromethane (1 mL) and chromatographed on silica gel (100 mL) with pentane (250 mL) under argon pressure as quickly as possible (< 30 s). A clear band containing **175** preceded a bright lemon yellow band of **18**. The solvent was removed from the clear band by rotary evaporation to leave **175** (91 mg, 1.1 % based on **72**) as a clear oil with odor of isoprene: ^{1}H NMR (500 MHz, $CDCl_3$) δ 7.70 (s, 1 H), 0.36 ppm (s, 9 H); ^{13}C NMR (125 MHz, $CDCl_3$) δ 159.4, 147.8, –1.3 ppm; IR (KBr) 2960, 2903, 2855, 1607, 1519, 1349, 1254, 982, 893, 851, 768, 725 cm^{-1}; MS *m/z* (rel intensity) 166/164 (M^+, 25/63), 104 (100), 73 (38).

The solvent was removed from the yellow band by rotary evaporation to afford **18** (391 mg, 5.9 %) as a lachrymatory, bright lemon-yellow, mobile liquid: mp –75 to –72 °C; bp 99 °C; ^{1}H NMR (400 MHz, $CDCl_3$) δ 0.31 ppm (s, 9 H); ^{13}C NMR (100 MHz, $CDCl_3$) δ 99.2 (t, J_{CN} = 28 Hz), 73.2, –1.30 ppm; IR (KBr) 2964, 2168, 1551, 1514, 1339, 1256, 1226, 1125, 961, 851, 803, 764, 729, 625 cm^{-1}; MS *m/z* (rel intensity) 128 (M^+ – 15, 100), 97 (35), 70 (23), 55 (10). DH_{50} (2.5 kg) 174 cm.

Reaction of bis(tributylstannyl)ethyne (171) with N_2O_4

To a stirred solution of **171** (608 mg, 1.01 mmol) in pentane (10 mL) was added a 0.058 M solution of N_2O_4 (17 mL, 9.2 mg, 1.00 mmol) in pentane. After 2 h, a dark red oil of unknown composition was separated from the golden yellow mother liquor by pipet: IR (film) 2957, 2925, 22857, 1463, 1633 (br), 1377, 1354, 1286, 1079, 1021, 675 cm^{-1}. The golden-colored solution was decanted through the atmosphere against argon backflow into a stirred solution of **23** (571 mg, 1.67 mmol) in toluene (30 mL). The reaction mixture was heated to 40 °C for 2 h and allowed to cool to RT under argon. Column chromatography of the reaction mixture on silica gel (400 mL) with pentane afforded brown and yellow bands that decomposed before the solvent could be removed.

Reaction of 1-nitro-2-(trimethylsilyl)ethyne (18) with NO_2BF_4 and 23

To a stirred slurry of NO_2BF_4 (150 mg, 1.2 mmol) in pentane (5 mL) was added a solution of **18** (210 mg, 1.5 mmol) in pentane (10 mL). Addition was accompanied by slight bubbling, and over 20 h, the light yellow solution darkened to a golden color. The mixture was transferred by canula to a solution of **23** (1.0 g, 3.1 mmol) in pentane (8 mL). Vigorous gas evolution subsided after 5 min. After 7 h, the solution was chromatographed on silica gel (300 mL) with pentane, giving a blood red band. The solvent was removed by rotary evaporation, affording **25** (55 mg, 10 %) as bright red needles.

Reaction of dimethyl acetylenedicarboxylate (197) with NH_4OH

To a jacketed beaker containing 15M NH_4OH (3.56 g, 101 mmol) maintained at –10 °C was added **197** (1.00 g, 7.04 mmol). The mixture immediately became cloudy. After 2 h, the precipitate was filtered and washed with ethanol at 0 °C (3 × 3 mL), leaving an

orange to tan solid insoluble in nitromethane, acetonitrile, acetone, diethyl ether, chloroform, and toluene, slightly soluble in water, and soluble in DMF and DMSO. The precipitate was crystallized from boiling water to afford an inseparable mixture of compounds as an amorphous yellow solid: mp 168–170 °C; ^{1}H NMR (400 MHz, DMSO-d_6) δ 8.34 (s, 3 H), 7.86 (s, 3 H), 5.10 (s, 1 H), 3.57 ppm (s, 3 H); ^{13}C NMR (100 MHz, DMSO-d_6) δ 169.9, 164.7, 152.6, 151.9, 82.0, 76.9, 50.2 ppm; IR (KBr) 3495, 3392, 2800, 1679, 1624, 1550, 1407, 1280, 1191, 1126, 976, 782, 742, 710, 626, 606, 559 cm^{-1}; MS *m/z* (rel intensity) 144 (97), 113 (40), 112 (30), 100 (55), 85 (20), 70 (15), 68 (100).

Reaction of but-2-ynedioic acid (199) with 23

Thermal:

To a stirred solution of **23** (420 mg, 1.2 mmol) in toluene (20 mL) was added **199** (130 mg, 1.1 mmol). The reaction mixture was heated to 50 °C for 5 d, at which time it was allowed to cool to RT. The cloudy brown-black reaction mixture was filtered through a Gooch crucible (30 mm, C frit), removing unreacted **199** as a light tan solid. The solvent was removed from the filtrate by rotary evaporation, leaving an intractable brown residue.

Sonication:

To a stirred solution of **23** (1.01 g, 2.95 mmol) in octane (30 mL) was added **199** (320 mg, 2.81 mmol). The reaction mixture was immersed in a sonication bath maintained at 50 °C for 8 h, at which time solvent was removed by rotary evaporation, leaving dark black crystals. Recrystallization from diethyl ether (40 mL) at –20 °C gave black-purple crystals: m.p. > 300 °C.

Attempted synthesis of [μ-1-propiolic acid-1,2-diyl]bis(tricarbonylcobalt)(*Co–Co*) (200)

Into a stirred solution of **23** (770 mg, 2.3 mmol) in toluene (30 mL) at 20 °C was injected **201** (0.14 mL, 160 mg, 2.3 mmol). Gas evolution was rapid at first, attenuating slowly over 105 min. The solvent was removed by rotary evaporation. The remaining solids were washed with pentane (6 × 7 mL), extracted with diethyl ether (5 × 1.5 mL), and filtered through a Gooch crucible (30 mm, F frit), leaving a bright red filtrate. The solvent was removed by rotary evaporation to afford a compound that could be **200** (200 mg, 25 %) as bright red needles: sublp 82–84 °C (760 torr); IR (KBr) 2106, 2068, 2033, 1664, 1476, 1249, 514, 452 cm^{-1}.

Reaction of but-2-ynedioic acid (199) with oxalyl chloride

Into a stirred slurry of **199** (281 mg, 2.46 mmol) in octane (30 mL) was injected oxalyl chloride (0.43 mL, 620 mg, 4.9 mmol) and DMF (1 drop). Addition of DMF immediately created a black precipitate and caused vigorous gas evolution. After 40 min, almost no precipitate remained, and the clear solution was sparged with nitrogen. No

carbonyl absorptions in the range of acid chlorides were detected by solution IR spectroscopy.

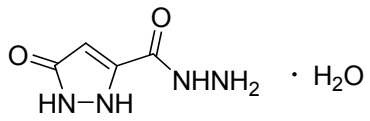

5-Oxo-3-pyrazoline-3-carboxhydrazide hydrate (214)[260]

Into a stirred solution of **213** (1.80 g, 10.6 mmol) in denatured ethanol (11 mL) was injected hydrazine hydrate (1.54 mL, 1.59 g, 31.8 mmol). The clear, colorless solution became transparent orange, and a mild exotherm was noted. The reaction mixture was heated at reflux for 24 h. The resulting solution, cloudy with precipitate, was filtered through a Gooch crucible (30 mm, C frit) and dried in the air. Two recrystallizations from hot (70 °C) water afforded **214** (320 mg, 21 %) as walnut colored crystals: mp 232 °C (lit.[260] 247–255 °C); ^{1}H NMR (500 MHz, DMSO-d_6) δ 9.5 (br, s, 2 H), 5.96 (s, 1 H), 4.4 (br, s, 1 H), 3.5 ppm (br, s, 2 H), 12.3 (br, s, 1 H) [lit.[260] (60 MHz, acetone-d_6) δ 6.03 ppm (br)]; ^{13}C NMR (125 MHz, DMSO-d_6) δ 161 (br), 159 (br), 136 (br), 88.8 ppm [lit.[260] (20 MHz, acetone-d_6) δ 160.08, 138.34 (J = 0.26 Hz), 88.9 ppm (J = 178 MHz)]; IR (KBr) 3449, 3274, 3124, 3045, 2887, 2627, 1650, 1582, 1526, 1438, 1317, 1257, 1206, 1166, 1131, 1031, 963, 867, 836, 765, 732, 654, 599 cm^{-1}; MS *m/z* (rel intensity) 142 (M^+, 65), 111 (100) [lit.[260] 111 (100)].

Reaction of diethyl acetylenedicarboxylate (213) with *N*-(*t*-butoxycarbonyl)hydrazide (215)

To a stirred solution of **213** (1.70 g, 10.0 mmol) in ethanol (11 mL) was added **215** (3.96 g, 30.0 mmol). The solution changed color from clear to yellow-green, and a mild exotherm was noted. The reaction mixture was heated at reflux for 28 h, changing color to transparent orange. The solvent was removed by rotary evaporation, leaving a transparent orange oil. The oil was chromatographed on silica gel (500 mL) with diethyl ether/pentane (4:1), to afford six bands that each contained multiple inseperable compounds (as evidenced by TLC). Without a clear product or means of further separation, the reaction mixture was discarded.

Reaction of [μ-1,2-bis(dimethylcarboxylate)ethyne-1,2-diyl]bis(tricarbonylcobalt)(*Co–Co*) (217) with N_2H_4

With anhydrous hydrazine:

Into a stirred solution of **217** (570 mg, 1.3 mmol) in methanol (10 mL) was injected hydrazine (90 mg, 3 mmol). The reaction mixture was heated to 50 °C for 1 h and monitored by TLC [eluted with diethyl ether/pentane (4:1)]. When no further change in components was noted, the reaction mixture was allowed to cool to RT and the solvent removed by rotary evaporation to furnish a dark red oil. The oil was chromatographed on silica gel (200 mL) with diethyl ether/pentane (1:4) to give an orange band. The solvent

was removed by rotary evaporation to recover **217** (290 mg, 51 % recovery) as red microcrystals.

With hydrazine hydrate:

To a stirred solution of **217** (1.09 g, 2.55 mmol) in methanol (10 mL) was added hydrazine hydrate (380 mg, 7.7 mmol). The reaction mixture was heated at reflux for 22 h, cooled, and filtered to give a fine brown solid that was insoluble in water, methanol, acetone, and DMSO. The solvent was removed from the filtrate by rotary evaporation, leaving only an intractable brown tar.

Reaction of [μ-1,2-bis(trimethylsilyl)ethyne-1,2-diyl]bis(tricarbonylcobalt)(*Co–Co*) (218) with NO_2BF_4

To a stirred solution of **218** (132 mg, 0.289 mmol) in nitromethane (5 mL) was added by canula transfer a solution of NO_2BF_4 (73 mg, 0.55 mmol) in nitromethane (5 mL). Gas evolution was noted, the solution darkened, and a pink precipitate formed immediately. Filtration furnished the pink solid, determined to be paramagnetic by NMR spectroscopy. The filtrate decomposed upon concentration by rotary evaporation, affording only an intractable brown residue.

Reaction of [μ-1,2-bis(trimethylsilyl)ethyne-1,2-diyl]bis(tricarbonylcobalt)(*Co–Co*) (218) with TBAF, $AlCl_3$ and PETN (3)

Into a stirred solution of **218** (85 mg, 0.19 mmol) in THF (5 mL) was injected a 1.0 M solution of TBAF (0.45 mL, 0.45 mmol). The mixture changed to a dark orange-brown immediately, and was transferred by canula to a stirred solution of **3** (120 mg, 0.370 mmol) and $AlCl_3$ (240 mg, 1.8 mmol) in THF (5 mL). The reaction mixture turned a deep green over the course of 5 min. The solvent was evaporated by nitrogen flow to leave a green solid that was insoluble in pentane and diethyl ether, and soluble in nitromethane. Analysis by TLC and NMR spectroscopy showed no cobalt carbonyl complexes.

Reaction of [μ-1,2-bis(trimethylsilyl)ethyne-1,2-diyl]bis(tricarbonylcobalt)(*Co–Co*) (218) with KF

To a stirred solution of **218** (13.2 mg, 0.0290 mmol) in acetone (2 mL) was added a solution of $KF{\cdot}2H_2O$ (233 mg, 2.47 mmol) in water (2 mL), open to the air. The color changed immedately to a light orange, and a pink precipitate formed. The reaction mixture was filtered through a plug of alumina to afford material determined to be paramagnetic by NMR spectroscopy.

Reaction of [μ-1,2-diphenylethyne-1,2-diyl]bis(tricarbonylcobalt)(*Co–Co*) (186) with TBAF

To a stirred solution of **186** (50 mg, 0.11 mmol) in THF (1.5 mL) was added a 1.0 M solution of TBAF (0.05 mL, 0.05 mmol) in THF. The color immediately changed to a light orange. Ethanol (2 mL) was added to quench the reaction and solvent was evaported under nitrogen flow, leaving an intractable solid determined to be paramagnetic by NMR spectroscopy.

Reaction of [μ-1,2-bis(trimethylsilyl)ethyne-1,2-diyl]bis(tricarbonylcobalt)(*Co–Co*) (218) with trifluoroacetic acid (TFA)

To a stirred solution of **218** (6.3 mg, 0.015 mmol) in $CDCl_3$ (0.7 mL) was added TFA (15 mg, 0.13 mmol). The reaction mixture was filtered through a plug of alumina, removing a fine pink solid. Examination by NMR spectroscopy revealed unreacted **218** and free alkyne **72**.

Reaction of [μ-1,2-bis(trimethylsilyl)ethyne-1,2-diyl]bis(tricarbonylcobalt)(*Co–Co*) (218) with potassium methoxide

To a stirred solution of **218** (6.1 mg, 0.013 mmol) in methanol (1 mL) was added an excess of K_2CO_3 in methanol (3 mL). The solution darkened and uncharacterizable brown solids precipitated, indicative of demetallation.

Deprotonation and subsequent attempted transfer nitration of [μ-1-(trimethylsilyl)ethyne-1,2-diyl]bis(tricarbonylcobalt)(*Co–Co*) (219) with tetryl (6)

Into a stirred solution of diisopropylamine (58 mg, 0.57 mmol) in THF (2 mL) was injected a freshly titrated 0.85 M solution of BuLi (0.67 mL, 36 mg, 0.57 mmol) at –40 °C. The solution was cooled to –65 °C and **219** (210 mg, 0.54 mmol) was added. After 20 min, a solution of **6** (157 mg, 0.547 mmol) in THF (2 mL) at –65 °C was then added by canula transfer, whereupon the color changed immediately to a dark red. After 5 min, the reaction was quenched with ethanol. Analysis by TLC evidenced only starting material and a dark, unmoving band (R_f = 0.0) consisting of uncharacterizable material.

Attempted deprotonation and low temperature nitration of [μ-1-(trimethylsilyl)ethyne-1,2-diyl]bis(tricarbonylcobalt)(*Co–Co*) (219)

A stirred solution of potassium hexamethyldisilizane (291 mg, 1.46 mmol) in THF (2 mL) at –72 °C was transferred by canula to a solution of **219** (514 mg, 1.34 mmol) in THF (2 mL) at –72 °C and manually agitated. The mixture immediately became dark brown. The reaction flask was immersed in a liquid nitrogen bath, and N_2O_4 (0.30 mL, 440 mg, 4.7 mmol) was frozen on top of the THF glass. The liquid nitrogen bath was replaced with a RT methanol bath and the reaction flask manually agitated behind a safety shield, while warming to RT over 10 min. Violent frothing quadrupled the volume

of the reaction mixture during melting of the N_2O_4. After 2.5 h of stirring at RT, solvent was removed under vacuum by manual agitation and the resulting solid dissolved in pentane (2 mL). The extract was chromatographed on silica gel (250 mL) with pentane/diethyl ether (95:5) to give light red and red-orange bands. The solvent was removed from the first fraction by rotary evaporation to give **221**[99] (11 mg, 3.4 %) as a red oil: ^{1}H NMR (400 MHz, $CDCl_3$) δ 0.33 (s, 9 H), 0.21 ppm (s, 9 H); IR (film) 2962, 2901, 2130, 2092, 2054, 2025, 1558, 1408, 1359, 1250, 1045, 842, 759, 696, 617 cm^{-1}; MS *m/z* (rel intensity) 480 (M^+, 5), 452 (15), 424 (40), 396 (55), 368 (50), 340 (100), 312 (65), 179 (28), 155 (34), 93 (32), 73 (56), 59 (27).

The solvent was removed from the second fraction by rotary evaporation to furnish a red oil (13 mg) of unknown composition: ^{1}H NMR (400 MHz, $CDCl_3$) δ 0.36 (s, 9 H), 0.23 ppm (s, 9 H); ^{13}C (100 MHz, $CDCl_3$) (incomplete) δ 0.51, 0.45 ppm; IR (film) 2962, 2101, 2092, 2062, 2029, 1635, 1595, 1505, 1409, 1361, 1261, 1097, 1026, 842, 802, 697 cm^{-1}; MS *m/z* (rel intensity) 654 (10), 598 (15), 570 (15), 542 (5), 514 (10), 480 (10), 452 (15), 424 (15), 396 (20), 340 (25), 312 (100), 73 (45).

Reaction of [μ-1-(trimethylsilyl)ethyne-1,2-diyl]bis(tricarbonylcobalt)(*Co–Co*) (219) with triphenylcarbonium tetrafluoroborate (222)

To a stirred solution of **219** (55.0 mg, 0.143 mmol) in methylene chloride (2 mL) was added a solution of **222** (46.8 mg, 0.142 mmol) in methylene chloride (2 mL). After 24 h, TLC analysis revealed only unreacted **219** and **222**.

Reaction of [μ-1-(tributylstannyl)ethyne-1,2-diyl]bis(tricarbonylcobalt)(*Co–Co*) (223) with NO_2BF_4

To a stirred slurry of NO_2BF_4 (44 mg, 0.33 mmol) in pentane or nitromethane (1.5 mL) was added a solution of **223** (180 mg, 0.28 mmol) in pentane or nitromethane (12 mL). After 48 h, no reaction was observed by TLC, and the reaction mixture was chromatographed on silica gel (50 mL) with pentane to afford **223** (48 mg, 27 % recovery).

Reaction of [μ-1-(tributylstannyl)ethyne-1,2-diyl]bis(tricarbonylcobalt)(*Co–Co*) (223) with N_2O_4

To a stirred solution of **223** (160 mg, 0.27 mmol) in pentane (1 mL) was added a 0.058 M solution of N_2O_4 (12 mg, 0.14 mmol) in pentane. The reaction was monitored by TLC, and after 18 h, only unreacted **223** and uncharacterizable material remained.

Reaction of [μ-1-(tributylstannyl)ethyne-1,2-diyl]bis(tricarbonylcobalt)(*Co–Co*) (223) with tetranitromethane (9)

To a stirred solution of **223** (32 mg, 0.052 mmol) in DMSO (2 mL) was added a 0.011 M solution of **9** (11 mg, 0.054 mmol) in DMSO. The solution changed color to orange-red.

After 20 h, the solution was decanted into water (30 mL), and this solution was extracted first with pentane (5 × 6 mL), and then with diethyl ether (4 × 6 mL). Neither the colorless pentane extracts, nor the yellow ether extracts exhibited any absorptions between 2000–1900 cm^{-1} in the IR spectrum, precluding the existence of cobalt carbonyl complexes.

Reaction of [μ-1-(tributylstannyl)ethyne-1,2-diyl]bis(tricarbonylcobalt)(*Co–Co*) (223) with BuLi and tetryl (6)

Into a stirred solution of **223** (66 mg, 0.10 mmol) in diethyl ether (50 mL) maintained at –78 °C, was injected freshly titrated 0.102 M BuLi (1.0 mL, 0.102 mmol). The color of the mixture changed from a red to orange over 30–60 s. After 5 min, **6** (30 mg, 0.11 mmol) was added, turning the color brown over 10 min. After 50 min, the reaction mixture was allowed to warm to RT and the solvent was evaporated by nitrogen flow. The resulting red solid was dissolved in pentane (5 mL) and chromatographed on silica gel (300 mL) with pentane to afford a single red-orange band. The solvent was evaporated by nitrogen flow to give **223** (36 mg, 55 % recovery).

Reaction of [μ-1-(tributylstannyl)ethyne-1,2-diyl]bis(tricarbonylcobalt)(*Co–Co*) (223) with BuLi and triflic acid

Into a stirred solution of **223** (79.3 mg, 0.123 mmol) in diethyl ether (5 mL) maintained at –78 °C, was injected freshly titrated 0.12 M BuLi (1.0 mL, 0.12 mmol). After 30 min, a strong red band at the baseline (R_f = 0.0) was noted by TLC (eluted with pentane). Triflic acid (0.06 mL, 101.4 mg, 0.675 mmol) was injected, and the mixture was allowed to warm to RT, during which time the color changed from red-brown to purple. The crude product was chromatographed on silica gel (150 mL) with pentane/diethyl ether (95:5), affording one fast moving purple band. The solvent was evaporated under nitrogen flow to leave an unidentified product as a purple oil: ^{1}H NMR (400 MHz, $CDCl_3$) δ 1.46 (s, 2 H), 1.30 (s, 2 H), 0.89 (s, 2 H), 0.80 ppm (s, 3 H); ^{13}C NMR (100 MHz, $CDCl_3$) δ 199 (br), 29.2, 27.4, 13.7, 8.7 ppm; IR (film) 2957, 2925, 2872, 2854, 2101, 2078, 2050, 2036, 2015, 1983, 1464, 1418, 1377, 1340, 1292, 1261, 1149, 1072, 1021, 960, 874 cm^{-1}; MS *m/z* (rel intensity) 401 (10), 355 (25), 281 (40), 221 (50), 207 (40), 147 (100).

Reaction of [μ-1-(tributylstannyl)ethyne-1,2-diyl]bis(tricarbonylcobalt)(*Co–Co*) (223) with triflic acid

Into a stirred solution of **223** (118 mg, 0.183 mmol) in pentane (7 mL) was injected triflic acid (0.09 mL, 150 mg, 1.0 mmol). No color change was noted, and after 90 min, TLC (eluted with pentane) evidenced only starting material (R_f ~ 0.8). The reaction mixture was chromatographed on silica gel (400 mL) with pentane. A red-brown band was collected, and the solvent was removed to afford **223** (40 mg, 34 % recovery).

Attempted synthesis of [μ-1-nitro-2-(trimethylstannyl)ethyne-1,2-diyl]bis(tricarbonylcobalt)(*Co–Co*) (167)

A stirred solution of **176** (38.4 mg, 0.0600 mmol) and **224** (18.7 g, 0.0610 mmol) in **225** (237.8 g, 2.260 mmol) was heated to 50 °C. After 8 d, the reaction mixture was chromatographed on silica gel (50 mL) with pentane/diethyl ether (9:1), furnishing a peach-colored band that followed a brown band. The solvent was removed from the peach-colored band by rotary evaporation to leave a trace of a compound that could be **167**: ^{1}H NMR (500 MHz, $CDCl_3$) δ 0.42 ppm (s, 9 H); IR (Nujol) 2723, 2093, 2056, 2029, 1261, 1192 cm^{-1}.

Reaction of [μ-1,2-bis(trimetylstannyl)ethyne-1,2-diyl]bis(tricarbonylcobalt)(*Co–Co*) (176) with *N*-nitropyrazole (226) and $AlCl_3$

To a stirred slurry of $AlCl_3$ (580 mg, 4.35 mmol) in methylene chloride (8 mL) maintained at 0 °C, was added **226** (460 mg, 4.07 mmol). The clear, colorless solution changed to transparent brown. This solution was transferred by canula to stirred, dry **176** (640 mg, 1.0 mmol) maintained at 0 °C. Vigorous gas evolution was noted at first, and after 30 min, the reaction mixture was allowed to warm to RT and stir for 1 h. The solution was then washed with saturated NH_4Cl, dried over $MgSO_4$, and concentrated by rotary evaporation. Analysis by TLC [eluted with methylene chloride:diethyl ether (2:1)] did not reveal any moving colored bands.

Reaction of [μ-1,2-bis(trimetylstannyl)ethyne-1,2-diyl]bis(tricarbonylcobalt)(*Co–Co*) (176) with *N*-3,4-trinitropyrazole (227) and $AlCl_3$

This reaction was performed as in the reaction of **176** with **226**, except with $AlCl_3$ (150 mg, 1.12 mmol), **176** (190 mg, 0.28 mmol), and **227** (540 mg, 0.28 mmol). The results were identical.

Reaction of [μ-1,2-bis(trimetylstannyl)ethyne-1,2-diyl]bis(tricarbonylcobalt)(*Co–Co*) (176) with propyl nitrate (225) and $AlCl_3$

To $AlCl_3$ (6.3 mg, 0.047 mmol) and **176** (31 mg, 0.049 mmol) was added **225** (540 mg, 5.1 mmol). Gas evolution was immediate, and analysis of the crude reaction mixture by TLC (eluted with pentane) evidenced only starting material (R_f ~0.8) and an unidentified brown baseline (R_f = 0.0).

Reaction of [μ-1,2-bis(trimetylstannyl)ethyne-1,2-diyl]bis(tricarbonylcobalt)(*Co–Co*) (176) with NO_2Cl and $AlCl_3$

This reaction was performed as in the reaction of **176** with **226**, except with $AlCl_3$ (130 mg, 0.97 mmol), **176** (158 mg, 0.25 mmol), and NO_2Cl (20 mg, 0.25 mmol). The results were identical.

Reaction of [μ-1,2-bis(trimetylstannyl)ethyne-1,2-diyl]bis(tricarbonylcobalt)(*Co–Co*) (176) with NO_2Cl

To a stirred solution of **176** (99.8 mg, 0.157 mmol) in methylene chloride (2 mL) maintained at –78 °C was added 0.605 M NO_2Cl (0.20 mL, 0.12 mmol) in methylene chloride. Analysis by TLC (eluted in pentane) showed starting material (R_f ~ 0.8) and an unidentified, unmoving pink band (R_f = 0.0), which remained unchanged after 30 min. The solution was warmed to room temperature and allowed to stand 60 min. No changes were noted by TLC. Repetition of this experiment at –40 °C gave identical results.

Attempted palladium tetrakis(triphenylphosphine) (228) catalyzed coupling of [μ-1,2-bis(trimetylstannyl)ethyne-1,2-diyl]bis(tricarbonylcobalt)(*Co–Co*) (176) with *N*-nitropyrazole (226)

To a stirred solution of **176** (103.4 mg, 0.162 mmol) and **226** (40.3 mg, 0.356 mmol) in methylene chloride (5 mL) was added **228** (18.9 mg, 0.0164 mmol, 10 mol %). Analysis by TLC (eluted with methylene chloride) showed no change after 24 h.

Attempted palladium tetrakis(triphenylphosphine) (228) catalyzed coupling of [μ-1,2-bis(trimetylstannyl)ethyne-1,2-diyl]bis(tricarbonylcobalt)(*Co–Co*) (176) with iodobenzene (229)

This reaction was performed as in the reaction of **176** with **226** and **228**, except with **176** (102 mg, 0.16 mmol), **229** (73 mg, 0.36 mmol), and **228** (18.9 mg, 0.0164 mmol, 10 mol %). After 5 d, analysis by TLC (eluted with methylene chloride) did not show any reaction.

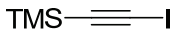

1-Iodo-2-(trimethylsilyl)ethyne (170)

To a stirred solution of **79** (480 mg, 4.89 mmol) in pentane (4.5 mL) at –50 °C was added dropwise a 2.5 M solution of BuLi (2.0 mL, 5 mmol) in hexanes, resulting in a cloudy white solution. After 15 min, the solution was cooled to –72 °C and allowed to stand for 75 min. A solution of iodine (1.26 g, 4.96 mmol) in diethyl ether (8 mL) was added by pressure equalized addition funnel over 15 min. The cooling bath was removed and the solution was allowed to come to RT over 3 h. The reaction was quenched with water (5 mL) and the organic layer was separated. The aqueous layer was extracted with pentane (1 × 5 mL) and the extract combined with the organic layer. The organic layer was washed successively with water (2 × 10 mL) and a 20 % solution of $Na_2S_2O_3$ (2.5 mL), then dried over $MgSO_4$. The solvent was removed by rotary evaporation to leave **170**[455] (329 mg, 30 %) as a clear oil: ^{1}H NMR (400 MHz, $CDCl_3$) δ 0.034 ppm (s, 9 H); ^{13}C NMR (100 MHz, $CDCl_3$) δ 103.8, 21.7, –0.50 ppm; IR (KBr) 2960, 2899, 2871, 2100, 1455, 1409, 1319, 1251, 1103, 1018, 843, 760, 745, 701, 619 cm^{-1}.

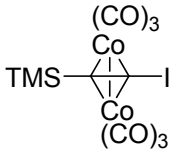

[μ-1-Iodo-2-(trimethylsilyl)ethyne-1,2-diyl]bis(tricarbonylcobalt)(*Co–Co*) (230)

To a stirred solution of **23** (610 mg, 1.78 mmol) in pentane (30 mL) was added **170** (0.329 g, 1.47 mmol), causing immediate gas evolution. The Schlenk reaction flask was connected to an oil bubbler to relieve pressure. The appearance of **230** (R_f = 0.82) was monitored by TLC eluted with pentane. After 8 h, solvent was reduced to ~ 10 mL by rotary evaporation, and the reaction mixture was chromatographed on silica gel (80 mL) with pentane, where **230** eluted as a red-brown band. The solvent was removed by rotary evaporation to afford **230** (240 mg, 32 %) as dark red plates: sublp 116 °C (760 torr); ^{1}H NMR (500 MHz, $CDCl_3$) δ 0.35 ppm (s, 9 H); ^{13}C NMR (125 MHz, $CDCl_3$) δ 199 (br), 83.5, 50.6, 0.12 ppm; ^{29}Si NMR (99 MHz, $CDCl_3$) δ 2.25 ppm; IR (KBr) 2962, 2094, 2058, 2032, 1485, 1250, 860, 841, 797, 640, 604, 513, 492, 450 cm^{-1}; MS *m/z* (rel intensity) 510 (M^+, 23) , 482 (72), 454 (13), 426 (15), 398 (22), 370 (16), 342 (57), 271 (13), 243 (15), 194 (15), 180 (20), 179 (100), 155 (26), 73 (68).

Reaction of [μ-1-iodo-2-(trimethylsilyl)ethyne-1,2-diyl]bis(tricarbonylcobalt)(*Co–Co*) (230) with $AgNO_2$

In diethyl ether:

To a stirred solution of **230** (100.3 mg, 0.1967 mmol) in diethyl ether (2 mL) was added $AgNO_2$ (80.0 mg, 0.520 mmol). Analysis by TLC (eluted in pentane) showed no change after 20 d.

In acetonitrile:

To a stirred solution of **230** (113.6 mg, 0.2227 mmol) in acetonitrile (5 mL) was added $AgNO_2$ (132.9 mg, 0.8637 mmol). The solution slowly became a black suspension over 2 d, and analysis by TLC (eluted in pentane) showed only a trace of starting material (R_f ~ 0.8). The solvent was removed by rotary evaporation, leaving an intractable, amorphous black solid.

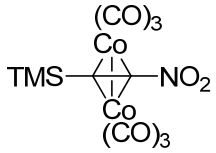

[μ-1-Nitro-2-(trimethylsilyl)ethyne-1,2-diyl]bis(tricarbonylcobalt)(*Co–Co*) (25)

To a Schlenk flask containing stirred solid **23** (1.56 g, 4.56 mmol) was added **18** (1.71 g, 11.94 mmol) in pentane (29 mL). Bubbling was vigorous, slowing within 15 min. Formation of **25** (R_f = 0.09) was monitored by TLC (eluted with pentane). After 2.5 h, the reaction mixture was chromatographed on silica gel (200 mL) with pentane, where **25** eluted as a blood red band after several yellow, brown, and blue bands. The solvent was removed by rotary evaporation, affording **25** (920 mg, 47 %) as dark red needles. X-ray quality prisms were obtained by sublimation: mp 104 °C (dec.); sublp 45 °C (0.1 torr); UV (pentane) λ_{max} 260 nm (log ε 2.01×10^4), 318 nm (log ε 8.83×10^3), 458 nm (log ε 8.57×10^2); ^{1}H NMR (500 MHz, $CDCl_3$) δ 0.34 ppm (s, 9 H); ^{13}C NMR (125 MHz, $CDCl_3$) δ 197 (br), 125.8, 73.4, 0.00 ppm; IR (KBr) 3044, 2964, 2110, 2075, 2046, 1609, 1566, 1503, 1451, 1407, 1384, 1323, 1288, 1268, 1253, 1049, 944, 845, 881, 792, 756, 715, 512, 493, 447 cm^{-1}; MS *m/z* (rel intensity) 429 (M^+, 30), 401 (25), 373 (40), 345 (22), 317 (14), 289 (32), 287 (20), 271 (70), 261 (70), 259 (12), 243 (70), 231 (70), 215 (72), 179 (45), 84 (58), 83 (32), 75 (100), 73 (46). Anal. Calcd for $C_{11}H_9NO_8Co_2Si$: C, 30.77; H, 2.10; N, 3.26. Found: C, 31.07; H, 1.96; N, 3.24. CV Starting E = 0 mV; High E = 1000 mV; Low E = –1300 mV; Initial sweep: negative; V = 200 mV/sec; Number of segments = 3; Sample interval = 1 mV; Solvent = CH_2Cl_2; Electrolyte = 0.1 M NBu_4PF_6. E_{pc} = 320, –955 mV; E_{pa} = 480, –0.815 mV. All events were reversible.

Reaction of [μ-1-nitro-2-(trimethylsilyl)ethyne-1,2-diyl]bis(tricarbonylcobalt)(*Co–Co*) (25) with NO_2BF_4

A solution of NO_2BF_4 (490 mg, 3.70 mmol) in acetonitrile (50 mL) maintained at –30 °C was transferred by canula to a stirred solution of **25** (99.6 mg, 0.232 mmol) in acetonitrile (5 mL) maintained at –30 °C. Within 2 min, the mixture had changed color from red to brown. Analysis by TLC showed only an intractable brown solid (R_f = 0.0). Repetition of this experiment at RT caused the color to change immediately, but otherwise gave identical results.

Reaction of [μ-1-nitro-2-(trimethylsilyl)ethyne-1,2-diyl]bis(tricarbonylcobalt)(*Co–Co*) (25) with TBAF and tetryl (6)

To a stirred solution of **25** (20 mg, 0.047 mmol) in THF (3 mL) was added 1.0 M TBAF (0.05 mL, 0.05 mmol). The color of the mixture changed from red to brown instantly. After 15 min, **6** (17 mg, 0.059 mmol) was added, causing the color to change to magenta. The reaction was quenched with ethanol (0.5 mL) and the solvent was evaporated by nitrogen flow. The resulting brown solids were transferred to a sublimator and heated to 70 °C under dynamic vacuum. No volatile material was collected. Repetition of this

experiment at –78 and –100 °C gave identical results, except that, at –100 °C, the red to brown color change of the solution of **25** occurred over 2 s rather than instantaneously.

Reaction of [μ-1-nitro-2-(trimethylsilyl)ethyne-1,2-diyl]bis(tricarbonylcobalt)(*Co–Co*) (25) with BuLi and tetryl (6)

Into a stirred solution of **25** (5.2 mg, 0.012 mmol) in pentane (2 mL) was injected freshly titrated 0.85 M BuLi (1.7 mg, 0.025 mmol). The red color of the solution disappeared and a black precipitate formed immediately. These changes were accompanied by a mild endotherm. The mixture was allowed to stand for 2 h, **6** (15.3 mg, 0.053 mmol) was added. After a further 1 h, the suspension was filtered through a plug of Celite, leaving only solvent in the filtrate.

Reaction of [μ-1-nitro-2-(trimethylsilyl)ethyne-1,2-diyl]bis(tricarbonylcobalt)(*Co–Co*) (25) with tributyltin fluoride (224) and propyl nitrate (225)

To a stirred solution of **25** (31 mg, 0.073 mmol) in **225** (0.5 mL, 500 mg, 5 mmol) was added **224** (22.6 mg, 0.073 mmol). The reaction mixture was heated to 50 °C for 24 h. Analysis by TLC (eluted with pentane) revealed only starting material ($R_f \sim 0.1$) and an intractable brown material.

Reaction of [μ-1-nitro-2-(trimethylsilyl)ethyne-1,2-diyl]bis(tricarbonylcobalt)(*Co–Co*) (25) with propyl nitrate (225) and NaOMe

To a stirred solution of **25** (456 mg, 1.06 mmol) in **225** (9.0 mL, 9.7 g, 92 mmol) was added NaOMe (1.3 mg, 0.020 mmol). Analysis by TLC [eluted in pentane/diethyl ether (9:1)] showed only **25** ($R_f \sim 0.9$) and a very weak band with $R_f = 0.6$ (assumed to be **26** from adventitious moisture because of similar R_f values). After 22 h, TLC analysis included an intractable brown solid ($R_f = 0.0$), but otherwise remained unchanged. The reaction mixture was heated to 50 °C for 2 h. No change was observed by TLC. The mixture was allowed to cool to RT, and the solvent was removed by rotary evaporation. The remaining dark red solid was dissolved in pentane (3 mL) and filtered through a plug of silica gel to afford **25** (210 mg, 46 % recovery).

Reaction of [μ-1-nitro-2-(trimethylsilyl)ethyne-1,2-diyl]bis(tricarbonylcobalt)(*Co–Co*) (25) with $NaBH_4$

To a stirred solution of **25** (47 mg, 0.11 mmol) in ethanol (1 mL) maintained at 0 °C was added $NaBH_4$ (22 mg, 0.58 mmol) and aqueous 2 M $CuSO_4$ (1 drop). The reaction mixture was allowed to warm to RT over 45 min, during which time the color changed from red to dark brown. Ethyl acetate (1 mL) was added, and then reaction was then quenched with water (1 mL), causing slight gas evolution. The mixture was centrifuged, and the ethyl acetate layer decanted, then dried over MgSO4. This layer was extracted with pentane (1 × 4 mL), giving a red-orange solution. The solvent was evaporated under

nitrogen flow to leave a mixture of **25** and **26** (12 mg) as a sticky red oil: ^{1}H NMR (400 MHz, $CDCl_3$): δ6.14 (s), 0.34 ppm (s).

Reaction of [μ-1-nitro-2-(trimethylsilyl)ethyne-1,2-diyl]bis(tricarbonylcobalt)(*Co–Co*) (25) with $LiAlH_4$

In THF:

A pressure-equalized addition funnel was charged with **25** (409.1 mg, 0.9533 mmol) in THF (7 mL). This solution was added dropwise to a slurry of $LiAlH_4$ (108.6 mg, 2.862 mmol) in THF (20 mL) over 10 min. Gas evolved, and the color changed from grey to dark black-red. The distinct odor of amines was noted. After 24 h, saturated NH_4Cl solution (6 mL) was added. After filtering through a Gooch crucible (30 mm, C frit) to remove precipitate, the organic layer was separated from the aqueous phase and dried over $MgSO_4$. The solvent was removed by rotary evaporation to furnish an intractable brown solid.

In diethyl ether:

A pressure-equalized addition funnel was charged with **25** (129.1 mg, 0.3008 mmol) in diethyl ether (10 mL). This solution was added dropwise to a slurry of $LiAlH_4$ (26.2 mg, 0.691 mmol) in diethyl ether (40 mL) over 45 min. The color changed from clear to cloudy and tan, and the temperature of the mixture rose from 20 to 22 °C. After 4 h, the reaction mixture was black, and saturated $MgCl_2$ solution (6 mL) was added. The slurry was filtered through a plug of Celite to remove the precipitate, and the solvent was removed by rotary evaporation to furnish brown-black solids containing traces of **25** and **219**.

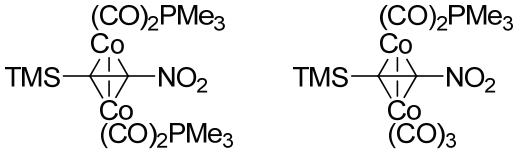

[μ-1-Nitro-2-(trimethylsilyl)ethyne-1,2-diyl]bis[dicarbonyl(trimethylphosphane)cobalt](*Co–Co*) (238) and [μ-1-nitro-2-(trimethylsilyl)ethyne-1,2-diyl](tricarbonylcobalt)[dicarbonyl(trimethylphosphane)cobalt](*Co–Co*) (237)

To a stirred solution of **25** (194.6 mg, 0.453 mmol) in hexanes (4.5 mL) was added trimethylphosphine (74 mg, 0.97 mmol) in hexanes (3 mL). Formation of **238** (R_f = 0.58) and **237** (R_f = 0.40) was monitored by silica gel TLC [eluted with pentane/diethyl ether (9:1)]. After 24 h, the reaction mixture was chromatographed on silica gel (75 mL) with pentane/diethyl ether (9:1, 250 mL). Compound **238** eluted as a dark brown-black band followed by **237** as a bright red-orange band. The solvent was removed by rotary

evaporation, leaving dark red fans of **238** and a red-orange film of **237**. Crystallization of the dark red fans from pentane afforded **238** (100 mg, 41 %) as dark red plates: ^{1}H NMR (400 MHz, $CDCl_3$) δ 1.39 (d, $^{2}J_{PH}$ = 8.7 Hz, 18 H), 0.31 ppm (s, 9 H), ; ^{13}C NMR (100 MHz, $CDCl_3$) (incomplete) δ 19.2 (d, J_{CP} = 26 Hz), 2.06 ppm; IR (KBr) 2965, 2910, 2030, 1993, 1980, 1978, 1953, 1946, 1627, 1492, 1469, 1421, 1380, 1301, 1287, 1246, 1173, 1102, 947, 841, 780, 756, 735, 692, 673, 622, 583, 532, 515, 498, 468, 434 cm^{-1}; MS *m/z* (rel intensity) 525 (M^+, 1), 497 (1), 469 (1), 441 (1), 423 (1), 413 (4), 383 (12), 367 (16), 337 (20), 291 (6), 179 (8), 155 (8), 135 (7), 97 (25), 92 (27), 84 (32), 83 (22), 77 (66), 76 (75), 75 (55), 73 (15), 61 (100), 59 (70), 57 (25).

Crystallization of the orange-red film from pentane afforded **237** (100 mg, 46 %) as red-orange needles: ^{1}H NMR (500 MHz, $CDCl_3$) δ 1.44 (d, $^{2}J_{PH}$ = 10.2 Hz, 9 H), 0.32 ppm (s, 9 H); ^{13}C NMR (125 MHz, $CDCl_3$) δ 199 (br), 121.4, 67.1, 19.4 (δ, J_{CP} = 28 Hz), 1.24 ppm; IR (KBr) 2962, 2917, 2827, 2076, 2026, 1976, 1637, 1494, 1422, 1384, 1314, 1290, 1249, 1180, 953, 846, 785, 739, 698, 677, 624, 514 cm^{-1}; MS *m/z* (rel intensity) 477 (M^+, 10), 449 (24), 421 (28), 337 (14), 319 (8), 307 (10), 291 (12), 179 (25), 155 (25), 97 (20), 92 (45), 84 (50), 83 (40), 77 (100), 76 (56), 75 (68), 73 (25), 61 (75), 59 (54), 57 (18).

Attempted nitration of [μ-1-nitro-2-(trimethylsilyl)ethyne-1,2-diyl]bis[dicarbonyl(trimethylphosphane)cobalt](*Co–Co*) (237) with NO_2BF_4

A pressure-equalized addition funnel was charged with NO_2BF_4 (20 mg, 0.15 mmol) in acetonitrile (25 mL). This solution was added dropwise to **237** (101 mg, 0.21 mmol) in acetonitrile (25 mL) maintained at –20 °C over 25 min. The solution was allowed to warm to 10 °C over 30 min. Analysis by TLC [eluted with pentane/diethyl ether (9:1)] showed a single red-orange band (R_f = 0.20). The solvent was removed by rotary evaporation to afford an intractable red solid.

Decomplexation of [μ-1-nitro-2-(trimethylsilyl)ethyne-1,2-diyl]bis(tricarbonylcobalt)(*Co–Co*) (25) with CAN

To a stirred solution of **25** (97.8 mg, 0.228 mmol) in CD_3CN (3 mL) was added $(NH_4)_2Ce(NO_3)_6$ (840.6 mg, 1.533 mmol). Gas evolved quickly, and the color of the mixture changed from dark red to light orange within 2 min. The solution was filtered through a 0.45 μm PTFE filter and observed by ^{1}H NMR spectroscopy, which showed that only **18** remained.

Reaction of [μ-1-nitro-2-(trimethylsilyl)ethyne-1,2-diyl]bis(tricarbonylcobalt)(*Co–Co*) (25) with TBAF

To a stirred solution of **25** (5.2 mg, 0.012 mmol) in methylene chloride (5 mL) was added 1.0 M TBAF (0.01 mL, 0.01 mmol) in THF. The red color of the disappeared and an intractable pink precipitate formed immediately, indicative of demetallation. This reaction was repeated in nitromethane, rendering a lighter colored solution and no

precipitate. This solution was analyzed by NMR and found to contain no desilylation products. In ethanol at –78 °C, this reaction also failed to give any desilylation products.

Reaction of [μ-1-nitro-2-(trimethylsilyl)ethyne-1,2-diyl]bis(tricarbonylcobalt)(*Co–Co*) (25) with KF

To a stirred solution of KF (30 mg, 0.32 mmol) in acetone/water (5:1) was added **25** (5.2 mg, 0.012 mmol) in acetone (2 mL). After 2 h, the solution had lost color and a black precipitate had formed, indicating demetallation.

Reaction of [μ-1-nitro-2-(trimethylsilyl)ethyne-1,2-diyl]bis(tricarbonylcobalt)(*Co–Co*) (25) with K_2CO_3 and MeOH

To a stirred solution of **25** (17 mg, 0.040 mmol) in methanol (3 mL) was added a solution of K_2CO_3 (20 mg, 0.14 mmol) in methanol (2 mL). The color of the reaction mixture darkened almost to black over 40 min. Water (15 mL) was added to quench the reaction, leaving a golden solution. The solvent was removed by rotary evaporation to afford an intractable orange-yellow solid.

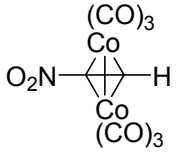

[μ-1-Nitroethyne-1,2-diyl]bis(tricarbonylcobalt)(*Co–Co*) (26)

A 6.2×10^{-3} M aqueous buffer solution of potassium carbonate and potassium bicarbonate (5.2 mL, 0.0032 mmol) in was added in air to a stirred solution of **25** (360 mg, 0.84 mmol) in methanol (25 mL) and the mixture sealed with a rubber septum. Within 1 min, the red solution became slightly darker and condensate appeared on the inside of the flask. The disappearance of **25** (R_f = 0.86) and the formation of **26** (R_f = 0.67) were monitored by silica gel TLC [eluted with pentane/diethyl ether (9:1)]. After 2 h, the reaction was quenched with water (10 mL) and the mixture extracted with diethyl ether/pentane (1.5:1, 2 × 25 mL). The red organic layers were combined, dried over $MgSO_4$, and concentrated by rotary evaporation below 20 °C (where sublimation begins) to afford **26** (0.18 g, 59.5 %) as red-orange prisms. X-ray quality single crystals were obtained by recrystallization from pentane: mp 49 °C (dec.); sublp 25 °C (0.1 torr); UV (pentane) λ_{max} 260 nm (log ε 2.86×10^4), 343 nm (log ε 6.61×10^3), 442 nm (log ε 1.04×10^3); ^{1}H NMR (500 MHz, $CDCl_3$) δ 6.14 ppm (s, 1 H); ^{13}C NMR (125 MHz, $CDCl_3$) δ 196 (br), 111.7, 65.2 ppm; IR (KBr) 2116, 2083, 2053, 1618, 1509, 1458, 1384, 1322, 1230, 1180, 1101, 796, 762, 732, 702, 562, 509, 491, 468, 451 cm^{-1}; MS *m/z* (rel intensity) 357 (M^+, 5) , 329 (65), 301 (45), 273 (30), 245 (5), 227 (12), 217 (17), 215 (15), 199 (75), 189 (17), 171 (75), 159 (25), 143 (90), 97 (100), 87 (26), 84 (17), 78 (65), 59 (55). Anal. Calcd for $C_8HNO_8Co_2$: C, 26.89; H, 0.28; N, 3.92. Found: C, 27.21; H, 0.22; N, 3.92. CV Starting E = 0 mV; High E = 1000 mV; Low E = –1300 mV; Initial sweep: negative; V = 200 mV/sec; Number of segments = 3; Sample interval = 1 mV;

Solvent = CH_2Cl_2; Electrolyte = 0.1 M NBu_4PF_6. E_{pc} = –961 mV. All events were irreversible.

Reaction of [μ-1-nitroethyne-1,2-diyl]bis(tricarbonylcobalt)(*Co–Co*) (26) with LiHMDS and NO_2Cl

Into a solution of **26** (30.6 mg, 0.086 mmol) in methylene chloride (2 mL) maintained at –98 °C was injected a freshly prepared solution of LiHMDS (14.4 mg, 0.086 mmol) in methylene chloride (1 mL). A black precipitate formed in 2 s. Into this was injected NO_2Cl (5.8 mg, 0.071 mmol) in methylene chloride (0.58 mL). No color change was observed. Analysis by TLC [eluted with pentane/diethyl ether (95:5)] showed only **26** (R_f = 0.6) and intractable black solids (R_f = 0.0). The reaction mixture was allowed to warm to –50 °C, and was then quenched with water (10 mL). The organic layer was separated, dried over Na_2SO_4, and decanted to remove the precipitate. The solvent was removed by rotary evaporation to leave a trace of **26**.

Reaction of [μ-1-nitroethyne-1,2-diyl]bis(tricarbonylcobalt)(*Co–Co*) (26) with LiHMDS and methyl triflate

Successive addition of reagents:

Into a solution of **26** (31 mg, 0.087 mmol) in methylene chloride (4 mL) maintained at –78 °C was injected a freshly prepared solution of LiHMDS (13.8 mg, 0.0825 mmol) in methylene chloride (1 mL). A black precipitate formed immediately. Into this was injected methyl triflate (26.9 mg, 0.164 mmol) in methylene chloride (0.5 mL). Analysis by TLC [eluted with pentane/diethyl ether (9:1)] showed only **26** (R_f = 0.6) and intractable black solids (R_f = 0.0). The solvent was removed by rotary evaporation to leave an intractable black solid with traces of **26**.

Reaction in the presence of methyl triflate:

This reaction was performed as in the reaction of **26** with LiHMDS and methyl triflate, except with **26** (32 mg, 0.090 mmol), LiHMDS (14.3 mg, 0.085 mmol), and methyl triflate (27 mg, 0.165 mmol) and the methyl triflate was combined with **26** prior to addition of LiHMDS. The results were identical.

Decomplexation of [μ-1-nitroethyne-1,2-diyl]bis(tricarbonylcobalt)(*Co–Co*) (26) with CAN

This reaction was performed as in the reaction of **25** with $(NH_4)_2Ce(NO_3)_6$, except with **26** (120.0 mg, 0.336 mmol) and $(NH_4)_2Ce(NO_3)_6$ (1.235 g, 2.252 mmol). Demetallation was accompanied by an exotherm. Complete decomposition of **26** without subsequent formation of **16** was observed by ^{1}H NMR spectroscopy.

Attempted Pauson-Khand reaction of [μ-1,2-bis(trimethylsilyl)ethyne-1,2-diyl]bis(tricarbonylcobalt)(*Co–Co*) (218) with vinyl benzoate (257) and NMO (258)

To a stirred solution of **218** (128 mg, 0.751 mmol) in methylene chloride (5 mL) was added **257** (139 mg, 0.939 mmol). A solution of **258** (876 mg, 7.48 mmol) in methylene chloride (30 mL) was injected by syringe pump over 3 h, causing precipitate to slowly form. The reaction mixture was filtered, and the resulting sky-blue filtrate concentrated by rotary evaporation to leave a blue-grey solid smelling of norbornene and spearmint. No Pauson-Khand products were observed by NMR spectroscopy.

Attempted Pauson-Khand reaction of [μ-1,2-bis(trimethylsilyl)ethyne-1,2-diyl]bis(tricarbonylcobalt)(*Co–Co*) (218) with cyclopentene (261) and TMANO (262)

A solution of **218** (101 mg, 0.221 mmol) in methylene chloride (2 mL) was transferred by canula to a stirred solution of **262** (81 mg, 1.078 mmol) in methylene chloride (6 mL) maintained at –78 °C. A balloon filled with O_2 was attached to the reaction flask, and **261** (85 mg, 1.245 mmol) was added. The solution color changed from dark red to dark blue over 1 h. After 4 h, the reaction was warmed to room temperature and filtered through a plug of alumina. The blue color remained on the alumina as a dark, royal-blue solid. The solvent was evaporated from the clear filtrate by nitrogen flow to leave a scant amount of an intractable clear gel.

Attempted Pauson-Khand reaction of [μ-1-(trimethylsilyl)ethyne-1,2-diyl]bis(tricarbonylcobalt)(*Co–Co*) (219) with vinyl benzoate (257) and NMO (258)

Into **219** (96.9 mg, 0.252 mmol) and **257** (332 mg, 2.24 mmol) was injected **258** (266 mg, 2.27 mmol) in methylene chloride (30 mL) by syringe pump over 4 h. The mixture changed color from red to dark purple during this addition. The solvent was removed by rotary evaporation to afford a black solid. Analysis by TLC (eluted in methylene chloride) showed only excess **257** and an unmoving black band ($R_f = 0.0$).

Pauson-Khand reaction of [μ-1-(trimethylsilyl)ethyne-1,2-diyl]bis(tricarbonylcobalt)(*Co–Co*) (219) with norbornene (250) and NH_4OH

To a stirred solution of **219** (390 mg, 1.02 mmol) and **250** (140 mg, 1.49 mmol) in 1,4-dioxane (3 mL) was added 2 M NH_4OH (9 mL, 18 mmol). The solution changed color from red to brown and a black precipitate formed. The mixture was heated to 86 °C, causing the color to change to black. After 1 h, the suspension was cooled to room temperature and filtered through a Gooch crucible (30 mm, F frit), then washed with water (15 mL), 5 % HCl (15 mL), and saturated $NaHCO_3$ solution (15 mL). The filtrate was dried over $MgSO_4$ and concentrated by rotary evaporation. The crude material was chromatographed on silica gel (100 mL) with pentane/diethyl ether (85:15) to give a single band visible under UV light. The solvent was removed by rotary evaporation to afford to afford **265** (130 mg, 58 %) as white crystals that smelled of isoprene and norbornene: ^{1}H NMR (400 MHz, $CDCl_3$) δ 7.54 (d, J = 2.6 Hz, 1 H), 2.62 (quar, J = 2.8

Hz, 1 H), 2.35 (d, *J* = 3.6 Hz, 1 H), 2.15 (d, *J* = 3.9 Hz, 1 H), 2.09 (d, *J* = 5.3 Hz, 1 H), 1.63 (m, 1 H), 1.54 (m, 1 H), 1.25 (m, 2 H), 0.90 (s, 2H), 0.14 ppm (s, 9 H) [lit.:[390] d 7.56 (d *J* = 2.8 Hz, 1 H), 2.37 (d, *J* = 4 Hz, 2 H), 2.12 (d, *J* = 5.2 Hz, 2 H), 1.54 (m, 2 H), 1.25 (m, 4 H), 0.5 ppm (s, 9 H)]; ^{13}C NMR (100 MHz, $CDCl_3$) δ 214.9, 173.0, 150.1, 54.3, 51.9, 39.1, 38.0, 31.0, 29.0, 28.3, –1.9 ppm [lit:[390] ($CDCl_3$) δ 173.1, 150.1, 54.3, 51.9, 39.1, 37.9, 31.0, 29.0, 28.3, –2.8 ppm].

Attempted Pauson-Khand reaction of [μ-1-nitro-2-(trimethylsilyl)ethyne-1,2-diyl]bis(tricarbonylcobalt)(*Co–Co*) (25) with norbornene (250) and NH_4OH

This reaction was performed as in the reaction of **219** with **250** and NH_4OH, except with **25** (210 mg, 0.49 mmol), **250** (70 mg, 0.74 mmol). The red suspension resulting from NH_4OH addition changed color to green after 15 min, and then again to aqua blue after a further 25 min. Following the same workup describe above, a clear, sticky solid resulted. Analysis by TLC (eluted with diethyl ether) showed it consisted of only unreacted **250**.

Attempted Pauson-Khand reaction of [μ-1-nitro-2-(trimethylsilyl)ethyne-1,2-diyl]bis(tricarbonylcobalt)(*Co–Co*) (25) with norbornene (250) and TMANO (262)

To a stirred solution of **25** (64 mg, 0.15 mmol) and **250** (76 mg, 0.81 mmol) in methylene chloride (4 mL) saturated with O_2, and maintained at 0 °C was added **262** (7 mg, 0.1 mmol). A balloon filled with O_2 was attached to the reaction flask. After 2 h, the reaction mixture was allowed to warm to RT. After 20 h, the reaction mixture was chromatographed on silica gel (40 mL) with methylene chloride to collect only one weak red band. The solvent was evaporated by nitrogen flow, affording a trace of red solid identified as **25** by NMR spectroscopy.

Attempted Pauson-Khand reaction of [μ-1-nitroethyne-1,2-diyl]bis(tricarbonylcobalt)(*Co–Co*) (26) with norbornene (250) and NH_4OH

This reaction was performed as in the reaction of **219** with **250** and NH_4OH, except with **26** (91.5 mg, 0.26 mmol), **250** (37.1 mg, 0.39 mmol). The red suspension resulting from NH_4OH addition changed color to brown after 10 min, and then again to green after a further 20 min. Following the same workup describe above, a dark brown solid was obtained. Analysis by TLC [eluted with pentane/diethyl ether (85:15)] showed only an unmoving band (R_f = 0.0). Analysis by NMR spectroscopy showed an absence of product.

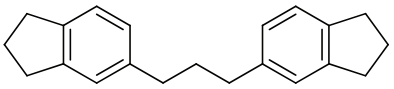

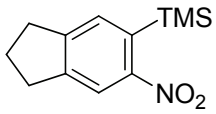

1,3-Bis(2,3-dihydro-1H-inden-5-yl)propane (312) and 6-nitro-7-(trimethylsilyl)indane (311)

To a stirred solution of **25** (161.4 mg, 0.376 mmol) in octane (7.5 mL) was added **271** (102.2 mg, 1.109 mmol). A Liebig condenser was attached, and the reaction mixture was heated at reflux (~150 °C) in an oil bath, open to the atmosphere. After 4 h, heating was discontinued and the black suspension was allowed to cool to RT. The solvent was removed by rotary evaporation and the remaining black solids were extracted with pentane (5 × 7.5 mL). The extract was vacuum filtered through silica gel (2 mL) over sand (2 mL), and washed down with pentane (20 mL). Formation of **311** (R_f = 0.15) was noted by TLC eluted with pentane. The solution was concentrated by rotary evaporation to ~ 5 mL, and chromatographed on a silica gel plate (2 mm thickness) by spinning band (Chromatotron), giving two UV-active bands. The solvent was removed from the first fraction by rotary evaporation to furnish **312** (2.8 mg, 2.7 %) as a clear oil: ^{1}H NMR (400 MHz, $CDCl_3$) δ 7.13 (d, J = 8 Hz, 2 H), 7.06 (s, 2 H), 6.96 (d, J = 8 Hz, 2 H), 2.87 (t, J = 8 Hz, 8 H), 2.62 (t, J = 8 Hz, 4 H), 2.06 ppm (m, 4 H) [lit.[348] (200 MHz, $CDCl_3$) δ 7.15–6.70 (m, 6 H), 2.86 (t, J = 7.1–7.3 Hz, 8 H), 2.62 (t, J = 7.2 Hz, 4 H), 2.19–1.62 (m, 6 H)]; 13C NMR (100 MHz, $CDCl_3$) δ 144.3, 141.5, 140.3, 126.2, 124.4, 124.1, 35.4, 33.6, 32.8, 32.4, 25.5 ppm

The solvent was removed from the second band to afford **311** (21.6 mg, 24.5 %) as a cloudy white oil: ^{1}H NMR (400 MHz, $CDCl_3$) δ 8.04 (s, 1 H), 7.53 (s, 1 H), 2.98 (t, J = 7.4 Hz, 4 H), 2.16 (quin, J = 7.4 Hz, 2 H), 0.33 ppm (s, 9 H); ^{13}C NMR (100 MHz, $CDCl_3$) δ 152.5, 150.7, 146.9, 134.5, 131.6, 120.2, 32.8, 32.5, 25.5, –0.2 ppm; ^{29}Si NMR (99 MHz, $CDCl_3$) δ –2.32 ppm; IR (film) 3065, 2954, 2901, 2845, 1566, 1519, 1461, 1434, 1372, 1347, 1311, 1251, 1218, 1109, 1037, 1001, 959, 891, 850, 776, 756, 684, 653, 622 cm^{-1}; MS *m/z* (rel intensity) 220 (M^+–15, 100), 190 (22), 175 (10), 115 (10).

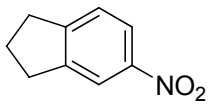

5-Nitroindane (313)

To a stirred solution of **26** (99.9 mg, 0.280 mmol) in hexanes (7 mL) was added **271** (79.8 mg, 0.870 mmol). A Liebig condenser was attached and the reaction mixture was heated at reflux (~70 °C) in an oil bath, open to the atmosphere. After 2.5 h, heating was discontinued and the black suspension allowed to cool to RT. The solvent was removed by rotary evaporation, and the remaining black solids were extracted with pentane (5 × 8 mL). Formation of (the product) (R_f = 0.31) was noted by TLC on silica gel (eluted with pentane). The solution was chromatographed on a silica gel plate (1 mm thickness) with pentane by spinning band (Chromatotron) to afford **313**[420,421,425] (0.6 mg, 1.3 %) as a

clear oil. ^{1}H NMR (500 MHz, $CDCl_3$) δ 8.06 (s, 1 H), 8.02 (dd, J = 8.0, 2.0 Hz, 1 H), 7.32 (d, J = 10.0 Hz, 1 H), 3.00 (m, J = 3.8 Hz, 4 H), 2.17 ppm (quin, J = 7.5 Hz, 2 H); MS *m/z* (rel intensity) 163 (M^+, 91), 146 (39), 117 (61), 116 (61), 115 (100), 91 (32).

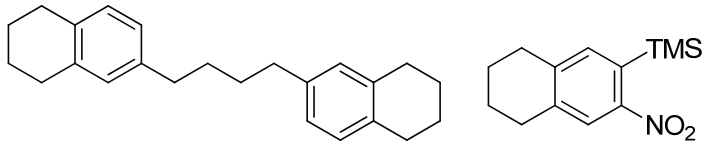

1,4-Bis(5,6,7,8-tetrahydronaphthalen-2-yl)butane (315) and 6-nitro-7-(trimethylsilyl)tetralin (314)

To a stirred solution of **25** (163 mg, 0.380 mmol) in octane (10 mL) was added **273** (120 mg, 1.130 mmol). A Liebig condenser was attached, and the reaction mixture was heated at reflux (~150 °C) in an oil bath, open to the atmosphere. After 4 h, heating was discontinued, and the now black suspension was allowed to cool to RT. The crude reaction mixture was chromatographed on a short column of silica gel (15 mL), eluted with pentane, to give a tan-colored band. This fraction was concentrated and purified by preparative TLC (eluted with pentane), to afford two colorless bands. The solvent was removed from the first band by rotary evaporation to give **315** (25 mg, 21 % based on **25**) as a yellow oil: ^{1}H NMR (500 MHz, $CDCl_3$) δ 6.96 (d, J = 7.7 Hz, 2 H), 6.92 (d, J = 8.5 Hz, 2 H), 6.88 (s, 2 H), 2.73 (br, 8 H), 2.56 (t, J = 6.8 Hz, 4 H), 1.79 (quin, J = 2.8 Hz, 8 H), 1.65 ppm (quin, J = 3.5 Hz, 4 H) [lit.[413] (300 MHz, $CDCl_3$) δ 7.0–6.8 (m, 3 H), 2.7 (br, 4 H), 2.55 (t, 2 H), 1.8 (m, 4 H), 1.65 (m, 2 H)]; ^{13}C NMR (125 MHz, $CDCl_3$) δ 139.7, 136.8, 134.3, 129.0, 128.9, 125.6, 35.4, 31.4, 29.4, 29.0, 23.3, 23.2 ppm; IR (KBr) 2925, 2854, 1613, 1574, 1500, 1433, 1349, 1245, 917, 874, 827, 809, 745 cm^{-1} [lit.[410] (KBr) 2985, 1613, 1575, 1502, 919, 908, 876, 864, 829, 811 cm^{-1}].

The solvent was removed from the second band by rotary evaporation to give **314** (37.2 mg, 39 %) as a clear oil: ^{1}H NMR (400 MHz, $CDCl_3$) δ 7.93 (s, 1 H), 7.36 (s, 1 H), 2.83 (t, J = 6.4 Hz, 4 H), 1.83 (quin, J = 3.2 Hz, 4 H), 0.33 ppm (s, 9 H); ^{13}C NMR (100 MHz, $CDCl_3$) δ 151.1, 143.5, 139.6, 137.1, 132.8, 124.7, 29.5, 29.1, 22.7, 22.6, –0.33 ppm; ^{29}Si NMR (99 MHz, $CDCl_3$) δ –3.11 ppm; IR (film) 2932, 2858, 1557, 1525, 1434, 1341, 1290, 1248, 1126, 926, 781, 847, 755, 682 cm^{-1}; MS *m/z* (rel intensity) 234 (M^+–15, 100), 212 (60), 197 (12), 183 (23), 171 (17), 158 (20), 145 (85), 129 (27), 115 (21). Anal. Calcd for $C_{13}H_{19}NO_2Si$: C, 62.61; H, 7.68; N, 5.62. Found: C, 63.80; H, 7.94; N, 5.29.

Attempted [2 + 2 + 2] cyclization of [μ-1-nitroethyne-1,2-diyl]bis(tricarbonylcobalt)(*Co–Co*) (26) with 1,7-octadiyne (273)

To a stirred solution of **26** (152.4 mg, 0.427 mmol) in octane (7 mL) was added **273** (136 mg, 1.28 mmol). The reaction mixture was heated at reflux for 2.5 h, and then allowed to cool to RT. The solvent was removed from the black suspension by rotary evaporation, and the resulting solid extracted with pentane (5 × 8 mL). This extraction was passed

through a short plug of silica gel, then chromatographed on a silica gel plate (2 mm thickness) by spinning band (Chromatotron) with pentane, giving one colorless band. The solvent was removed by rotary evaporation to leave **315** (5.5 mg, 18 % based on **26**) as a clear oil.

Attempted [2 + 2 + 2] cyclization of [μ-1-nitro-2-(trimethylsilyl)ethyne-1,2-diyl]bis(tricarbonylcobalt)(*Co–Co*) (25) with DMAD (197)

To a stirred solution of **25** (215.6 mg, 0.502 mmol) in xylenes (5.5 mL) was added **197** (430 mg, 3.03 mmol). The mixture was heated at reflux for 2.5 h, and then allowed to cool to RT. The solvent was removed by rotary evaporation, and the resulting black solid extracted with methylene chloride (5 × 8 mL). The extract was filtered through a plug of silica gel, then chromatographed on a silica gel plate (2 mm thickness) by spinning band (Chromatotron) with diethyl ether to give two light yellow bands. The solvent was removed from the first band to give a complex mixture of inseparable products as a yellow oil (30 mg). The solvent was removed from the second band to afford a complex mixture of unidentified compounds as an off-white amorphous solid (140 mg). Analysis by NMR showed that neither fraction contained TMS groups or an aromatic system substituted by esters.

Attempted [2 + 2 + 2] cyclization of [μ-1-nitro-2-(trimethylsilyl)ethyne-1,2-diyl]bis(tricarbonylcobalt)(*Co–Co*) (25) with diphenylacetylene (182)

This reaction was performed as in the reaction of **25** with **197**, except with **25** (101.2 mg, 0.236 mmol), **182** (258.1 mg, 1.448 mmol), and with octane as the solvent. Following workup with pentane, four bands were separated by chromatography on silica gel (with diethyl ether). The solvent was removed from these bands by rotary evaporation. Their descriptions are as follows: band 1: white solid (20 mg); band 2: clear oil (< 10 mg); band 3: off white solid (70 mg); band 4: yellow oil (120 mg). All were found to be complex mixtures of aromatic compounds, and only band 3 contained evidence of TMS groups by NMR spectroscopy.

Attempted [2 + 2 + 2] cyclization of [μ-1-nitro-2-(trimethylsilyl)ethyne-1,2-diyl]bis(tricarbonylcobalt)(*Co–Co*) (25)

A stirred solution of **25** (1.73 g, 4.03 mmol) in octane (12 mL) was heated at reflux for 3 h, then allowed to cool to RT. Analysis by TLC (eluted with pentane) showed only an unidentified, very weak, yellow-orange band (R_f = 0.86), and a very strong purple band (R_f = 0.80). The purple band was assumed to be a larger cobalt cluster because of the similarity in elution time to **23**. No aromatic compounds were observed when viewed in UV light.

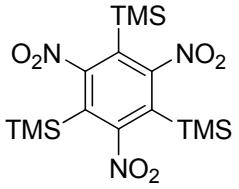

325

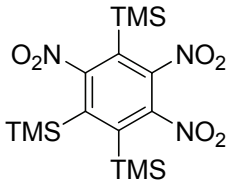

322

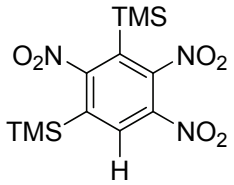

324

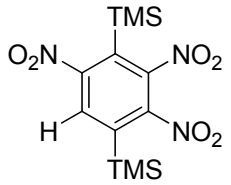

323

1,3,5-Trinitro-2,4,6-tris(trimethylsilyl)benzene (325), 1,2,4-trinitro-3,5,6-tris(trimethylsilyl)trinitrobenzene (322), 1,2,4-trinitro-3,5-bis(trimethylsilyl)benzene (324), and 1,3,4-trinitro-1,4-bis(trimethylsilyl)-2,4,5-trinitrobenzene (323)

To a stirred solution of **25** (431 mg, 1.00 mmol) in octane (7 mL) was added **18** (860 mg, 6.00 mmol). A Liebig condenser was attached, and the reaction mixture was heated at reflux (~150 °C) in a heating mantle, open to the atmosphere. After 2.5 h, heating was discontinued and the black suspension allowed to cool to RT. Formation of **325** (R_f = 0.28) and several side products (R_f ~ 0.09) were noted by TLC on silica gel (eluted with pentane). The solvent was removed by rotary evaporation, and the remaining black solids were extracted with pentane (5 × 7.5 mL). The extract was vacuum filtered through silica gel (2 mL) over sand (2 mL), and washed down with pentane (20 mL). The solvent was removed from the pentane extract to afford **325** (110 mg, 26 %) as white needles. X-ray quality single crystals were obtained by recrystallization from pentane: sublp 246 °C (760 torr); ^{1}H NMR (500 MHz, $CDCl_3$) δ 0.32 ppm (s, 9 H); ^{13}C NMR (125 MHz, $CDCl_3$) δ 162.7, 126.3, –0.5 ppm; IR (KBr) 1543, 1516, 1376, 1257, 1098, 857, 799, 762 cm^{-1}; MS *m/z* (rel intensity) 465 (M^+ + 36, 26), 414 (M^+ – 15, 100), 369 (24), 295 (44), 73 (65). Anal. Calcd for $C_{15}H_{27}N_3O_6Si_3$: C, 41.93; H, 6.33; N, 9.78. Found: C, 41.97; H, 6.23; N, 9.41.

The black solids were extracted as described above with diethyl ether. The solution was concentrated by rotary evaporation and the resulting orange oil extracted with pentane (1 × 8 mL). Analysis by TLC (eluted with pentane) showed **325** (R_f = 0.27), **322** (R_f = 0.13), and a complex band at R_f = 0.09, along with several smaller unidentified bands (R_f ~ 0.0–0.19). The solution was chromatographed on a silica gel plate (2 mm thickness) by spinning band (Chromatotron) to afford **325**, **322**, **324** and **323**. The solvent was removed by rotary evaporation to afford **325** (2.6 mg, 0.61 %) as a white microcrystalline solid. This fraction was combined with the **325** isolated from the initial pentane extract as described above. The solvent was removed from the second band to afford **322** (18.6 mg, 4.3 %) as a thermally unstable, amorphous white powder: ^{1}H NMR (500 MHz, $CDCl_3$) δ 0.442 (s, 1 H), 0.438 (s, 9 H), 0.35 ppm (s, 9 H); MS *m/z* (rel intensity) 414 (M^+–15, 75), 342 (58), 295 (10), 270 (10), 223 (25), 147 (20), 133 (25), 104 (18), 73 (100).

The solvent was removed from the third band by rotary evaporation, leaving **324** (4.1 mg, 1.1 %) as a white microcrystalline solid: ^{1}H NMR (500 MHz, $CDCl_3$) δ 8.140 (s, 1 H), 0.378 (s, 9 H), 0.365 ppm (s, 9 H).

The solvent was removed from the final band by rotary evaporation to afford **323** (9.6 mg, 2.7 %) as a light yellow microcrystalline solid: ^{1}H NMR (400 MHz, $CDCl_3$) δ 8.46 (s, 1 H), 0.47 (s, 9 H), 0.45 ppm (s, 9 H); ^{13}C NMR (100 MHz, $CDCl_3$) δ 163.8, 157.8, 156.8, 151.8, 150.0, 120.1, 3.1, 2.6 ppm; ^{29}Si NMR (99 MHz, $CDCl_3$) δ 4.74, 3.61 ppm; IR (KBr) 1564, 1550, 1536, 1381, 1344, 1254, 1226, 1128, 1091, 893, 855, 784, 755, 745, 688, 634 cm^{-1}; MS *m/z* (rel intensity) 342 (M^{+}–15, 75), 223 (55), 147 (25), 133 (35), 73 (100).

References

1. Lancaster, R. *Fireworks Principles and Practice*, 3rd Ed.; Chemical Publishing Co.: New York, 1998; p 77.
2. Davis, T.L. *The Chemistry of Powder and Explosives*; Angriff Press: Las Vegas, 1943; p 28.
3. Davis, T.L. *The Chemistry of Powder and Explosives*; Angriff Press: Las Vegas, 1943; p 195.
4. Davis, T.L. *The Chemistry of Powder and Explosives*; Angriff Press: Las Vegas, 1943; pp 244–245.
5. Nobel, A.B. Finnish Patent 77, December 9, 1864.
6. Nobel, A.B. Improvement in Exploding Nitro-glycerine. U.S. Patent 50,617, October 24, 1865.
7. Urbanski, T. *Chemistry and Technology of Explosives*, Academic Press: New York, 1964; Vol. 1; p 4.
8. Nitration. *Encyclopedia of Explosives and Related Items*; Picatinny Arsenal: New Jersey, 1978; Vol. 8; pp N41–N42.
9. Cooper, P.W. *Explosives Engineering*; Wiley: New York, 1996; pp 19–20.
10. Banert, K.; Joo, Y.; Rueffer, T.; Walfort, B.; Lang, H. *Angew. Chem. Int. Ed.* **2007**, *46*, 1168–1171.
11. Miller, D.R.; Swenson, D.C.; Gillan, E.G. *J. Am. Chem. Soc.* **2004**, *126*, 5372–5373.
12. Urbanski, T. *Chemistry and Technology of Explosives*, Academic Press: New York, 1964; Vol. 1; pp 188–189.
13. Luo, Y.R. *Comprehensive Handbook of Chemical Bond Energies*; CRC Press: Boca Raton, 2007; pp 348–351, 398–399, 406–411.
14. Davis, T.L. *The Chemistry of Powder and Explosives*; Angriff Press: Las Vegas, 1943; p 332.
15. Davis, T.L. *The Chemistry of Powder and Explosives*; Angriff Press: Las Vegas, 1943; p 334.
16. Davis, T.L. *The Chemistry of Powder and Explosives*; Angriff Press: Las Vegas, 1943; p 292.
17. Pentaerythritoltetranitrate. *Encyclopedia of Explosives and Related Items*; Picatinny Arsenal: New Jersey, 1978; Vol. 8; p P93.
18. Explosia Inc. http://www.explosia.cz/en/?show=semtex, (accessed Jan 5, 2011).
19. Davis, T.L. *The Chemistry of Powder and Explosives*; Angriff Press: Las Vegas, 1943; pp 163–164, 166.
20. Cady, H.H.; Larson, A.C. *Acta Crystallogr.* **1965**, *18*, 485–496.
21. Trinitrotoluene. *Encyclopedia of Explosives and Related Items*; Picatinny Arsenal: New Jersey, 1980; Vol. 9; pp T236–T298.
22. Picric acid. *Encyclopedia of Explosives and Related Items*; Picatinny Arsenal: New Jersey, 1978; Vol. 8; p P286.
23. Ammonium Picrate. *Encyclopedia of Explosives and Related Items*; Picatinny Arsenal: New Jersey, 1978; Vol. 8; p P276.
24. Hardt, A.P. *Pyrotechnics*; Pyrotechnica Publications: Post Falls, ID, 2001; p 135.

25. Davis, T.L. *The Chemistry of Powder and Explosives*; Angriff Press: Las Vegas, 1943; pp 72–73.
26. Wilbrand, J. *Ann.* **1863**, *128*, 178–179.
27. Davis, T.L. *The Chemistry of Powder and Explosives*; Angriff Press: Las Vegas, 1943; p 153.
28. Hardt, A.P. *Pyrotechnics*; Pyrotechnica Publications: Post Falls, ID, 2001; p 145.
29. Tetryl. *Encyclopedia of Explosives and Related Items*; Picatinny Arsenal: New Jersey, 1980; p T165.
30. Michler, W.; Meyer, K. *Ber.* **1879**, *12*, 1791–1793.
31. Triaminotrinitrobenzene. *Encyclopedia of Explosives and Related Items*; Picatinny Arsenal: New Jersey, 1980; pp T34–35.
32. Akopyan, Z.A.; Struchkov, Yu.T.; Dashevskii, V.G. *Zh. Strukt. Khim.* **1966**, *7*, 408.
33. Nielsen, A.T.; Atkins, R.L.; Norris, W.P. *J. Org. Chem.* **1979**, *44*, 1181–1182.
34. Nielsen, A.T. *Nitrocarbons*; VCH: New York, 1995; p 97.
35. Zhang, M.; Eaton, P.E.; Gilardi, R. *Angew. Chem. Int. Ed.* **2000**, *39*, 401–404.
36. Nielsen, A.T. *Nitrocarbons*; VCH: New York, 1995; pp 71–72, 118.
37. Liang, P. *Organic Syntheses Collective Vol. III*, **1955**, 803–805.
38. Tetranitromethane. *Encyclopedia of Explosives and Related Items*; Picatinny Arsenal: New Jersey, 1978; pp M83–M85.
39. Schischkoff, L. *Ann.* **1861**, *119*, 247–248.
40. Palmer, W.G.; Small, M.J.; Dacre, J.C.; Eaton, J.C. Toxicology and Environmental Hazards. In *Organic Energetic Compounds*; Nova Science Publishers: Commack, NY, 1996; pp 307–311.
41. Gilardi, R.D.; Koale *J. Chemistry of Energetic Materials*; Academic Press: San Diego, 1991; p 2.
42. Eaton, P.E.; Zhang, M.; Gilardi, R.; Gelber, N.; Iyer, S.; Surapaneni, R. *Prop., Expl., Pyro.* **2002**, *27*, 1–6.
43. Eaton, P.E.; Gilardi, R.L.; Zhang, M. *Adv. Mater.* **2000**, *12*, 1143–1148.
44. Eaton, P.E.; Xiong, Y.; Gilardi, R. *J. Am. Chem. Soc.* **1993**, *115*, 10195–10202.
45. Eaton, P.E.; Xiong, Y.; Zhou, J.P. *J. Org. Chem.* **1992**, *57*, 4277–4281.
46. Urbanski, T. *Chemistry and Technology of Explosives*, Academic Press: New York, 1964; Vol. 3; p 13.
47. Henning, G.F. Verfahren zur Darstellung eines Nitrokörpers aus Hexamethylentetramin. German Patent 104,280, June 14, 1899.
48. Composition C4. *Encyclopedia of Explosives and Related Items*; Picatinny Arsenal: New Jersey, 1966; Vol. 3; p C485.
49. VonHerz, E. Explosive. U.S. Patent 1,402,693, October 3, 1922.
50. VonHerz, E. Improvements relating to Explosives. British Patent 145,791, July 2, 1920.
51. Davis, T.L. *The Chemistry of Powder and Explosives*; Angriff Press: Las Vegas, 1943; p 369.
52. Simpson, R.L.; Urtiew, P.A.; Ornellas, D.L.; Moody, G.L.; Scribner, K.J.; Hoffman, D.M. *Prop., Expl. Pyro.* **1997**, *22*, 249–255.
53. Nielsen, A.T.; Chafin, A.P.; Christian, S.L.; Moore, D.W.; Nadler, M.P.; Nissan, R.A.; Vanderah, D.J. *Tetrahedron* **1998**, *54*, 11793–11812.

54. Griffin, T.S.; Baum, K. *J. Org. Chem.* **1980**, *45*, 2880–2883.
55. Baum, K. *Chemistry of Polynitroethane Derivatives*; ADA249264; DTIC: Research Triangle Park, NC, 1992.
56. Baum, K.; Tzeng, D. *J. Org. Chem.* **1985**, *50*, 2736–2739.
57. Baum, K.; Bigelow, S.S.; Tzeng, D.; Archibald, T.C. *Chemistry of Polynitroethane Derivatives*; ADA197044; DTIC: Research Triangle Park, NC, 1988.
58. Marshall, H.P.; Borgardt, F.G.; Noble, P. *J. Phys. Chem.* **1968**, *72*, 1513–1516.
59. Baum, K.; Bigelow, S.S.; Nguyen, N.V.; Archibald, T.G.; Gilardi, R.; Flippen–Anderson, J.L.; George, C. *J. Org. Chem.* **1992**, *57*, 235–241.
60. Baum, K.; Archibald, T.G.; Tzeng, D.; Gilardi, R.; Flippen–Andersen, J.L.; George, C. *J. Org. Chem.* **1991**, *56*, 537–539.
61. Latypov, N.V.; Bergman, J.; Langlet, A.; Wellmar, U.; Bemm, U. *Tetrahedron* **1998**, *54*, 11525–11536.
62. Tzeng, D.; Baum, K. *J. Org. Chem.* **1983**, *48*, 5384–5385.
63. Nielsen, A.T. *Nitrocarbons*; VCH: New York, 1995; pp 87–91.
64. Baum, K.; Griffin, T.S. *J. Org. Chem.* **1981**, *46*, 4811–4813.
65. Jäger, V.; Viehe, H.G. *Angew. Chem. Int. Ed.* **1969**, *8*, 273–274.
66. Viehe, H. G.; Jäger, V.; Compernolle, F. *Angew. Chem. Int. Ed.* **1969**, *8*, 979.
67. Krüerke, U.; Hübel, W. *Chem. Ber.* **1961**, *94*, 2829–2856.
68. Jäger, V.; Viehe, H.G. *Angew. Chem. Int. Ed.* **1970**, *9*, 795–796.
69. Schmitt, R.J.; Krempp, M.; Bierbaum, V.M. *Int. J. Mass Spec. and Ion Processes* **1992**, *117*, 621–632.
70. Gibson, S.E.; Stevenazzi, A. *Angew. Chem. Int. Ed.* **2003**, *42*, 1800–1810.
71. Berthelot, M. *Compt. Rend. Acad. Sci.* **1866**, *62*, 905–910.
72. Reppe, W.; Schlichting, O.; Klager, K.; Toepel, T. *Ann.* **1948**, *560*, 1–92.
73. Bowden, F.L.; Lever, A.B.P. *Organomet. Chem. Rev.* **1968**, *3*, 227–279.
74. Sekiguchi, A.; Tanaka, M.; Matsuo, T.; Watanabe, H. *Angew. Chem. Int. Ed.* **2001**, *40*, 1675–1677.
75. Rausch, M.D.; Higbie, F.A.; Westover, G.F.; Clearfidld, A.; Gopal, R.; Troup, J.M.; Bernal, I. *J. Organomet. Chem.* **1978**, *149*, 245–264.
76. Ville, G.A.; Vollhardt, K.P.C.; Winter, M.J. *Organometallics* **1984**, *3*, 1177–1187.
77. Gleiter, R.; Werz, D. *Organometallics* **2005**, *24*, 4316–4329.
78. Katritzky, A.R.; Zhang, Y.; Singh, S.K. *Heterocycles* **2003**, *60*, 1225–1239.
79. Baryshnikov, A.T.; Erashko, V.I.; Zubanova, N.I.; Ugrak, B.I.; Shevelev, S.A.; Fainzilberg, A.A.; Semenov, V.V. *Izv. Akad. Nauk, Ser. Khim.* **1992**, *9*, 2123–2131.
80. Vereshchagin, L.I.; Tikhonova, L.G.; Maksikova, A.V.; Serebryakova, E.S.; Proidakov, A.G.; Filippova, T.M. *Z. Org. Khim.* **1980**, *16*, 730–738.
81. Bottaro, J.; Schmitt. R.; Bedford, C.; Gilardi, R.; George, C. *J. Org. Chem.* **1990**, *55*, 1916–1919.
82. Pelosi, L.F.; Miller, W.T. *J. Am. Chem. Soc.* **1976**, *98*, 4311–4312.
83. Miller, W.T.; Hummel, R.J.; Pelosi, L.F. *J. Am. Chem. Soc.* **1973**, *95*, 6850–6851.
84. Nielsen, A.T. *Nitrocarbons*; VCH: New York, 1995; p 103.

85. Dewar, M.J.S.; Ritchie, J.P.; Alster *J. J. Org. Chem.* **1985**, *50*, 1031–1036.
86. Dewar, M.J.S. *Dinitroacetylene and Related Compounds*; ADA128954; DTIC: Research Triangle Park, NC, 1983.
87. Stevens, T.E.; Emmons, W.D. *J. Am. Chem. Soc.* **1958**, *80*, 338–341.
88. Baschieri, D.A. *Gazz. Chim. Ital.* **1901**, *31*, 461–472.
89. Venugopal, M.; Srinivasulu, D.; Shechter, H. *Synthesis of 1,2,3,4-Tetrazines, 1,2,3,4-Tetrazine Di-N-oxides, Pentazole Derivatives, Pentazine Poly-N-oxides, and Nitroacetylenes*; ADA430332; DTIC: Research Traingle Park, NC, 2004.
90. Woltermann, C.J. Studies of Syntheses of Mono- and Dinitroacetylenes, Acetylenic Nitrities and Nitrosoketenes. Ph.D. Dissertation, The Ohio State University, Columbus, OH, 1996.
91. Politzer, P.; Lane, P.; Weiner, J.J.M. *Cyclooligomerizations as Possible Routes to Cubane–like Systems*; ADA364287; DTIC: Research Triangle Park, NC, 1999.
92. Politzer, P.; Lane, P.; Sjoberg, P.; Grice, M.E.; Shechter, H. *Struct. Chem.* **1995**, *6*, 217–223.
93. Politzer, P.; Bar–Adon, R. *J. Am. Chem. Soc.* **1987**, *109*, 3529–3534.
94. Crabtree, R.H. *The Organometallic Chemistry of the Transition Metals*, 4th Ed.; Wiley: Hoboken, 2005; pp 14–16.
95. Happ, B.; Bartik, T.; Zucchi, C.; Rossi, M. C.; Ghelfi, F.; Palyi, G.; Varadi, G.; Szalontai, G.; Horvath, I. T.; Chiesi–Villa, A.; Guastini, C. *Organometallics* **1995**, *14*, 809–819.
98. Seyferth, D.; White, D.L. *J. Organomet. Chem.* **1971**, *32*, 317–322.
96. Cetini, G.; Gambino, O.; Rossetti, R.; Sappa, E. *J. Organomet. Chem.* **1967**, *8*, 149–154.
99. Magnus, P.; Becker, D. P. *J. Chem. Soc. Chem. Commun.* **1985**, 640–642.
97. Nicholas, K.M.; Pettit, R. *Tetrahedron Lett.* **1971**, *12*, 3475–3478.
100. Schottelius, M.J.; Chen, P. *Helv. Chim. Acta* **1998**, *81*, 2341–2347.
101. Gibson, S.; Mainolfi, N. *Angew. Chem. Int. Ed.* **2005**, *44*, 3022–3037.
102. Houk, K. N.; Gandour, R. W.; Strozier, R. W.; Rondan, N. G.; Paquette, L. A. *J. Am. Chem. Soc.*, **1979**, *101*, 6797–6802.
103. Bach, R. D.; Wolber, G. J.; Schlegel, H. B. *J. Am. Chem. Soc.* **1985**, *107*, 2837–2841.
104. Jäger, V. Nitroacetylenes. Ph.D. Dissertation, Friedrich-Alexander-Universität, Nürnberg, 1970.
105. Laszlo, P.; Schleyer, P.R. *J. Am. Chem. Soc.* **1963**, *85*, 2709–2712.
106. Walsh, A.D. *Disc. Farad. Soc.* **1947**, *2*, 18–25.
107. Zhang, M.; Eaton, P.E.; Steele, I.; Gilardi, R. *Synthesis* **2002**, *14*, 2013–2018.
108. Schmitt, R.J.; Bedford, C.D. *Synthesis* **1986**, 132–133.
109. Schmitt, R. J.; Bottaro, J.C.; Malhotra, R.; Bedford, C.D. *J. Org. Chem.* **1987**, *52*, 2294–2297.
110. Schmitt, R.J.; Bottaro, J.C. *New Nitration Concepts*; ADA187518; DTIC: Research Triangle Park, NC, 1987.
111. Jäger, V.; Motte, J.; Viehe, H. G. *Chimia* **1975**, *29*, 516–517.
112. Jäger, V.; Viehe, H.G. Process for Producing Nitroacetylenes. U.S. Patent 3,626,013, December 7, 1971.
113. Braude, E.A.; Jones, E.R.H.; Rose, G.G. *J. Chem. Soc.* **1947**, 1104.

114. Kashin, A.N.; Bumagin, N.A.; Bessonova, M.P.; Beletskaya, I.P.; Reutov, O.A. *J. Org. Chem. USSR* **1980**, *16*, 1153–1159.
115. Eaton, P.E.; Zhang, M. unpublished results.
116. Motte, J.; Viehe, H. G. *Chimia* **1975**, *29*, 515–516.
117. Rall, K.B.; Vil'avskaya, A.I.; Petrov, A.A. Russ. *Chem. Rev.* **1975**, *44*, 373–379.
118. Petrov, A.A.; Zavgorodnii, V.S.; Rall, K.B.; Vil'davskaya, A.I.; Bogoradovskii, E.T. *Z. Obshc. Khim.* **1978**, *48*, 943–944.
119. Petrov, A.A.; Zavgorodnii, V.S.; Rall, K.B.; Vil'davskaya, A.I.; Bogoradovskii, E.T. Nitroacetylenes. Russian Patent SU401136, March 6, 1978.
120. Kuznetsova, O.V.; Egorochkin, A.N.; Mushtina, T.G.; Bogoradovskii, E.T. *Russ. J. Gen. Chem.* **2004**, *74*, 384–392.
121. Lin–Vien, D., Colthup, N.B.; Fateley, W.G.; Grasselli, J.G. *The Handbook of Infrared and Raman Characteristic Frequencies of Organic Molecules*; Academic Press: Boston, 1991; pp 179–189.
122. Bellamy, L.J. *Advances in Infrared Group Frequencies*, 1st Ed.; Meuthen and Co.: Suffolk, 1968; Col. 2; pp 229–232.
123. Bellamy, L.J. *The Infrared Spectra of Complex Molecules*, 3rd Ed.; Chapman and Hall: London, 1975; pp 79–81.
124. Windler, G.K. Nitroacetylenes Harnessed by Cobalt. Ph.D. Dissertation, University of California - Berkeley, Berkeley, 2011.
125. Yamabe, K.; Yasutake, A. *Sasebo Kogyo Koto Senmon Gakko Kenkyu Hokoku* **1979**, *16*, 63–64.
126. Gross, J.H. *Mass Spectrometry*; Springer: Berlin, 2004; pp 247, 308–310.
127. Becker, E.D. *High Resolution NMR*; Academic Press: New York, 1980; p 192.
128. Harris, R.K. *Nuclear Magnetic Resonance Spectroscopy A Physicochemical View;* Pitman: London, 1983; pp 130–137.
129. Acetylene. *Encyclopedia of Explosives and Related Items*; Picatinny Arsenal: New Jersey, 1960; Vol. 1; p A67.
130. Clark, H.G.; Plummer, C.W.; Hoffman, S.A. The Preparation of Polynitro Derivatives of Methane. U.S. Patent 3,067,261, December 4, 1962.
131. Krauz, C.; Stepanek *J. Chem. Abstr.* **1936**, *30*, 3403.
132. Mager, H. *Chem. Abstr.* **1961**, *55*, 2484.
133. Wieland, H. *Ann.* **1903**, *328*, 154–255.
134. Novikov, S.S.; Belikov, V.M.; Dem'yaneko, V.F.; Lapshina, L.V. *Russ. Chem. Bull.* **1960**, *9*, 1200–1202.
135. Robson, E.; Tedder, J.M.; Woodcock, D.J. *J. Chem. Soc. (C)* **1968**, 1324–1328.
136. Woltermann, C.J.; Shechter, H. *Helv. Chim. Acta* **2005**, *88*, 354–369.
137. Loevenich, J.; Koch, J.; Pucknat, U. *Ber.* **1930**, *63*, 636–646.
138. Loevenich, J.; Gerber, H. *Ber.* **1930**, *63*, 1707–1713.
139. Viehe, H.G.; Merényi, R.; Oth, J.F.M; Valange, P. *Angew. Chem. Int. Ed.* **1964**, *3*, 746.
140. Gais, H.J.; Hafner, K.; Neuenschwander, M. *Helv. Chim. Acta* **1969**, *52*, 2641–2657.
141. Stang, P.J. *Russ. Chem. Bull.* **1993**, *42*, 12–23.

142. Olah, G.A.; Malhotra, R.; Narang, S.C. *Nitration Methods and Mechanisms*; VCH: New York, 1989; p 243.
143. Tani, K.; Lukin, K.; Eaton, P.E. *J. Am. Chem. Soc.* **1997**, *119*, 1476–1477.
144. Ciaccio, L.L.; Marcus, R.A. *J. Am. Chem. Soc.* **1962**, *84*, 1838–1841.
145. Olah, G.A. personal communication.
146. Shechter, H.; Venugopal, M.; Srinivasulu, D. Syntheses of 1,2,3,4-Tetrazine Di-N-oxides, Pentazole Derivatives, Pentazine Poly-N-oxides, and Nitroacetylenes. ADA445136; DTIC: Research Triangle Park, NC, 2004.
147. Nguyen, N.V.; Baum, K. *Tetrahedron Lett.* **1992**, *33*, 2949–2952.
148. Diels, O.; Alder, K. *Ber.* **1929**, *62*, 2337–2372.
149. Wittig, G.; Mayer, U. *Chem. Ber.* **1963**, *96*, 342–348.
150. Weis, C.D. *J. Org. Chem.* **1962**, *27*, 3520–3524.
151. Nielsen, A.T. *Nitrocarbons*; VCH: New York, 1995; pp 104–105.
152. Chung, Y.; Duerr, B.F.; McKelvey, T.A.; Nanjappan, P.; Czarnik, A.W. *J. Org. Chem.* **1989**, *54*, 1018–1032.
153. Grundmann, C.; Mini, V.; Dean, J.M.; Frommeld, H. *Ann.* **1965**, *687*, 191–214.
154. Zhang, M. personal communication.
155. Viehe, H.G. *Angew. Chem. Int. Ed.* **1965**, *4*, 746–751.
156. Glaser, C. *Ber.* **1869**, *2*, 422–424.
157. Dvorko,G.F. *Chem Abstr.* **1960**, *54*, 2162c.
158. Gompper, R.; Seybold, G. *Angew. Chem. Int. Ed.* **1968**, *7*, 824–826.
159. Ghosez, L.; Haveaux, B.; Viehe, H.G. *Angew. Chem. Int. Ed.* **1969**, *8*, 454–455.
160. Neuenschwander, M.; Niederhauser, A. *Chimia*, **1968**, *22*, 491–492.
161. Breslow, R.; Kivelevich, D.; Mitchell, M.J.; Fabian, W.; Wendel, K. *J. Am. Chem. Soc.* **1965**, *87*, 5132–5139.
162. Battaglia, A.; Dondoni, A. *Tetrahedron Lett.* **1970**, 1221–1224.
163. Morrocchi, S.; Ricca, A.; Zanarotti, A.; Bianchi, G.; Gandolfi, R.; Grunanger, P. *Tetrahedron Lett.* **1969**, 3329–3332.
164. Christl, M.; Huisgen, R. *Tetrahedron Lett.* **1968**, 5209–5213.
165. Denmark, S.E.; Thorarensen, A. *Chem. Rev.* **1996**, *96*, 137–166.
166. Fang, Y.; Liu, L.; Feng, Y.; Li, X.; Guo, Q. *J. Phys. Chem. A* **2002**, *106*, 4669–4678.
167. Tomonari, M.; Ookubo, N.; Takada, T. *Syn. Met.* **1996**, *81*, 137–142.
168. Xia, Y.; Li, Y.; Li, W. *J. Organomet. Chem.* **2008**, *693*, 3722–3728.
169. Prall, M.; Wittkopp, A.; Fokin, A.A.; Schreiner, P.R. *J. Comp. Chem.* **2001**, *22*, 1605–1614.
170. Musch, P.W.; Remenyi, C.; Helten, H.; Engels, B. *J. Am. Chem. Soc.* **2002**, *124*, 1823–1828.
171. Tomonari, M.; Ookubo, N.; Takada, T. *Chem. Phys. Lett.* **1997**, *266*, 488–498.
172. Weimer, M.; Hieringer, W.; Sala, F.D.; Görling, A. *Chem. Phys.* **2005**, *309*, 77–87.
173. Giuffreda, M.G.; Bruschi, M.; Lüthi, H.P. *Chem. Eur. J.* **2004**, *10*, 5671–5680.
174. Kuznetsova, O.V.; Egorochkin, A.N. *Russ. Chem. Bull., Int. Ed.* **2006**, *55*, 624–631.
175. Prochnow, E.; Zuer, A.A.; Banert, K. *J. Phys. Chem. A* **2007**, *111*, 9945–9951.

176. Jakt, M.; Johannissen, L.; Rzepa, H.S.; Widdowson, D.A.; Wilhelm, R. *J. Chem. Soc., Perkins Trans. 2* **2002**, 576–581.
177. Vianello, R.; Peran, N.; Maksic, Z.B. *J. Phys. Chem. A* **2006**, *110*, 12870–12881.
178. Golovin, A.V.; Takhistov, V.V. *J. Mol. Struct.* **2004**, *701*, 57–91.
179. Mulliken, R.S.; Rieke, C.A.; Brown, W.G. *J. Am. Chem. Soc.* **1941**, *63*, 41–56.
180. Vijayakumar, S.; Kolandaivel, P. *J. Mol. Struct. (Theochem)* **2006**, *770*, 23–30.
181. Jursic, B.S. *J. Mol. Struct. (Theochem)* **1999**, *459*, 215–220.
182. Walton, D.R.M.; Webb, M.J. *J. Organomet. Chem.* **1972**, *37*, 41–43.
183. Amatore, C.; Blart, E.; Genêt, J.P.; Jutand, A.; Lemaire–Audoire, S.; Savignac, M. *J. Org. Chem.* **1995**, *60*, 6829–6839.
184. Olah, G.A.; Malhotra, R.; Narang, S.C. *Nitration Methods and Mechanisms*; VCH: New York, 1989; p 60.
185. Iwashita, Y.; Ishikawa, A.; Kainosho, M. *Spectrochim. Acta A* **1971**, *27*, 271–277.
186. Bellamy, L.J. *The Infrared Spectra of Complex Molecules*, 3rd Ed.; Chapman and Hall: London, 1975; pp 37–60.
187. Lin–Vien, D., The Handbook of Infrared and Raman Characteristic Frequencies of Organic Molecules, Academic Press: Boston, 1991, 10–11, 255–258.
188. Bellamy, L.J. *The Infrared Spectra of Complex Molecules*, 3rd Ed.; Chapman and Hall: London, 1975; pp 375–383.
189. Bellamy, L.J. *The Infrared Spectra of Complex Molecules*, 3rd Ed.; Chapman and Hall: London, 1975; pp 331–337.
190. *LLNL Explosives Handbook*; Lawrence Livermore National Laboratory: Livermore, CA; p 9-4.
191. King, W.D.; Barnes, C.E.; Orvis, J.A. *Organometallics* **1997**, *16*, 2152–2159.
192. Solà, J.; Riera, A.; Verdaguer, X.; Maestro, M.A. *Organometallics* **2006**, *25*, 5795–5799.
193. Sternberg, H.W.; Greenfield, H.; Friedel, R.A.; Wotiz, J.; Markby, R.; Wender, I. *J. Am. Chem. Soc.* **1954**, *76*, 1457–1458.
194. Bennett, M.A.; Schwemlein, H.P. *Angew. Chem. Int. Ed., Engl.* **1989**, *28*, 1296–1320.
195. Bor, G.; Kettle, S.F.A.; Stanghellini, P.L. *Inorg. Chim. Acta* **1976**, *18*, L18–L20.
196. Medina, R.M.; Moreno, C.; Marcos, M.L.; Castro, J.A.; Benito, F.; Arnanz, A.; Delgado, S.; Gonzalez–Velasco, J.; Macazaga, M.J. *Inorg. Chim. Acta* **2004**, *357*, 2069–2080.
197. Varadi, G.; Palyi, G. *Inorg. Chim. Acta.* **1976**, *20*, L33–L34.
198. Dickson, R.S.; Fraser, P.J. *Adv. Organomet. Chem.* **1974**, *12*, 323–377.
199. Ungváry, F.; Marko, L. *Inorg. Chim. Acta* **1970**, *4*, 324–326.
200. Bor, G.; Dietler, U.K. *J. Organomet. Chem.* **1980**, *191*, 295–302.
201. Aime, S.; Milone, L.; Rossetti, R.; Stanghellini, P.L. *Inorg. Chim. Acta* **1977**, *22*, 135–139.
202. Pepermans, H.; Willem, R.; Hoogzand, C. *Bull. Soc. Chim. Belg.* **1987**, *96*, 563–574.
203. Dickson, R.S.; Yawney, D.B.W. *Aust. J. Chem.* **1968**, *21*, 1077–1080.
204. Dickson, R.S.; Yawney, D.B.W. *Aust. J. Chem.* **1968**, *21*, 97–102.

205. Birchall, J.M.; Bowden, F.L.; Haszeldine, R.N.; Lever, A.B.P. *J. Chem. Soc. (A)* **1967**, 747–753.
206. Dickson, R.S.; Kirsch, H.P. *Aust. J. Chem.* **1972**, *25*, 1815–1818.
207. Meyer, A.; Bigorgne, M. *Organometallics* **1984**, *3*, 1112–1118.
208. Iwashita, Y.; Tamura, F.; Nakamura, A. *Inorg. Chem.* **1969**, *8*, 1179–1183.
209. Iwashita, Y. *Inorg. Chem.* **1970**, *9*, 1178–1182.
210. Dickson, R.S.; Yawney, D.B.W. *Inorg. Nucl. Chem. Lett.* **1967**, *3*, 209–214.
211. Dickson, R.S.; Yawney, D.B.W. *Aust. J. Chem.* **1967**, *20*, 77–84.
212. Vollhardt, K.P.C.; Schore, N.E. *Organic Chemistry: Structure and Function*, 4th Ed.; W.H. Freeman: New York, 2003, p 411.
213. Pauling, L. *General Chemistry*; Dover: Mineola, NY, 1970; pp 161–164.
214. Hoffman, D.M.; Hoffman, R.; Fisel, C.R. *J. Am. Chem. Soc.* **1982**, *104*, 3858–3875.
215. Zumdahl, S.S. *Chemical Principles*, 1st Ed.; Heath: Lexington, MA, 1992; pp 602–605.
216. Cotton, F.A.; Jamerson, J.D.; Stults, B.R. *J. Am. Chem. Soc.* **1976**, *98*, 1774–1779.
217. Gregson, D.; Howard, J.A. *Acta Crystallogr., Sect. C: Cryst. Struct. Commun.* **1983**, *39*, 1027–1027.
218. Zirngast, M.; Marschner, C.; Baumgartner *J. Organometallics* **2006**, *25*, 4897–4908.
219. Deschamps, N.M.; Kaldis, J.H.; Lock, P.E.; Britten, J.F.; McGlinchey, M.J. *J. Org. Chem.* **2001**, *66*, 8585–8591.
220. Low, P.J.; Udachin, K.A.; Enright, G.D.; Carty, A.J. *J. Organomet. Chem.* **1999**, *578*, 103–114.
221. Werz, D.B.; Schulte, J.H.; Rausch, B.J.; Gleiter, R.; Rominger, F. *Eur. J. Inorg. Chem.* **2004**, 2585–2593.
222. Clarke, L.P.; Davies, J.E.; Raithby, P.R.; Rennie, M.; Shields, G.P.; Sparr, E. *J. Organomet. Chem.* **2000**, *609*, 169–176.
223. Berenbaum, A.; Ginzburg–Margau, M.; Coombs, N.; Lough, A.J.; Safa–Sefat, A.; Greedan, J.E.; Ozin, G.A.; Manners, I. *Adv. Mater.* **2003**, *15*, 51–55.
224. Chan, W.Y.; Berenbaum, A.; Clendenning, S.B.; Lough, A.J.; Manners, I. *Organometallics* **2003**, *22*, 3796–3808.
225. Dunn, J.A.; Harrington, L.E.; McGlinchey, M.J. *J. Organomet. Chem.* **2004**, *689*, 8–13.
226. Zhang, L.; Jones, R.A.; Lynch, V.M. *Chem. Commun.* **2002**, 2986–2987.
227. Draper, S.M.; Delamesiere, M.; Champeil, E.; Twamley, B.; Byrne, J.J.; Long, C. *J. Organomet. Chem.* **1999**, *589*, 157–167.
228. Kuhnen, T.; Stradiotto, M.; Ruffolo, R.; Ulbrich, D.; McGlinchey, M.J.; Brook, M.A. *Organometallics* **1997**, *16*, 5048–5057.
229. Stradiotto, M.; Brook, M.A.; McGlinchey, M.J. *Inorg. Chem. Commun.* **1998**, *1*, 105–108.
230. Hong, F.; Liaw, J.; Chien, B.; Chang, Y.; Lin, C.; Wang, S.; Liao, F. *Polyhedron* **1999**, *18*, 2737–2747.
231. Delgado, E.; Alcalde, M.I.; Donnadieu, B.; Hernandez, E.; Sanchez–Nieves, J. *Acta Crystallogr., Sect. E: Struct Rep. Online* **2003**, *59*, m207–m209.

232. Back, S.; Gossage, R.A.; Lutz, M.; del Río, I.; Spek, A.L.; Lang, H.; van Koten, G. *Organometallics* **2000**, *19*, 3296–3304.
233. Brook, M.A.; Ramacher, B.; Dallaire, C.; Gupta, H.K.; Ulbrich, D.; Ruffolo, R., *Inorg. Chim. Acta* **1996**, *250*, 49–57.
234. Baert, F.; Guelzim, A. *Acta Crystallogr., Sect. B: Struct. Sci.* **1984**, *40*, 590–595.
235. Henkel, T.; Klauck, A.; Seppelt, K. *J. Organomet. Chem.* **1995**, *501*, 1–6.
236. Calvo–Perez, V.; Vega, A.; Cortes, P.; Spodine, E. *Inorg. Chim. Acta* **2002**, *333*, 15–24.
237. Arewgoda, M.; Rieger, P.H.; Robinson, B.H.; Simpson, J.; Visco, S.J. *J. Am. Chem. Soc.* **1982**, *104*, 5633–5640.
238. Osella, D.; Fiedler, J. *Organometallics* **1992**, *11*, 3875–3878.
239. Osella, D.; Stein, E.; Jaouen, G.; Zanello, P. *J. Organomet. Chem.* **1991**, *401*, 37–47.
240. Duffy, N.; McAdam, J.; Nervi, C.; Osella, D.; Ravera, M.; Robinson, B.; Simpson, J. *Inorg. Chim. Acta* **1996**, *247*, 99–104.
241. Dosa, P.I.; Erben, C.; Iyer, V.S.; Vollhardt, K.P.C.; Wasser, I.M. *J. Am. Chem. Soc.* **1999**, *121*, 10430–10431.
242. Murray, R.W.; Rajadhyaksha, S.N.; Mohan, L. *J. Org. Chem.* **1989**, *54*, 5783–5788.
243. Eaton, P.E.; Wicks, G.E. *J. Org. Chem.* **1988**, *53*, 5353–5355.
244. Díaz, D.; Betancort, J.M.; Martín, V.S. *Synlett* **2007**, 343–359.
245. vanBaar, B.; Koch, W.; Lebrilla, C.; Terlouw, J.K.; Weiske, T.; Schwarz, H. *Angew. Chem. Int. Ed., Engl.* **1986**, *25*, 827–828.
246. Saggiomo, A.J. *J. Org. Chem.* **1957**, *22*, 1171–1175.
247. Baumgarten, H.E.; Smith, H.L.; Staklis, A. *J. Org. Chem.* **1975**, *40*, 3554–3561.
248. Moureu, C.; Bongrand, J.C. *Ann. Chim.* **1920**, *14*, 9.
249. Eaton, P.E.; Shankar, B.K.R.; Price, G.D.; Pluth, J.J.; Gilbert, E.E.; Alster, J.; Sandus, O. *J. Org. Chem.* **1984**, *49*, 185–186.
250. Banthorpe, D.V. Rearrangements Involving Azide Groups. In *The Chemistry of the Azido Group*; Patai, S., Ed.; Wiley: New York, 1971; p 397.
251. Scriven, E.F.V.; Turnbull, K. *Chem. Rev.* **1988**, *88*, 297–368.
252. Diels, O.; Thiele, W.E. *Ber.* **1938**, *71*, 1173–1178.
253. Sugihara, T.; Yamaguchi, M.; Nishizawa, M. *Rev. Heteroat. Chem.* **1999**, *21*, 179–194.
254. Morrison, R.T.; Boyd, R.N. *Organic Chemistry*, 3rd Ed.; Allyn and Bacon: Boston, 1973, p 374.
255. Maier, G.; Jung, W.A. *Chem. Ber.* **1982**, *115*, 804–807.
256. Fan, Y.L. *Macromolecules* **1977**, *10*, 469–473.
257. Frazer, A.H.; Wallenberger, F.T. *J. Polymer Sci. A* **1964**, *2*, 1137–1145.
258. Hamciuc, E.; Bruma, M.; Köpnick, T.; Kaminorz, Y.; Schulz, B. *Polymer* **2001**, *45*, 1809–1815.
259. Mikroyannidis, J.A.; Hlídkova, H.; Vyprachticky, D.; Cimrová, V. *J. Polymer Chem. A* **2005**, *43*, 3079–3090.
260. Patterson, J.M.; Braun, L.L.; Haidar, N.F.; Smith, W.T. *J. Org. Chem.* **1978**, *43*, 3039–3041.

261. Melikyan, G.G.; Mkrtchyan, V.M.; Atanesyan, K.A.; Azaryan, G.Kh.; Badanyan, Sh.O. *Russ. J. Bioorg. Chem.* 1990, *16*, 565–566.
262. Nicholas, K.M.; Pettit, R. *J. Organomet. Chem.* **1972**, *44*, C21–C24.
263. Olah, G.A.; Malhotra, R.; Narang, S.C. *Nitration Methods and Mechanisms*; VCH: New York, 1989; pp 80–83, 241–243, 265–266.
264. Olah, G.A.; Malhotra, R.; Narang, S.C. *Nitration Methods and Mechanisms*; VCH: New York, 1989; p 68.
265. Corey, E.J.; Estreicher, H. *Tetrahedron Lett.* **1980**, *21*, 1113–1116.
266. Tanaka, S.; Tsukiyama, T.; Isobe, M. *Tetrahedron Lett.* **1993**, *34*, 5757–5760.
267. Olah, G.A.; Malhotra, R.; Narang, S.C. *Nitration Methods and Mechanisms*; VCH: New York, 1989; pp 37–38.
268. Lo Sterzo, C.; Stille, J.K. *Organometallics* **1990**, *9*, 687–694.
269. Cummins, C.H. *Tetrahedron Lett.* **1994**, *35*, 857–860.
270. Prakash, G.K.S.; Mathew, T. *Angew. Chem. Int. Ed.* **2010**, *49*, 1726–1728.
271. Kornblum, N.; Lichtin, N.N.; Patton, J.T.; Iffland, D.C. *J. Am. Chem. Soc.* **1947**, *69*, 307–313.
272. Kornblum, N.; Smiley, R.A.; Blackwood, R.K.; Iffland, D.C. *J. Am. Chem. Soc.* **1955**, *77*, 6269–6280.
273. Meyer, V.; Stüber, O. *Chem. Ber.* **1872**, *5*, 203–205.
274. Meyer, V.; Stüber, O. *Chem. Ber.* **1872**, *5*, 399–406.
275. Meyer, V.; Stüber, O. *Chem. Ber.* **1872**, *5*, 514–518.
276. Meyer, V.; Chojnacki, C. *Chem. Ber.* **1872**, *5*, 1034–1038.
277. Meyer, V. *Ann. Chem.* **1874**, *171*, 1.
278. Olah, G.A.; Malhotra, R.; Narang, S.C. *Nitration Methods and Mechanisms*; VCH: New York, 1989; pp 96–97.
279. Denmark, S.E.; Wang, Z. *Org. Syn.* **2005**, *81*, 42–46.
280. Webb, J.A.; Klijn, J.E.; Hill, P.A.; Bennett, J.L.; Goroff, N.S. *J. Org. Chem.* **2004**, *69*, 660–664.
281. Cullen, W.R.; Leeder, W.R. *Inorg. Chem.* **1966**, *5*, 1004–1008.
282. Haszeldine, R.N.; Leedham, K. *J. Chem. Soc.,* **1954**, 1261–1264.
283. Finnegan, W.G.; Norris, W.P. *J. Org. Chem.* **1963**, *28*, 1139–1140.
284. Chung, M.; Sakurai, A.; Akita, M.; Moro-oka, Y. *Organometallics* **1999**, *18*, 4684–4691.
285. Bradley, D.H.; Khan, M.A.; Nicholas, K.M. *Organometallics* **1989**, *8*, 554–556.
286. Dellaca, R.J.; Penfold, B.R.; Robinson, B.H.; Robinson, W.T.; Spencer, J.L. *Inorg. Chem.* **1970**, *9*, 2197–2203.
287. Carriedo, G.A.; Riera, V.; Miguel, D.; Lanfredi, A.M.M.; Tiripicchio, A. *J. Organomet. Chem.* **1984**, *272*, C17–C20.
288. Akita, M.; Terada, M.; Moro-oka, Y. *Organometallics* **1992**, *11*, 1825–1830.
289. Keller, H.; Daran, J.C.; Lang, H. *J. Organomet. Chem.* **1994**, *482*, 63–66.
290. Wadepohl, H.; Wolf, A.; Pritzkow, H. *J. Organomet. Chem.* **1996**, *506*, 287–292.
291. Cheng, M.; Shu, H.; Lee, G.; Peng, S.; Liu, R. *Organometallics* **1993**, *12*, 108–115.

292. Standard Test Method for Thermally Unstable Materials Using Differential Scanning Calorimetry and the Flynn/Wall/Ozawa Method. E 698–05, ASTM: West Conshohocken, PA, 2006.
293. Freeman, E.S.; Carroll, B. *J. Phys. Chem.* **1958**, *62*, 394–397.
294. Torfs, J.C.M.; Deij, L.; Dorrepaal, A.J.; Heijens, J.C. *Anal. Chem.* **1984**, *56*, 2863–2867.
295. Lowry, T.H.; Richardson, K.S. *Mechanism and Theory in Organic Chemistry*, 3rd Ed.; Harper Collins: New York, 1987; p 519.
296. Rim, C.; Son, D.Y. *Arch. Org. Chem.* **2006**, 265–291.
297. Yoo, S.; Lee, S. *Synlett* **1990**, 419–420.
298. Nystrom, R.F.; Brown, W.G. *J. Am. Chem. Soc.* **1948**, *70*, 3738–3740.
299. Zachwieja, U.; Preut, H.; Mitchell, T.; Zavgorodnii, V.S.; Golosovskii, A.V.; Karpov, M.G. *Acta Crystallogr.* **2001**, *E57*, m533–m534.
300. Chia, L.S.; Cullen, W.R.; Franklin, M.; Manning, A.R. *Inorg. Chem.* **1975**, *14*, 2521–2526.
301. Varadi, G.; Vizi–orosz, A.; Vastag, S.; Palyi, G. *J. Organomet. Chem.* **1976**, *108*, 225–233.
302. Marcos, M.L.; Macazaga, M.J.; Medina, R.M.; Moreno, C.; Castro, J.A.; Gomez, J.L.; Delgado, S.; Gonzalez–Velasco, J. *Inorg. Chim. Acta* **2001**, *312*, 249–255.
303. Castro, J.; Moyano, A.; Pericas, M.A.; Riera, A.; Alvarez–Larena, A.; Piniella, J.F. *J. Organomet. Chem.* **1999**, *585*, 53–58.
304. Castro, J.; Moyano, A.; Pericas, M.A.; Riera, A.; Alvarez–Larena, A.; Piniella, J.F. *J. Am. Chem. Soc.* **2000**, *122*, 7944–7952.
305. Galow, P.; Sebald, A.; Wrackmeyer, B. *J. Organomet. Chem.* **1983**, *259*, 253–268.
306. Iwasawa, N.; Satoh, H. *J. Am. Chem. Soc.* **1999**, *121*, 7951–7952.
307. Meyer, A.; Gorgues, A.; LeFloc'h, Y.; Pineau, Y.; Guillevic, J.; LeMarouille, J.Y. *Tetrahedron Lett.* **1981**, *22*, 5181–5182.
308. Bellamy, L.J. *The Infrared Spectra of Complex Molecules*, 3rd Ed.; Chapman and Hall: London, 1975, p 359.
309. Seyferth, D.; Wehman, A.T. *J. Am. Chem. Soc.* **1970**, *92*, 5520–5522.
310. Cullen, W.R.; Waldman, M.C. *Can. J. Chem.* **1969**, *47*, 3093–3098.
311. Abou–Ghazaleh, B.; Laurent, P.; Blancou, H.; Commeyras, A. *J. Fluor. Chem.* **1994**, *68*, 21–24.
312. LeBlanc, M.; Santini, G.; Jeanneaux, F.; Riess, J.G. *J. Fluor. Chem.* **1976**, *7*, 525–530.
313. Burton, D.J.; Spawn, T.D. *J. Fluor. Chem.* **1988**, *38*, 119–123.
314. Calleja–Rubio, S.; Crette, S.; Blancou, H. *Synthesis* **2003**, 361–364.
315. Fei, Z.; Zhao, D.; Scopelliti, R.; Dyson, P.J. *Organometallics* **2004**, *23*, 1622–1628.
316. Melikyan, G.G.; Sepanian, S.; Riahi, B.; Villena, F.; Jerome, J.; Ahrens, B.; McClain, R.; Matchett, J.; Scanlon, S.; Abrencia, E.; Paulsen, K.; Hardcastle, K.I. *J. Organomet. Chem.* **2003**, *683*, 324–330.
317. Lake, K.; Dorrell, M.; Blackman, N.; Khan, M.A.; Nicholas, K.M. *Organometallics* **2003**, *22*, 4260–4264.

318. Melikyan, G.G.; Deravakian, A.; Myer, S.; Yadegar, S.; Hardcastle, K.I.; Ciurash, J.; Toure, P. *J. Organomet. Chem.* **1999**, *578*, 68–75.
319. Hong, F.; Huang, Y.; Chen, H. *J. Organomet. Chem.* **2004**, *689*, 3449–3460.
320. Zhang, J.; Chen, X.; Yin, Y.; Wang, W.; Huang, X. *J. Organomet. Chem.* **1999**, *582*, 252–258.
321. Chen, X.; Zhang, J.; Ding, E.; Yin, Y.; Sun, J. *Polyhedron* **1999**, *18*, 1555–1560.
322. Gasser, G.; Neukamm, M.A.; Ewers, A.; Brosch, O.; Weyhermüller, T.; Metzler-Nolte, N. *Inorg. Chem.* **2009**, *48*, 3157–3166.
323. Rosillo, M.; Domínguez, G.; Casarrubios, L.; Pérez-Castells, J. *J. Org. Chem.* **2005**, *70*, 10611–10614.
324. Mikaelyan, G.S.; Smit, V.A.; Batsanov, A.S.; Struchkov, Y.T. *Russ. Chem. Bull.* **1984**, *33*, 1922–1931.
325. Franken, A.; McGrath, T.D.; Stone, F.G.A. *Organometallics* **2008**, *27*, 908–917.
326. Schottenberger, H.; Wurst, K.; Horvath, U.E.I.; Cronje, S.; Lukasser, J.; Polin, J.; McKenzie, J.M.; Raubenheimer, H.G. *Dalton Trans.* **2003**, 4275–4281.
327. Chen, X.; Zhang, J.; Wu, S.; Yin, Y.; Wang, W.; Sun, J. *J. Chem. Soc., Dalton Trans.* **1999**, 1987–1991.
328. Bird, P.H.; Fraser, A.R. *J. Chem. Soc. (D) Chem. Commun.* **1970**, 681–682.
329. Pérez, J.; Riera, L.; Riera, V.; García–Granda, S.; García–Rodriguez, E.; Churchill, D.G.; Churchill, M.R.; Janik, T.S. *Inorg. Chim. Acta* **2003**, *347*, 189–193.
330. Montaña, A.M.; Nicholas, K.M.; Khan, M.A. *J. Org. Chem.* **1988**, *53*, 5193–5201.
331. El-Amouri, H.; Gruselle, M.; Jaouen, G.; Daran, J.C.; Vaissermann, J. *Inorg. Chem.* **1990**, *29*, 3238–3242.
332. Coogan, M.P.; Stanton, L.S.; Walther, T. *J. Organomet. Chem.* **2003**, *677*, 125–132.
333. Stepnicka, P.; Císarová, I. *J. Organomet. Chem.* **2006**, *691*, 2863–2871.
334. Liu, J.; Wei, A. *Chem. Commun.* **2009**, 4254–4256.
335. Chen, X.; Zhang, J.; Yin, Y.; Huang, X. *Organometallics* **1999**, *18*, 3164–3169.
336. Schottenberger, H.; Lukasser, J.; Reichel, E.; Müller, A.G.; Steiner, G.; Kopacka, H.; Wurst, K.; Ongania, K.H. *J. Organomet. Chem.* **2001**, *637*, 558–576.
337. Ganesh, P.; Nicholas, K.M. *J. Org. Chem.* **1997**, *62*, 1737–1747.
338. Calvo–Pérez, V.; Vega, A.; Spodine, E. *Organometallics* **2006**, *25*, 1953–1960.
339. Zhu, B.; Hu, B.; Hong, H.; Yin, Y.; Sun, J. *J. Organomet. Chem.* **2006**, *691*, 485–490.
340. Vega, A.; Calvo, V.; Spodine, E.; Zárate, A.; Fuenzalida, V.; Saillard, J. *Inorg. Chem.* **2002**, *41*, 3389–3395.
341. Zhang, Y.; Lao, W.; Liu, Y.; Yin, Y.; Wu, J.; Huang, Z. *Polyhedron* **2001**, *20*, 1107–1113.
342. Lang, H.; Weinmann, S.; Herres, M.; Weinmann, M.; Walter, O.; Nuber, B.; Zsolnai, L. *J. Organomet. Chem.* **1996**, *524*, 49–61.
343. Mathur, P.; Manimaran, B.; Trivedi, R.; Satyanarayana, C.V.V.; Chadha, R.K. *J. Cluster Sci.* **1998**, *9*, *45*–62.
344. Suo, Q.; Zhu, N.; Han, L.; Wang, Y.; Bai, Y.; Weng, L. *Polyhedron* **2006**, *25*, 3209–3214.

345. Dare, S.; Ducroix, B.; Bernard, S.; Nicholas, K.M. *Tetrahedron Lett.* **1996**, *37*, 4341–4344.
346. Hong, F.; Tsai, Y.; Chang, Y.; Ko, B. *Inorg. Chem.* **2001**, *40*, 5487–5488.
347. Choualeb, A.; Rosé, J.; Braunstein, P.; Welter, R. *Organometallics* **2003**, *22*, 2688–2693.
348. Battaglia, L.P.; Delledonne, D.; Nardelli, M.; Predieri, G.; Chiusoli, G.P.; Costa, M.; Pelizzi, C. *J. Organomet. Chem.* **1989**, *363*, 209–222.
349. Lee, J.; Chang, Y.; Ho, Y.; Chu, K.; Chen, H.; Hong, F. *Polyhedron* **2008**, *26*, 2987–2996.
350. Lang, H.; Leise, M.; Zsolnai, L. *Organometallics* **1993**, *12*, 2393–2397.
351. Melikyan, G.G.; Combs, R.C.; Lamirand, J.; Khand, M.; Nicholas, K.M. *Tetrahedron Lett.* **1994**, *35*, 363–366.
352. Clément, S.; Guyard, L.; Knorr, M.; Dilsky, S.; Strohmann, C.; Arroyo, M. *J. Organomet. Chem.* **2007**, *692*, 839–850.
353. Weber, L.; Barlmeyer, M.; Quasdorff, J.; Sievers, H.L.; Stammler, H.; Neumann, B. *Organometallics* **1999**, *18*, 2497–2504.
354. Lee, I.S.; Shin, D.M.; Yoon, Y.; Shin, S.M.; Chung, Y.K. *Inorg. Chim. Acta* **2003**, *343*, 41–50.
355. García–Escudero, L.A.; Miguel. D.; Turiel, J.A. *J. Organomet. Chem.* **2006**, *691*, 3434–3444.
356. Vega, A.; Calvo, V.; Manzur, J.; Spodine, E.; Saillard, J. *Inorg. Chem.* **2002**, *41*, 5382–5387.
357. Hong, F.; Chen, C.; Chang, Y. *J. Chem. Soc., Dalton Trans.* **2002**, 2951–2953.
358. Wong, W.; Choi, K.; Lin, Z. *Eur. J. Inorg. Chem.* **2002**, 2112–2120.
359. Osella, D.; Galeotti, F.; Cavigiolio, G.; Nervi, C.; Hardcastle, K.I.; Vessières, A.; Jaouen, G. *Helv. Chim. Acta* **2002**, *85*, 2918–2925.
360. Chetcuti, M.J.; Devoille, M.J.; Othman, A.B.; Souane, R.; Thuéry, P.; Vicens, J. *Dalton Trans.* **2009**, 2999–3008.
361. Gu, Y.; Pritzkow, H.; Siebert, W. *Eur. J. Inorg. Chem.* **2001**, 373–379.
362. Albanesi, G.; Tovaglieri, M. *Chim. Ind.* **1959**, *41*, 189–194.
363. Hübel, W.; Hoogzand, C. *Chem. Ber.* **1960**, *93*, 103–115.
364. Khand, I.U.; Knox, G.R.; Pauson, P.L.; Watts, W.E. *Chem. Commun.* **1971**, 36.
365. Khand, I.U.; Knox, G.R.; Pauson, P.L.; Watts, W.E. *J. Chem. Soc. Perkins Trans. I* **1973**, 975–977.
366. Khand, I.U.; Knox, G.R.; Pauson, P.L.; Watts, W.E.; Foreman, M.I. *J. Chem. Soc. Perkins Trans. I* **1973**, 977–981.
367. Magnus, P.; Principe, L.M. *Tetrahedron Lett.* **1985**, *26*, 4851–4854.
368. Banide, E.V.; Müller–Bunz, H.; Manning, A.R.; Evans, P.; McGlinchey, M.J. *Angew. Chem. Int. Ed.* **2007**, *46*, 2907–2910.
369. Itami, K.; Mitsudo, K.; Yoshida, J. *Angew. Chem. Int. Ed.* **2002**, *41*, 3481–3484.
370. Geis, O.; Schmalz, H. *Angew. Chem. Int. Ed.* **1998**, *37*, 911–914.
371. Ahmar, M.; Chabanis, O.; Gauthier, J.; Cazes, B. *Tetrahedron Lett.* **1997**, *38*, 5277–5280.
372. Antras, F.; Ahmar, M.; Cazes, B. *Tetrahedron Lett.* **2001**, *42*, 8157–8160.

373. Rios, R.; Paredes, S.; Pericas, M.; Moyano, A. *J. Organomet. Chem.* **2005**, *690*, 358–362.
374. Rivero, M.; Adrio, J.; Carretero, J. *Synlett* **2005**, 26–41.
375. Kerr, W.J.; McLaughlin, M.; Pauson, P.L.; Robertson, S.M. *Chem. Commun.* **1999**, 2171–2172.
376. Lagunas, A.; Payeras, A.M.; Jimeno, C.; Pericas, M.A. *Org. Lett.* **2005**, *7*, 3033–3036.
377. Perez del Valle, C.; Milet, A.; Gimbert, Y.; Greene, A.E. *Angew. Chem. Int. Ed.* **2005**, *44*, 5717–5719.
378. Brown, D.S.; Campbell, E.; Kerr, W.J.; Lindsay, D.M.; Morrison, A.J.; Pike, K.G.; Watson, S.P. *Synlett* **2000**, 1573–1576.
379. Park, K.H.; Son, S.U.; Chung, Y.K. *Chem. Commun.* **2003**, 1898–1899.
380. Kerr, W.J.; Lindsay, D.M.; Watson, S.P. *Chem. Commun.* **1999**, 2551–2552.
381. Kerr, W.J.; Lindsay, D.M.; McLaughlin, M.; Pauson, P.L. *Chem. Commun.* **2000**, 1467–1468.
382. Maier, G.; Neudert, J.; Wolf, O. *Angew. Chem. Int. Ed.* **2001**, *40*, 1674–1675.
383. Revés, M.; Achard, T.; Solà, J.; Riera, A.; Verdaguer, X. *J. Org. Chem.* **2008**, *73*, 7080–7087.
384. Mukai, C.; Kozaka, T.; Suzuki, Y.; Kim, I.J. *Tetrahedron Lett.* **2002**, *43*, 8575–8578.
385. Mohamed, A.; Green, J.; Masuda, J. *Synlett* **2005**, 1543–1546.
386. Itami, K.; Mitsudo, K.; Fujita, Y.; Ohashi, Y.; Yoshida *J. J. Am. Chem. Soc.* **2004**, *126*, 11058-11066.
387. Jeong, N.; Chung, Y.K.; Lee, B.Y.; Lee, S.H.; Yoo, S. *Synlett* **1991**, *3*, 204–206.
388. Chung, Y.K. *Coord. Chem. Rev.* **1999**, *188*, 297–341.
389. Krafft, M.E.; Romero, R.H.; Scott, I.L. *Synlett* **1995**, 577–578.
390. Coleman, A.C.; Long, C.; Meetsma, A.; Feringa, B.L.; Browne, W.R.; Pryce, M.T. *Dalton Trans.* **2009**, 7885–7887.
391. Montenegro, E.; Moyano, A.; Pericas, M.A.; Riera, A.; Alvarez–Larena, A.; Piniella, J.F. *Tetrahedron: Asymmetry* **1999**, *10*, 457–471.
392. Robert, F.; Milet, A.; Gimbert, Y.; Konya, D.; Greene, A.E. *J. Am. Chem. Soc.* **2001**, *123*, 5396–5400.
393. Shibata, T.; Takagi, K. *J. Am. Chem. Soc.* **2000**, *122*, 9852–9853.
394. Añorbe, L.; Poblador, A.; Dominguez, G.; Pérez–Castells, J. *Tetrahedron Lett.* **2004**, *45*, 4441–4444.
395. Krafft, M.E.; Romero, R.H.; Scott, I.L. *J. Org. Chem.* **1992**, *57*, 5277–5278.
396. Fonquerna, S.; Moyano, A.; Pericàs, M.A.; Riera, A. *Tetrahedron* **1995**, *51*, 4239–4254.
397. Fonquerna, S.; Moyano, A.; Pericas, M.A.; Riera, A. *J. Am. Chem. Soc.* **1997**, *119*, 10225–10226.
398. Vázquez, J.; Fonquerna, S.; Moyano, A.; Pericas, M.A.; Riera, A. *Tetrahedron: Asymmetry* **2001**, *12*, 1837–1850.
399. Kobayashi, T.; Koga, Y.; Narasaka, K. *J. Organomet. Chem.* **2001**, *624*, 73–87.
400. Fonquerna, S.; Rios, R.; Moyano, A.; Pericas, M.A.; Riera, A. *Eur. J. Org. Chem.* **1999**, 3459–3478.
401. Krafft, M.E.; Juliano, C.A. *J. Org. Chem.* **1992**, *57*, 5106–5115.

402. Corey, E.J.; Estreicher, H. *Tetrahedron Lett.* **1981**, *22*, 603–606.
403. Sugihara, T.; Yamada, M.; Ban, H.; Yamaguchi, M.; Kaneko, C. *Angew. Chem. Int. Ed., Engl.* **1997**, *36*, 2801–2804.
404. Khand, I.U.; Pauson, P.L. *J. Chem. Soc. Perkins Trans. I* **1976**, 30–32.
405. deBruin, T.J.M.; Milet, A.; Greene, A.E.; Gimbert, Y. *J. Org. Chem.* **2004**, *69*, 1075–1080.
406. Baxter, R.J.; Knox, G.R.; Moir, J.H.; Pauson, P.L.; Spicer, M.D. *Organometallics* **1999**, *18*, 206–214.
407. Baxter, R.J.; Knox, G.R.; Pauson, P.L.; Spicer, M.D. *Organometallics* **1999**, *18*, 197–205.
408. Baxter, R.J.; Knox, G.R.; Pauson, P.L.; Spicer, M.D. *Organometallics* **1999**, *18*, 215–218.
409. Gandon, V.; Leca, D.; Aechtner, T.; Vollhardt, K.P.C.; Malacria, M.; Aubert, C. *Org. Lett.* **2004**, *6*, 3405–3407.
410. Hubert, A.J.; Dale, J. *J. Chem. Soc.,* **1965**, 3160–3170.
411. Gesing, E.R.F.; Sinclair, J.A.; Vollhardt, K.P.C. *J. Chem. Soc. Chem. Commun.* **1980**, 286–287.
412. Aalbersberg, W.G.L.; Barkovich, A.J.; Funk, R.L.; Hillard, R.L.; Vollhardt, K.P.C. *J. Am. Chem. Soc.* **1975**, *97*, 5600–5602.
413. Srinivasan, R.; Farona, M.F. *J. Mol. Catal.* **1989**, *53*, 203–208.
414. Arnett, E.M.; Bollinger, J.M. *J. Am. Chem. Soc.* **1964**, *86*, 4729–4731.
415. Arnett, E.M.; Bollinger, J.M.; Sanda, J.C. *J. Am. Chem. Soc.* **1965**, *87*, 2050–2051.
416. Hoogzand, C.; Hübel, W. Cyclic Polymerization of Acetylenes by Metal Carbonyl Compounds. In *Organic Syntheses via Metal Carbonyls*; Wender, I.; Pino, P., Eds.; Interscience: New York, 1968; Vol. 1; pp 343–371.
417. Dickson, R.S.; Yawney, D.B.W. *Aust. J. Chem.* **1969**, *22*, 533–541.
418. Giordano, R.; Sappa, E.; Predieri, G. *Inorg. Chim. Acta* **1995**, *228*, 139–146.
419. Grigg, R.; Scott, R.; Stevenson, P. *J. Chem. Soc., Perkins Trans. I* **1988**, 1357–1364.
420. Fuller, J.F.; Valente, E.J. *J. Chem. Cryst.* **1996**, *26*, 815–821.
421. Pailer, M.; Grünhaus, H., *Monatsh. Chem.* **1974**, *105*, 1362–1373.
422. Brown, J.F. *J. Am. Chem. Soc.* **1955**, *77*, 6341–6351.
423. Bellamy, L.J. *The Infrared Spectra of Complex Molecules*, 3rd Ed.; Chapman and Hall: London, 1975; pp 84–91.
424. Tuominen, J.; Wickstrom, K.; Pyysalo, H. *J. High Res. Chromatog.* **1986**, *9*, 469–471.
425. Tanida, H.; Muneyuki, R. *Tetrahedron Lett.* **1964**, *5*, 2787–2790.
426. Zhang, M.X.; Dave, P.R.; Yang, K.; Duddu, R.G.; Gelber, N.; Damavarapu, R.; Rao, S. *Abstracts of Papers*, 232nd ACS National Meeting, San Francisco, CA, September 10–14, 2006; American Chemical Society: Washington, DC, 2006; ORGN–468.
427. Polonsky, J.; Fouquey, C.; Gaudemer, M.A. *Bull. Soc. Chim. Fr.* **1962**, 1255–1258.
428. Hübel, W.; Merényi, R. *Chem. Ber.* **1963**, *96*, 930–943.

429. Yu, Y.; Bond, A.D.; Leonard, P.W.; Lorenz, U.J.; Timofeeva, T.V.; Vollhardt, K.P.C.; Whitener, G.D.; Yakovenko, A.A. *Chem. Commun.* **2006**, 2572–2574.
430. Ebata, K.; Inada, T.; Kabuto, C.; Sakurai, H. *J. Am. Chem. Soc.* **1994**, *116*, 3595–3596.
431. Klein, R.; Schmid, G.; Thewalt, U.; Sedmera, P.; Hanus, V.; Mach, K. *J. Organomet. Chem.* **1994**, *466*, 125–131.
432. Rüdinger, C.; Bissinger, P.; Beruda, H.; Schmidbaur, H. *Organometallics* **1992**, *11*, 2867–2873.
433. Sakurai, H.; Ebata, K.; Kabuto, C.; Sekiguchi, A. *J. Am. Chem. Soc.* **1990**, *112*, 1799–1803.
434. Hillard, R.L.; Vollhardt, K.P.C. *J. Am. Chem. Soc.* **1977**, *99*, 4058–4069.
435. Jackman, L.M.; Sternhell, S. *Applications of Nuclear Magnetic Resonance Spectroscopy in Organic Chemistry*; Pergamon: Oxford, 1969; pp 201–204.
436. Spectral Database for Organic Compounds SDBS, phenyltrimethylsilane. http://riodb01.ibase.aist.go.jp/sdbs/cgi-bin/img_disp.cgi?disptype=disp3&imgdir=hsp&fname=HSP49023&sdbsno=15629 (Accessed Jan 5, 2011).
437. Leonard, P.W. personal communication.
438. Windler, G.K. unpublished results.
439. Trinitrotoluene. *Encyclopedia of Explosives and Related Items*; Picatinny Arsenal: New Jersey, 1980; Vol. 9; p T235.
440. Trinitrobenzene. *Encyclopedia of Explosives and Related Items*; Picatinny Arsenal: New Jersey, 1962; Vol. 2; p B48.
441. Chance, J.M.; Kahr, B.; Buda, A.B.; Siegel, J.S. *J. Am. Chem. Soc.* **1989**, *111*, 5940–5944.
442. Wolff, J.J.; Nelsen, S.F.; Petillo, P.A.; Powell, D.R. *Chem. Ber.* **1991**, *124*, 1719–1725.
443. Adam, D.; Karakhiosoff, K.; Klapotke, T.M.; Holl, G.; Kaiser, M. *Prop. Expl. Pyro.* **2002**, *27*, 7–11.
444. Rosokha, S.V.; Lu, J.; Dibrov, S.M.; Kochi, J.K. *Acta Crystallogr., Sect. C: Cryst. Struct. Commun.* **2006**, *62*, o464–o466.
445. Zeng, Z.; Guo, Y.; Twamley, B.; Shreeve, J.M. *Chem. Commun.* **2009**, 6014–6016.
446. Johnston, B.F.; Mitzel, N.W.; Rankin, D.W.H.; Robertson, H.E.; Rüdinger, C.; Schmidbaur, H. *Dalton Trans.* **2005**, 2292–2299.
447. Choi, C.S.; Abel, J.E. *Acta Crystallogr., Sect. B: Struct. Sci.* **1972**, *B28*, 193–201.
448. Fink, W. *Helv. Chim. Acta* **1974**, *57*, 1010–1015.
449. Eaborn, C. *J. Organomet. Chem.* **1975**, *100*, 43–57.
450. Kaplan, R.; Shechter, H. *Inorg. Syn.* **1953**, *4*, 52–55.
451. Davis, T.L. *The Chemistry of Powder and Explosives*; Angriff Press: Las Vegas, 1943; pp 278–281.
452. Greenfield, H.; Sternberg, H.W.; Friedel, R.A.; Wotiz, J.H.; Markby, R.; Wender, I. *J. Am. Chem. Soc.* **1956**, *78*, 120–124.
453. Pagoria, P.F. unpublished results.
454. Shriver, D.F.; Drezdzon, M.A. *The Manipulation of Air–Sensitive Compounds*; Wiley: New York, 1986.

455. Ejchart, A.; Gryff–Keller, A. *J. Mag. Res. A* **1996**, *118*, 272–278.
456. Davis, T.L. *The Chemistry of Powder and Explosives*; Angriff Press: Las Vegas, 1943; pp 1–4.
457. Rongzu, H.; Xingsen, L.; Yingao, F. *J. Energetic Mater.* **1993**, *11*, 219–241.
458. Cooper, P.W. *Explosives Engineering*; Wiley: New York, 1996; pp 42, 258.
459. Cooper, P.W. *Explosives Engineering*; Wiley: New York, 1996; pp 24–26.
460. Cooper, P.W. *Explosives Engineering*; Wiley: New York, 1996 pp 131–132.

Appendix A: Definitions and Formulae

A1 Explosive Terminology

Brisance (*n*) the shock produced upon explosion, commonly measured in detonation velocity[456]

Deflagration (*n*) an explosion in which the shockwave is subsonic, usually achieved through the combustion of a propellant

Detonation (*n*) 1. an explosive chemical reaction in which all bonds of an explosive break and the constituent atoms form radical species, recombining into the lowest thermodynamic products 2. an explosion in which the shockwave is supersonic

Detonation pressure (*n*) the pressure a shockwave exerts on its surroundings, usually measured in katm or GPa

Detonation temperature (*n*) the temperature of an explosion, measured in K

Detonation velocity (*n*) the speed at which a shockwave travels, usually measured in m/s or km/s

Explosion (*n*) "a loud noise and the sudden going away of things from the place where they have been."[456]

Explosive (*n*) a substance capable of undergoing a sudden transformation accompanied by the liberation of energy[456]

High explosive (*n*) a primary or secondary explosive

Initiation (*n*) the beginning of the chemical process of detonation, accompanied by the formation of a shockwave

Initiator (*n*) see primary explosive

Low explosive (*n*) see propellant

Propellant (*n*) also: low explosive. a combustible material containing within itself all the oxygen necessary for its combustion, which burns but does not explode, and functions by producing gas which produces an explosion. Black powder is an example of a propellant.[456]

Primary explosive (*n*) also: initiator. a substance that, without confinement, detonates (and does not burn) when heated or subjected to shock. Mercury fulminate, lead azide, and cuprous acetylide are examples of primary explosives.[456]

Secondary explosive (*n*) a substance that detonates (and does not burn) under the influence of the shock of a primary explosive. Not all secondary explosives are combustible, but most can be ignited and will sustain combustion without detonation. Most are less sensitive to initiation than primary explosives and are generally more powerful and brisant. Dynamite, TNT, and nitrocellulose are examples of secondary explosives.[456]

Shockwave (*n*) the initial compression component of the longitudinal wave generated by an explosion, typically 0.2 mm in thickness, traveling at 1000–9000 m/s, at a temperature of ~10,000 K, and at a pressure of 200,000–500,000 atm

A2 Explosive Detonation Velocities

Table 35. Explosives with the greatest detonation velocities.

Rank	Compound	Structure	V_{det} (km/s)
1	2,4,6,8,10,12-hexanitro-2,4,6,8,10,12-hexaaza-tricyclo (7,3,0,$0^{3,7}$) dodecane-5,11-dione, HHTDD (**342**)	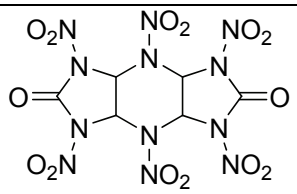	9.75[457]
2	**8** (HNB)	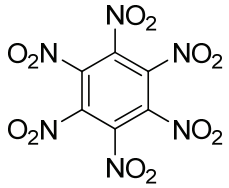	9.50[34]
3	**13** (CL-20)	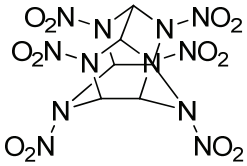	9.21[52]
4	tetranitroglycouril, TNGU (**343**)	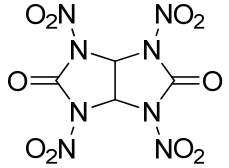	9.15[458]
5	**12** (HMX)	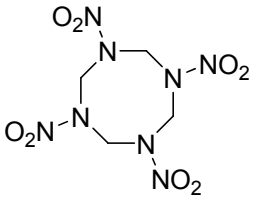	9.11[458]

A3 Oxygen Balance

Oxygen balance (OB) is a measure of the completeness of oxidation of an explosive on detonation, expressed in weight percent of excess oxygen. Underoxidized materials are expressed as a negative percent, while overoxidized compounds have positive values. As a rule of thumb, power of an explosive increases as the OB approaches zero.

For a pure CHNO molecule where x is the number of carbon atoms, y is the number of hydrogen atoms, and z is the number of oxygen atoms in the molecule, OB is expressed as the weight of oxygen unused in oxidizing the C and H atoms divided by the molecular weight (MW) of the explosive:[459]

$$\text{OB \%} = \frac{15.9994 \text{ amu } O_2 \times (z - 2x - y/2)}{\text{MW}_{\text{explosive}}}$$

For example, **5** (TNT) is severely underoxidized (–74 %), ammonium nitrate is overoxidized (20 %), and **10** (octanitrocubane) has a perfect OB (0 %).

A4 Explosive Heats of Formation

The heat of reaction when an explosive detonates is called the heat of detonation, denoted $\Delta H°_d$.[460] The expression is given as:

$$\Delta H°_d = \Sigma \Delta H°_f(\text{detonation products}) - \Delta H°_f(\text{explosive})$$

As is obvious from the equation above, an explosive with a larger $\Delta H°_f$ is more likely to have a greater energy output, but this is only a rough guide, as the initial density, temperature, degree of confinement, particle size and morphology, and dimensions and shape of the charge affect the equilibrium at the detonation front and thus conditions are far from ideal.[460] This is also a poor estimate for underoxidized explosives, as a sizeable quantity of energy can be released through the afterburn of such materials.[460]

Appendix B: Crystallographic Data

B1 [μ-1-Nitro-2-(trimethylsilyl)ethyne-1,2-diyl]bis(tricarbonylcobalt)(*Co–Co*) (25)

Empirical Formula	$Co_2SiO_8NC_{11}H_9$
Formula Weight	429.15
Crystal Color, Habit	red, bladelike
Crystal Dimensions	0.12 X 0.13 X 0.38 mm
Crystal System	monoclinic
Lattice Type	C-centered
Lattice Parameters	a = 13.881(1)Å b = 10.1471(8) Å c = 12.517(1) Å β = 105.394(1)° V = 1699.8(2) Å^3
Space Group	Cc (#9)
Z value	4
D_{calc}	1.677 g/cm^3
F_{000}	856.00
μ(MoKα)	20.58 cm^{-1}

Intensity Measurements

Diffractometer	Bruker APEX CCD
Radiation	MoKα (λ = 0.71069 Å) graphite monochromated
Detector Position	60.00 mm
Exposure Time	10.0 seconds per frame.
Scan Type	ω (0.3 degrees per frame)
$2\theta_{max}$	52.7°
No. of Reflections Measured	Total: 4893 Unique: 1968 (R_{int} = 0.024)
Corrections	Lorentz-polarization
Absorption	Tmax = 1.00, Tmin = 0.81

Structure Solution and Refinement

Structure Solution	Direct Methods (SIR97)
Refinement	Full-matrix least-squares
Function Minimized	Σ w (|Fo| - |Fc|)^2
Least Squares Weights	$1/\sigma^2(Fo) = 4Fo^2/\sigma^2(Fo^2)$
p-factor	0.0300
Anomalous Dispersion	All non-hydrogen atoms
No. Observations (I>3.00σ(I))	2286
No. Variables	206
Reflection/Parameter Ratio	11.10
Residuals: R; Rw; Rall	0.021; 0.026; 0.021
Goodness of Fit Indicator	1.11

Max Shift/Error in Final Cycle	0.00
Maximum peak in Final Diff. Map	0.24 $e^-/Å^3$
Minimum peak in Final Diff. Map	–0.53 $e^-/Å^3$

Atomic coordinates and B_{iso}/B_{eq} for 25

atom	x	y	z	B_{eq}
Co1	–0.0861	0.07187(4)	0.0253	1.973(8)
Co2	0.09296(4)	0.11053(4)	0.11960(4)	1.996(8)
Si1	–0.03190(7)	0.41657(7)	0.04054(8)	2.24(2)
O1	0.1294(2)	0.1696(3)	–0.1354(2)	4.69(7)
O2	–0.0275(2)	0.1582(3)	–0.2193(2)	3.97(6)
O3	–0.2643(2)	0.1254(3)	–0.1575(2)	4.01(6)
O4	–0.0744(2)	–0.2149(2)	–0.0094(3)	4.40(7)
O5	–0.1707(2)	0.1044(3)	0.2167(2)	4.03(7)
O6	0.2757(2)	0.2581(3)	0.1238(2)	4.40(7)
O7	0.0762(2)	0.1506(3)	0.3478(2)	3.67(6)
O8	0.1732(2)	–0.1599(3)	0.1143(2)	4.30(7)
N1	0.0420(2)	0.1581(2)	–0.1355(2)	2.43(6)
C1	–0.0080(2)	0.2369(3)	0.0354(2)	1.86(5)
C2	0.0190(2)	0.1438(3)	–0.0292(2)	1.90(5)
C3	0.0777(3)	0.5009(3)	0.0098(4)	4.07(9)
C4	–0.0435(3)	0.4609(4)	0.1801(3)	4.38(9)
C5	–0.1495(3)	0.4523(3)	–0.0674(3)	3.17(7)
C6	–0.1958(2)	0.1053(3)	–0.0870(3)	2.67(7)
C7	–0.0806(3)	–0.1058(3)	0.0046(3)	2.87(7)
C8	–0.1391(2)	0.0893(3)	0.1444(3)	2.55(7)
C9	0.2063(2)	0.1998(3)	0.1242(3)	2.81(7)
C10	0.0841(2)	0.1340(3)	0.2613(3)	2.41(6)
C11	0.1418(3)	–0.0577(3)	0.1187(3)	2.85(7)
H1	0.0571	0.5833	–0.0248	4.8772
H2	0.1036	0.4473	–0.0383	4.8772
H3	0.1280	0.5149	0.0769	4.8772
H4	–0.0542	0.5531	0.1832	5.2609
H5	–0.0984	0.4149	0.1943	5.2609
H6	0.0161	0.4373	0.2341	5.2609
H7	–0.1640	0.5438	–0.0671	3.8131
H8	–0.1419	0.4281	–0.1381	3.8131
H9	–0.2027	0.4033	–0.0524	3.8131

$B_{eq} = 8/3\ \pi^2(U_{11}(aa^*)^2 + U_{22}(bb^*)^2 + U_{33}(cc^*)^2 + 2U_{12}(aa^*bb^*)\cos\gamma + 2U_{13}(aa^*cc^*)\cos\beta + 2U_{23}(bb^*cc^*)\cos\alpha)$

Anisotropic Displacement Parameters

atom	U_{11}	U_{22}	U_{33}	U_{12}	U_{13}	U_{23}
Co1	0.0231(2)	0.0236(2)	0.0283(2)	–0.0015(1)	0.0067(1)	0.0020(2)

Co2	0.0231(2)	0.0273(2)	0.0249(2)	0.0003(2)	0.0054(1)	0.0019(2)
Si1	0.0289(4)	0.0222(4)	0.0332(4)	0.0007(3)	0.0068(3)	–0.0025(3)
O1	0.041(1)	0.100(2)	0.044(2)	–0.008(1)	0.025(1)	–0.002(2)
O2	0.051(2)	0.072(2)	0.025(1)	0.002(1)	0.005(1)	0.002(1)
O3	0.035(1)	0.064(2)	0.044(2)	0.001(1)	–0.004(1)	0.009(1)
O4	0.061(2)	0.027(1)	0.087(2)	–0.005(1)	0.033(2)	–0.006(1)
O5	0.048(2)	0.067(2)	0.046(2)	0.004(1)	0.025(1)	0.006(1)
O6	0.033(1)	0.075(2)	0.060(2)	–0.019(1)	0.013(1)	0.001(1)
O7	0.048(1)	0.064(2)	0.030(1)	–0.005(1)	0.013(1)	–0.002(1)
O8	0.059(2)	0.042(1)	0.062(2)	0.018(1)	0.015(1)	0.003(1)
N1	0.038(2)	0.028(1)	0.028(1)	–0.001(1)	0.012(1)	–0.002(1)
C1	0.022(1)	0.022(1)	0.025(1)	–0.000(1)	0.005(1)	0.003(1)
C2	0.024(1)	0.025(1)	0.024(1)	–0.002(1)	0.006(1)	0.000(1)
C3	0.040(2)	0.029(2)	0.084(3)	–0.008(1)	0.015(2)	0.001(2)
C4	0.068(3)	0.053(2)	0.044(2)	0.014(2)	0.014(2)	–0.016(2)
C5	0.036(2)	0.032(2)	0.048(2)	0.005(1)	0.004(1)	0.005(1)
C6	0.030(2)	0.034(2)	0.038(2)	–0.005(1)	0.008(1)	0.001(1)
C7	0.034(2)	0.030(2)	0.049(2)	–0.001(1)	0.018(2)	0.003(1)
C8	0.027(2)	0.035(2)	0.035(2)	–0.001(1)	0.008(1)	0.004(1)
C9	0.031(2)	0.045(2)	0.031(2)	–0.000(1)	0.008(1)	0.000(1)
C10	0.028(1)	0.032(2)	0.031(2)	–0.003(1)	0.007(1)	0.003(1)
C11	0.034(2)	0.038(2)	0.035(2)	0.003(1)	0.007(1)	0.004(1)

The general temperature factor expression:
$\exp(-2\pi^2(a^{*2}U_{11}h^2 + b^{*2}U_{22}k^2 + c^{*2}U_{33}l^2 + 2a^*b^*U_{12}hk + 2a^*c^*U_{13}hl + 2b^*c^*U_{23}kl))$

B2 [μ-1-Nitroethyne-1,2-diyl]bis(tricarbonylcobalt)(*Co–Co*) (26)

Empirical Formula	$Co_2O_8NC_8H$
Formula Weight	356.96
Crystal Color, Habit	red, blocky
Crystal Dimensions	0.09 X 0.12 X 0.32 mm
Crystal System	monoclinic
Lattice Type	Primitive
Lattice Parameters	a = 6.7001(7)Å b = 13.771(1) Å c = 12.683(1) Å β = 93.981(2)° V = 1167.4(2) Å^3
Space Group	$P2_1/n$ (#14)
Z value	4
D_{calc}	2.031 g/cm^3
F_{000}	696.00
μ(MoKα)	28.77 cm^{-1}

Intensity Measurements

Diffractometer	Bruker APEX CCD
Radiation	MoKα (λ = 0.71069 Å) graphite monochromated
Detector Position	60.00 mm
Exposure Time	10.0 seconds per frame.
Scan Type	ω (0.3 degrees per frame)
$2\theta_{max}$	52.7°
No. of Reflections Measured	Total: 6505
	Unique: 2597 (R_{int} = 0.020)
Corrections	Lorentz-polarization
Absorption	Tmax = 1.00, Tmin = 0.74

Structure Solution and Refinement

Structure Solution	Direct Methods (SIR97)
Refinement	Full-matrix least-squares
Function Minimized	Σ w (|Fo| - |Fc|)^2
Least Squares Weights	$1/\sigma^2(Fo) = 4Fo^2/\sigma^2(Fo^2)$
p-factor	0.0300
Anomalous Dispersion	All non-hydrogen atoms
No. Observations (I>3.00σ(I))	1925
No. Variables	176
Reflection/Parameter Ratio	10.94
Residuals: R; Rw; Rall	0.022; 0.026; 0.029
Goodness of Fit Indicator	1.19
Max Shift/Error in Final Cycle	0.00
Maximum peak in Final Diff. Map	0.29 $e^-/Å^3$
Minimum peak in Final Diff. Map	–0.18 $e^-/Å^3$

Atomic Coordinates and B_{iso}/B_{eq} for 26

atom	x	y	z	B_{eq}
Co1	0.44739(4)	0.40053(2)	0.26145(2)	1.839(6)
Co2	0.47496(4)	0.29600(2)	0.10395(2)	1.840(6)
O1	0.0648(3)	0.1706(1)	0.1839(1)	2.93(4)
O2	0.0431(3)	0.2622(1)	0.3209(1)	3.65(4)
O3	0.8468(3)	0.4929(1)	0.2861(1)	3.82(4)
O4	0.1902(3)	0.5502(1)	0.1538(1)	3.18(4)
O5	0.3475(3)	0.4120(1)	0.4833(1)	3.31(4)
O6	0.2611(3)	0.4180(1)	–0.0592(1)	3.29(4)
O7	0.8927(3)	0.3364(1)	0.0578(2)	4.26(5)
O8	0.3927(3)	0.1031(1)	0.0107(1)	3.85(5)
N1	0.1272(3)	0.2352(1)	0.2434(1)	2.20(4)
C1	0.5055(4)	0.2627(2)	0.2529(2)	2.07(5)
C2	0.3138(3)	0.2823(1)	0.2221(2)	1.80(4)
C3	0.6944(4)	0.4584(2)	0.2757(2)	2.53(5)

C4	0.2888(3)	0.4952(2)	0.1984(2)	2.24(5)
C5	0.3849(3)	0.4097(2)	0.3978(2)	2.33(5)
C6	0.3401(3)	0.3700(2)	0.0027(2)	2.22(5)
C7	0.7327(4)	0.3193(2)	0.0738(2)	2.63(5)
C8	0.4283(4)	0.1771(2)	0.0445(2)	2.64(5)
H1	0.579(4)	0.218(2)	0.294(2)	3.8(6)

$B_{eq} = 8/3\ \pi^2(U_{11}(aa^*)^2 + U_{22}(bb^*)^2 + U_{33}(cc^*)^2 + 2U_{12}(aa^*bb^*)\cos\gamma + 2U_{13}(aa^*cc^*)\cos\beta + 2U_{23}(bb^*cc^*)\cos\alpha)$

Anisotropic Displacement Parameters

atom	U_{11}	U_{22}	U_{33}	U_{12}	U_{13}	U_{23}
Co1	0.0251(2)	0.0217(2)	0.0231(2)	–0.0024(1)	0.0017(1)	0.0007(1)
Co2	0.0236(2)	0.0237(2)	0.0227(2)	0.0017(1)	0.0029(1)	0.0012(1)
O1	0.039(1)	0.0312(9)	0.0402(10)	–0.0113(8)	–0.0032(8)	0.0011(7)
O2	0.047(1)	0.052(1)	0.042(1)	–0.0132(9)	0.0217(9)	–0.0069(9)
O3	0.035(1)	0.067(1)	0.043(1)	–0.020(1)	–0.0011(8)	0.0092(9)
O4	0.044(1)	0.0313(9)	0.044(1)	0.0080(8)	–0.0029(8)	0.0016(8)
O5	0.048(1)	0.051(1)	0.0268(9)	–0.0067(9)	0.0079(8)	–0.0041(8)
O6	0.043(1)	0.049(1)	0.0327(9)	0.0052(9)	–0.0019(8)	0.0123(8)
O7	0.027(1)	0.070(1)	0.065(1)	0.0053(10)	0.0109(9)	0.029(1)
O8	0.062(1)	0.035(1)	0.050(1)	–0.0022(9)	0.0101(10)	–0.0135(9)
N1	0.030(1)	0.0257(10)	0.028(1)	–0.0016(8)	0.0009(8)	0.0071(8)
C1	0.033(1)	0.022(1)	0.024(1)	0.0004(10)	0.0023(9)	0.0052(9)
C2	0.028(1)	0.019(1)	0.022(1)	–0.0038(9)	0.0029(9)	0.0009(8)
C3	0.035(1)	0.035(1)	0.026(1)	–0.005(1)	0.0032(10)	0.0034(10)
C4	0.031(1)	0.022(1)	0.032(1)	–0.003(1)	0.0039(10)	–0.0031(10)
C5	0.030(1)	0.026(1)	0.033(1)	–0.0057(10)	0.0023(10)	–0.0016(9)
C6	0.028(1)	0.031(1)	0.026(1)	–0.001(1)	0.0041(9)	0.0003(9)
C7	0.031(1)	0.036(1)	0.033(1)	0.007(1)	0.005(1)	0.009(1)
C8	0.034(1)	0.035(1)	0.031(1)	0.004(1)	0.007(1)	–0.002(1)

The general temperature factor expression:
$\exp(-2\pi^2(a^{*2}U_{11}h^2 + b^{*2}U_{22}k^2 + c^{*2}U_{33}l^2 + 2a^*b^*U_{12}hk + 2a^*c^*U_{13}hl + 2b^*c^*U_{23}kl))$

B3 1,3,5-Tris(trimethylsilyl)-2,4,6-trinitrobenzene (325)

Empirical Formula	$C_{15}H_{27}N_3O_6Si_3$
Formula Weight	429.67
Crystal Color, Habit	colorless, polyhedral
Crystal Dimensions	0.12 x 0.08 x 0.08 mm
Crystal System	Monoclinic
Lattice Type	C-centered
Lattice Parameters	a = 11.062(3) Å
	b = 19.067(5) Å

	c = 21.187(5) Å
	α= 90 °
	β= 96.226(4) °
	γ = 90°
	V = 4442.2(19) Å3
Space Group	C 2/c
Z value	8
D_{calc}	1.285 g/cm^3
F_{000}	1824
μ(MoK)	0.25 cm^{-1}

Intensity Measurements

Diffractometer	Bruker APEX I
Radiation	MoK(λ = 0.71073 □) graphite monochromated
Detector Position	60.00 mm
Exposure Time	30 seconds per frame.
Scan Type	ω (0.3 degrees per frame)
θ max	22.01°
No. of Reflections Measured	Total: 8618 Unique: 2729 (R_{int} = 0.0720)
Corrections	Lorentz-polarization
Absorption	Tmax = 1.0, Tmin = 0.79

Structure Solution and Refinement

Structure Solution	direct (SHELXS-97 (Sheldrick, 1990))
Refinement	Full-matrix least-squares
Function Minimized	$\Sigma w(\|F_o\|^2 - \|F_c\|^2)^2$
Least Squares Weighting scheme	$w = 1/[\sigma^2(F_o^2) + (qP)^2 + 0.000P]$ where $P = [F_o^2 + 2F_c^2]/3$
q-factor	0.10
Anomalous Dispersion	All non-hydrogen atoms
No. Observations (I>2.00σ(I))	1542
No. Variables	282
Reflection/Parameter Ratio	5.5
Residuals: R; wR_2; Rall	0.0740; 0.1830; 0.1375
Goodness of Fit Indicator	1.143
Max Shift/Error in Final Cycle	0.001
Maximum peak in Final Diff. Map	0.407 e$^-$/Å^3
Minimum peak in Final Diff. Map	–0.326 e$^-$/Å^3

Atomic Coordinates, U_{iso}/U_{eq}, and Occupancy for 325

atom	x	y	z	Ueq	Occupancy
Si1	–0.1474(2)	0.1860(1)	–0.1270(1)	0.053(1)	1
Si2	0.3168(2)	0.3353(1)	–0.1215(1)	0.050(1)	1
Si3	0.3071(2)	0.0278(1)	–0.1266(1)	0.057(1)	1
O1A	0.4767(11)	0.1959(8)	–0.0781(6)	0.097(5)	0.65(2)
O2A	0.4530(10)	0.1668(8)	–0.1756(6)	0.082(5)	0.65(2)
O1B	0.4698(14)	0.1508(11)	–0.0680(8)	0.051(8)	0.35(2)
O2B	0.4658(16)	0.2038(9)	–0.1624(8)	0.054(7)	0.35(2)
O3	0.0290(6)	0.0230(4)	–0.0776(4)	0.096(2)	1
O4	–0.0325(7)	0.0390(4)	–0.1743(4)	0.120(3)	1
O5	0.0384(7)	0.3432(4)	–0.0733(4)	0.111(3)	1
O6	–0.0178(7)	0.3343(4)	–0.1719(4)	0.102(3)	1
N1	0.4132(7)	0.1819(3)	–0.1229(3)	0.067(2)	1
N2	0.0264(5)	0.0570(4)	–0.1263(4)	0.061(2)	1
N3	0.0357(5)	0.3117(4)	–0.1240(4)	0.059(2)	1
C1	0.0283(6)	0.1845(4)	–0.1260(3)	0.035(2)	1
C2	0.1012(6)	0.2441(4)	–0.1243(3)	0.032(2)	1
C3	0.2263(6)	0.2482(4)	–0.1227(3)	0.031(2)	1
C4	0.2793(5)	0.1817(4)	–0.1223(3)	0.034(2)	1
C5	0.2218(7)	0.1172(4)	–0.1250(3)	0.036(2)	1
C6	0.0982(7)	0.1230(4)	–0.1259(3)	0.037(2)	1
C7	–0.1976(8)	0.2661(5)	–0.0838(5)	0.091(5)	0.892(10)
C8	–0.2135(10)	0.1866(8)	–0.2087(4)	0.117(6)	0.892(10)
C9	–0.2003(8)	0.1117(6)	–0.0794(5)	0.082(4)	0.892(10)
C7B	–0.212(5)	0.2679(17)	–0.166(2)	0.05(2)	0.108(10)
C8B	–0.214(5)	0.111(2)	–0.177(2)	0.05(2)	0.108(10)
C9B	–0.200(6)	0.178(3)	–0.0481(14)	0.07(3)	0.108(10)
C10B	0.4660(16)	0.3216(14)	–0.0702(10)	0.055(8)	0.316(11)
C11B	0.239(2)	0.4062(13)	–0.0801(11)	0.076(10)	0.316(11)
C12B	0.340(2)	0.3595(14)	–0.2003(7)	0.065(9)	0.316(11)
C10	0.3696(15)	0.3586(9)	–0.0416(5)	0.122(9)	0.684(11)
C11	0.2203(12)	0.4087(6)	–0.1609(7)	0.090(6)	0.684(11)
C12	0.4423(12)	0.3265(7)	–0.1737(7)	0.102(6)	0.684(11)
C13B	0.236(2)	–0.0452(13)	–0.0894(12)	0.106(12)	0.352(9)
C14B	0.4647(15)	0.0402(14)	–0.0854(10)	0.072(9)	0.352(9)
C15B	0.323(2)	0.0095(15)	–0.2114(7)	0.088(10)	0.352(9)
C13	0.3398(13)	–0.0028(8)	–0.0437(5)	0.089(6)	0.648(9)
C14	0.4414(12)	0.0342(8)	–0.1672(7)	0.102(7)	0.648(9)
C15	0.2036(11)	–0.0396(6)	–0.1696(6)	0.076(5)	0.648(9)
H7A	–0.2864	0.2660	–0.0848	0.136	0.892(10)
H7B	–0.1717	0.3086	–0.1046	0.136	0.892(10)
H7C	–0.1607	0.2652	–0.0396	0.136	0.892(10)
H8A	–0.3024	0.1874	–0.2103	0.176	0.892(10)
H8B	–0.1881	0.1444	–0.2301	0.176	0.892(10)
H8C	–0.1859	0.2283	–0.2300	0.176	0.892(10)

H9A	–0.2890	0.1134	–0.0805	0.124	0.892(10)
H9B	–0.1633	0.1156	–0.0354	0.124	0.892(10)
H9C	–0.1762	0.0671	–0.0974	0.124	0.892(10)
H7BA	–0.3009	0.2677	–0.1657	0.074	0.108(10)
H7BB	–0.1918	0.2701	–0.2095	0.074	0.108(10)
H7BC	–0.1782	0.3088	–0.1421	0.074	0.108(10)
H8BA	–0.3023	0.1116	–0.1782	0.073	0.108(10)
H8BB	–0.1814	0.0668	–0.1595	0.073	0.108(10)
H8BC	–0.1915	0.1165	–0.2207	0.073	0.108(10)
H9BA	–0.2892	0.1794	–0.0522	0.110	0.108(10)
H9BB	–0.1678	0.2174	–0.0214	0.110	0.108(10)
H9BC	–0.1714	0.1339	–0.0286	0.110	0.108(10)
H10A	0.5136	0.3650	–0.0688	0.082	0.316(11)
H10B	0.5117	0.2838	–0.0882	0.082	0.316(11)
H10C	0.4499	0.3088	–0.0271	0.082	0.316(11)
H11A	0.2871	0.4495	–0.0803	0.114	0.316(11)
H11B	0.2324	0.3920	–0.0362	0.114	0.316(11)
H11C	0.1580	0.4142	–0.1022	0.114	0.316(11)
H12A	0.3855	0.4036	–0.1995	0.097	0.316(11)
H12B	0.2609	0.3657	–0.2255	0.097	0.316(11)
H12C	0.3858	0.3226	–0.2193	0.097	0.316(11)
H10D	0.4152	0.4027	–0.0414	0.184	0.684(11)
H10E	0.4227	0.3214	–0.0225	0.184	0.684(11)
H10F	0.3000	0.3644	–0.0172	0.184	0.684(11)
H11D	0.2682	0.4521	–0.1596	0.135	0.684(11)
H11E	0.1486	0.4159	–0.1383	0.135	0.684(11)
H11F	0.1944	0.3962	–0.2052	0.135	0.684(11)
H12D	0.4882	0.3705	–0.1732	0.153	0.684(11)
H12E	0.4076	0.3161	–0.2172	0.153	0.684(11)
H12F	0.4968	0.2883	–0.1580	0.153	0.684(11)
H13A	0.2853	–0.0875	–0.0925	0.160	0.352(9)
H13B	0.1544	–0.0530	–0.1111	0.160	0.352(9)
H13C	0.2305	–0.0343	–0.0446	0.160	0.352(9)
H14A	0.5095	–0.0041	–0.0856	0.108	0.352(9)
H14B	0.4598	0.0551	–0.0415	0.108	0.352(9)
H14C	0.5071	0.0762	–0.1076	0.108	0.352(9)
H15A	0.3655	–0.0351	–0.2150	0.132	0.352(9)
H15B	0.3695	0.0473	–0.2287	0.132	0.352(9)
H15C	0.2421	0.0068	–0.2353	0.132	0.352(9)
H13D	0.3827	–0.0478	–0.0431	0.133	0.648(9)
H13E	0.2633	–0.0087	–0.0249	0.133	0.648(9)
H13F	0.3907	0.0319	–0.0192	0.133	0.648(9)
H14D	0.4815	–0.0117	–0.1670	0.152	0.648(9)
H14E	0.4972	0.0686	–0.1456	0.152	0.648(9)
H14F	0.4186	0.0491	–0.2112	0.152	0.648(9)
H15D	0.2465	–0.0845	–0.1703	0.113	0.648(9)

H15E	0.1798	–0.0239	–0.2132	0.113	0.648(9)
H15F	0.1309	–0.0455	–0.1475	0.113	0.648(9)

U_{eq} is defined as one third of the orthogonalized U_{ij} tensor

Anisotropic Displacement Parameters

atom	U_{11}	U_{22}	U_{33}	U_{12}	U_{13}	U_{23}
Si1	0.028(1)	0.070(2)	0.061(2)	0.014(1)	0.004(1)	0.001(1)
Si2	0.050(2)	0.041(2)	0.059(2)	–0.004(1)	0.006(1)	–0.014(1)
Si3	0.060(2)	0.041(2)	0.070(2)	–0.006(1)	–0.002(1)	0.018(1)
O3	0.111(6)	0.075(5)	0.103(6)	0.021(5)	0.021(5)	–0.034(4)
O4	0.172(8)	0.098(6)	0.085(6)	–0.005(5)	–0.020(6)	–0.071(6)
O5	0.159(8)	0.085(6)	0.090(6)	–0.015(5)	0.028(5)	0.055(5)
O6	0.133(7)	0.085(6)	0.088(6)	0.021(4)	0.007(5)	0.052(5)
N1	0.074(6)	0.060(5)	0.065(6)	–0.018(5)	–0.003(5)	–0.001(4)
N2	0.061(5)	0.046(5)	0.073(7)	–0.001(5)	–0.006(5)	0.000(4)
N3	0.053(5)	0.049(5)	0.075(6)	0.001(5)	0.011(4)	–0.002(4)
C1	0.032(4)	0.032(5)	0.041(5)	0.000(4)	0.003(3)	–0.002(4)
C2	0.030(5)	0.023(5)	0.043(5)	0.004(4)	0.010(3)	0.009(4)
C3	0.028(5)	0.030(5)	0.036(5)	–0.002(4)	0.007(3)	0.005(4)
C4	0.003(4)	0.055(6)	0.046(5)	–0.002(4)	0.004(3)	0.000(4)
C5	0.020(4)	0.041(5)	0.047(5)	–0.006(4)	0.000(3)	–0.003(4)
C6	0.049(6)	0.020(4)	0.041(5)	–0.001(4)	0.000(4)	–0.014(4)
C7	0.042(7)	0.117(11)	0.121(11)	0.012(8)	0.043(6)	0.031(7)
C8	0.060(8)	0.220(19)	0.068(9)	0.015(10)	–0.016(6)	–0.010(9)
C9	0.037(6)	0.113(11)	0.101(9)	0.019(8)	0.022(6)	–0.011(6)
C10	0.18(2)	0.128(17)	0.051(10)	–0.019(10)	–0.015(11)	–0.087(15)
C11	0.103(12)	0.041(9)	0.125(14)	0.033(9)	0.008(10)	–0.019(8)
C12	0.095(13)	0.068(11)	0.153(16)	0.018(11)	0.062(11)	–0.035(10)
C13	0.109(13)	0.073(12)	0.076(12)	0.026(9)	–0.032(9)	0.025(10)
C14	0.099(14)	0.067(12)	0.147(18)	–0.013(11)	0.053(12)	0.023(10)
C15	0.082(11)	0.042(9)	0.100(13)	–0.021(8)	–0.003(9)	0.022(8)
Si1	0.028(1)	0.070(2)	0.061(2)	0.014(1)	0.004(1)	0.001(1)
Si2	0.050(2)	0.041(2)	0.059(2)	–0.004(1)	0.006(1)	–0.014(1)
Si3	0.060(2)	0.041(2)	0.070(2)	–0.006(1)	–0.002(1)	0.018(1)
O3	0.111(6)	0.075(5)	0.103(6)	0.021(5)	0.021(5)	–0.034(4)
O4	0.172(8)	0.098(6)	0.085(6)	–0.005(5)	–0.020(6)	–0.071(6)
O5	0.159(8)	0.085(6)	0.090(6)	–0.015(5)	0.028(5)	0.055(5)
O6	0.133(7)	0.085(6)	0.088(6)	0.021(4)	0.007(5)	0.052(5)
N1	0.074(6)	0.060(5)	0.065(6)	–0.018(5)	–0.003(5)	–0.001(4)
N2	0.061(5)	0.046(5)	0.073(7)	–0.001(5)	–0.006(5)	0.000(4)
N3	0.053(5)	0.049(5)	0.075(6)	0.001(5)	0.011(4)	–0.002(4)
C1	0.032(4)	0.032(5)	0.041(5)	0.000(4)	0.003(3)	–0.002(4)
C2	0.030(5)	0.023(5)	0.043(5)	0.004(4)	0.010(3)	0.009(4)
C3	0.028(5)	0.030(5)	0.036(5)	–0.002(4)	0.007(3)	0.005(4)
C4	0.003(4)	0.055(6)	0.046(5)	–0.002(4)	0.004(3)	0.000(4)

C5	0.020(4)	0.041(5)	0.047(5)	–0.006(4)	0.000(3)	–0.003(4)
C6	0.049(6)	0.020(4)	0.041(5)	–0.001(4)	0.000(4)	–0.014(4)
C7	0.042(7)	0.117(11)	0.121(11)	0.012(8)	0.043(6)	0.031(7)
C8	0.060(8)	0.220(19)	0.068(9)	0.015(10)	–0.016(6)	–0.010(9)
C9	0.037(6)	0.113(11)	0.101(9)	0.019(8)	0.022(6)	–0.011(6)
C10	0.18(2)	0.128(17)	0.051(10)	–0.019(10)	–0.015(11)	–0.087(15)
C11	0.103(12)	0.041(9)	0.125(14)	0.033(9)	0.008(10)	–0.019(8)
C12	0.095(13)	0.068(11)	0.153(16)	0.018(11)	0.062(11)	–0.035(10)
C13	0.109(13)	0.073(12)	0.076(12)	0.026(9)	–0.032(9)	0.025(10)
C14	0.099(14)	0.067(12)	0.147(18)	–0.013(11)	0.053(12)	0.023(10)
C15	0.082(11)	0.042(9)	0.100(13)	–0.021(8)	–0.003(9)	0.022(8)
Si1	0.028(1)	0.070(2)	0.061(2)	0.014(1)	0.004(1)	0.001(1)
Si2	0.050(2)	0.041(2)	0.059(2)	–0.004(1)	0.006(1)	–0.014(1)
Si3	0.060(2)	0.041(2)	0.070(2)	–0.006(1)	–0.002(1)	0.018(1)
O3	0.111(6)	0.075(5)	0.103(6)	0.021(5)	0.021(5)	–0.034(4)
O4	0.172(8)	0.098(6)	0.085(6)	–0.005(5)	–0.020(6)	–0.071(6)
O5	0.159(8)	0.085(6)	0.090(6)	–0.015(5)	0.028(5)	0.055(5)
O6	0.133(7)	0.085(6)	0.088(6)	0.021(4)	0.007(5)	0.052(5)
N1	0.074(6)	0.060(5)	0.065(6)	–0.018(5)	–0.003(5)	–0.001(4)
N2	0.061(5)	0.046(5)	0.073(7)	–0.001(5)	–0.006(5)	0.000(4)
N3	0.053(5)	0.049(5)	0.075(6)	0.001(5)	0.011(4)	–0.002(4)
C1	0.032(4)	0.032(5)	0.041(5)	0.000(4)	0.003(3)	–0.002(4)
C2	0.030(5)	0.023(5)	0.043(5)	0.004(4)	0.010(3)	0.009(4)
C3	0.028(5)	0.030(5)	0.036(5)	–0.002(4)	0.007(3)	0.005(4)
C4	0.003(4)	0.055(6)	0.046(5)	–0.002(4)	0.004(3)	0.000(4)
C5	0.020(4)	0.041(5)	0.047(5)	–0.006(4)	0.000(3)	–0.003(4)
C6	0.049(6)	0.020(4)	0.041(5)	–0.001(4)	0.000(4)	–0.014(4)
C7	0.042(7)	0.117(11)	0.121(11)	0.012(8)	0.043(6)	0.031(7)
C8	0.060(8)	0.220(19)	0.068(9)	0.015(10)	–0.016(6)	–0.010(9)
C9	0.037(6)	0.113(11)	0.101(9)	0.019(8)	0.022(6)	–0.011(6)
C10	0.18(2)	0.128(17)	0.051(10)	–0.019(10)	–0.015(11)	–0.087(15)
C11	0.103(12)	0.041(9)	0.125(14)	0.033(9)	0.008(10)	–0.019(8)
C12	0.095(13)	0.068(11)	0.153(16)	0.018(11)	0.062(11)	–0.035(10)
C13	0.109(13)	0.073(12)	0.076(12)	0.026(9)	–0.032(9)	0.025(10)
C14	0.099(14)	0.067(12)	0.147(18)	–0.013(11)	0.053(12)	0.023(10)
C15	0.082(11)	0.042(9)	0.100(13)	–0.021(8)	–0.003(9)	0.022(8)
Si1	0.028(1)	0.070(2)	0.061(2)	0.014(1)	0.004(1)	0.001(1)
Si2	0.050(2)	0.041(2)	0.059(2)	–0.004(1)	0.006(1)	–0.014(1)
Si3	0.060(2)	0.041(2)	0.070(2)	–0.006(1)	–0.002(1)	0.018(1)
O3	0.111(6)	0.075(5)	0.103(6)	0.021(5)	0.021(5)	–0.034(4)
O4	0.172(8)	0.098(6)	0.085(6)	–0.005(5)	–0.020(6)	–0.071(6)
O5	0.159(8)	0.085(6)	0.090(6)	–0.015(5)	0.028(5)	0.055(5)
O6	0.133(7)	0.085(6)	0.088(6)	0.021(4)	0.007(5)	0.052(5)
N1	0.074(6)	0.060(5)	0.065(6)	–0.018(5)	–0.003(5)	–0.001(4)
N2	0.061(5)	0.046(5)	0.073(7)	–0.001(5)	–0.006(5)	0.000(4)
N3	0.053(5)	0.049(5)	0.075(6)	0.001(5)	0.011(4)	–0.002(4)

C1	0.032(4)	0.032(5)	0.041(5)	0.000(4)	0.003(3)	–0.002(4)
C2	0.030(5)	0.023(5)	0.043(5)	0.004(4)	0.010(3)	0.009(4)
C3	0.028(5)	0.030(5)	0.036(5)	–0.002(4)	0.007(3)	0.005(4)
C4	0.003(4)	0.055(6)	0.046(5)	–0.002(4)	0.004(3)	0.000(4)
C5	0.020(4)	0.041(5)	0.047(5)	–0.006(4)	0.000(3)	–0.003(4)
C6	0.049(6)	0.020(4)	0.041(5)	–0.001(4)	0.000(4)	–0.014(4)
C7	0.042(7)	0.117(11)	0.121(11)	0.012(8)	0.043(6)	0.031(7)

The general temperature factor expression:
$\exp(-2\pi^2(a^{*2}U_{11}h^2 + b^{*2}U_{22}k^2 + c^{*2}U_{33}l^2 + 2a^*b^*U_{12}hk + 2a^*c^*U_{13}\,hl + 2b^*c^*U_{23}kl))$

Appendix C: Numbered List of Compounds

Chapter 1

Number	Structure
1	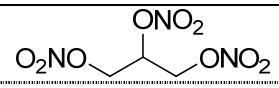
2	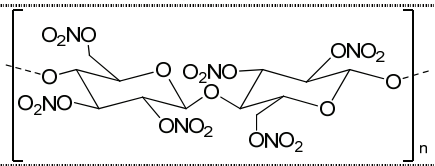
3	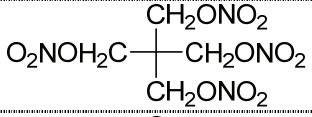
4	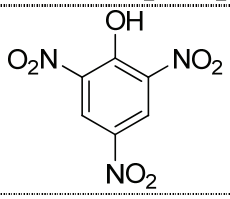
5	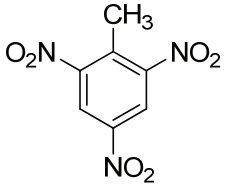
6	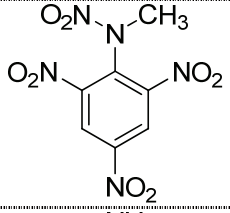
7	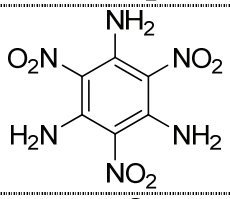
8	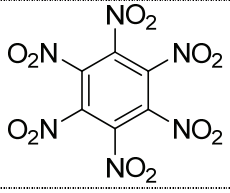
9	$C(NO_2)_4$
10	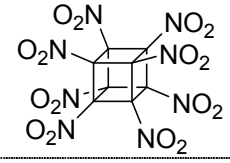
11	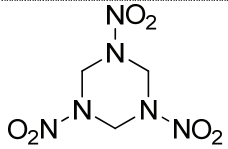
12	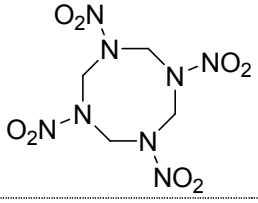
13	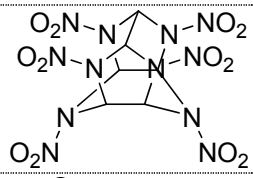
14	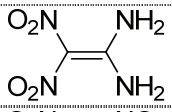
15	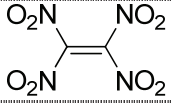
16	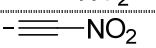
16a	
17	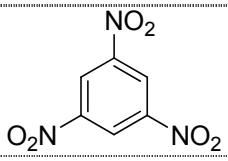
18	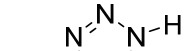
19	
20	
21	
22	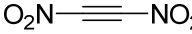
23	$Co_2(CO)_8$
24	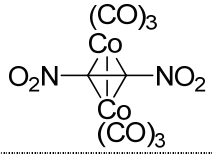

25	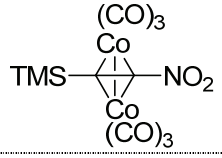
26	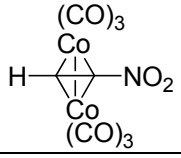

Chapter 2

Number	Structure
27	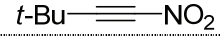
28	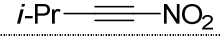
29	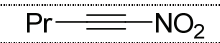
30	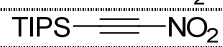
31	
32	
33	
34	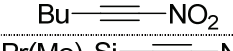
35	
36	
37	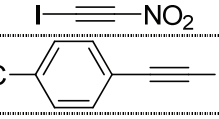
38	
39	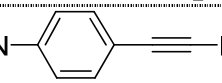
40	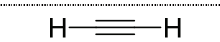
41	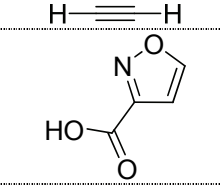
42	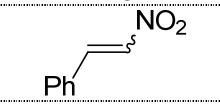
43	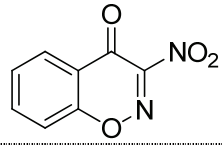
44	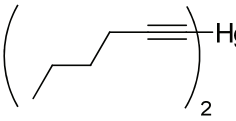
45	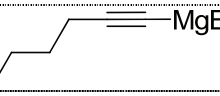
46	
47	
48	
49	
50	
51	
52	
53	
54	
55	
56	
57	
58	
59	

60	
61	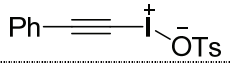
62	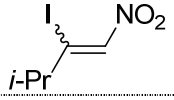
63	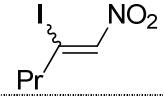
64	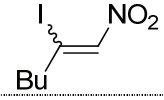
65	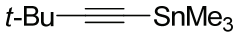
66	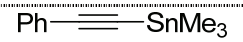
67	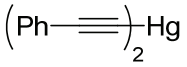
68	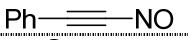
69	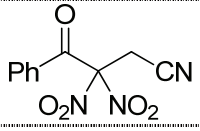
70	
71	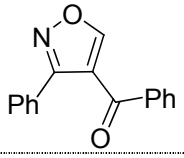
72	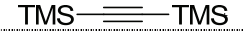
73	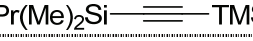
74	
75	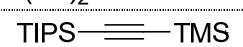
76	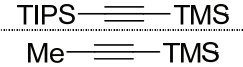
77	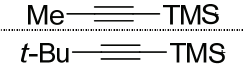
78	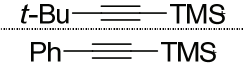
79	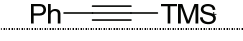
80	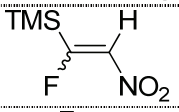
81	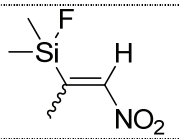
82	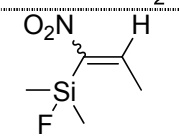
83	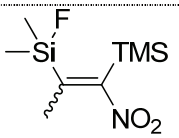

84	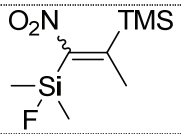
85	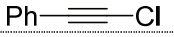
86	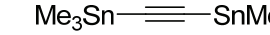
87	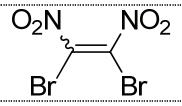
88	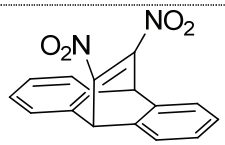
89	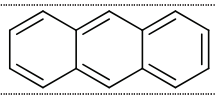
90	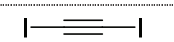
91a	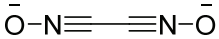
91b	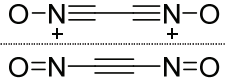
92	
93	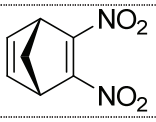
94	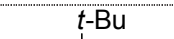
95	
96	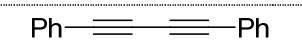
97	
98	
99	
100	
101a	
101b	

102	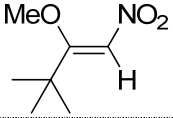
103	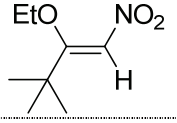
104	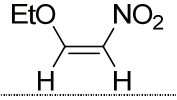
105	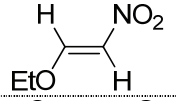
106	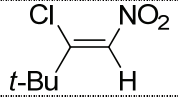
107	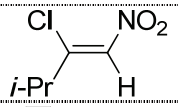
108	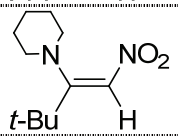
109	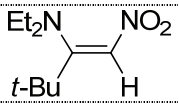
110	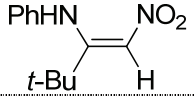
111	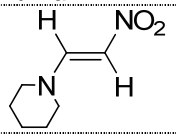
112	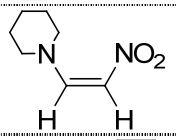
113	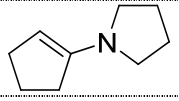
114	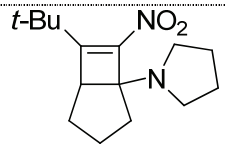
115	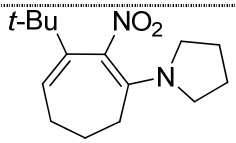

116	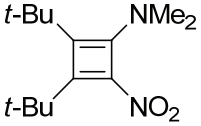
117	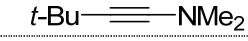
118	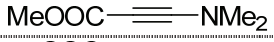
119	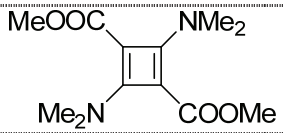
120	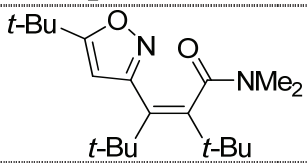
121	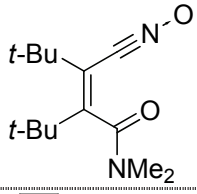
122	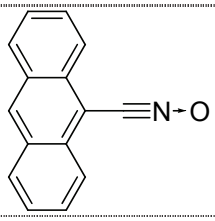
123	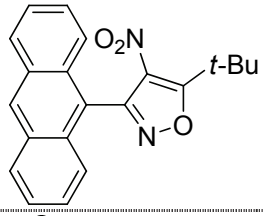
124	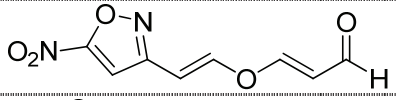
125	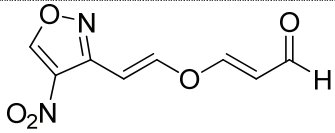
126	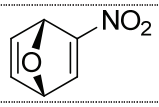
127	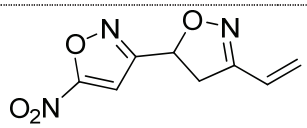
128	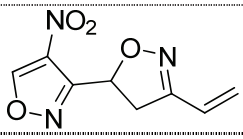

129	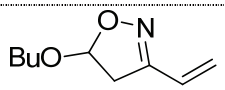
130	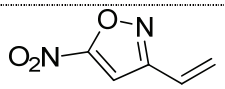
131	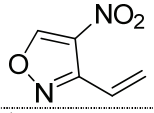
132	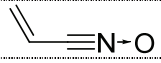
133	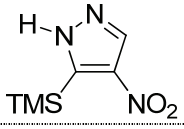
134	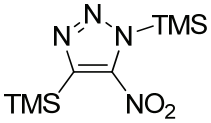
135	
136	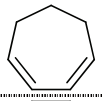
137	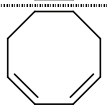
138	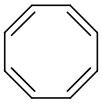
139	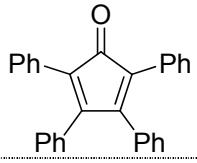
140	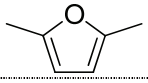
141	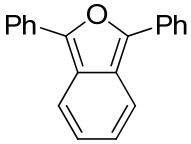
142	
143	
144	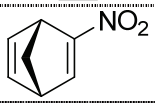

145	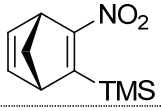
146	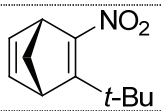
147	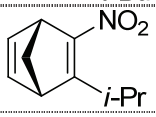
148	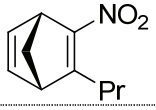
149	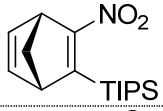
150	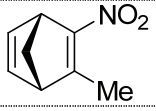
151	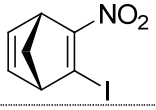
152	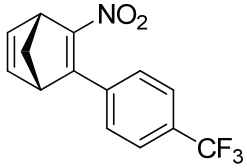
153	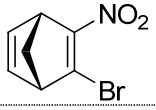
154	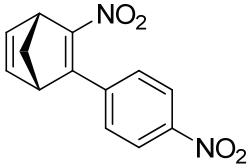
155	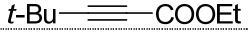
156	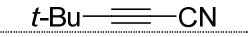
157	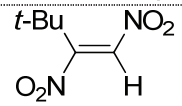
158	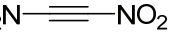
159	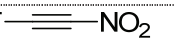
160	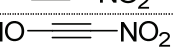
161	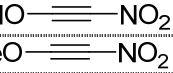
162	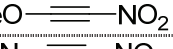
163	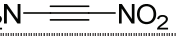
164	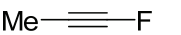

165	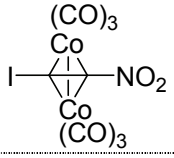
166	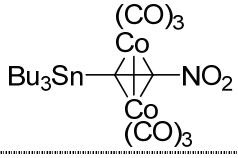
167	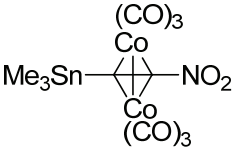
168	
169	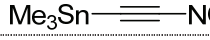
170	
171	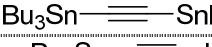
172	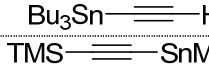
173	
174	
175	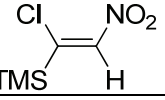

Chapter 3

Number	Structure
176	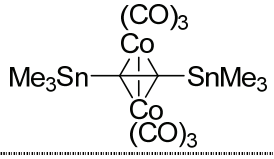
177	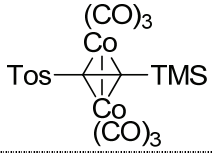
178	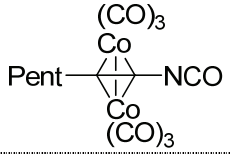
179	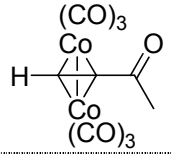
180	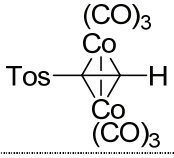
181	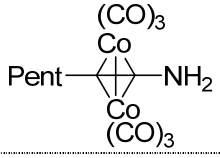
182	
183	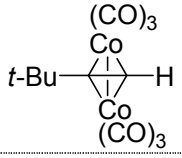
184	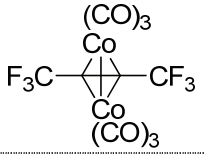
185	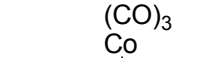
186	
187	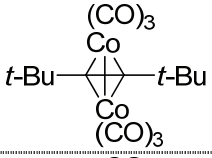
188	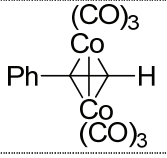
189	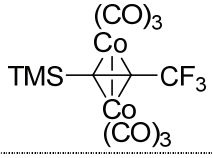

190	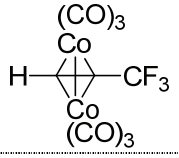
191	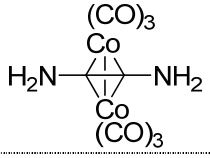
192	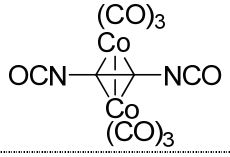
193	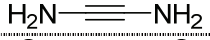
194	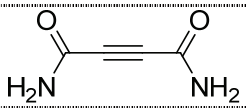
195	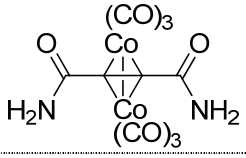
196	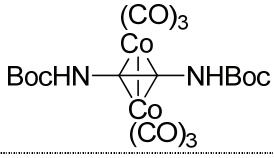
197	
198	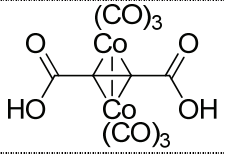
199	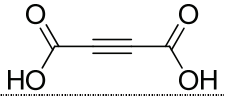
200	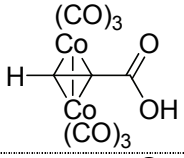
201	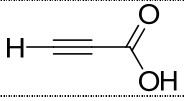
202	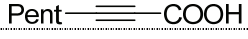
203	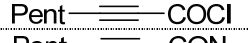
204	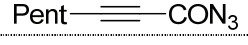
205	
206	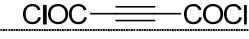

207	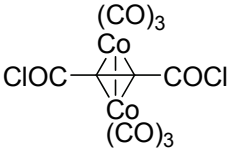
208	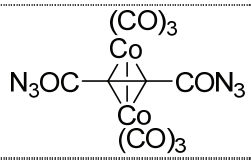
209	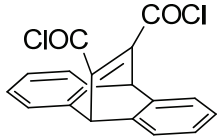
210	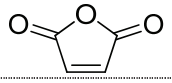
211	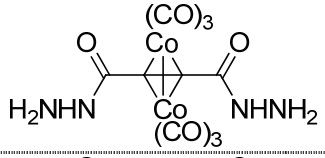
212	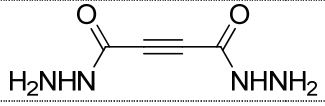
213	
214	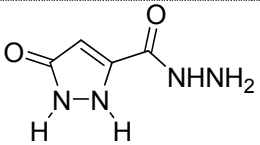
215	
216	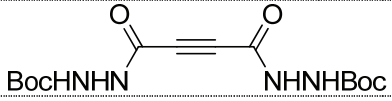
217	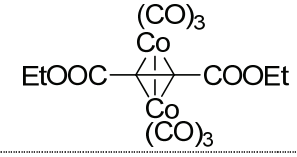
218	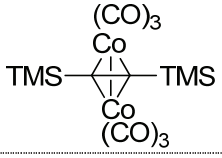
218a	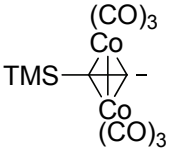

219	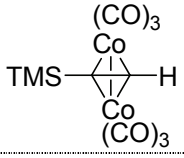
220	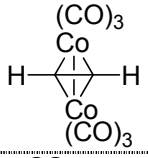
221	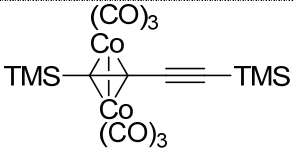
222	Ph_3CBF_4
223	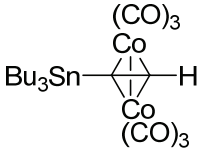
224	Bu_3SnF
225	$PrONO_2$
226	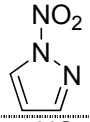
227	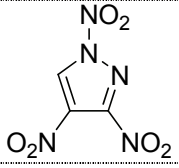
228	$Pd(PPh_3)_4$
229	PhI
230	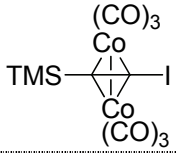
231	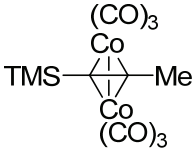
232	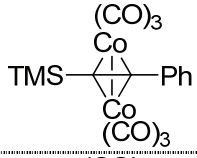
233	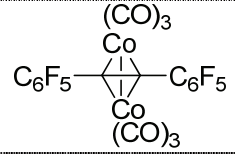
234	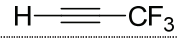
235	
236	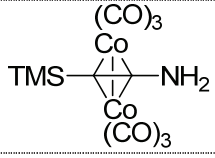
237	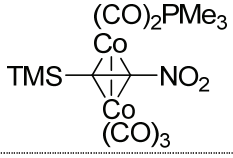
238	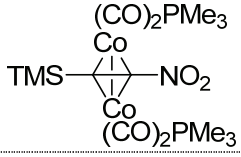
239	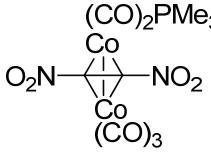
240	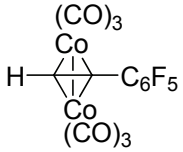
241	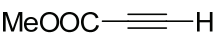
242	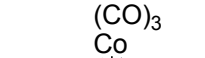
243	
244	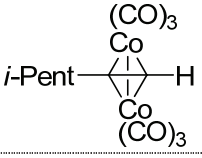
245	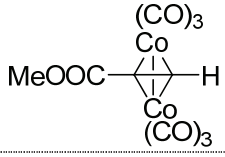
246	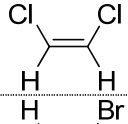
247	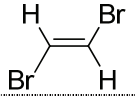

248	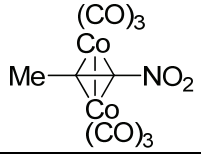

Chapter 4

Number	Structure
249	
250	
251	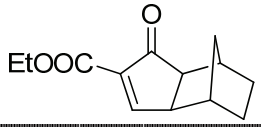
252	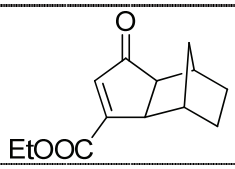
253	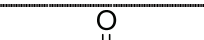
254	
255	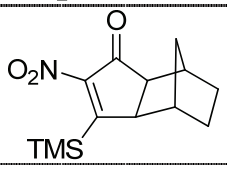
256	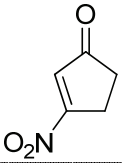
257	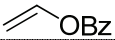
258	NMO
259	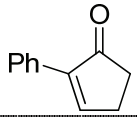
260	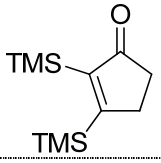

261	
262	TMANO
263	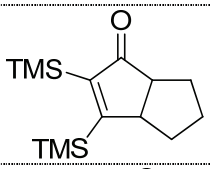
264	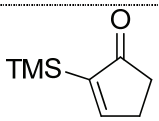
265	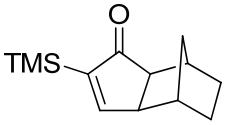
266	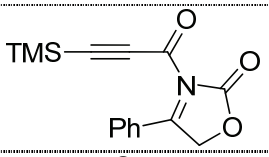
267	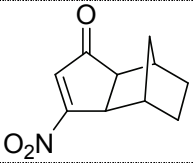
268	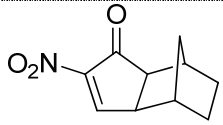
269	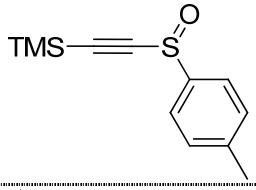
270	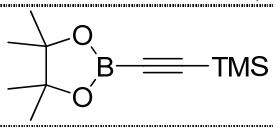
271	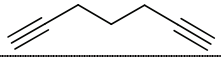

272	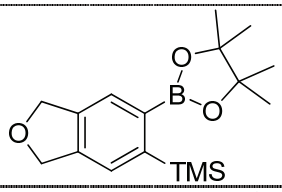
273	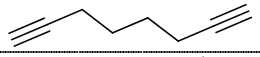
274	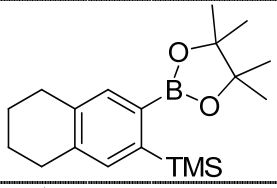
275	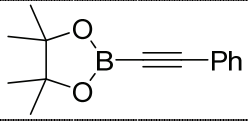
276	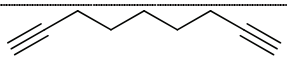
277	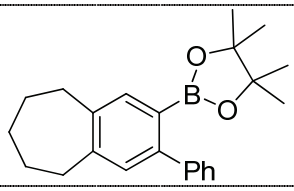
278	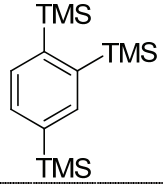
279	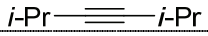
280	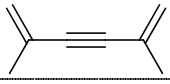
281	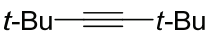
282	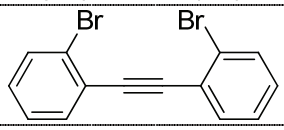
283	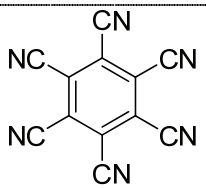
284	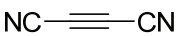
285	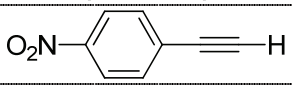
286	
287	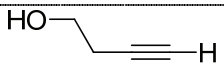
288	

289	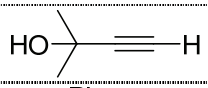
290	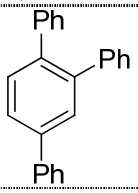
291	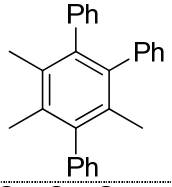
292	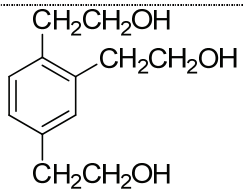
293	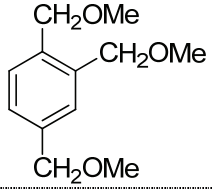
294	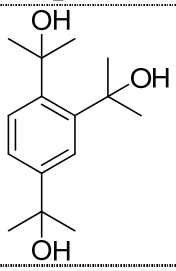
295	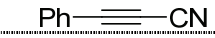
296	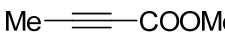
297	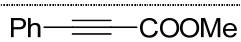
298	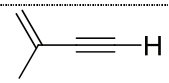
299	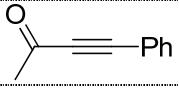
300	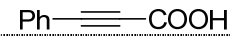
301	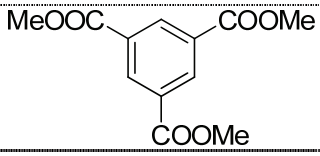

302

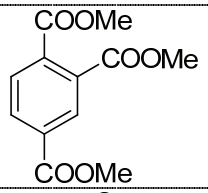

303

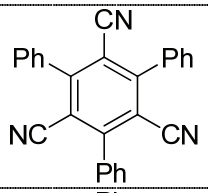

304

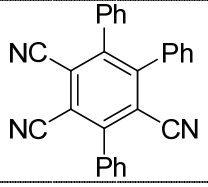

305

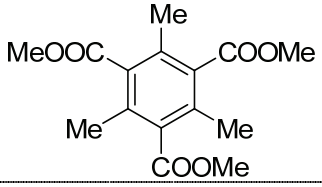

306

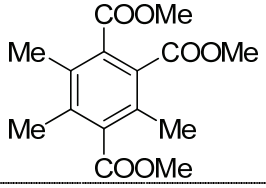

307

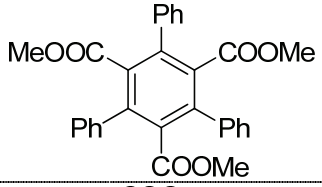

308

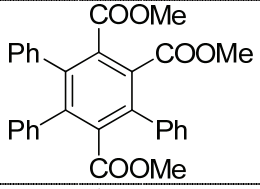

309

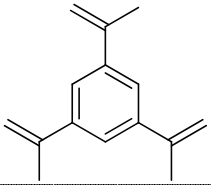

310

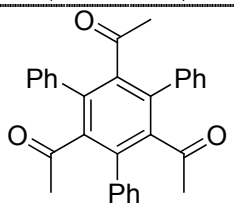

311

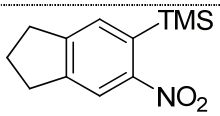

312

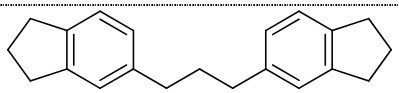

313

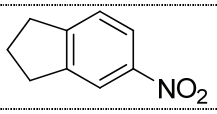

314

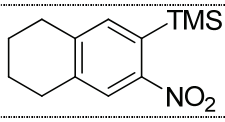

315

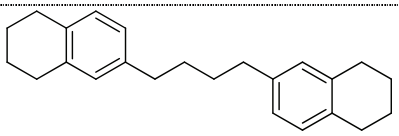

316

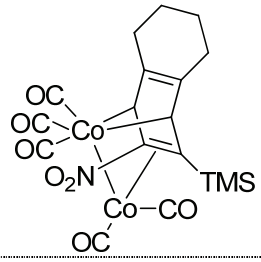

317

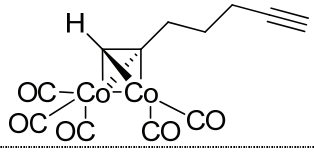

318

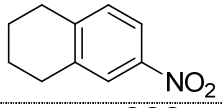

319

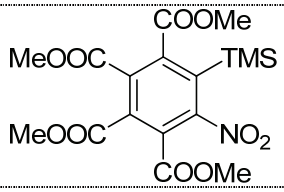

319a

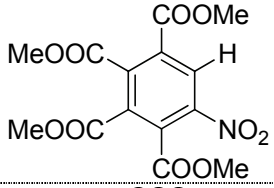

320

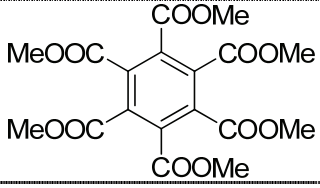

321	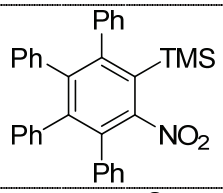
322	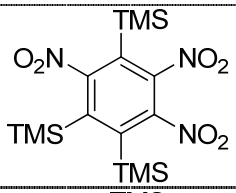
323	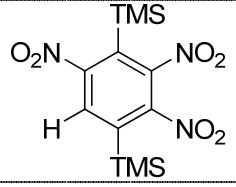
324	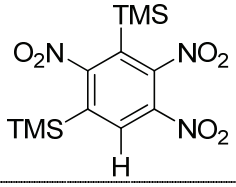
325	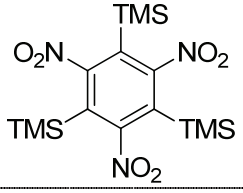
326	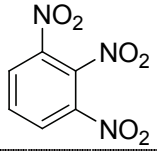
327	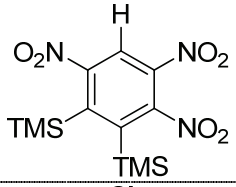
328	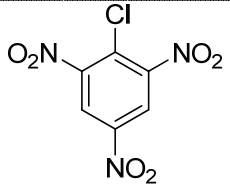
329	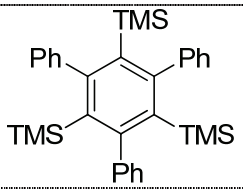
330	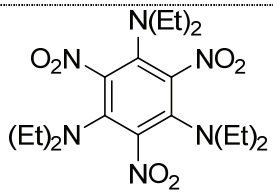
331	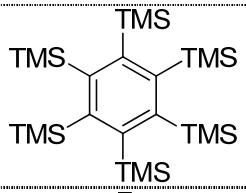
332	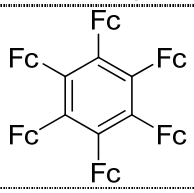
333	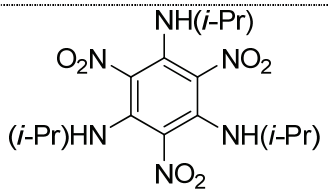
334	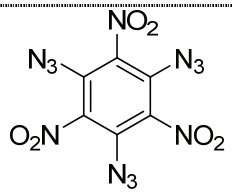
335	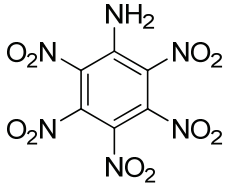
336	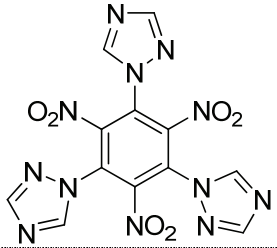
337	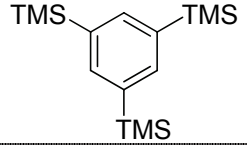

338	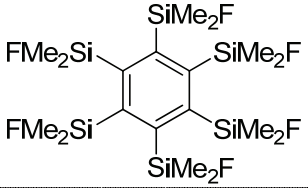
339	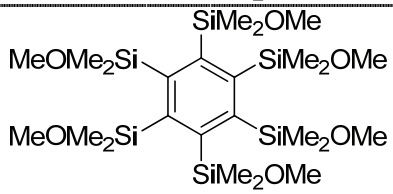
340	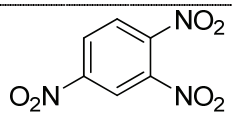

341	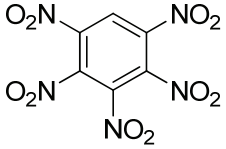

Appendix A

Number	Structure
342	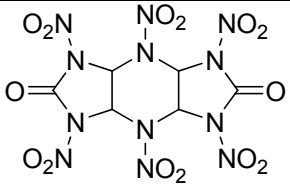
343